Title

Trait-based and phylogenetic approaches to understanding community assembly processes in eelgrass beds

Author

Gross, Collin Patrick

Publication Date

2023

Peer reviewed|Thesis/dissertation

Trait-based and phylogenetic approaches to understanding community assembly processes in eelgrass beds

by

COLLIN PATRICK GROSS

DISSERTATION

Submitted in partial satisfaction of the requirements for the degree of

DOCTOR OF PHILOSOPHY

in

Population Biology

in the

OFFICE OF GRADUATE STUDIES

of the

UNIVERSITY OF CALIFORNIA

DAVIS

Approved:

_____

John J. Stachowicz, Chair

_____

Sharon Lawler

_____

Eric Sanford

Committee in Charge

2023

ABSTRACT

The field of community ecology is fundamentally concerned with the assembly and maintenance of diversity across space and time. Two of the most fundamental questions in the field, then, are 1) why do we see variation in composition and diversity across space and time, and 2) how are diversity and assemblage structures maintained? A common model for beginning to understand these questions is the idea of ecological "filters" that restrict species from a regional pool. Different kinds of filters apply different kinds of selective pressures, and because species' traits are what allow them to pass through filters, studying the distributions and dispersion of traits within the community can help us understand how these filters act on the species pool. A variety of factors may cause communities to have traits that are overdispersed – more disparate than expected by chance – or underdispersed or clustered – more similar than expected by chance.

My dissertation attempts to address these fundamental questions in communities associated with eelgrass (*Zostera marina*) – an herbaceous marine angiosperm (seagrass) that forms monospecific beds across nearly 40º of latitude in the northern hemisphere. Eelgrass is home to a diversity of epifaunal invertebrate mesograzers – animals that live on the leaves of the plant and feed on fouling microalgal epiphytes, as well as macroalgae and fresh and decaying eelgrass tissue. Peracarid crustaceans are one of the most abundant and diverse of the mesograzers. These crustaceans – amphipods, isopods, and their relatives – are found worldwide and are especially susceptible to predation by the diverse suite of resident and juvenile fishes that also call eelgrass beds home.

My first chapter draws on data from a global experimental network to examine how the functional structure of eelgrass peracarid communities varies across space and with different ecological filters. I found that dispersion strongly increased with increasing predation and decreasing latitude – communities at low-latitude sites and those that experienced high predation intensity were more overdispersed than those at high latitudes and with low predation intensity. Ocean and epiphyte load appeared as secondary predictors; Pacific communities were more overdispersed while Atlantic communities were more clustered, and increasing epiphytes were associated with increased clustering. Together these results point to the importance of both biotic interactions and the historical legacies of distinct species pools in structuring communities.

My second chapter narrows in on eelgrass beds in Northern California to investigate the role of diverse suites of predator (fish) community traits as ecological filters that drive patterns of dispersion in prey (peracarid) communities. Fish traits related to prey detection and capture selected for more overdispersed peracarid communities, particularly with respect to body size and activity level, suggesting that prey may be pushed to disparate areas of trait space to avoid consistent detection by predators across the community. I also found correlations between the trait dispersions of predator and prey communities that strengthened after accounting for the effects of habitat filters on predator dispersion, suggesting that habitat filtering effects on predator species pools may hinder their ability to affect prey community assembly. Specific predator traits may have measurable impacts on the community assembly of prey, inviting experimental tests of predator trait means on community assembly, and explicit comparisons of how the relative effects of habitat filters and intraguild competition on predators impact their ability to affect prey community assembly.

Finally, my third chapter returns to the global experimental network from the first chapter to address more coarse-scale patterns of community structure beyond peracarids. This time, I examined in epifauna communities dominated by peracarids and gastropods. The abundance of these two taxa exhibited a strong latitudinal cline in turnover, with gastropods abundant at high-latitude sites, and peracarids abundant at low-latitude sites, especially in the Atlantic. This pattern appeared to be driven by greater eelgrass genetic diversity at lower latitudes, which strongly influenced both the richness and abundance of peracarids, but less so for gastropods. The two taxa exhibited functional complementarity, and so global variation in genetic diversity led to geographic variation in the distribution of functional traits across the range of eelgrass. These results add to a growing body of literature that suggests that variation in traits underlaid by genetic differences within species has important bottom-up consequences for assemblage variation and ecosystem function across broad spatial scales.

ACKNOWLEDGMENTS

I'd first like to thank my mother, Sarah Funk, for instilling in me both a sense of creativity and an appreciation for all organisms, from fishes to amphipods. Whether those qualities were hereditary or not, they have been the driving force behind my love of science since I can remember.

I also extend my thanks to all of the people at the University of Washington who saw in me the potential to succeed in and encouraged me to pursue academic science. To the graduate students – Dr. Katie Dobkowski, Dr. Emily Grason, Dr. Hilary Hayford, Iris Kemp, Dr. Alex Lowe and Dr. Mo Turner – who so graciously let me get my feet wet (sometimes literally) in volunteer lab work, field work, and my very first research projects. To the faculty and other seasoned mentors – Dr. Megan Dethier, Dr. Cinde Donoghue, Dr. Ben Kerr, and especially Dr. Jennifer Ruesink. Jen, I will never forget the time you first took me out for my first eelgrass field trip at midnight in December on Hood Canal. The menagerie of tiny squirming bugs, slugs, and worms has captured my heart ever since. Thank you for fostering my love for eelgrass and its inhabitants, teaching me how to enjoy writing, and emphasizing the scientific value of natural history observations.

To the inimitable Dr. Jay Stachowicz – I could never have asked for a more patient, supportive, and encouraging PhD advisor. Jay, I have never left a meeting with you feeling confused, discouraged, or lacking confidence in my abilities. Thank you for being my biggest cheerleader and helping me realize that yes, I do have programming skills. You've also brought together the most amazing team of scientists, colleagues, and friends I could have ever hoped for. To the rest of the Stach Labbies, past and present – Dr. Deanna Beatty, Dr. Gina Chaput, Dr. Katie Dubois, Dr. Melissa Kardish, Dr. Nicole Kollars, Serina Moheed, Claire Murphy, Karolina Zabinski – thank you for your willingness to turn around and talk about anything from mixed effects models to Downton Abbey, and for truly making me excited to go back to Storer every week. Of course, I have to acknowledge my Stach Lab triplets, Hannah Higuera and Isabelle Neylan. It's been so inspiring to learn from you and witness all of the things you've accomplished these past 6 years. How fitting that we're now finishing up our dissertations just as we started them, totally in sync!

This dissertation would not be in the shape it's in (whatever that means) without the rest of my committee helping me both with this finished product and its nascent stages during my

qualifying exam. Dr. Eric Sanford and Jackie Sones are to me the most important fixtures of the Bodega Marine Lab. Their dedication to and knowledge of natural history and science communication is unparalleled, and I am so grateful to have gotten to learn from them both inside and outside of the classroom. It was always so heartening when, after staring at dead animals all day in the lab or labeling the 120th pee cup, they would let me know they'd found an interesting (live!) amphipod or isopod and invite me in to check it out under their microscope. My heartfelt thanks also extends to Dr. Ted Grosholz, Dr. Emilio Laca, Dr. Sharon Lawler, Dr. Sharon Strauss, and Dr. Peter Wainwright. Thank you for your incredible support in all aspects of science and career development.

I thank the Center for Population Biology, my PBGG cohort, and all the other Platypodes that have made this experience truly excellent, in science and beyond. Thank you to the staff in the Department of Evolution and Ecology and the Bodega Marine Lab, past and present – Kitty Brown, Brenda Cameron, Al Carranza, Debbie Davidson, Sally Harmsworth, Ivana Li, Phong Mai, Sherri Mann, Carla Muñoz, Joe Patrocinio, Philip Smith, and Ruby Wu – I would be nowhere without your patience and willingness to help.

No dissertation research can be completed without the indispensable help of those willing to put in long and odd hours helping with data collection. I extend my gratitude to the original team of ZENterns – thank you for your dedication to quantifying and identifying hundreds of epifaunal samples, not only across taxa but collected from three different continents. To all of the amazing undergraduate interns and volunteers and others that have helped me collect data from my own surveys and experiments, whether it was in the eelgrass before first light or in the lab staring into a microscope until your eyeballs fell out. I extend my thanks to Rylee Alexander, Emma Deen, Sophie Allen, Monica Burnett, Gabriel Hernandez, Lara Hsia, Anna Lee, Naomi Murray, Sindhu Bala, Reyana Balotcopo, Nathan Dao, Julia Delamare, Olivia Diana, Zoe Fricker, Kaley Hamane, Tracie Hayes, Alex Lei, Andie Lindeman, Michael Liu, Lila Magbilang, Chloe McCormick, Armand McFarland, Kendall Menard, Emily Myers, Sophia Pelletier, Adri Penix, Kenzie Pollard, Kevin Sanchez, Alondra Sandoval, Chloe Sears, Chelsea Souza, and Mary Yang.

I'm so incredibly lucky to have had an amazing group of friends with me this whole time. All of my friends and found family in Davis and Seattle have proved to be an unending font of

love, support, and cackling, and I thank them all – Daphna Khen, Daneil Newcomb, the Nut House, and the Queerios.

My partner, Jasen Liu, has been an incredible source of joy throughout this whole experience. Jasen, I'm so lucky to have had your support during uncertain and stressful times, and your amazing ability to say whatever it is in the moment that will make me laugh my ass off. Thank you for taking me out to look at birds, getting up every Wednesday with me during a global pandemic to look at insects and dodder in the marsh, making the best cinnamon rolls I've ever had, and being incredibly stupid with me. I love you.

Finally, this dissertation goes out to the eelgrass and all of the creatures that call it home. Thank you for continuing to inspire me and reinvigorate me every time I stick my hands (and sometimes face) in the water. To the 241 fish and the hundreds of thousands of epifaunal invertebrates that gave their lives for this dissertation (including the un-analyzed caging samples), thank you for teaching me about how the natural world works and helping me put my own little dent in the circle of human knowledge.

TABLE OF CONTENTS

CHAPTER 1: The biogeography of community assembly: latitude and predation drive variation in community trait distribution in a guild of epifaunal crustaceans[1]

ABSTRACT

While considerable evidence exists of biogeographic patterns in the intensity of species interactions, the influence of these patterns on variation in community structure is less clear. Studying how the distributions of traits in communities vary along global gradients can inform how variation in interactions and other factors contribute to the process of community assembly. Using a model selection approach on measures of trait dispersion in crustaceans associated with eelgrass (*Zostera marina*) spanning 30º of latitude in two oceans, we found that dispersion strongly increased with increasing predation and decreasing latitude. Ocean and epiphyte load appeared as secondary predictors; Pacific communities were more overdispersed while Atlantic communities were more clustered, and increasing epiphytes were associated with increased clustering. By examining how species interactions and environmental filters influence community structure across biogeographic regions, we demonstrate how both latitudinal variation in species interactions and historical contingency shape these responses. Community trait distributions have implications for ecosystem stability and functioning, and integrating large-scale observations of environmental filters, species interactions, and traits can help us predict how communities may respond to environmental change.

INTRODUCTION

Community ecology is fundamentally concerned with the assembly and maintenance of diversity across space and time. Key to this endeavor is the idea that the composition of a local community is the result of multiple ecological filters selecting species from a regional pool (Poff 1997; Thompson *et al.* 2020). Different kinds of filters apply different kinds of selective pressures on the species pool, and because species' traits are what allow them to pass through filters, studying the distribution of traits within the community can help us understand how these filters act on the species pool as a whole. Strong environmental filters (i.e., abiotic filters *sensu* Kraft *et al.* 2015) such as climate are thought to act on large spatial scales to constrain trait diversity such that species are more alike (clustered) in traits that respond to these factors than

[1] Published as: Gross, C.P., et al. (2022). The biogeography of community assembly: latitude and predation drive variation in community trait distribution in a guild of epifaunal crustaceans. *Proceedings of the Royal Society B,* 289: 20211762. doi: 10.1098/rspb.2021.1762

we would expect under a purely random assembly process (Webb *et al.* 2002; Cavender-Bares *et al.* 2009; Starko *et al.* 2020; Thompson *et al.* 2020). Biotic filters, such as competition, then act at smaller spatial scales to enhance or reduce trait diversity among species with broadly similar abiotic tolerances, depending on which traits are affected (Mayfield & Levine 2010). When traits related to the acquisition of distinct resources are considered, competition for these resources drives the distribution of traits to be wider than expected by chance (overdispersed) as there are multiple resource niche optima that can be occupied (Webb *et al.* 2002; Cavender-Bares *et al.* 2009; Pavoine & Bonsall 2011). In contrast, competition for a single, dominant limiting resource can also act as a filter, selecting for traits related to acquiring this resource to converge around an optimal value, because species deviating from the optimum are otherwise competitively excluded. All else being equal, as richness increases, an increase in trait dispersion may point to stronger stabilizing mechanisms and limiting similarity, while a decrease in trait dispersion can suggest stronger equalising mechanisms promoting unstable coexistence. (Chesson 2000; Mayfield & Levine 2010).

Despite well-known geographic patterns in the strength of both biotic interactions and environmental filters (Schemske *et al.* 2009; Reynolds *et al.* 2018; Longo *et al.* 2019; Zvereva & Kozlov 2021), few studies have examined the global-scale consequences of geographic variation in these filters for community trait distributions (Ford & Roberts 2018, Skeels *et al.* 2020). In particular, intense predation, competition, and mutualistic interactions at lower latitudes (Freestone & Osman 2011; Longo *et al.* 2019; Zvereva & Kozlov 2021), may lead to the predominance of biotic interactions over environmental filters in structuring low-latitude communities. This may cause stronger trait clustering near the poles that shifts towards more overdispersed communities at lower latitudes. On the other hand, selection for tolerance of extreme heat conditions could also cause trait clustering at low latitudes. Finally, patterns in community structure along latitudinal gradients could be dominated by idiosyncratic and historically-contingent effects of predators, prey, competitors, and mutualists that vary among biogeographic provinces (Sanford & Bertness 2009; Mittelbach & Schemske 2015; Ford & Roberts 2019; Whalen *et al.* 2020). Local abiotic factors, habitat complexity, assemblage composition, and adaptation to these local factors could further obscure broader geographic patterns of community assembly (Sanford & Bertness 2009; Lavender *et al.* 2017), stressing the importance of assessing patterns across multiple independent species pools. For example, the

effects of regional gradients in predation may be overshadowed by local increases in habitat complexity, which can decrease predation pressure (Reynolds *et al.* 2018) and increase trait dispersion as species assort into disparate microhabitat niches (Best & Stachowicz 2014). Understanding trait distributions and their drivers should provide insight into the likely responses of communities to environmental fluctuations or perturbations in the same way that understanding the diversity of traits within a population can inform us on its evolutionary potential (Cadotte *et al.* 2011; Rumm *et al.* 2018).

Here we examine geographic patterns in the trait distribution of epifaunal invertebrates living on eelgrass throughout the northern hemisphere to assess the extent and causes of geographic variation in the drivers of the assembly of these communities. Eelgrass (*Zostera marina*) is the world's most widespread species of temperate seagrass, a marine angiosperm found throughout the Northern Hemisphere from 30º to 67º N latitude in both the Atlantic and Pacific Oceans (den Hartog 1970; Green & Short 2003). Much of the animal community in eelgrass beds is made up of invertebrate mesograzers that primarily feed on the epiphytic microalgae fouling the seagrass blades (Valentine & Duffy 2006). Competition for food and microhabitat space occurs among mesograzers, and can significantly affect community composition (Edgar 1990; Best *et al.* 2013; Best & Stachowicz 2014; Amundrud *et al.* 2015). Peracarid crustaceans (amphipods, isopods, and tanaids) are the most widespread, abundant, and species-rich mesograzer taxon in these eelgrass beds, and they experience elevated predation in low-latitude eelgrass beds (Reynolds *et al.* 2018) which could either cause clustering of communities around traits that increase resistance or tolerance to predation, or cause dispersion of communities due to competition for enemy-free space. *Z. marina*'s wide range across latitudes provides an opportunity to assess the role of gradients of ecological filters on global scales without the confounding influence of changing habitat type. We predicted: (1) that trait dispersion would increase with decreasing latitude as species interactions become more intense and (2) that abiotic filters would be strongest and result in clustering at higher latitudes and where biotic interactions are weak. While marine systems often show non-linear variation in species diversity and interaction strength with latitude (peaking at mid-latitudes; Chaudhary *et al.* 2017; Whalen *et al.* 2020), our predictions are reasonable within the range of latitudes occupied by eelgrass (~30-70ºN). We test these predictions in separate ocean basins with largely unique fauna, allowing us to assess whether the unique histories of these zoogeographic

provinces result in different patterns and drivers of trait distribution in each ocean basin (Roy *et al.* 2009; Dyer & Forister 2019).

METHODS

Study design and sample collection. Between May and September 2014, we sampled 42 sites across the range of *Z. marina*, spanning 30 degrees of latitude along both coasts of Eurasia and North America (30.4ºN to 60.1ºN; Fig. 1.1) to characterize the biological and physical structure of eelgrass beds using standardized measurements. We implemented a hierarchical sampling design consisting of two oceans (Atlantic and Pacific), each with two coasts (east and west), each with 6-14 sites, each with 20 plots, for a total of 840 plots in 42 sites sampled as part of the *Zostera* Experimental Network (ZEN; Fig. A1.1). Plots were 1 m^2 and spaced 2 m apart at each site. Along each coastline, sites were separated by 4.9 km (Virginia, USA) to 485.4 km (Washington State, USA) of water.

Assessing eelgrass habitat characteristics. We sampled eelgrass biomass by haphazardly placing and pushing a 20-cm diameter core tube 20 cm into the sediment within each plot. We gathered all shoots rooted within the core bottom area into the core tube to ensure that no shoots were cut off during sampling. We then removed the shoots from the sediment, transferred the core contents into a mesh bag. In the lab, we rinsed the core contents, removed fouling algae and sediment from the eelgrass tissue, and separated above- and belowground biomass by cutting the plant above the rhizome. In addition to eelgrass, we also removed all of the macroalgae from the plot. All eelgrass and macroalgal tissue was dried to a constant weight at 60ºC and weighed. From five haphazardly collected eelgrass shoots per plot, we also collected 3-cm lengths of tissue from a healthy, unfouled inner leaf and processed these samples for tissue nitrogen using a CHN analyser (Thermo Fisher Scientific Inc., Waltham, MA, USA).

We quantified eelgrass habitat structure at the plot level by measuring shoot density and canopy height. We estimated shoot density by counting the number of shoots emerging within a 20-cm diameter ring placed haphazardly in the plot. In plots where density was particularly low (less than 50 shoots m^{-2}, about 5% of plots), we counted all of the shoots in the plot. We measured canopy height by haphazardly collecting five shoots from each plot and measuring their length from the tip of the longest leaf to the leaf sheath.

We sampled epiphyte load on the eelgrass blades by selecting four shoots from each plot and removing them from the substrate either by gently uprooting or clipping at the meristem and

placing them in a plastic bag on ice for transport. In the lab, we scraped both sides of all the leaves with a glass slide to remove fouling material, which was then filtered, transferred to an aluminium pan, dried to a constant weight at 60ºC, and weighed.

Measuring predation intensity. Predation intensity was quantified by tethering locally-collected prey ("gammarid" amphipods) in each plot for 24 hours. These data and methods are reported in detail in Reynolds et al. (2018). Briefly, each individual amphipod was glued to a 10-cm piece of monofilament line 0.133 mm in diameter (Berkley Fireline™, Spirit Lake, IA, USA) tied to a transparent acrylic stake anchored in the sediment, so that it could swim freely in the water column and cling to adjacent eelgrass blades. After 24 hours, we removed the stakes and scored prey as present (uneaten) or absent (eaten); partially-consumed prey were considered eaten, and moulted prey were excluded from analyses. Site-level predation was calculated by averaging scores across plots.

Abiotic environmental variables. To characterize the abiotic environment experienced by epifauna across the range of eelgrass, we measured in-situ temperature and salinity at each site at the time of sampling. To characterize the overall abiotic environment of each site, we also retrieved estimates of annual mean sea surface temperature (SST), photosynthetically active radiation (PAR), and surface chlorophyll A (Chl a) from the surrounding region, available in the Bio-ORACLE data set (Tyberghein *et al.* 2012). These data were taken from monthly readings of the Aqua-MODIS and SeaWiFS satellites at a 9.6 km^2 spatial resolution from 2002 to 2009. We used the raster package in R v. 3.6.3 (Hijmans & Etten 2020; R Development Core Team 2021) to extract the annual mean SST, SST range, PAR, and Chl a from all cells within 10 km of each site, and averaged these cell-level estimates to generate site-level predictors. Other water quality parameters, including dissolved nitrate and other nutrients, were spatially interpolated based on surface measurements in the World Ocean Database 2009 (Garcia *et al.* 2010).

Epifaunal community composition. To sample the macrofauna associated with the eelgrass blades, we carefully placed an open-mouthed fine-mesh drawstring bag (500 µm mesh, 18 cm diameter) over a clump of shoots in the centre of the plot so that the mouth of the bag was flush with the sediment surface. We then cut the shoots where they emerged from the sediment and quickly closed the drawstring to capture the shoots and associated animals. The shoots were transferred to the lab on ice, rinsed and hand-inspected to dislodge the epifauna, which were then passed through a 1-mm sieve and ultimately transferred into 70% ethanol. Epifauna were then

identified to the lowest possible taxonomic level (typically species). Epifaunal abundance was standardized by the aboveground biomass of the eelgrass sample from which they were collected.

We scored all peracarids (amphipods, isopods, and tanaids) for a series of traits based on information available in the literature, including body size, fecundity, body shape, living habit, motility, bioturbation, and diet components (Table 1.1, Appendix 2 for literature). Due to a paucity of data on intraspecific trait variation for most species, literature values were assumed to be representative for all individuals in our study. For subsequent analyses, we categorized each of these traits as related to microhabitat or dietary niche; we also performed analyses with all traits ungrouped. While we acknowledge that these broad categories may overlap, we elected to sort traits into these categories because they represent two potential components of trait dispersion exhibited by peracarids in field studies and laboratory experiments (Best *et al.* 2013; Best & Stachowicz 2014). Correlations among traits were generally weak, save for strong positive relationships between eating live seagrass tissue and macroalgae, detritivory and consuming seagrass detritus, and suspension feeding and bioturbation (Fig. A1.2).

Characterizing community dispersion. For all the peracarid species observed in our dataset, we used the trait dataset to generate three matrices of Gower distances between species: one of all traits, one for diet traits, and one for microhabitat traits using the FD package in R (Laliberté *et al.* 2014). Using subsets of these matrices for communities at the site level (summed across 20 plots at each site, n = 42), we measured the trait distance between species as the Mean Pairwise Distance (MPD) and Mean Nearest Taxon Distance (MNTD) for each set of traits (Webb *et al.* 2002; Sessa *et al.* 2018). MPD is the average of the trait distances between all pairs of species found within a given sample unit (site), while MNTD is the average minimum distance between species pairs in a site. Both are independent of species richness, but the two metrics can behave differently depending on the clustering of species in trait space within a sample (Sessa *et al.* 2018).

To determine whether the observed species traits in each community differed from those expected by chance, we standardized MPD and MNTD against null distributions generated according to two permutation algorithms. The first, independent swap, is a semi-constrained model that randomly re-assembles the sample-by-species community matrix while maintaining the species richness of each sample and the presence/absence of each species across samples.

The second, tip shuffle, is a more constrained model that directly shuffles the traits of the species in the community while maintaining richness, occurrence, and trait distances between community members, effectively moving the tip labels on a trait dendrogram. Imposing more constraints on permutation controls for patterns in the data that are not directly relevant to the question at hand, such as species richness, occurrence, or identity, ultimately reducing type I error rates (Swenson 2014). Because of the relatively low overlap in species pools across the range of our study, comparing the results relative to both types of models can be informative of the importance of species identity in these types of permutations, and also facilitate comparison with other studies in which the independent swap algorithm has been used together with less constrained permutations (e.g., Best and Stachowicz 2014). These permutations were each completed 999 times for each community, and null distributions of MPD and MNTD were generated based on values calculated from randomized communities.

We examined the effect of the species pool on community dispersion, using varying degrees of constraint on the matrix and trait dendrogram used to generate null distributions. To make comparisons among sites, we permuted within the global species pool (all sites) and ocean-level Atlantic and Pacific species pools. Using a global pool in our permutations is appropriate because while all species were not present in all regions, there were no traits that were exclusive to any region (Fig. A1.2).

Each observed value of community trait distance was then compared to the corresponding null distribution by calculating the standard effect size (SES_{MPD} or SES_{MNTD}). A positive value of SES indicates that the observed community trait distance (as measured by MPD or MNTD) is greater than the null mean, meaning that community members are more dissimilar than expected under a random draw (overdispersion), while a negative SES indicates that trait distance is less than the null mean, meaning that community members are more similar to each other than expected under a random draw (clustering). MPD, MNTD, null distributions and SES values were calculated using the picante package in R (Kembel *et al.* 2010).

Data analysis. Two distance metrics (MPD and MNTD), two permutation algorithms (independent swap and tip shuffle), three species pools (global, Pacific, and Atlantic), and three trait sets (all, diet, and microhabitat) totalled 36 sets of SES values. However due to missing diet data for some species, we were unable to calculate diet SES_{MNTD} with the tip shuffle algorithm, leaving us with a total of 33 sets. For each distance metric, algorithm, species pool, and trait set,

SES values were used as response variables in a set of 16 linear models incorporating latitude, ocean, continental margin (east vs. west), in-situ temperature and salinity, annual mean and range of SST, total crustacean abundance and median crustacean size, epifaunal and peracarid richness, macroalgal biomass, average predation intensity, epiphyte load, Chl a, PAR, water column nitrate, mean leaf nitrogen content, and two axes of eelgrass habitat structure as derived from a principal component analysis incorporating shoot density, leaf sheath width and length, longest leaf length, and aboveground biomass (PC1 and 2, Fig. A1.4) as predictor variables, as well as select interactions between them (Table 1.2). Predictors were log-, square-root-, or arcsin-transformed where appropriate to conform to a normal distribution based on Shapiro-Wilk normality tests and visual examinations of histograms. Collinearity of predictors was accounted for using variance inflation factors (VIF) for variables in composite models using the car package in R (Fox & Weisberg 2019). Predictors with a VIF greater than five were removed from composite models. We also examined the effects of predictors on the SES of individual traits to understand what traits may drive the patterns we see across environmental gradients (Appendix 2).

We ranked these initial hypothesis-driven models of SES using AICc scores (MuMIn package; Bartoń 2020), and then incorporated predictors from the three lowest-scoring models of each set into a set of composite models to examine the combined effects of multiple predictor types. We then used backwards elimination to select the lowest-scoring model from these composite models. Where two models had a ΔAICc less than 3 units, we selected the model with the fewest parameters for interpretation.

RESULTS

Peracarid assemblages at Pacific sites had greater trait dispersion than Atlantic sites, and dispersion increased with increasing predation and decreasing latitude, though there were some differences among the two oceans that we outline below. Across our sites, we found a total of 105 species, 55 of which were found in the Atlantic, and 60 of which were found in the Pacific, with 10 species found in both oceans. There were 15 species in the Northwest Pacific, 48 species in the Northeast Pacific, 36 species in the Northwest Atlantic, and 24 species in the Northeast Atlantic (Fig. A1.3). The patterns and predictors of trait dispersion were robust across SES metrics and permutation algorithms (Fig. A1.5); here we present and interpret the results of

model selection on SES_{MNTD} calculated using the tip shuffle algorithm, with exceptions presented where relevant.

Dispersion of traits by ocean basin. Of the set of all traits examined, communities at Atlantic sites were on average clustered (SES < 0) relative to the global null, particularly for body size and living habit (Fig. A3.2) – species clustered around a mean body size of 14.09 mm (47.5% smaller than the mean Pacific body size), and most were free-living. Communities at Pacific sites were overdispersed (SES > 0) on average relative to the global null (Fig. 1.2, Table A1.1). This pattern held for both metrics and null models but was significant only for SES_{MPD} (SES_{MPD} independent swap $t_{38.097} = 2.43$, $p = 0.020$; SES_{MPD} tip shuffle $t_{38.242} = 2.31$, $p = 0.027$; two-sample t tests). Within the global pool, the separate calculations of SES using microhabitat and feeding traits showed a similar pattern; for microhabitat traits, Pacific communities were more overdispersed and Atlantic communities more clustered (SES_{MNTD} tip shuffle $t_{35.654} = 3.64$, $p = 0.00086$; Fig. 1.2).

Correlates of among-site variation in trait dispersion. Predation intensity, latitude, epiphyte load, and ocean basin (within the global species pool) were the strongest and most consistent predictors of SES across all species pools and all trait sets (Fig. A1.5). In-situ temperature, bed characteristics, epifaunal richness, continental margin, nitrate, and salinity also appeared occasionally (less than 30% of models) across the best models of SES. Mean annual sea surface temperature, epifaunal richness, salinity, nitrate, in-situ temperature, and crustacean abundance also varied significantly with latitude (Fig. A1.8).

In all of the best models, peracarid communities at sites with higher predation intensity had more overdispersed traits, whereas those with less intense predation had more clustered traits relative to a random draw from the species pool (Fig. 1.3a, Fig. A1.5a-c). Predation (removal of amphipod baits) varied from 20% in Quebec to 100% in Sweden, San Francisco Bay, Ireland, Korea, and British Columbia; the average predation rate was significantly greater in the Pacific than in the Atlantic Ocean (Table A1.2, Fig. A1.7, A1.8), but this did not translate to a difference in the effect of predation on dispersion across the two basins when permuting within the global pool ($p = 0.48$; Fig. 1.3a). Across the three species pools, the predation effect was stronger on average when permuting within the Pacific than the Atlantic or global pools, (Fig. A1.5a), and strongest in models of the dispersion of all traits together (Fig. A1.5b).

As predicted, trait dispersion decreased with increasing latitude in the best models (global species pool, microhabitat traits); communities became more clustered at higher latitude, while communities toward the equatorward edge of *Z. marina*'s range were more overdispersed (Fig. 1.3b, Fig. A1.5d-f). These latitude effects were stronger in the Pacific Ocean than in the Atlantic ($F_{1,38} = 7.95$, $p = 0.0076$; Fig. 1.3b) although they did not appear in the top models when permuting within the Pacific species pool (Fig. A1.5d); the best model including latitude was 1.3 AICc units better than the top model, but it was not selected as the top model because of the small difference in AICc score and greater number of parameters. Like predation, the latitude effect was strongest in models including all traits together (Fig. A1.5e).

Communities were more clustered (more negative SES) at sites with high epiphyte loads, but this effect was most obvious in the Atlantic species pool when only microhabitat traits were considered (Fig. 1.3c; Fig. A1.5g-h). There was rarely an effect of epiphyte load on SES when using other species pools (Fig. A1.5g) and never for diet traits (Fig. A1.5h).

DISCUSSION

Using a global dataset of eelgrass-associated peracarid crustaceans, we found a strong increase in community trait dispersion with decreasing latitude and increasing predation (Fig. 1.3a, b). Latitudinal clines in different ecological filters have been well-characterized in a wide variety of systems (Schemske *et al.* 2009; Reynolds *et al.* 2018; Zvereva & Kozlov 2021), particularly temperature and the strength of species interactions (Schemske *et al.* 2009; Longo *et al.* 2019; Zvereva & Kozlov 2021), both of which decrease at high latitudes. Stronger biotic interactions, in particular stabilizing interactions (*sensu* Chesson 2000), at lower latitudes may select for an overdispersed community (Webb *et al.* 2002; Mayfield & Levine 2010; Pavoine & Bonsall 2011), while stronger abiotic filters (or relatively weaker biotic filters) at either end of range (e.g. cold at the poleward edge or hot at the equatorward edge) could select for a clustered community (Webb *et al.* 2002; Cavender-Bares *et al.* 2009; Kraft *et al.* 2015). We found similar total numbers of species in the two oceans (Fig. A1.3) given similar sampling effort, and all traits were found in both oceans, so the differences we observe among oceans are not simply the result of different diversities in the underlying species pool.

Several lines of evidence point to the relatively greater effect of biotic interactions over temperature in structuring our communities. First, temperature rarely appeared as a significant factor in our best models (Fig. 1.3d). Second, latitudinal clines in dispersion were more

dependent on ocean basin than continental margins, which differ significantly in their temperature gradients (western side of oceans are warmer at an equivalent latitude; Fig. 1.3b; Reynolds *et al.* 2018). Third, predation in this system decreases with latitude, as it does in many others (Reynolds *et al.* 2018; Longo *et al.* 2019; Zvereva & Kozlov 2021). Fourth, we observed greater dispersion in living habit, motility, and macroalgae consumption at lower latitudes (Fig. A3.1b-d), all of which can be reasonably linked to stabilizing competition for food or enemy-free space. Finally, for some traits (body size, fecundity), we would expect clustering at both ends of a thermal gradient, but around different optima: large-bodied and highly fecund peracarids at cool sites, and small-bodied peracarids that produce fewer eggs at warm sites (Sainte-Marie 1991; Jaramillo *et al.* 2017). However, in ectotherms like peracarids, decreases in temperature at higher latitudes are less likely to be strong drivers of community structure than increases in temperature at lower latitudes as a result of asymmetrical performance curves (Martin & Huey 2008; Vasseur *et al.* 2014). While we saw that high-latitude sites tended to have species with high fecundity (65 to <135 eggs per brood; part of a general trend for clustered sites to have high or very high fecundity; Fig. A3.1a), we saw no similar trend towards clustering at low latitudes around low fecundity values or any other traits.

The decline in trait dispersion with latitude was significantly greater in the Pacific than the Atlantic. This difference in latitudinal clines and trait dispersion more generally between the two ocean basins (Fig. 1.2, Fig. 1.3b) may be in part due to differences in these assemblages' biogeographic and evolutionary histories (Mittelbach & Schemske 2015). First, glaciation in the north Atlantic during the last Ice Age means that many of the areas in which eelgrass now occurs would have been colonized after glaciers retreated (Vermeij 1991; Olsen *et al.* 2004), leaving less time for in-situ adaptation and specialization that might lead to increased trait dispersion (Cavender-Bares *et al.* 2009). Similarly, given *Z. marina*'s origin in the Pacific and more recent Pleistocene expansion into the Atlantic (Olsen *et al.* 2004), we might also generally expect Atlantic species to have colonized eelgrass from other Atlantic-native habitats, perhaps predisposing them to be less overdispersed in their traits as they cluster around a single mean. Consistent with this, we found that species in Atlantic sites were clustered around a smaller mean body size, which may be selected for by the denser eelgrass habitat in the Atlantic (Fig. A1.4, Fig. A3.2a; Bartholomew *et al.* 2000). Finally, gastropod relative abundance increases with latitude, and gastropods are a more abundant and speciose component of the epifaunal

community in the north Atlantic than in the Pacific (See Chapter 3). Competition with gastropods for epiphytes or other shared resources may push the peracarids there into a more constrained area of trait space, leading to the clustering we observed.

The precise impacts of these and other historical factors are difficult to quantify but may be further investigated with analyses of phylogenetic dispersion or more detailed studies of trait distributions in the regional species pool (Denelle *et al.* 2019; Skeels *et al.* 2020). However, we currently lack a phylogeny of peracarids with sufficient resolution and taxon sampling with which to evaluate underlying differences in phylogenetic diversity between the two ocean basins. We do note that richness of species, genera and families did not vary substantially between the ocean basins (Fig. A1.3).

One of the most striking results of our study was the positive effect of predation intensity on community dispersion among sites that was consistent in both oceans (Fig. 1.3a); peracarid species were more dissimilar in their traits than expected by chance in sites with high predation intensity. This effect appeared across trait sets, species pools, dispersion metrics and methods, although we rarely saw this signal at the level of individual traits (Table A3.1, Fig. A3.3). Changes in predator community structure, predation intensity, or both could lead to an increase in competition for predator-free space, an ecological selective filter that may result in overdispersion, particularly with respect to microhabitat and predator avoidance traits (Best & Stachowicz 2014). Herbivorous arthropods in both marine and terrestrial systems are known to select their microhabitat niches based largely on their effectiveness as shelter from predators rather than the availability or quality of food (Bernays & Graham 1988; Duffy & Hay 1991; Lasley-Rasher *et al.* 2011). Consequently, competition for enemy-free space can be an important factor structuring communities. Alternatively, predation could affect trait dispersion by reducing competition (Pianka 1966; Amundrud *et al.* 2015), but we would expect this to lead to an increase in dispersion from strongly clustered (SES < 0) to random communities (SES = 0) as stabilizing competition lessened, rather than the observed shift from clustered to overdispersed (SES > 0, Fig. 1.3a, Fig. A1.5b).

Latitudinal patterns of species interactions are now broadly appreciated (Schemske *et al.* 2009; Freestone & Osman 2011; Reynolds *et al.* 2018; Longo *et al.* 2019; Whalen *et al.* 2020; Zvereva & Kozlov 2021), but rarely are these results explicitly connected to variation in the structure of communities. By examining both how species interactions and environmental drivers

vary within a single habitat type across a broad geographic gradient, we demonstrate an important role for latitudinal variation in species interactions in driving patterns of community assembly. Diversity in important traits can increase the completeness with which epiphytes are removed, leading to increased seagrass growth (Duffy *et al.* 2003), an effect that is strongest in the presence of predators (Duffy *et al.* 2005). More generally, trait clustering and dispersion have implications for redundancy, stability, and ecosystem functioning (Cavender-Bares *et al.* 2009; Cadotte *et al.* 2011; Leibold *et al.* 2017). For instance, communities may be less resilient to environmental change if they are clustered by environmental filters (Cadotte *et al.* 2011, Rumm *et al.* 2018). Clustering that occurs as a result of equalizing mechanisms (*sensu* Chesson 2000) can weaken the relationship between diversity and ecosystem functioning, or certain ecosystem functions may be enhanced in communities with overdispersed effect traits, especially if diversity-function relationships arise through complementarity (Leibold *et al.* 2017; Thompson *et al.* 2020). Thus, historical contingency and broad-scale ecological drivers may play an important role in constraining not only the assembly of local communities, but the resulting trait diversity can affect the functioning of the entire ecosystem. This approach, if applied broadly, offers the potential for developing a predictive understanding of how entire communities respond to environmental change.

ACKNOWLEDGMENTS

We thank the many lab and field assistants that participated in this research and whose contributions of time and effort were invaluable for making this project happen. The manuscript was improved with comments from SP Lawler, ED Sanford, SY Strauss, and two anonymous referees. This research was funded by National Science Foundation grants to JED, JJS, and KAH (NSF-OCE 1336206, OCE 1336905, and OCE 1336741). CB was funded by the Åbo Akademi University Foundation.

REFERENCES

Amundrud, S. L., D. S. Srivastava, and M. I. O'Connor. 2015. Indirect effects of predators control herbivore richness and abundance in a benthic eelgrass (*Zostera marina*) mesograzer community. Journal of Animal Ecology 84:1092–1102.

Bartholomew, A., R. J. Diaz, and G. Cicchetti. 2000. New dimensionless indices of structural habitat complexity: predicted and actual effects on a predator[1]s foraging success. Marine Ecology Progress Series 206:45–58.

Bartoń, K. 2020, April 14. Multi-Model Inference. R.

Bernays, E., and M. Graham. 1988. On the evolution of host specificity in phytophagous arthropods. Ecology 69:886–892.

Best, R. J., N. C. Caulk, and J. J. Stachowicz. 2013. Trait vs. phylogenetic diversity as predictors of competition and community composition in herbivorous marine amphipods. Ecology Letters 16:72–80.

Best, R. J., and J. J. Stachowicz. 2014. Phenotypic and phylogenetic evidence for the role of food and habitat in the assembly of communities of marine amphipods. Ecology 95:775–786.

Cadotte, M. W., K. Carscadden, and N. Mirotchnick. 2011. Beyond species: functional diversity and the maintenance of ecological processes and services. Journal of Applied Ecology 48:1079–1087.

Cavender-Bares, J., K. H. Kozak, P. V. A. Fine, and S. W. Kembel. 2009. The merging of community ecology and phylogenetic biology. Ecology Letters 12:693–715.

Chaudhary, C., H. Saeedi, and M. J. Costello. 2017. Marine species richness is bimodal with latitude: a reply to Fernandez and Marques. Trends in Ecology & Evolution 32:234–237.

Chesson, P. 2000. Mechanisms of maintenance of species diversity. Annual Review of Ecology and Systematics 31:343–366.

Denelle, P., C. Violle, and F. Munoz. 2019. Distinguishing the signatures of local environmental filtering and regional trait range limits in the study of trait–environment relationships. Oikos 128:960–971.

Duffy, J. E., and M. E. Hay. 1991. Food and shelter as determinants of food choice by an herbivorous marine amphipod. Ecology 72:1286–1298.

Duffy, J. E., J. P. Richardson, and E. A. Canuel. 2003. Grazer diversity effects on ecosystem functioning in seagrass beds. Ecology Letters 6:637–645.

Duffy, J. E., J. P. Richardson, and K. E. France. 2005. Ecosystem consequences of diversity depend on food chain length in estuarine vegetation. Ecology Letters 8:301–309.

Dyer, L. A., and M. L. Forister. 2019. Challenges and advances in the study of latitudinal gradients in multitrophic interactions, with a focus on consumer specialization. Current Opinion in Insect Science 32:68–76.

Edgar, G. J. 1990. Population regulation, population dynamics and competition amongst mobile epifauna associated with seagrass. Journal of Experimental Marine Biology and Ecology 144:205–234.

Ford, B. M., and J. D. Roberts. 2018. Latitudinal gradients of dispersal and niche processes mediating neutral assembly of marine fish communities. Marine Biology 165:94.

Ford, B. M., and J. D. Roberts. 2019. Evolutionary histories impart structure into marine fish heterospecific co-occurrence networks. Global Ecology and Biogeography 28:1310–1324.

Fox, J., and S. Weisberg. 2019. An R companion to applied regression. Third edition. Sage, Thousand Oaks, CA.

Freestone, A. L., and R. W. Osman. 2011. Latitudinal variation in local interactions and regional enrichment shape patterns of marine community diversity. Ecology 92:208–217.

Garcia, H. E., R. A. Locarnini, T. P. Boyer, J. I. Antonov, M. M. Zweng, O. K. Baranova, and D. R. Johnson. 2010. World Ocean Atlas 2009, Volume 4: Nutrients (phosphate, nitrate, silicate). Page (S. Levitus, Ed.). U.S. Government Printing Office, Washington, D.C.

Green, E. P., and F. T. Short. 2003. World atlas of seagrasses. University of California Press, Berkeley, CA, USA.

den Hartog, C. 1970. The seagrasses of the world. North Holland Publishing Co., Amsterdam.

Hijmans, R. J., and J. van Etten. 2020, November 14. raster: geographic data analysis and modeling. R.

Jaramillo, E., J. E. Dugan, D. M. Hubbard, H. Contreras, C. Duarte, E. Acuña, and D. S. Schoeman. 2017. Macroscale patterns in body size of intertidal crustaceans provide insights on climate change effects. PLOS ONE 12:e0177116.

Kembel, S. W., P. D. Cowan, M. R. Helmus, W. K. Cornwell, H. Morlon, D. D. Ackerly, S. P. Blomberg, and C. O. Webb. 2010. Picante: R tools for integrating phylogenies and ecology. Bioinformatics 26:1463–1464.

Kraft, N. J. B., P. B. Adler, O. Godoy, E. C. James, S. Fuller, and J. M. Levine. 2015. Community assembly, coexistence and the environmental filtering metaphor. Functional Ecology 29:592–599.

Laliberté, É., P. Legendre, and B. Shipley. 2014, August 19. Measuring functional diversity (FD) from multiple traits, and other tools for functional ecology. R.

Lasley-Rasher, R. S., D. B. Rasher, Z. H. Marion, R. B. Taylor, and M. E. Hay. 2011. Predation constrains host choice for a marine mesograzer. Marine Ecology Progress Series 434:91–99.

Lavender, J. T., K. A. Dafforn, M. J. Bishop, and E. L. Johnston. 2017. An empirical examination of consumer effects across twenty degrees of latitude. Ecology 98:2391–2400.

Leibold, M. A., J. M. Chase, and S. K. M. Ernest. 2017. Community assembly and the functioning of ecosystems: how metacommunity processes alter ecosystems attributes. Ecology 98:909–919.

Longo, G. O., M. E. Hay, C. E. L. Ferreira, and S. R. Floeter. 2019. Trophic interactions across 61 degrees of latitude in the Western Atlantic. Global Ecology and Biogeography 28:107–117.

Martin, T. L., and R. B. Huey. 2008. Why "suboptimal" is optimal: Jensen's Inequality and ectotherm thermal preferences. The American Naturalist 171:E102–E118.

Mayfield, M. M., and J. M. Levine. 2010. Opposing effects of competitive exclusion on the phylogenetic structure of communities. Ecology Letters 13:1085–1093.

Mittelbach, G. G., and D. W. Schemske. 2015. Ecological and evolutionary perspectives on community assembly. Trends in Ecology & Evolution 30:241–247.

Olsen, J. L., W. T. Stam, J. A. Coyer, T. B. H. Reusch, M. Billingham, C. Boström, E. Calvert, H. Christie, S. Granger, R. L. Lumière, N. Milchakova, M.-P. Oudot-Le Secq, G. Procaccini, B. Sanjabi, E. Serrão, J. Veldsink, S. Widdicombe, and S. Wyllie-Echeverria. 2004. North Atlantic phylogeography and large-scale population differentiation of the seagrass Zostera marina L. Molecular Ecology 13:1923–1941.

Pavoine, S., and M. B. Bonsall. 2011. Measuring biodiversity to explain community assembly: a unified approach. Biological Reviews 86:792–812.

Pianka, E. R. 1966. Latitudinal gradients in species diversity: a review of concepts. The American Naturalist 100:33–46.

Poff, N. L. 1997. Landscape filters and species traits: towards mechanistic understanding and prediction in stream ecology. Journal of the North American Benthological Society 16:391–409.

R Development Core Team. 2022. R: a language and environment for statistical computing.

Reynolds, P. L., J. J. Stachowicz, K. Hovel, C. Boström, K. Boyer, M. Cusson, J. S. Eklöf, F. G. Engel, A. H. Engelen, B. K. Eriksson, F. J. Fodrie, J. N. Griffin, C. M. Hereu, M. Hori, T. C. Hanley, M. Ivanov, P. Jorgensen, C. Kruschel, K.-S. Lee, K. McGlathery, P.-O. Moksnes, M. Nakaoka, M. I. O'Connor, N. E. O'Connor, R. J. Orth, F. Rossi, J. Ruesink, E. E. Sotka, J. Thormar, F. Tomas, R. K. F. Unsworth, M. A. Whalen, and J. E. Duffy. 2018. Latitude, temperature, and habitat complexity predict predation pressure in eelgrass beds across the Northern Hemisphere. Ecology 99:29–35.

Roy, K., G. Hunt, D. Jablonski, A. Z. Krug, and J. W. Valentine. 2009. A macroevolutionary perspective on species range limits. Proceedings of the Royal Society B: Biological Sciences 276:1485–1493.

Rumm, A., F. Foeckler, F. Dziock, C. Ilg, M. Scholz, R. M. B. Harris, and M. Gerisch. 2018. Shifts in mollusc traits following floodplain reconnection: Testing the response of functional diversity components. Freshwater Biology 63:505–517.

Sainte-Marie, B. 1991. A review of the reproductive bionomics of aquatic gammaridean amphipods: variation of life history traits with latitude, depth, salinity and superfamily. Hydrobiologia 223:189–227.

Sanford, E., and M. Bertness. 2009. Latitudinal gradients in species interactions. Pages 357–391 *in* J. Witman and K. Roy, editors. Marine Macroecology. University of Chicago Press.

Schemske, D. W., G. G. Mittelbach, H. V. Cornell, J. M. Sobel, and K. Roy. 2009. Is there a latitudinal gradient in the importance of biotic interactions? Annual Review of Ecology, Evolution, and Systematics 40:245–269.

Sessa, E. B., S. M. Chambers, D. Li, L. Trotta, L. Endara, J. G. Burleigh, and B. Baiser. 2018. Community assembly of the ferns of Florida. American Journal of Botany 105:549–564.

Skeels, A., D. Esquerré, and M. Cardillo. 2020. Alternative pathways to diversity across ecologically distinct lizard radiations. Global Ecology and Biogeography 29:454–469.

Starko, S., K. W. Demes, C. J. Neufeld, and P. T. Martone. 2020. Convergent evolution of niche structure in Northeast Pacific kelp forests. Functional Ecology 34:2131–2146.

Swenson, N. G. 2014. Functional and Phylogenetic Ecology in R. Springer-Verlag, New York.

Thompson, P., M. Guzman, L. De Meester, Z. Horváth, R. Ptacnik, B. Vanschoenwinkel, D. Viana, and J. Chase. 2020. A process-based metacommunity framework linking local and regional scale community ecology. Ecology Letters 23.

Tyberghein, L., H. Verbruggen, K. Pauly, C. Troupin, F. Mineur, and O. D. Clerck. 2012. Bio-ORACLE: a global environmental dataset for marine species distribution modelling. Global Ecology and Biogeography 21:272–281.

Valentine, J. F., and J. E. Duffy. 2006. The Central Role of Grazing in Seagrass Ecology. Pages 463–501 *in* A. W. D. Larkum, R. J. Orth, and C. M. Duarte, editors. Seagrasses: biology, ecology and conservation. Springer Netherlands, Dordrecht.

Vasseur, D. A., J. P. DeLong, B. Gilbert, H. S. Greig, C. D. G. Harley, K. S. McCann, V. Savage, T. D. Tunney, and M. I. O'Connor. 2014. Increased temperature variation poses a greater risk to species than climate warming. Proceedings of the Royal Society B: Biological Sciences 281:20132612.

Vermeij, G. J. 1991. Anatomy of an invasion: the Trans-Arctic Interchange. Paleobiology 17:281–307.

Webb, C. O., D. D. Ackerly, M. A. McPeek, and M. J. Donoghue. 2002. Phylogenies and community ecology. Annual Review of Ecology and Systematics 33:475–505.

Whalen, M. A., R. D. B. Whippo, J. J. Stachowicz, P. H. York, E. Aiello, T. Alcoverro, A. H. Altieri, L. Benedetti-Cecchi, C. Bertolini, M. Bresch, F. Bulleri, P. E. Carnell, S. Cimon, R. M. Connolly, M. Cusson, M. S. Diskin, E. D'Souza, A. A. V. Flores, F. J. Fodrie, A. W. E. Galloway, L. C. Gaskins, O. J. Graham, T. C. Hanley, C. J. Henderson, C. M. Hereu, M. Hessing-Lewis, K. A. Hovel, B. B. Hughes, A. R. Hughes, K. M. Hultgren, H. Jänes, D. S. Janiak, L. N. Johnston, P. Jorgensen, B. P. Kelaher, C. Kruschel, B. S. Lanham, K.-S. Lee, J. S. Lefcheck, E. Lozano-Álvarez, P. I. Macreadie, Z. L. Monteith, N. E. O'Connor, A. D. Olds, J. K. O'Leary, C. J. Patrick, O. Pino, A. G. B. Poore, M. A. Rasheed, W. W. Raymond, K. Reiss, O. K. Rhoades, M. T. Robinson, P. G. Ross, F. Rossi, T. A. Schlacher, J. Seemann, B. R. Silliman, D. L. Smee, M. Thiel, R. K. F. Unsworth, B. I. van Tussenbroek, A. Vergés, M. E. Yeager, B. K. Yednock, S. L. Ziegler, and J. E. Duffy. 2020. Climate drives the geography of marine consumption by changing predator communities. Proceedings of the National Academy of Sciences 117:28160–28166.

Zvereva, E. L., and M. V. Kozlov. 2021. Latitudinal gradient in the intensity of biotic interactions in terrestrial ecosystems: sources of variation and differences from the diversity gradient revealed by meta-analysis. Ecology Letters 24:2506–2520.

Table 1.1. Traits used in analyses of ZEN peracarid communities. Full citations, as well as sources for individual species traits, are listed in Appendix 2.

Trait	Type	Values	Category	Interpretation	Citations
Maximum fecundity (number of eggs)	Ordered categorical	Very low (0 to <18), Low (18 to <31), Medium (31 to <65), High (65 to <135), Very high (>135)	Neither	Competitive ability, population resilience, population density	Sainte-Marie 1991, Best and Stachowicz 2013, Lefcheck and Duffy 2015, Ashford *et al.* 2018
Maximum adult length	Continuous	2-50 mm	Microhabitat	Susceptibility to predators, ability to occupy physical space	Sainte-Marie 1991, Best and Stachowicz 2013, Lefcheck and Duffy 2015, Ashford *et al.* 2018
Body shape	Categorical	Laterally compressed, Dorsoventrally compressed, Vermiform	Microhabitat	Ability to occupy physical space, palatability	Lefcheck and Duffy 2015
Living habit	Categorical	Free, Parasite/direct commensal, Tube/burrow dweller	Microhabitat	Degree of substrate association, substrate type, population density	Best and Stachowicz 2013, Ashford *et al.* 2018
Motility	Categorical	Swimmer, Crawler	Microhabitat	Susceptibility to predators, dispersal ability, degree of substrate association	Lefcheck and Duffy 2015, Ashford *et al.* 2018
Bioturbator?	Binary		Microhabitat	Degree of substrate association, substrate type	Ashford *et al.* 2018
Microalgae feeding	Binary		Diet	Dietary niche partitioning	Duffy and Harvilicz 2001, Best and Stachowicz 2012, 2013
Macroalgae feeding	Binary		Diet		
Seagrass feeding	Binary		Diet		
Seagrass detritus feeding	Binary		Diet		
Suspension feeding	Binary		Diet		
Detritivory, deposit feeding	Binary		Diet		

Carnivory, parasitism, scavenging	Binary	Diet

Table 1.2. A priori models used to analyse site-level SES values. These 16 models were separately applied to 33 sets of SES values for different trait distance metrics, permutation algorithms, species pools, and trait sets, for a total of 528 models.

Model name	Predictors				
Biogeography 1	Latitude				
Biogeography 2	Latitude	Continental Margin	Ocean		
Biogeography 3	Latitude	Continental Margin	Latitude × Continental Margin		
Biogeography 4	Latitude	Continental Margin	Ocean	Latitude × Continental Margin	
Biogeography 5	Latitude	Continental Margin	Ocean	Latitude × Continental Margin	Latitude × Ocean
Abiotic Environment	in-situ Temperature	in-situ Salinity	Mean Leaf % N		
Temperature Regime 1	Mean SST				
Temperature Regime 2	SST Range				
Temperature Regime 3	Mean SST	SST Range	Mean SST × SST Range		
Community	log(Mean Standard Total Crustacean Abundance)	Median Crustacean Size			
Total Biodiversity	log(Site Epifaunal Richness)				
Peracarid Biodiversity	log(Site Peracarid Richness)				
Habitat	PC1	PC2	log(Macroalgal Biomass + 1)		
Predation	arcsin(Mean Amphipod Predation)				
Resource 1	log(Mean Epiphyte load)	log(Mean Chl a)			
Resource 2	$\sqrt{NO_2}$	Mean PAR			

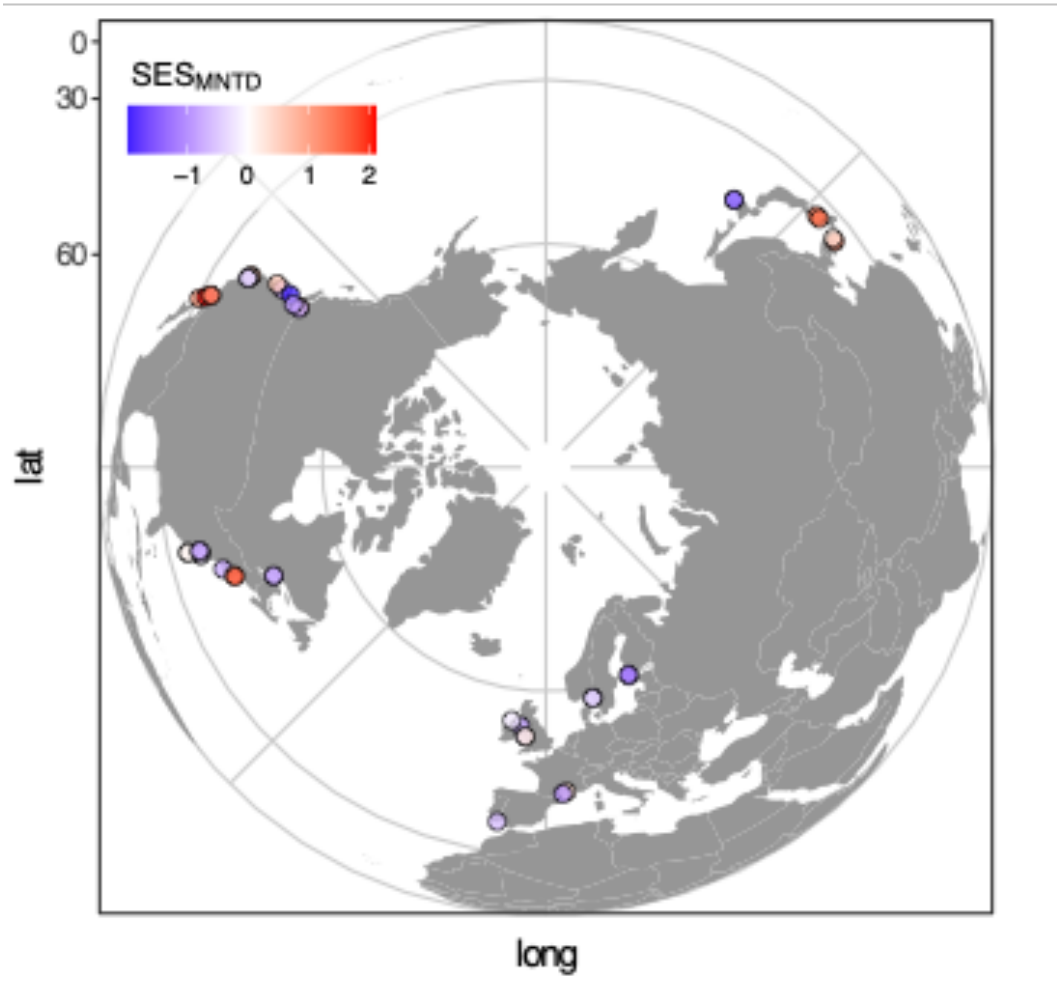

Figure 1.1. *Zostera* Experimental Network (ZEN) sites used in our analyses. Sites spanned 30º of latitude on the Pacific and Atlantic coasts of North America and Eurasia, including the Baltic and Mediterranean seas, covering most of the range of *Zostera marina* (eelgrass). Colors indicate trait dispersion (SES_{MNTD} calculated using the tip shuffle algorithm); positive values of SES_{MNTD} indicate greater dispersion in traits than expected from a random draw from the global species pool, whereas negative values of SES_{MNTD} indicate clustering in traits relative to a random draw. See Fig. A1.1 for more detailed information about site locations.

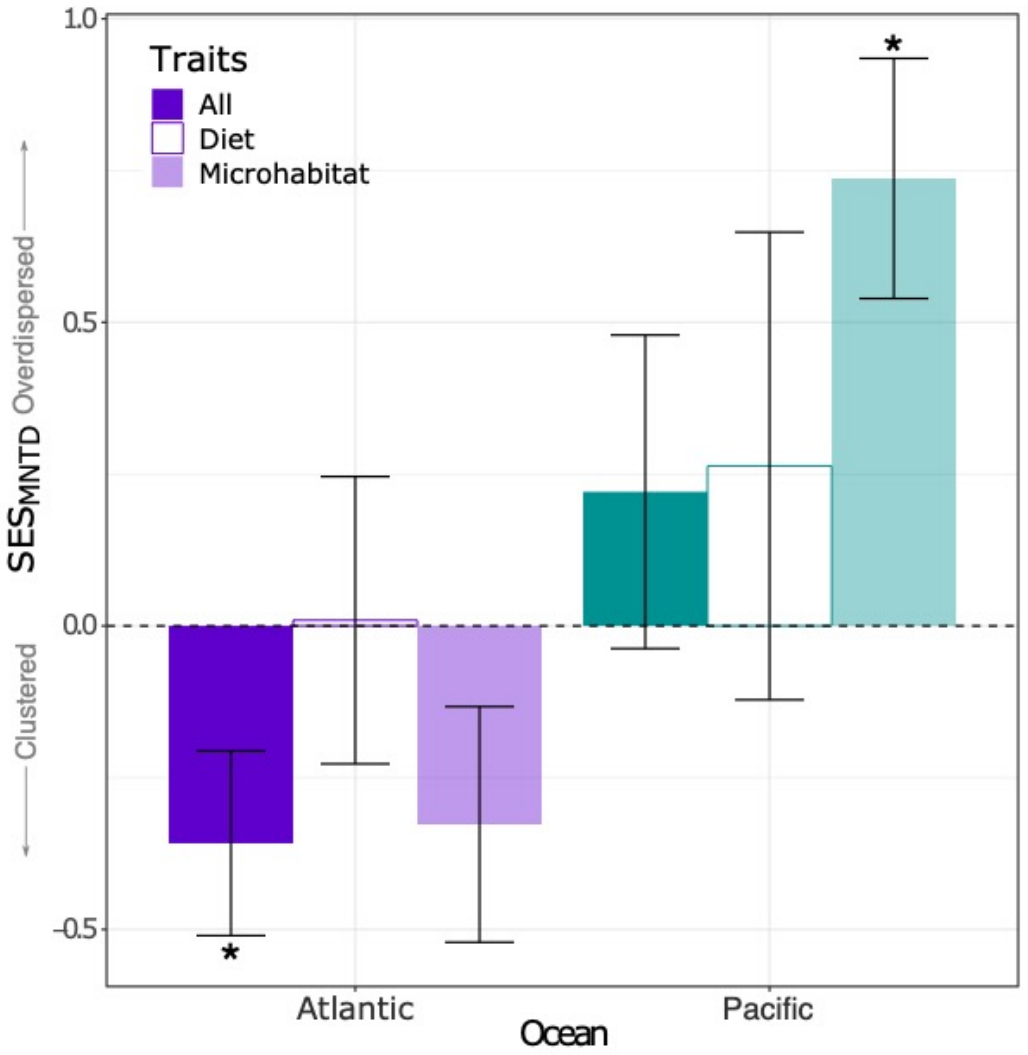

Figure 1.2. Trait dispersion (SES_{MNTD}) in eelgrass-associated peracarid crustacean communities across trait sets. In general, communities at sites in the Pacific Ocean were more overdispersed, while communities at Atlantic sites were less dispersed than expected. The dashed horizontal line represents an SES_{MNTD} value of 0, indicating random assembly. Asterisks indicate means significantly different from zero (two-tailed one-sample t tests; see table A1.1); error bars represent standard errors. Figure shows SES_{MNTD} calculated according to the Tip Shuffle permutation algorithm; results were comparable across permutation algorithms and SES values.

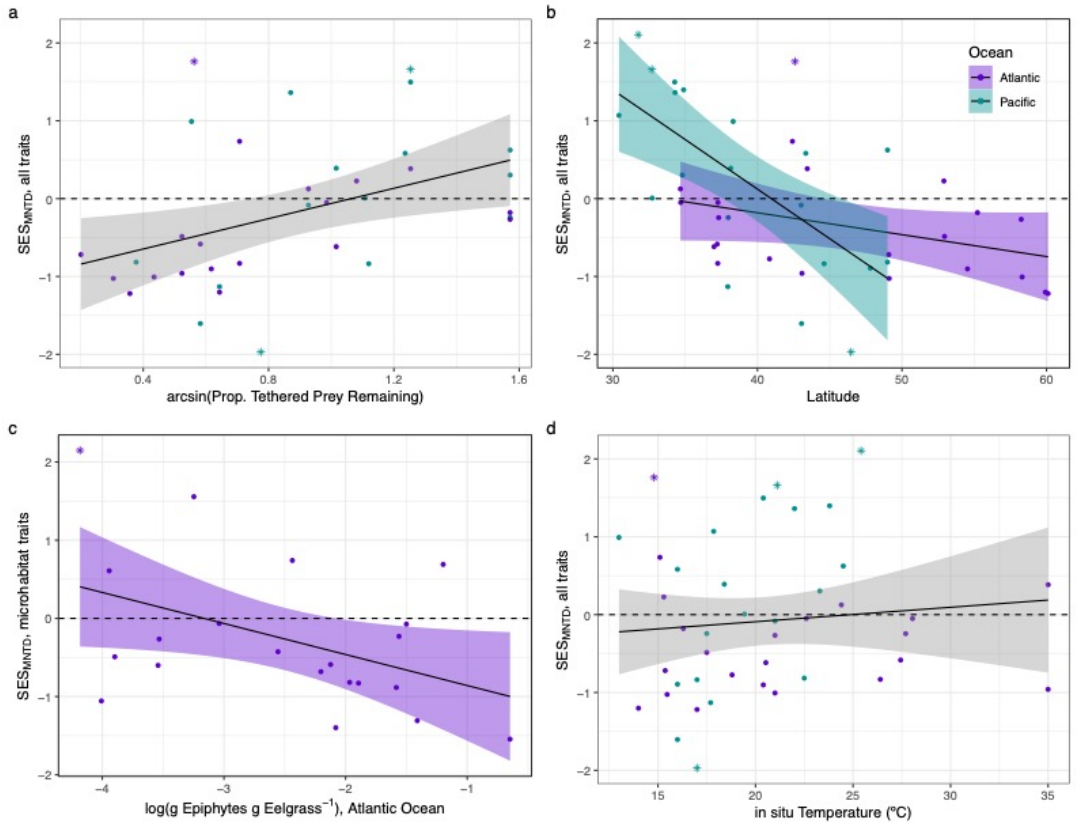

Figure 1.3. The effects of predation (a), latitude (b), epiphyte load (c), and in-situ temperature (d) on trait dispersion (SES_{MNTD} using the tip shuffle algorithm) in univariate analyses. In all of the best models of dispersion, sites with higher predation intensity had more overdispersed communities, while those with lower predation intensity had more clustered communities (a; $R^2 = 0.15$, $p = 0.012$). In the best models that had a non-zero latitude effect, sites at lower latitudes had more overdispersed communities, while those at higher latitudes had more clustered communities. This effect was stronger in the Pacific than the Atlantic species pool (b; $R^2 = 0.36$, interaction $p = 0.0076$). In the best models with a non-zero epiphyte effect, sites where eelgrass had lower epiphyte density had more overdispersed communities, while sites with more heavily fouled blades had clustered communities (c; plot shows SES_{MNTD} for microhabitat traits in the Atlantic species pool; $R^2 = 0.15$, $p = 0.046$). In-situ temperature appeared only sporadically across permutations and dispersion metrics, and was not significant for total trait dispersion ($R^2 = 0.0094$, $p = 0.54$). The dashed horizontal line represents an SES value of 0, indicating random assembly; sites in bold italics are those for which SES is significantly different from 0 at $\alpha = 0.05$.

CHAPTER 2: Extending trait dispersion across trophic levels: functionally diverse predator assemblages act as top-down filters on prey community traits

ABSTRACT

Studies of community assembly typically focus on the effects of abiotic environmental filters and stabilizing competition on functional trait dispersion within single trophic levels. Predation is a well-known driver of trait distributions within communities, but the role of functionally diverse predator communities in filtering prey community traits has received less attention. We examined functionally diverse communities of predators (fishes) and prey (epifaunal crustaceans) in eelgrass (*Zostera marina*) beds in two Northern California estuaries to evaluate the filtering effects of predator traits on community assembly, and how filters acting on predators influence their ability to mediate prey community assembly. Fish traits related to prey detection and capture selected for more overdispersed epifauna communities, particularly with respect to body size and activity level, suggesting that prey may be pushed to disparate areas of trait space to avoid consistent detection by predators across the community. We also found correlations between the trait dispersions of predator and prey communities that strengthened after accounting for the effects of habitat filters on predator dispersion, suggesting that habitat filtering effects on predator species pools may hinder their ability to affect prey community assembly. Our results present compelling observational evidence that specific predator traits have measurable impacts on the community assembly of prey, inviting experimental tests of predator trait means on community assembly, and explicit comparisons of how the relative effects of habitat filters and intraguild competition on predators impact their ability to affect prey community assembly. Integrating our understanding of traits at multiple trophic levels can help us better predict the impacts of community composition on food web dynamics as regional species pools shift with climate change and anthropogenic introductions.

INTRODUCTION

One of the key goals of community ecology is to understand the mechanisms by which communities assemble from a regional species pool (Poff 1997, Thompson et al. 2020). Ecological filters such as temperature, habitat structure, and interspecific competition exert selective pressures in multiple different directions on the species pool. Because species' traits are what allow them to pass through these filters, studying the distribution of traits within the community provides insight into how filters have acted on the species pool. Strong

environmental filters (i.e., abiotic filters *sensu* Kraft *et al.* 2015) such as climate are thought to act on large spatial scales to constrain trait diversity such that species are more alike (clustered) in traits that respond to these factors than would be expected under a purely random assembly process (Webb et al. 2002, Cavender-Bares et al. 2009, Starko et al. 2020, Thompson et al. 2020). Biotic filters, such as competition, act at smaller spatial scales to enhance or reduce trait diversity among species with broadly similar abiotic tolerances, depending on which traits are affected (Mayfield and Levine 2010). When traits related to the acquisition of distinct resources are considered, competition for these resources drives the distribution of traits to be wider than expected by chance (overdispersed) as there are multiple resource niche optima that can be occupied (Webb et al. 2002, Cavender-Bares et al. 2009, Pavoine and Bonsall 2011). In contrast, competition for a single limiting resource can also act as a filter, selecting for traits related to resource acquisition to converge around an optimal value as species deviating from the optimum are competitively excluded (Mayfield and Levine 2010).

To the extent that traits are phylogenetically conserved, phylogenetic diversity may provide an integrated picture of functional distinctiveness across many traits, and might thus provide a proxy for ecological differences between species (Webb et al. 2002, Swenson et al. 2006, Cavender-Bares et al. 2009, Cadotte et al. 2017). However, the extent to which this assumption holds depends on the degree of trait convergence between distantly related taxa, intraspecific trait variation due to plasticity or adaptation, the species used to build the reference phylogeny, and other factors (Cadotte et al. 2017, Tucker et al. 2018). Nevertheless, the distribution of phylogenetic and functional trait distances among species in a community may reveal patterns in community functional or phylogenetic structure that allow us to draw inferences about the processes that determine community composition in nature.

The assumption that limiting similarity and environmental filters are the two main opposing forces in community assembly that lead to either overdispersion or clustering, respectively (Kraft et al. 2015, Cadotte et al. 2017) is pervasive, despite nuances in the effects of different filters on the functional (and phylogenetic) structure of communities. Less attention has been paid to other possible selective filters, such as predation. Yet predators are widely known to govern community structure, species coexistence, and even adaptive divergence among prey species (McPeek 1995, Vamosi 2005) by both consumptive and nonconsumptive effects (Paine 1966, Sommers and Chesson 2019, Dellinger et al. 2022). For example, predators affect prey

behavior and habitat use, and may determine which prey traits are important for facilitating prey coexistence. In the presence of predators, competition for enemy-free space may drive community assembly and promote divergence in microhabitat use (Best and Stachowicz 2014, Lürig et al. 2016, Gross et al. 2022), while in predator-free environments, prey may compete more for food (Best et al. 2013, Beermann et al. 2018). Predator traits may influence prey coexistence and community assembly by selecting for prey with traits that aid in predator evasion (McPeek 1995, Schmid et al. 2019), or by reducing the abundance of a dominant competitor (Paine 1966).

Despite the wealth of knowledge of how predators influence prey community structure, studies of functional and phylogenetic diversity and community assembly rarely examine the potential role of speciose predator communities in producing these patterns, both in terms of their traits and how those traits are distributed among predator species in the community. Instead, studies typically focus on one or two predator species or morphotypes (Post et al. 2008, Holdridge et al. 2017, Schmid et al. 2019) or coarse measures of community-level predation intensity without directly investigating the predator community itself (Palkovacs et al. 2009, Gross et al. 2022). Yet predators and their prey are affected by broader ecological filters, and the influences of predator selection on prey communities may carry the fingerprints of of environmental filters, competition, or other factors that limit the suite of predator traits that can act to filter prey (Chang et al. 2021; Fig. 2.1a).

Looking specifically at the role that community-wide predator trait distributions might play in structuring prey communities, four general patterns of dispersion can be considered between guilds (Fig. 2.1b). First, an overdispersed predator community may lead to an overdispersed prey community, as a wide range of predator feeding modes may prevent the dominance of a single set of prey traits. Second, an overdispersed predator community may lead to a clustered prey community if diffuse pressure from predator traits in all directions pushes prey into a single refuge in trait space (Sih et al. 1998). Third, a clustered predator community might be associated with a clustered prey community, either because they respond to the same environmental filters, or because prey are forced into a single trait space that reduces their predation risk outside the range of predator traits. Finally, a clustered predator community might be associated with an overdispersed prey community if prey reduce their competition for enemy-free space by moving into different niches that are inaccessible to predators.

We investigated patterns of clustering and overdispersion in communities of mesopredatory fishes and their epifaunal invertebrate mesograzer prey found in eelgrass (*Zostera marina*) beds of northern California, USA. We addressed two major questions: (1) Does the trait composition of fish communities act as a selective filter to affect epifaunal community assembly? and (2) How do ecological filters acting on fishes affect the direction and magnitude of their selective pressure on the epifaunal species pool? We specifically chose to focus on peracarid crustaceans (amphipods, isopods, and tanaids), because they are the most widespread, abundant, and speciose mesograzer taxon in these eelgrass beds (Ha and Williams 2018, Gross et al. 2022), are monophyletic, and are more susceptible to predation than other taxa such as gastropods (Reynolds et al. 2018), increasing the likelihood that predation and predators will act as filters. Understanding the effect of fish traits and trait distributions on peracarid traits and trait distributions is particularly interesting in seagrass beds, unique among marine benthic habitats in that mesograzers typically feed on fouling epiphytic algae, rather than on the seagrass tissue itself (Jernakoff et al. 1996, Valentine and Duffy 2006). The "mutualistic mesograzer model" (Reynolds et al. 2014) predicts that increased secondary consumption by mesopredators will indirectly harm the seagrass by decreasing the numbers of epiphyte-removing mesograzers, increasing competition between seagrass and epiphytes for light (Jackson et al. 2001, Estes et al. 2011). However, in communities of epiphyte grazers, relative abundances, interspecific variation in epiphyte feeding rates, and differences in mesopredator susceptibility due to predator-prey trait matching or mismatching may lead to idiosyncratic outcomes from experimental trophic cascades (Best and Stachowicz 2012). In light of these studies and others in which variation in predator traits leads to differences in prey community structure and alters trophic cascades (Post et al. 2008, Schmid et al. 2019), it is likely that the traits of both mesograzers and the predators that feed on them can have dramatic impacts on the strength and outcome of trophic cascades in eelgrass.

METHODS

Study sites and sampling. In the summers of 2019 and 2021, we sampled three eelgrass beds each in Bodega Harbor (38°19'N 123°03'W) and Tomales Bay (38°09'N 122°54'W), or a total of 12 site-by-year samples across both estuaries. Bodega Harbor is a small (approximately 5 km^2) shallow bar-enclosed embayment characterized by extensive mudflats (Abbott et al. 2018), while Tomales Bay is a long (16 km) and narrow (2 km) drowned river estuary characterized by

strong environmental gradients (Cheng and Grosholz 2016, DuBois et al. 2022). We chose eelgrass beds across gradients of temperature and water residence time in each estuary.

We sampled fishes in 6 sets of a custom beach seine net when the water level was at or below 1 m above the seafloor. The seine sampled a circular area of 11 m^2. We counted, identified to the lowest possible taxonomic level (typically species), and released animals retained in the seine. We additionally grouped some species into discrete size classes (large or small, Table A4.2) based on earlier seining efforts (C.P. Gross, unpublished), keeping in mind that allometric growth may lead to ontogenetic differences in morphometric traits (Karachle et al. 2012). We retained two individuals of each species and size class from each estuary (in 2019) or each site (in 2021) to be euthanized for morphometric analyses. To get our final list of fish species and size classes, we removed singletons, species that only occurred in a single site-year combination, and species with 4 or fewer individuals across the entire dataset (Table A4.1).

At each site, we collected peracarid crustaceans and other epifauna along six 20-meter transects. Three transects were parallel to the shoreline at shallow subtidal elevations in the eelgrass, while three were parallel to these at a higher intertidal elevation in the same grass bed. At 4 and 16 meters along each transect, we collected each epifaunal sample by everting an open-mouth drawstring mesh bag (500 μm mesh size) over a clump of shoots in the eelgrass bed so that the mouth of the bag was flush with the sediment surface. We then severed the shoots where they emerged from the sediment and closed the drawstring to capture shoots, macroalgae, and associated animals. We transferred the shoots to the laboratory on ice, rinsed and hand-inspected them to dislodge the epifauna, which we then passed through a 500 μm sieve and ultimately transferred into 70% ethanol. We then identified epifauna to the lowest possible taxonomic level (typically species), and removed singletons and species that only occurred in one site-year combination. We standardized epifaunal abundance by the total aboveground biomass of macrophytes in the sample from which they were collected (Appendix Table A4.5).

In addition to sampling fishes and epifauna, we also collected data on total eelgrass shoot density m^{-2}, flowering shoot density m^{-2}, percent cover, canopy height, and epiphyte dry weight mm^{-2} eelgrass as described by Aoki et al. (2022). We also measured mean in-situ summer temperatures by averaging hourly temperatures at the upper (intertidal) transect level between June and August as recorded by HOBO MX 2201 pendant temperature loggers (Onset). We also

quantified macroalgal abundance in each site-by-year sample as the total macroalgal wet mass collected in epifaunal grab samples.

Traits and phylogeny. For the 23 most abundant species of peracarids in our surveys, we assigned values for 11 traits putatively related to predator avoidance and microhabitat niche. We collected three of these traits (maximum body size, shape, and living habit) from the literature. We determined the tube fidelity for each species according to observations of living and preserved specimens along a four-point ordered scale as follows: none (species lacks silk glands to build tubes), low (species has silk glands but was never observed in a tube alive or preserved in ethanol), medium (species has silk glands and was observed in tubes when alive but readily flees tube when exposed to ethanol), and high (species has silk glands, is tubicolous when alive, and is regularly found inside tubes after preservation in ethanol). We measured mean body size (length from rostrum to telson), relative eye diameter, and relative antenna lengths from 10-20 preserved individuals collected across sites and years. We measured activity levels as fractions of time spent swimming, walking, and still (unmoving) from one-minute video recordings of 10-20 live individuals per species across sites and years. We log-transformed peracarid traits where appropriate to conform to a normal distribution. A more detailed discussion of peracarid traits including how we defined and measured each, any transformations prior to analysis, and mean values for each species is included in Appendix 4 (Table A4.6, Table A4.7, Fig. A4.3).

We assigned two categorical (vertical position and foraging mode) and one continuous trait (trophic level) to the 16 most abundant fishes based on the literature. We fuzzy-coded vertical position and foraging mode among 5 and 3 levels, respectively, to accommodate species that could be classified among multiple levels (Ashford et al. 2018). We collected linear morphometric measurements of fishes (body and head dimensions, fin lengths, eye size and position, and mouth height and protrusion) from 2-26 specimens per species and size class collected from seines as described above, and standardized them for ease of comparison across species. We log-transformed fish traits where appropriate to conform to a normal distribution. We also used principal component analysis (PCA) to condense variation among fish species' linear morphometric traits into 16 axes, the first three of which explained 66% of variation among species (Fig. A4.2). Detailed discussion of fish traits, including how each was defined and measured, any transformations prior to analysis, and mean values for each species, is included in Appendix 4 (Table A4.3, Table A4.4, Fig. A4.1).

To address the potential effects of evolutionary history on peracarid community responses to predators, we built a phylogeny of our species by subsetting from the peracarid supertree published by Ashford et al. (2018). Species in our dataset that were not included in the supertree were substituted in for congeners or closely-related confamilials.

Community dispersion. Hereafter, "community" refers to the sum of individual fishes from 6 seines or peracarids from 12 grab samples for each of the 12 site-by-year combinations. For peracarids, we used the trait dataset to create a matrix of weighted Gower distances, which incorporate both continuous and categorical variables, between species using the gawdis package in R (de Bello et al. 2021). This method iteratively assigns weights to traits that ensure the equal contribution of each trait to the mean Gower distances between taxa, and accounts for correlations between traits by grouping them so that the group as a whole contributes equally to the mean Gower distances rather than the individual elements of the group. We grouped tube fidelity and living habit a priori, because species for which living habit was anything other than "tubicolous" automatically was assigned a tube fidelity of "none." We also calculated Gower distances between species for their individual traits to pinpoint which community trait distributions may be subject to top-down control by the predator community.

For fishes, we calculated overall Gower distances by averaging weighted Gower distances based on fuzzy-coded traits (foraging mode and vertical position) and continuous traits (linear morphometric measurements and trophic level, with correlated modules grouped based on Pearson correlation coefficients greater than 0.6) calculated separately. Correlated continuous trait modules were dorsal fin length, anal fin length, and caudal peduncle length; eye diameter and body depth; and mouth height, pectoral fin length, and caudal fin length. To examine how specific fish traits in the community might exert differential selective pressures on peracarid communities, we also calculated the community-weighted mean value of each fish trait and PC axis for each community.

We measured the trait distance between species within peracarids and within fishes as the Mean Pairwise Distance (MPD) and Mean Nearest Taxon Distance (MNTD; Webb et al. 2002, Sessa et al. 2018). MPD is the average of the trait distances between all pairs of species found within a given community, while MNTD is the average minimum distance between species pairs in a community. Both are independent of species richness, but the two metrics can behave differently depending on the clustering of species in trait space within a community (Sessa et al.

2018). For peracarids, we also calculated MPD and MNTD for phylogenetic distances within each community, based on total branch length within the subset of the phylogeny contained in each community.

To determine whether the traits of observed species in each community differed from those expected by chance (fishes and peracarids) or phylogenetic relationships (peracarids), we standardized MPD and MNTD against null distributions generated according to two permutation algorithms. The first, independent swap, is a semi-constrained model that randomly re-assembles the community-by-species matrix while maintaining the species richness of each community and the presence/absence of each species across communities. The second, tip shuffle, is a more constrained model that directly shuffles the traits of the species in the community while maintaining richness, occurrence, and trait distances between community members, effectively moving the tip labels on a trait dendrogram or phylogeny. Imposing more constraints on permutation controls for patterns in the data that are not directly relevant to the question at hand, such as species richness, occurrence, or identity, which ultimately reduces type I error rates (Swenson 2014). We completed each permutation 999 times for each community, and generated null distributions of MPD and MNTD based on values calculated from randomized communities.

We then compared each observed value of community trait distance to the corresponding null distribution by calculating the standard effect size (SES_{MPD} or SES_{MNTD}). A positive value of SES indicates that the observed community trait distance (as measured by MPD or MNTD) is greater than the null mean, meaning that community members are more dissimilar than expected under a random draw (overdispersion), while a negative SES indicates that trait distance is less than the null mean, meaning that community members are more similar to each other than expected under a random draw (clustering). We calculated MPD, MNTD, null distributions and SES values using the picante package in R (Kembel et al. 2010).

Data analyses. To estimate the overall influence of multivariate habitat and fish community structure on peracarid traits and phylogenetic relationships, we used Mantel tests. Using matrices of habitat differences between communities and fish trait differences between communities, we modeled peracarid trait and phylogenetic distances between communities. We also conducted partial Mantel tests, which accounted for variation in habitat distances between communities when modeling the relationship between fish community trait distances and peracarid community trait and phylogenetic distances.

To account for the background effects of habitat filters that may mask the direct filtering effects of fishes on peracarid communities, we focused on the residuals of overall peracarid trait and phylogenetic dispersion from multiple regression against our habitat variables as response variables in linear models with community-weighted mean fish trait values as predictors. Aware of the possibility of temporal autocorrelation between years within sites, we examined correlations between site-level dispersion in both years, but found no significant correlations. We thus continued our analyses using each community as an independent observation. We conducted these analyses twice: once using community-weighted mean PC scores as predictors (16 tests), and once more using individual fish trait means (19 tests). We felt it important to examine all PC axes as predictors in order to capture potential "keystone" traits that explain a small percentage of morphological variation in the species pool but disproportionately affect prey community composition. To account for multiple comparisons, we applied Bonferroni corrections and compared our statistical results to α levels of 0.00313 (PC scores) and 0.00263 (individual traits). Based on these initial analyses, we performed post-hoc tests of relationships between residual SES for individual peracarid traits and fish mean PC8 scores (positively associated with anal fin length, eye position, and mouth protrusion), PC16 scores (positively associated with eye diameter, eye position, and pectoral fin length; hereafter "eye index"), and body depth below midline (BDBM) values. To account for multiple comparisons across 11 peracarid traits we applied a Bonferroni correction and compared our statistical results to an α level of 0.00455. We then measured the phylogenetic signal of peracarid traits that exhibited significant responses to fish traits as Blomberg's K and Pagel's λ to understand how individual traits might drive the response of peracarid phylogenetic dispersion to fish traits (Best and Stachowicz 2013).

To examine the indirect effects of filters on peracarids mediated through fish traits, we modeled residual peracarid SES as a function of fish SES. This time we focused on total fish trait dispersion, PC8 dispersion, eye index dispersion, and BDBM dispersion as predictors; and total peracarid trait dispersion, phylogenetic dispersion, maximum body size dispersion, antenna length 1 and 2 dispersion, and activity level dispersion (measured as percent still) as response variables based on results from our first set of analyses. We repeated these analyses twice: once with unaltered values of fish trait dispersion to accommodate habitat variables that might be affecting fish dispersion, and once more using residual values of fish dispersion regressed against habitat variables to focus on intraguild competition or other filtering processes acting on fish

communities. Statistical results were compared to an α level of 0.0083 to account for 6 types of peracarid dispersion as response variables. All statistical analyses were conducted in R v.4.2.2 (R Development Core Team 2022).

RESULTS

Across both years and all six sites, we found a total of 35 fish species and 28 peracarid species, of which 16 and 23 species were retained in our analyses, respectively. The epifaunal community overall was dominated by peracarids, making up 87% of individual epifauna across both estuaries and years. The most speciose peracarid community in our dataset had 18 species, while the most speciose fish community had 13 species. Four fish species (*Cymatogaster aggregata, Gasterosteus aculeatus, Porichthys notatus,* and *Sebastes carnatus*) were present in two discrete size cohorts; we considered each of these cohorts as a different predator type.

Habitat differences across communities explained variation in peracarid trait structure (Mantel $r = 0.270$, $p = 0.044$), but did not explain phylogenetic structure across communities. Fish taxonomic and trait structure did not have any significant effects on any aspect of peracarid community structure both when accounting for habitat variation and not.

However, dispersion in the trait and phylogenetic distribution of peracarid communities was strongly correlated with both mean state and dispersion in the traits of the fish assemblage. Patterns and predictors of peracarid trait and phylogenetic dispersion were robust across SES metrics and permutation algorithms; here we present and interpret the results of modeling fish trait effects on SES_{MNTD} calculated using the tip shuffle algorithm, with exceptions presented where relevant. Detailed results using other metrics and permutation algorithms are presented in Tables A4.1-A4.3. Of the community-weighted mean predator traits that we modeled as predictors of residual prey community dispersion, only one – PC axis 16 of fish morphology (eye index) – emerged as a strong predictor of both trait ($R^2 = 0.657$, $p < 0.001$; Fig. 2.2a) and phylogenetic dispersion ($R^2 = 0.826$, $p < 0.001$; Fig. 2.2b). This axis ranges from fishes with relatively large eyes located high up on the head (positive values) to fishes with small eyes located relatively low on the head (negative values). This index was positively correlated with peracarid trait dispersion; fish communities with larger average eye indices co-occurred with more overdispersed peracarid communities. For phylogenetic dispersion, we additionally observed a strong positive correlation between community-weighted fish PC8 score and dispersion (longer anal fins, higher eye position, and less protrusive jaws; $R^2 = 0.590$, $p =$

0.0022; Fig. 2.3a), and a strong negative correlation between community weighted fish body depth below midline (BDBM) and dispersion ($R^2 = 0.671$, $p < 0.001$; Fig. 2.3b).

No individual peracarid trait showed a significant response to these mean predator traits, but we did observe trends towards increased dispersion of maximum body size ($R^2 = 0.381$, $p = 0.019$), antenna 1 length ($R^2 = 0.419$, $p = 0.0136$), and activity level (measured as % still; $R^2 = 0.300$, $p = 0.0380$) with increasing mean eye index (Fig. 2.2c, d, f), and decreased dispersion of antenna 2 length with increasing mean eye index ($R^2 = 0.361$, $p = 0.0228$; Fig. 2e). Dispersion of antenna 1 length also increased with increasing mean PC8 score ($R^2 = 0.307$, $p = 0.0359$; Fig. 2.3c); decreased dispersion of maximum body size ($R^2 = 0.308$, $p = 0.0356$; Fig. 2.3d) and antenna 1 length ($R^2 = 0.352$, $p = 0.0247$; Fig. 2.3e) with mean BDBM; and increased dispersion of antenna 2 length with mean BDBM ($R^2 = 0.303$, $p = 0.0372$; Fig. 2.3f). Where peracarids were clustered for particular traits, there was no apparent consistency in the mean trait value across communities (Fig. 2.2c-f, Fig. 2.3c-f). Both antenna lengths showed significant phylogenetic signal (antenna 1: $K = 1.88$, $p = 0.001$; $\lambda = 0.946$, $p < 0.001$; antenna 2: $K = 0.960$, $p = 0.024$; $\lambda = 1.00$, $p = 0.0493$).

To examine the potential indirect effects of habitat filters on peracarid communities via fishes, we used fish community dispersion – due to habitat filters and other factors – as predictors of peracarid community dispersion. Surprisingly, total fish trait dispersion and dispersion along PC8 and eye index had no significant relationships with peracarid residual trait dispersion, phylogenetic dispersion, or the dispersion of any one trait in the community. In contrast, dispersion of fish BDBM was strongly negatively correlated with peracarid trait dispersion (Fig. 2.4a; $R^2 = 0.549$, $p = 0.00355$), phylogenetic (Fig. 2.4c; $R^2 = 0.726$, $p < 0.001$), maximum body size (Fig. 2.4d; $R^2 = 0.463$, $p = 0.00889$), and antenna 1 length dispersion (Fig. 2.4g; $R^2 = 0.0107$, $p = 0.0107$). We also saw negative relationships between fish BDBM dispersion and dispersion of peracarid activity level (% still), but only when peracarid dispersion was measured as SES_{MPD} (Table A5.2). In other words, fish communities that were more clustered, particularly with less body depth below midline (Fig. 2.4), co-occurred with peracarid communities that were more overdispersed.

Examining the residual dispersion of fish communities as a predictor of peracarid dispersion allowed us to focus on potential fish-mediated indirect effects on peracarid communities. Controlling for habitat filtering of fish communities strengthened the relationships

between fish BDBM dispersion and peracarid dispersion for all traits (Fig. 2.4b; $R^2 = 0.732$, $p < 0.001$), phylogeny (Fig. 2.4d; $R^2 = 0.960$, $p < 0.001$), body size (Fig. 2.4f; $R^2 = 0.622$, $p = 0.0014$), and antenna 1 length (Fig. 2.4h; $R^2 = 0.598$, $p = 0.00194$). These analyses also revealed positive effects of fish trait dispersion on peracarid phylogenetic dispersion (Fig. 2.5c; Fig. $R^2 = 0.537$, $p = 0.00406$), maximum body size dispersion (Fig. 2.5e; $R^2 = 0.603$, $p = 0.0018$), and antenna 1 length dispersion (Fig. 2.5g; $R^2 = 0.883$, $p < 0.001$), and a nonsignificant but notable positive effect of fish trait dispersion on peracarid trait dispersion (Fig. 2.5a; $R^2 = 0.302$, $p = 0.0374$). That is, fish communities that were more overdispersed in their traits co-occurred with peracarid communities that were more overdispersed with respect to traits and phylogeny, even after accounting for habitat effects. Residual fish PC8 dispersion exhibited strong negative relationships with residual trait (Fig. 2.5b; $R^2 = 0.570$, $p = 0.00274$), phylogenetic (Fig. 2.5d; $R^2 = 0.927$, $p < 0.001$) and body size dispersion (Fig. 2.5f; $R^2 = 0.712$, $p < 0.001$), and a nonsignificant but notable negative relationship with antenna 1 length dispersion (Fig. 2.5h; $R^2 = 0.336$, $p = 0.0283$) that was significant when other methods of calculating fish and peracarid dispersion were applied (Table A5.3). In particular, fish communities clustered around higher average PC8 scores tended to select for more overdispersed peracarid communities. The effect of eye index dispersion was largely dependent on the method used to calculate it. Eye index SES_{MNTD} had no significant effect when calculated with the tip shuffle algorithm, but had strong positive effects when we used the independent swap algorithm to randomize communities; and we saw no significant effect of eye index SES_{MPD} when calculated with the independent swap algorithm, but strong negative effects when we used the tip shuffle algorithm to randomize (Table A5.3).

DISCUSSION

In our examination of peracarid community assembly in Northern California eelgrass beds, we found that the dispersion of traits in the peracarid community responded strongly to a particular set of community-weighted mean fish traits. Peracarid communities were more overdispersed when exposed to fish communities with larger eyes high up on the head (high PC16 score), a pattern that held for all traits combined and for phylogenetic dispersion (Fig 2.2). While PC16 (eye index) accounts for only 0.028% of the morphological variation in the fish species pool, our analyses focus on local fish communities that have already undergone filtering from the regional pool, and the explanatory power of individual PC axes on species pool

variability is not relevant to our study. In this sense, eye index acts as a "keystone trait" that has a disproportionate effect on prey communities despite its encompassing a small part of predator morphospace. The strong effect of eye index on peracarid community dispersion is particularly noteworthy because of its correlation with traits including eye size, which is strongly related to fish visual acuity (Myrberg and Fuiman 2002, Caves et al. 2017, Lisney et al. 2020). Correspondingly, prey activity level and body size both contribute to detectability by and susceptibility to gape-limited predators like fishes (McPeek 1990, Urban 2007), and we found that higher mean eye index lead to increased dispersion of both maximum prey body size and the amount of time prey spent not moving, which may hinder the ability of visually oriented predators to detect or form a consistent search image for prey.

In contrast, mean fish body depth below midline (BDBM) was strongly negatively correlated with peracarid phylogenetic dispersion. By itself, BDBM may serve as a proxy for bottom orientation (Pease et al. 2012); in our dataset, it is highest in benthically-oriented fishes with low gape limitation such as sculpins (Cottidae) or midshipmen (*Porichthys notatus*) and lowest in laterally compressed fishes that occupy the water column such as surfperches (Embiotocidae) and rockfishes (*Sebastes* spp.; Fig. 2.3b). This suggests that large-mouthed benthic fishes, many of which are sit-and wait-predators, select for a narrow range of phylogenetically-conserved traits such as body size and antenna length. While maximum body size of peracarids as defined in this study showed no significant phylogenetic signal, biomass has shown to be phylogenetically conserved in other studies of these peracarid communities (Best and Stachowicz 2013).

In all cases where we observed correlations between clustered peracarid communities and particular mean fish traits, we saw few apparent consistencies in the direction to which peracarids are clustered for specific response traits (Fig. 2.2c-f, Fig. 2.3c-f). For example, although low average eye indices were associated with clustered prey communities, these clustered communities did not have consistently low body sizes or activity levels, despite the fact that these could minimize detection by small-eyed fishes (Fig. 2.2c, f; Myrberg and Fuiman 2002, Caves et al. 2017, Lisney et al. 2020). This suggests three non-mutually exclusive possibilities. First, that these fish traits may be exerting strong selection on unmeasured phylogenetically conserved peracarid traits that exhibited strong genetic correlations with traits like body size, antenna length, and activity level. Second, only fish traits at one extreme may

drive overdispersion, while those at the other extreme have minimal effects on clustering, and the clustering we observed may be driven by other forces. Finally, the direction of fish traits' effects on peracarid trait clustering in the summer may be contingent on processes occurring earlier in the year when predation was lower and other factors were more important in community assembly. Broader factors such as dispersal limitation, competition for resources, and stochasticity in community composition may be important in determining how specific traits are distributed early on in the community assembly process before the predator community exerts any selective pressure (Hein and Gillooly 2011, Pelinson et al. 2022). Of note here is the fact that many of these fishes are juveniles of outer rocky reef species that recruit to estuarine habitats such as eelgrass every year to use as nursery habitats (McDevitt-Irwin et al. 2016, Beheshti et al. 2022, Obaza et al. 2022), and that predation rates in eelgrass are seasonally variable (Ruesink et al. 2019, C.E. Murphy, unpublished).

The trait dispersion of predator communities was a strong predictor of prey community dispersion; additionally, accounting for habitat filters on predator community assembly strengthened these relationships. Overall, these results suggest that habitat filtering on the fish species pool tended to diminish or antagonize selection acting on peracarids by fishes. In other words, habitat filtering on fishes tended to select for trait values that were weaker drivers of peracarid dispersion. To some degree, both predator and prey communities are assembled according to the same set of habitat filters, which may act in the same or opposite direction as filters such as predation or competition that act on smaller spatial scales (Kraft et al. 2015). These different selective pressures may act concurrently on the same or different sets of traits to produce the emergent pattern (Grime 2006, Ingram and Shurin 2009, Fitzgerald et al. 2017), and traits that respond differentially to selective pressures in one trophic level could produce different responses in another (Daniel and Rooney 2022).

On one hand, we found negative correlations between PC8 and BDBM dispersion and peracarid trait dispersion (Fig. 2.4), suggesting that prey may reduce competition for enemy-free space by moving into multiple niche optima that reduce their susceptibility to predation when predators are clustered, while pressure from overdispersed predator traits push prey into a single refuge in trait space, potentially reflecting equalizing competition (Fig. 2.1b, quadrants i and iii). On the other hand, we observed a positive correlation between total fish trait dispersion and peracarid dispersion (Fig. 2.5). In this case, a wide range of predation strategies across traits in

overdispersed predator communities may have prevented the dominance of a single predator avoidance strategy, leading to stabilizing competition for enemy-free space, while clustered predator communities forced prey to a single niche optimum that avoids the similarly small range of predator traits in the community (Fig. 2.1b, quadrants ii and iv). However, the lack of consistent trait means we observed in clustered peracarid communities suggests that the single trait optimum for evading clustered predators varies from community to community according to either idiosyncratic factors including the specific clustering pattern of the predator community or external environmental filters that lead to clustering at both trophic levels. In some cases, selection appeared to have no effect whatsoever on fish communities' strength as filters on the peracarid species pool – mean fish eye index had strong effects on peracarid dispersion, but the distribution of this trait and its response to ecological filters had no consistent predictive power (Table A5.2, A4.3). For traits like eye index that show little variation in the species pool, ecological selection may not be able to further constrain communities beyond the mean value of the species pool and thus have a negligible top-down effect.

Throughout this study we have operated under the assumption that the relationships we observed between predator and prey communities are the result of top-down control. While a bottom-up interpretation (prey traits filtering predator traits) is a valid approach to understanding these communities, we lack the means to apply this interpretation confidently with our trait dataset, as we focused on prey traits thought to be important for predator avoidance and microhabitat niche, and predator traits that were more broadly associated with feeding, movement, and habitat use. Additionally, predation is already known as an important driver of peracarid community structure in eelgrass beds, even for traits that are not necessarily directly affected by predators a priori (Gross et al. 2022). Furthermore, we saw no significant relationships between the mean or distribution of fish gape sizes and prey body sizes, or any other trait-trait relationships that might be reasonably expected under bottom-up control by prey communities.

Although the roles of predators in affecting prey community assembly through both predation and non-consumptive effects are now well-appreciated, much of this work focuses on species-depauperate predator assemblages (Post et al. 2008, Holdridge et al. 2017, Schmid et al. 2019), and rarely considers the potential top-down effects of community assembly of predators on the community assembly of their prey. We present compelling observational evidence that

specific predator traits have measurable impacts on the community assembly of prey, and that habitat filtering effects on predator species pools may hinder their ability to affect prey community assembly. While these results are not conclusive, they invite experimental tests of predator mean trait values on community assembly, and explicit comparisons of how the relative effects of habitat filters and intraguild competition on predators impact their ability to affect prey community assembly, especially in systems that exhibit strong top-down control. Integrating our understanding of traits at multiple trophic levels can help us better predict the impacts of community composition on food web dynamics, especially as regional species pools shift with climate change and anthropogenic introductions.

ACKNOWLEDGMENTS

Fieldwork and sampling for this project was conducted on the unceded traditional lands of the Coast Miwok people. We are grateful for the help of numerous assistants and volunteers in the field and laboratory who helped to collect and process fish and invertebrate samples, including RA Alexander, EA Deen, S Bala, DS Beatty, M Burnett, E Cruz-Rivera, N Dao, O Diana, KA Dubois, T Hayes, LG Hsia, A Lee, A Lei, A Lindeman, M Liu, A McFarland, E Meyers, CE Murphy, N Murray, S Pelletier, A Penix, KN Pollard, A Sandoval, C Sears, C Souza, M Yang, and KL Zabinski. Funding for this project was supported by UC Natural Reserve System Matthias, American Philosophical Society, and UC Davis Center for Population Biology grants to CPG, and by National Science Foundation awards OCE-1829921, OCE-1829922, OCE-1829992, and OCE-1829890 to JJS. This manuscript was prepared as a chapter for CPG's doctoral dissertation, and improved by comments from SP Lawler, E Sanford, and SY Strauss.

REFERENCES

Abbott, J. M., K. DuBois, R. K. Grosberg, S. L. Williams, and J. J. Stachowicz. 2018. Genetic distance predicts trait differentiation at the subpopulation but not the individual level in eelgrass, *Zostera marina*. Ecology and Evolution 8:7476–7489.

Aoki, L. R., B. Rappazzo, D. S. Beatty, L. K. Domke, G. L. Eckert, M. E. Eisenlord, O. J. Graham, L. Harper, T. L. Hawthorne, M. Hessing-Lewis, K. A. Hovel, Z. L. Monteith, R. S. Mueller, A. M. Olson, C. Prentice, J. J. Stachowicz, F. Tomas, B. Yang, J. E. Duffy, C. Gomes, and C. D. Harvell. 2022. Disease surveillance by artificial intelligence links

eelgrass wasting disease to ocean warming across latitudes. Limnology and Oceanography 67:1577–1589.

Ashford, O. S., A. J. Kenny, C. R. S. Barrio Froján, M. B. Bonsall, T. Horton, A. Brandt, G. J. Bird, S. Gerken, and A. D. Rogers. 2018. Phylogenetic and functional evidence suggests that deep-ocean ecosystems are highly sensitive to environmental change and direct human disturbance. Proceedings of the Royal Society B: Biological Sciences 285:20180923.

Beermann, J., K. Boos, L. Gutow, M. Boersma, and A. C. Peralta. 2018. Combined effects of predator cues and competition define habitat choice and food consumption of amphipod mesograzers. Oecologia 186:645–654.

Beheshti, K. M., S. L. Williams, K. E. Boyer, C. Endris, A. Clemons, T. Grimes, K. Wasson, and B. B. Hughes. 2022. Rapid enhancement of multiple ecosystem services following the restoration of a coastal foundation species. Ecological Applications 32:e02466.

de Bello, F., Z. Botta-Dukát, J. Lepš, and P. Fibich. 2021. Towards a more balanced combination of multiple traits when computing functional differences between species. Methods in Ecology and Evolution 12:443–448.

Best, R. J., N. C. Caulk, and J. J. Stachowicz. 2013. Trait vs. phylogenetic diversity as predictors of competition and community composition in herbivorous marine amphipods. Ecology Letters 16:72–80.

Best, R. J., and J. J. Stachowicz. 2012. Trophic cascades in seagrass meadows depend on mesograzer variation in feeding rates, predation susceptibility, and abundance. Marine Ecology Progress Series 456:29–42.

Best, R. J., and J. J. Stachowicz. 2013. Phylogeny as a Proxy for Ecology in Seagrass Amphipods: Which Traits Are Most Conserved? PLOS ONE 8:e57550.

Best, R. J., and J. J. Stachowicz. 2014. Phenotypic and phylogenetic evidence for the role of food and habitat in the assembly of communities of marine amphipods. Ecology 95:775–786.

Cadotte, M. W., T. J. Davies, and P. R. Peres-Neto. 2017. Why phylogenies do not always predict ecological differences. Ecological Monographs 87:535–551.

Cavender-Bares, J., K. H. Kozak, P. V. A. Fine, and S. W. Kembel. 2009. The merging of community ecology and phylogenetic biology. Ecology Letters 12:693–715.

Caves, E. M., T. T. Sutton, and S. Johnsen. 2017. Visual acuity in ray-finned fishes correlates with eye size and habitat. Journal of Experimental Biology 220:1586–1596.

Chang, F.-H., J. W. Yang, A. C.-H. Liu, H.-P. Lu, G.-C. Gong, F.-K. Shiah, and C. Hsieh. 2021. Community Assembly Processes as a Mechanistic Explanation of the Predator-Prey Diversity Relationship in Marine Microbes. Frontiers in Marine Science 8.

Cheng, B. S., and E. D. Grosholz. 2016. Environmental stress mediates trophic cascade strength and resistance to invasion. Ecosphere 7:e01247.

Daniel, J., and R. C. Rooney. 2022. Functional dispersion of wetland birds, invertebrates, and plants more strongly influenced by hydroperiod than each other. Ecosphere 13:e3971.

Dellinger, J. A., C. R. Shores, A. D. Craig, S. M. Kachel, M. R. Heithaus, W. J. Ripple, and A. J. Wirsing. 2022. Predators reduce niche overlap between sympatric prey. Oikos 2022.

DuBois, K., K. N. Pollard, B. J. Kauffman, S. L. Williams, and J. J. Stachowicz. 2022. Local adaptation in a marine foundation species: Implications for resilience to future global change. Global Change Biology 28:2596–2610.

Estes, J. A., J. Terborgh, J. S. Brashares, M. E. Power, J. Berger, W. J. Bond, S. R. Carpenter, T. E. Essington, R. D. Holt, J. B. C. Jackson, R. J. Marquis, L. Oksanen, T. Oksanen, R. T. Paine, E. K. Pikitch, W. J. Ripple, S. A. Sandin, M. Scheffer, T. W. Schoener, J. B. Shurin, A. R. E. Sinclair, M. E. Soulé, R. Virtanen, and D. A. Wardle. 2011. Trophic Downgrading of Planet Earth. Science 333:301–306.

Fitzgerald, D. B., K. O. Winemiller, M. H. S. Pérez, and L. M. Sousa. 2017. Using trophic structure to reveal patterns of trait-based community assembly across niche dimensions. Functional Ecology 31:1135–1144.

Grime, J. P. 2006. Trait convergence and trait divergence in herbaceous plant communities: Mechanisms and consequences. Journal of Vegetation Science 17:255–260.

Gross, C. P., J. E. Duffy, K. A. Hovel, M. R. Kardish, P. L. Reynolds, C. Boström, K. E. Boyer, M. Cusson, J. Eklöf, A. H. Engelen, B. K. Eriksson, F. J. Fodrie, J. N. Griffin, C. M. Hereu, M. Hori, A. R. Hughes, M. V. Ivanov, P. Jorgensen, C. Kruschel, K.-S. Lee, J. Lefcheck, K. McGlathery, P.-O. Moksnes, M. Nakaoka, M. I. O'Connor, N. E. O'Connor, J. L. Olsen, R. J. Orth, B. J. Peterson, H. Reiss, F. Rossi, J. Ruesink, E. E. Sotka, J. Thormar, F. Tomas, R. Unsworth, E. P. Voigt, M. A. Whalen, S. L. Ziegler, and J. J. Stachowicz. 2022. The biogeography of community assembly: latitude and predation

drive variation in community trait distribution in a guild of epifaunal crustaceans. Proceedings of the Royal Society B: Biological Sciences 289:20211762.

Ha, G., and S. L. Williams. 2018. Eelgrass community dominated by native omnivores in Bodega Bay, California, USA. Bulletin of Marine Science 94:1333–1353.

Hein, A. M., and J. F. Gillooly. 2011. Predators, prey, and transient states in the assembly of spatially structured communities. Ecology 92:549–555.

Holdridge, E. M., G. E. Flores, and C. P. terHorst. 2017. Predator trait evolution alters prey community composition. Ecosphere 8:e01803.

Ingram, T., and J. B. Shurin. 2009. Trait-based assembly and phylogenetic structure in northeast Pacific rockfish assemblages. Ecology 90:2444–2453.

Jackson, J. B. C., M. X. Kirby, W. H. Berger, K. A. Bjorndal, L. W. Botsford, B. J. Bourque, R. H. Bradbury, R. Cooke, J. Erlandson, J. A. Estes, T. P. Hughes, S. Kidwell, C. B. Lange, H. S. Lenihan, J. M. Pandolfi, C. H. Peterson, R. S. Steneck, M. J. Tegner, and R. R. Warner. 2001. Historical Overfishing and the Recent Collapse of Coastal Ecosystems. Science 293:629–637.

Jernakoff, P., A. Brearley, and J. Nielsen. 1996. Factors affecting grazer-epiphyte interactions in temperate seagrass meadows. Oceanography and Marine Biology: An Annual Review.

Karachle, P. K., K. I. Stergiou, P. K. Karachle, and K. I. Stergiou. 2012. Morphometrics and Allometry in Fishes. Page Morphometrics. IntechOpen.

Kembel, S. W., P. D. Cowan, M. R. Helmus, W. K. Cornwell, H. Morlon, D. D. Ackerly, S. P. Blomberg, and C. O. Webb. 2010. Picante: R tools for integrating phylogenies and ecology. Bioinformatics 26:1463–1464.

Kraft, N. J. B., P. B. Adler, O. Godoy, E. C. James, S. Fuller, and J. M. Levine. 2015. Community assembly, coexistence and the environmental filtering metaphor. Functional Ecology 29:592–599.

Lisney, T. J., S. P. Collin, and J. L. Kelley. 2020. The effect of ecological factors on eye morphology in the western rainbowfish, *Melanotaenia australis*. Journal of Experimental Biology 223:jeb223644.

Lürig, M. D., R. J. Best, and J. J. Stachowicz. 2016. Microhabitat partitioning in seagrass mesograzers is driven by consistent species choices across multiple predator and competitor contexts. Oikos 125:1324–1333.

Mayfield, M. M., and J. M. Levine. 2010. Opposing effects of competitive exclusion on the phylogenetic structure of communities. Ecology Letters 13:1085–1093.

McDevitt-Irwin, J. M., J. C. Iacarella, and J. K. Baum. 2016. Reassessing the nursery role of seagrass habitats from temperate to tropical regions: a meta-analysis. Marine Ecology Progress Series 557:133–143.

McPeek, M. A. 1990. Behavioral differences between *Enallagma* species (Odonata) influencing differential vulnerability to predators. Ecology 71:1714–1726.

McPeek, M. A. 1995. Morphological evolution mediated by behavior in the damselflies of two communities. Evolution 49:749–769.

Myrberg, A. A., and L. A. Fuiman. 2002. Chapter 6 - The Sensory World of Coral Reef Fishes. Pages 123–148 *in* P. F. Sale, editor. Coral Reef Fishes. Academic Press, San Diego.

Obaza, A. K., A. Bird, R. Sanders, R. Ware, and D. W. Ginsburg. 2022. Variable fish habitat function in two open-coast eelgrass species. Marine Ecology Progress Series 696:15–27.

Paine, R. T. 1966. Food web complexity and species diversity. The American Naturalist 100:65–75.

Palkovacs, E. P., M. C. Marshall, B. A. Lamphere, B. R. Lynch, D. J. Weese, D. F. Fraser, D. N. Reznick, C. M. Pringle, and M. T. Kinnison. 2009. Experimental evaluation of evolution and coevolution as agents of ecosystem change in Trinidadian streams. Philosophical Transactions of the Royal Society B: Biological Sciences 364:1617–1628.

Pavoine, S., and M. B. Bonsall. 2011. Measuring biodiversity to explain community assembly: a unified approach. Biological Reviews 86:792–812.

Pease, A. A., A. A. González-Díaz, R. Rodiles-Hernández, and K. O. Winemiller. 2012. Functional diversity and trait–environment relationships of stream fish assemblages in a large tropical catchment. Freshwater Biology 57:1060–1075.

Pelinson, R. M., M. A. Leibold, and L. Schiesari. 2022. Community variability in pond metacommunities: interactive effects of predators and isolation on stochastic community assembly. Oikos 2022:e08798.

Poff, N. L. 1997. Landscape filters and species traits: towards mechanistic understanding and prediction in stream ecology. Journal of the North American Benthological Society 16:391–409.

Post, D. M., E. P. Palkovacs, E. G. Schielke, and S. I. Dodson. 2008. Intraspecific variation in a predator affects community structure and cascading trophic interactions. Ecology 89:2019–2032.

R Development Core Team. 2022. R: a language and environment for statistical computing.

Reynolds, P. L., J. P. Richardson, and J. E. Duffy. 2014. Field experimental evidence that grazers mediate transition between microalgal and seagrass dominance. Limnology and Oceanography 59:1053–1064.

Reynolds, P. L., J. J. Stachowicz, K. Hovel, C. Boström, K. Boyer, M. Cusson, J. S. Eklöf, F. G. Engel, A. H. Engelen, B. K. Eriksson, F. J. Fodrie, J. N. Griffin, C. M. Hereu, M. Hori, T. C. Hanley, M. Ivanov, P. Jorgensen, C. Kruschel, K.-S. Lee, K. McGlathery, P.-O. Moksnes, M. Nakaoka, M. I. O'Connor, N. E. O'Connor, R. J. Orth, F. Rossi, J. Ruesink, E. E. Sotka, J. Thormar, F. Tomas, R. K. F. Unsworth, M. A. Whalen, and J. E. Duffy. 2018. Latitude, temperature, and habitat complexity predict predation pressure in eelgrass beds across the Northern Hemisphere. Ecology 99:29–35.

Ruesink, J. L., C. Gross, C. Pruitt, A. C. Trimble, and C. Donoghue. 2019. Habitat structure influences the seasonality of nekton in seagrass. Marine Biology 166:75.

Schmid, D. W., M. D. McGee, R. J. Best, O. Seehausen, and B. Matthews. 2019. Rapid divergence of predator functional traits affects prey composition in aquatic communities. The American Naturalist 193:331–345.

Sessa, E. B., S. M. Chambers, D. Li, L. Trotta, L. Endara, J. G. Burleigh, and B. Baiser. 2018. Community assembly of the ferns of Florida. American Journal of Botany 105:549–564.

Sih, A., G. Englund, and D. Wooster. 1998. Emergent impacts of multiple predators on prey. Trends in Ecology & Evolution 13:350–355.

Sommers, P., and P. Chesson. 2019. Effects of predator avoidance behavior on the coexistence of competing prey. The American Naturalist 193:E132–E148.

Starko, S., K. W. Demes, C. J. Neufeld, and P. T. Martone. 2020. Convergent evolution of niche structure in Northeast Pacific kelp forests. Functional Ecology 34:2131–2146.

Swenson, N. G. 2014. Functional and Phylogenetic Ecology in R. Springer-Verlag, New York.

Swenson, N. G., B. J. Enquist, J. Pither, J. Thompson, and J. K. Zimmerman. 2006. The problem and promise of scale dependency in community phylogenetics. Ecology 87:2418–2424.

Thompson, P., M. Guzman, L. De Meester, Z. Horváth, R. Ptacnik, B. Vanschoenwinkel, D. Viana, and J. Chase. 2020. A process-based metacommunity framework linking local and regional scale community ecology. Ecology Letters 23.

Tucker, C. M., T. J. Davies, M. W. Cadotte, and W. D. Pearse. 2018. On the relationship between phylogenetic diversity and trait diversity. Ecology 99:1473–1479.

Urban, M. C. 2007. The growth–predation risk trade-off under a growing gape-limited predation threat. Ecology 88:2587–2597.

Valentine, J. F., and J. E. Duffy. 2006. The central role of grazing in seagrass ecology. Pages 463–501 *in* A. W. D. Larkum, R. J. Orth, and C. M. Duarte, editors. Seagrasses: biology, ecology and conservation. Springer Netherlands, Dordrecht.

Vamosi, S. M. 2005. On the role of enemies in divergence and diversification of prey: a review and synthesis. Canadian Journal of Zoology 83:894–910.

Webb, C. O., D. D. Ackerly, M. A. McPeek, and M. J. Donoghue. 2002. Phylogenies and community ecology. Annual Review of Ecology and Systematics 33:475–505.

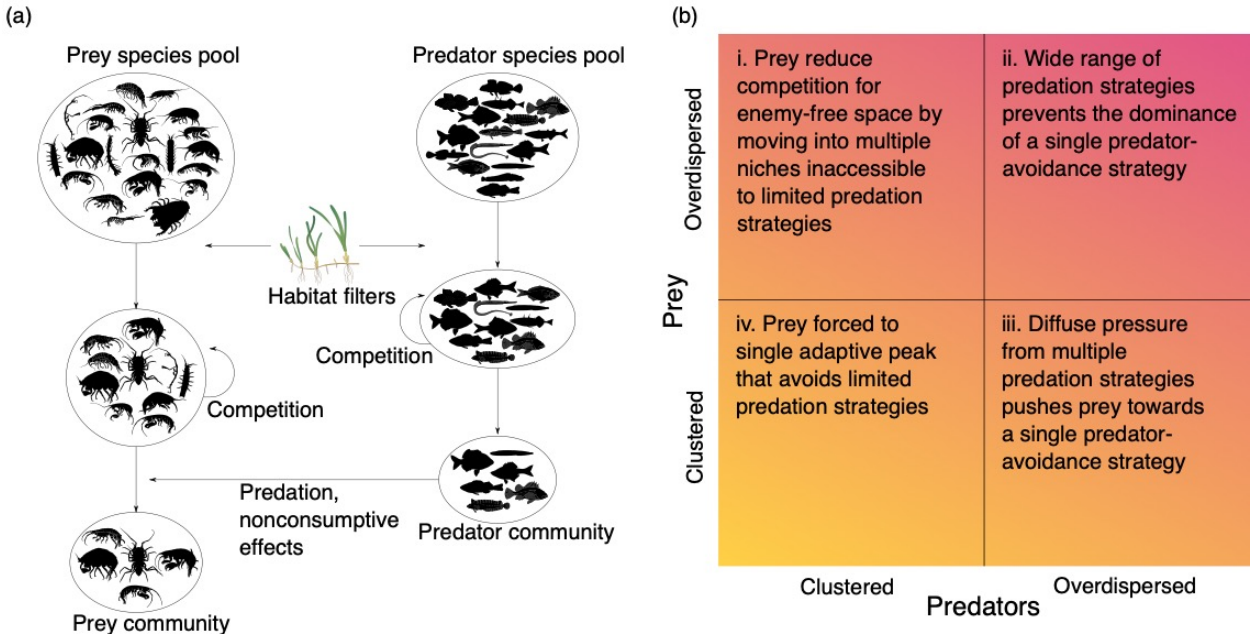

Figure 2.1. a) Species pools of both predators and prey are subject to abiotic and habitat filters as well as competition within trophic guilds, all of which exert selective pressure to restrict species from the local community. The local predator community, shaped by selection from other ecological filters, can act on the prey species pool to shape the final prey community. b) To the extent that predators act as filters on the prey species pool, predator trait dispersion patterns may exert selective pressure in directions that cause prey communities to mirror or oppose predator communities in terms of trait dispersion. Animal silhouettes by CPG; *Zostera* image by C. Collier, James Cook University (ian.umces.edu/media-library).

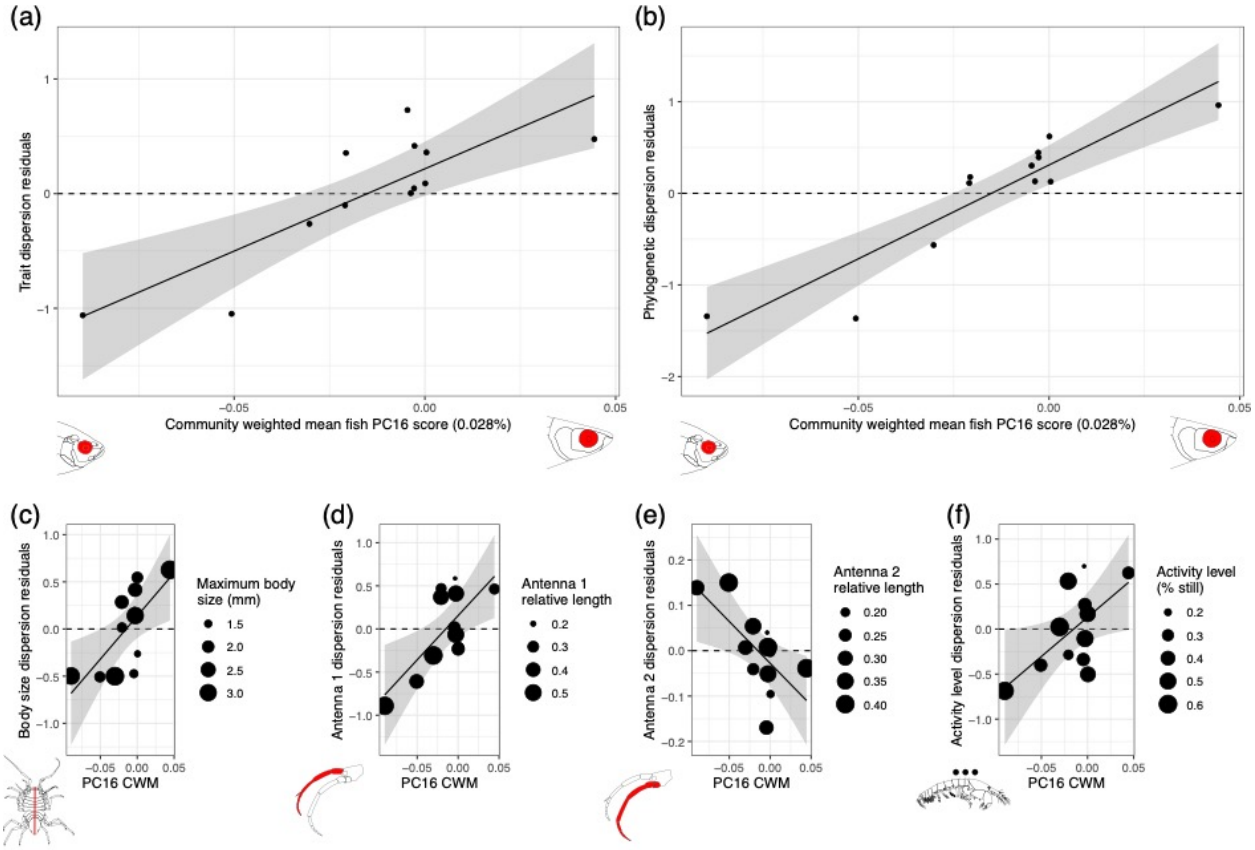

Figure 2.2. Responses of residual peracarid trait (a; $R^2 = 0.656$, $p < 0.001$) and phylogenetic (b; $R^2 = 0.826$, $p < 0.001$) dispersion to community-weighted mean (CWM) fish PC16 scores. Four traits showed noteworthy responses in their residual dispersion to PC16, although none were significant at $\alpha = 0.0045$: maximum body size (c; $R^2 = 0.381$, $p = 0.019$), antenna 1 length (d; $R^2 = 0.419$, $p = 0.0136$), antenna 2 length (e; $R^2 = 0.361$, $p = 0.0228$), and activity level measured as % still (f; $R^2 = 0.300$, $p = 0.0380$). In panels c-f, point size varies with CWM values for each individual trait examined. The dashed horizontal line represents a randomly assembled peracarid community ($SES_{MNTD} = 0$; calculated using the tip shuffle algorithm). Drawings by CPG.

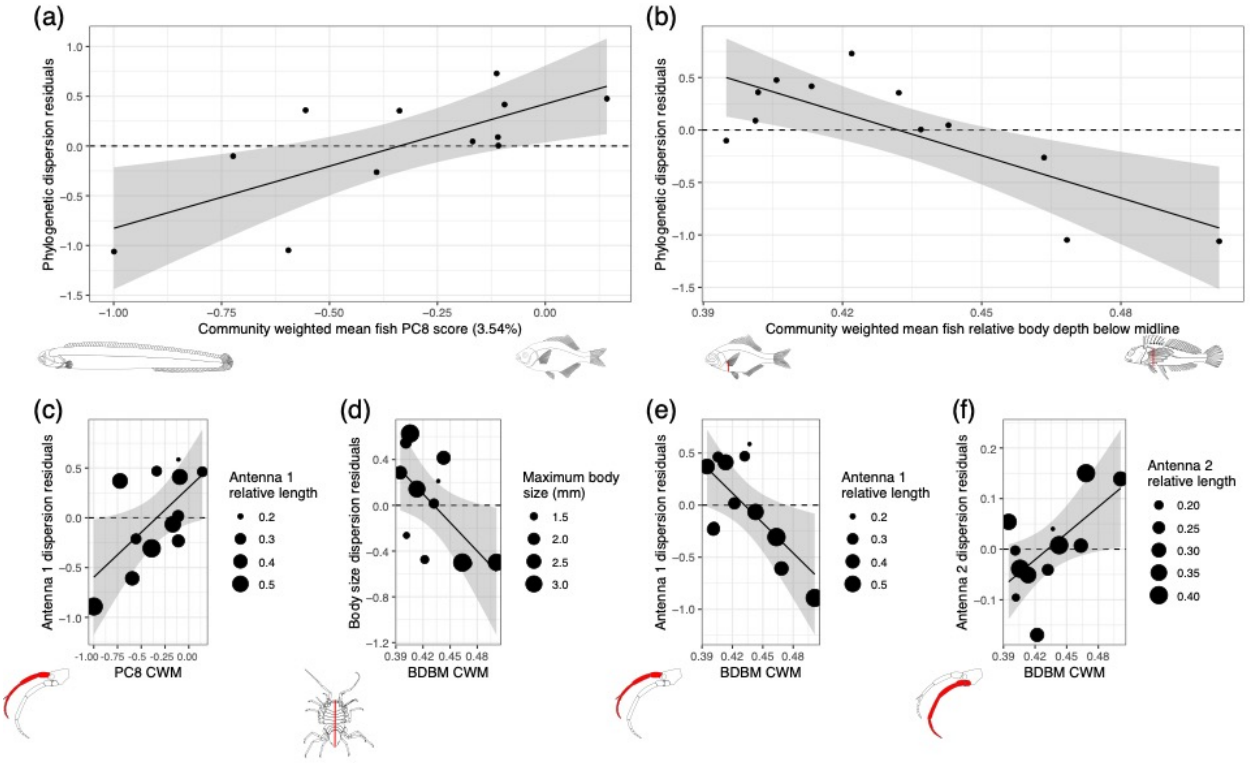

Figure 2.3. Responses of residual peracarid phylogenetic dispersion to community-weighted mean (CWM) fish PC8 scores (a; $R^2 = 0.590$, $p = 0.00215$) and body depth below midline (BDBM; b; $R^2 = 0.671$, $p < 0.001$). Antenna 1 length showed a noteworthy albeit nonsignificant positive correlation with community weighted mean PC8 score (c; $R^2 = 0.307$, $p = 0.0359$). Residual dispersion of maximum body size, antenna 1 length, and antenna 2 length were all correlated with community weighted mean BDBM (d: $R^2 = 0.308$, $p = 0.0356$; e: $R^2 = 0.352$, $p = 0.0247$; f: $R^2 = 0.303$, $p = 0.0372$), although none of these were significant at $\alpha = 0.0045$. In panels c-f, point size varies with community weighted mean values for each individual trait examined. The dashed horizontal line represents a randomly assembled peracarid community ($SES_{MNTD} = 0$; calculated using the tip shuffle algorithm). Drawings by CPG.

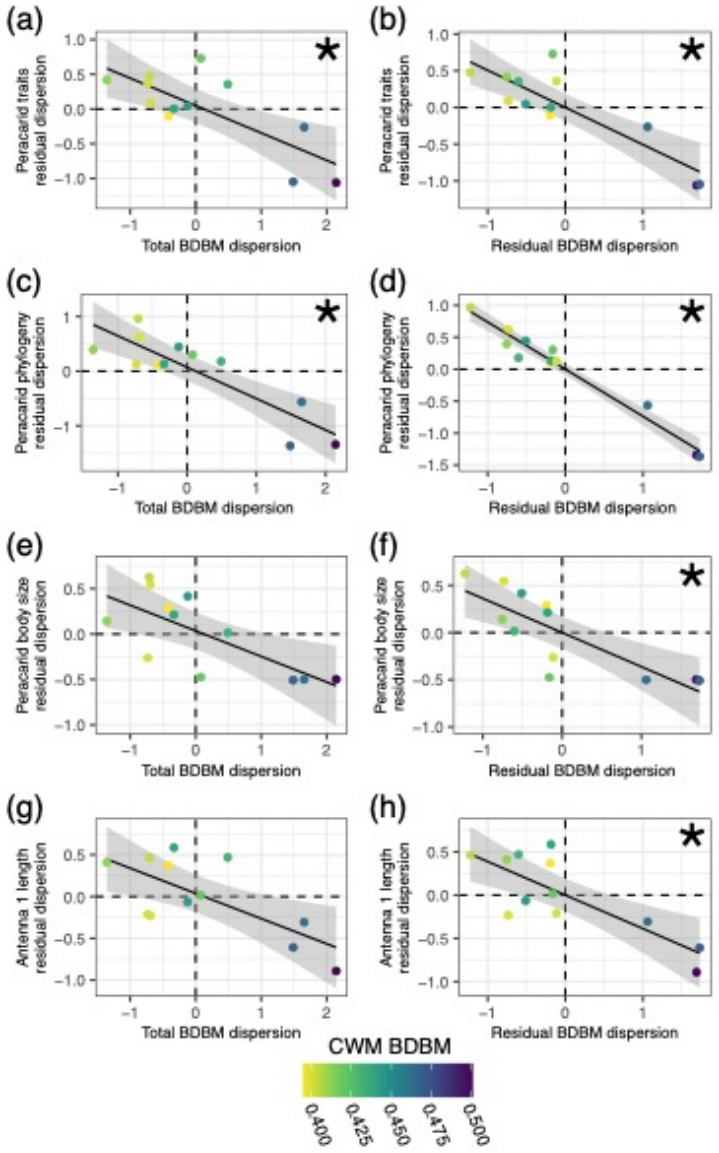

Figure 2.4. Responses of residual peracarid community dispersion to fish body depth below midline (BDBM) dispersion. Fish communities clustered around smaller BDBMs co-occur with peracarid communities that are more overdispersed when including (a, c, e, g) and controlling for the influence of habitat filters (b, d, f, h) for all traits (a, $R^2 = 0.549$, $p = 0.00355$; b, $R^2 = 0.732$, $p < 0.001$), phylogenetic distance (c, $R^2 = 0.726$, $p < 0.001$; d, $R^2 = 0.960$, $p < 0.001$), maximum body size (e, $R^2 = 0.463$, $p = 0.00889$; f, $R^2 = 0.622$, $p = 0.0014$), and antenna 1 length (g, $R^2 = 0.444$, $p = 0.0107$; h, $R^2 = 0.598$, $p = 0.00194$). Colors indicate the community weighted mean BDBM of each fish community. The dashed horizontal and vertical lines represent randomly assembled peracarid and fish communities, respectively ($SES_{MNTD} = 0$; calculated using the tip shuffle algorithm). Asterisks indicate a significant relationship at $\alpha = 0.0083$

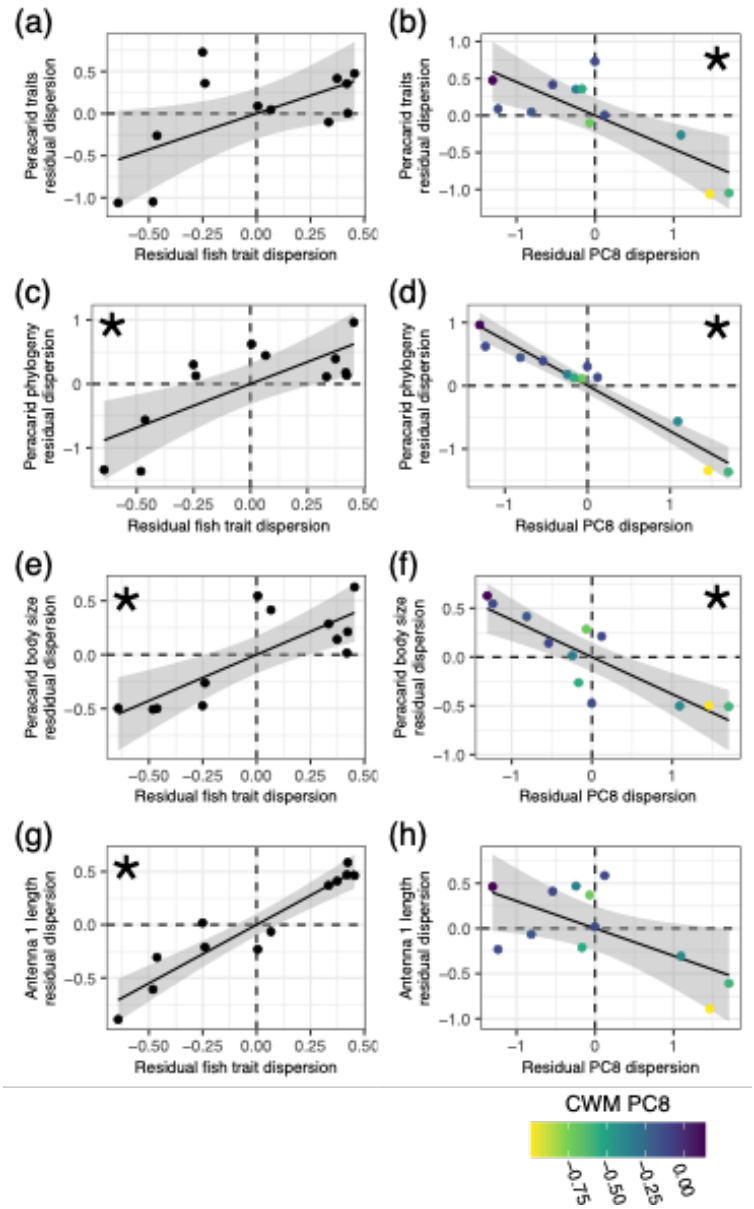

Figure 2.5. Residual fish trait dispersion (a, c, e, g) and PC8 dispersion (b, d, f, h) as predictors of residual peracarid trait dispersion (a, $R^2 = 0.302$, $p = 0.0374$; b, $R^2 = 0.570$, $p = 0.00274$), phylogenetic dispersion (c, $R^2 = 0.537$, $p = 0.00406$; d, $R^2 = 0.927$, $p < 0.001$), body size dispersion (e, $R^2 = 0.603$, $p = 0.0018$; f, $R^2 = 0.712$, $p < 0.001$), and antenna 1 length dispersion (g, $R^2 = 0.883$, $p < 0.001$; h, $R^2 = 0.336$, $p = 0.0283$). The dashed horizontal and vertical lines represent randomly assembled peracarid and fish communities, respectively ($SES_{MNTD} = 0$; calculated using the tip shuffle algorithm). In panels b, d, f, and h, colors indicate fish community-weighted mean scores of PC8. Asterisks indicate a significant relationship at $\alpha = 0.0083$.

CHAPTER 3: Eelgrass genetic diversity is strongly associated with a novel latitudinal cline in taxonomic turnover

ABSTRACT

Structural complexity within and among populations of habitat-forming foundation species is important for facilitating mobile animal diversity and abundance. Yet not all animal taxa respond equally to different axes of structural complexity and microhabitat space provided by foundation species, and because of functional differences among these taxa, variation in structural complexity may cascade upwards to affect ecosystem function. We examined global patterns in communities of epifaunal mesograzers dominated by peracarid crustaceans and gastropod molluscs in eelgrass (*Zostera marina*) beds, where variation in shoot morphology is underlaid by intraspecific genetic diversity. The abundance of peracarids and gastropods exhibited a strong latitudinal cline in turnover, with gastropods abundant at high-latitude sites, and peracarids abundant at low-latitude sites, especially in the Atlantic. This pattern appeared to be driven by greater eelgrass genetic diversity at lower latitudes, which strongly influenced both the richness and abundance of peracarids, but less so for gastropods. The two taxa exhibited functional complementarity, and so variation in eelgrass genetic diversity across latitudes and between ocean basins led to geographic variation in the distribution of functional traits across the range of eelgrass. Our results add to a growing body of literature that suggests that variation in traits underlaid by genetic differences within species has important consequences for assemblage variation and ecosystem function across broad spatial scales.

INTRODUCTION

The variety of microhabitats created by structurally complex foundation species can be an important driver of diversity in animal communities in both marine and terrestrial systems (MacArthur and MacArthur 1961, Hughes et al. 2002, Loke and Chisholm 2022). Different taxa may coexist by physically partitioning niche space in these habitats, based on the utility of microhabitats for feeding, avoiding predators, or optimizing physiological performance (Schmitz and Suttle 2001, Lindo and Winchester 2013, Lürig et al. 2016). In habitats composed of monospecific stands of foundation species, intraspecific trait variation, whether as a result of plasticity or standing genetic variation, can influence foundation species' suitability as habitat for numerous organisms.

Yet not all taxa may respond equally to the same aspects of structural complexity that may be underlaid by inter- or intraspecific variation in genetic architecture. Diverse trophic guilds across ecosystems are often composed of distinct lineages of taxa that have converged upon similar niches, despite separate origins (Scheltema 1997, Lefcheck and Duffy 2015). Despite their functional similarity, these lineages' may have distinct morphologies or other traits that may be favored by different aspects of structural complexity (e.g., Montalbetti et al. 2022), imposing a separate set of filters on the parts of a habitat they can occupy or the types of foundation species that may facilitate them. For taxa that are especially deeply diverged in time, these filters play out on a background of differences in biogeographic or phylogenetic history, differential responses to abiotic environmental filters, and other factors that can influence how they are distributed across broad spatial scales. Understanding the drivers behind differences in distributions among otherwise functionally similar taxa is key to generalizing how functional and phylogenetic differences affect species distributions, abundance, and community composition.

Worldwide, habitats formed by submerged marine angiosperms (seagrasses) are often composed of clonal individuals of just one or a few species (Hughes et al. 2009, Serra et al. 2010, Leopardas et al. 2014, Duffy et al. 2022). In these species-depauperate systems, plasticity within beds and genetic differences between individual clones are responsible for variation in shoot density, numbers of leaves, canopy height, and other aspects of structural complexity that make these habitats suitable for diverse communities of epifaunal macroinvertebrates (Hughes et al. 2009, Abbott et al. 2017, 2018). Gastropod molluscs and peracarid crustaceans form an important component of these epifaunal communities around the world (Jernakoff and Nielsen 1997, Lefcheck and Duffy 2015, Ha and Williams 2018). Both are typically included in the herbivorous "mesograzer" guild, feeding on epiphytic microalgae that foul seagrass blades, as well as detritus, macroalgae, and live seagrass tissue itself. Yet these taxa are phylogenetically distinct, separated by more than 550 million years of evolutionary history. In some seagrass systems, they are also differentially susceptible to predation, with peracarids being much more vulnerable to consumption than gastropods at the same sites (Reynolds et al. 2018). Direct development is common to all peracarids and when coupled with short generation times can lead to rapid population increases compared to gastropods which have slower individual growth and more diverse developmental modes. Whether global seagrass communities dominated by gastropods or peracarids are functionally distinct in other ways, including their responses to the

structural complexity provided by seagrasses, can have major implications for understanding their broader patterns of distribution and the ability of whole epifaunal communities to promote seagrass growth by suppressing algae (Hughes et al. 2004).

Here, using a global dataset of epifaunal invertebrate communities associated with the world's most widespread seagrass species (eelgrass, *Zostera marina*), we describe how epifaunal community composition and functional trait distributions vary with environmental parameters including aspects of eelgrass habitat structure on broad biogeographic scales, including between ocean basins and across latitudes. We were specifically interested in documenting any patterns of turnover exhibited between higher taxonomic groups, particularly peracarid crustaceans and gastropod molluscs, across space, with the goal of uncovering the likely drivers underlying spatial turnover in taxonomic dominance as well as its consequences for ecosystem function in these imperiled habitats.

METHODS

Study design and sample collection. Between May and September 2014, we sampled 49 sites across the range of *Z. marina*, spanning 37 degrees of latitude along both coasts of Eurasia and North America (30.4ºN to 67.3ºN; Fig. 3.1; Table A4.1, Fig. A4.1) to characterize the biological and physical structure of eelgrass beds using standardized measurements. Each site had 20 plots, for a total of 980 plots sampled as part of the *Zostera* Experimental Network (ZEN). Plots were 1 m^2 and spaced 2 m apart at each site. We sampled eelgrass biomass and quantified eelgrass habitat structure at the plot level as described by Gross et al. (2022) – briefly, we quantified eelgrass aboveground biomass, shoot density, canopy height, and leaf nitrogen, as well as macroalgal biomass from 20-cm diameter cores in each plot. We quantified epiphyte load by scraping fouling microalgae from four eelgrass shoots per plot and drying to a constant weight. We additionally quantified eelgrass genotypic richness as the average site-level genetic dissimilarity (Rozenfeld distance) between individual shoots based on 24 microsatellite loci, and allelic richness as the average number of alleles per locus, normalized to 7 genets (Duffy et al. 2022).

Abiotic environmental variables. To characterize the abiotic environment experienced by epifauna across the range of eelgrass, we measured in-situ temperature and salinity at each site at the time of sampling. To characterize the overall abiotic environment of each site, we also retrieved estimates of annual mean sea surface temperature (SST), photosynthetically active

radiation (PAR), surface chlorophyll a (Chl a), salinity, and pH from the surrounding region, available in the Bio-ORACLE data set (Tyberghein et al. 2012). These data were taken from monthly readings of the Aqua-MODIS and SeaWiFS satellites at a 9.6 km^2 spatial resolution from 2002 to 2009. We used the raster package in R v. 3.6.3 (Hijmans and Etten 2020, R Development Core Team 2022) to extract the annual mean SST, SST range, PAR, and Chl a from all cells within 10 km of each site, and averaged these cell-level estimates to generate site-level predictors. Other water quality parameters, including dissolved nitrate and other nutrients, were spatially interpolated based on surface measurements in the World Ocean Database 2009 (Garcia et al. 2010).

Measuring predation intensity. Predation intensity was quantified with prey tethering units (PTUs) – locally-collected prey (shelled gastropods and "gammarid" amphipods) as well as standardized prey types (dried squid and kale) were tethered in each plot for 24 hours. Data and methods for amphipod and gastropod prey are reported in detail in Reynolds et al. (2018). Standardized squid prey were 1 cm^2 pieces of dried squid attached by monofilament line to one acrylic rod in each plot (Duffy et al. 2015, Whalen et al. 2020). Pieces of organic curly-leaf green kale measuring approximately 5 x 3 cm were wrapped around acrylic rods to measure macroherbivory pressure at each site. Each PTU type was deployed in each of the four corners of each plot. After 24 hours, we removed the stakes and scored prey as present (uneaten) or absent (eaten); partially-consumed prey were considered eaten, and molted prey were excluded from analyses. Site-level predation was calculated by averaging scores across plots. We calculated site-level consumption of each prey type by averaging scores across plots.

Epifaunal community composition. To sample the macrofauna associated with the eelgrass blades, we carefully placed an open-mouthed fine-mesh drawstring bag (500 μm mesh, 18 cm diameter) over a clump of shoots in the centre of the plot so that the mouth of the bag was flush with the sediment surface. We then cut the shoots where they emerged from the sediment and quickly closed the drawstring to capture the shoots and associated animals. We transferred shoots to the lab on ice and rinsed and hand-inspected them to dislodge the epifauna. We preserved all epifauna that remained on a 1-mm sieve in 70% ethanol and then identified them to the lowest possible taxonomic level (typically species). We standardized epifaunal abundance by the aboveground biomass of the eelgrass sample from which they were collected. We separated epifaunal species into 7 coarse taxonomic groups, including peracarid crustaceans (amphipods,

isopods, tanaids, and mysids), gastropod molluscs, polychaete annelids, bivalve molluscs, decapod crustaceans, anemones, and others (including but not limited to barnacles, nemertean worms, echinoderms, ostracods, and chironomid midge larvae). Peracarids and gastropods were by far the most abundant and speciose groups in these global epifaunal communities (comprising 21.6% and 39.9% of individuals and 116 and 91 species, respectively), and have known functional roles as grazers of eelgrass and associated epiphytes, so we chose to focus subsequent analyses on these taxa.

We scored all peracarid and gastropods for a common series of traits based on information available in the literature, including maximum body size, parental care, developmental mode, tolerance of brackish and fresh water, grazer diet components (fresh eelgrass tissue, eelgrass detritus, macroalgae, microalgae), and alternate non-grazing feeding modes (suspension feeder, carnivore/parasite/scavenger). We also used a series of nested sieves to group individual epifauna into size classes, and used these to approximate mean, mode, medium, and maximum observed sizes for each species. We additionally estimated each species' latitudinal range as the difference between the two most extreme point observations regardless of hemisphere (to account for introduced species and others that span the equator), and latitudinal mean as the mean latitude absolute latitude value of point observations, available online from the Ocean Biodiversity Information System (OBIS) and the Global Biodiversity Information Facility (GBIF) (UNESCO 2023, GBIF 2023). A more detailed discussion of traits including how we defined and measured each, and any transformations we applied prior to analysis is included in Table A4.2.

Functional trait ordination and clustering. To examine how communities dominated by peracarids and gastropods varied across trait space, we calculated continuous community weighted mean trait values for each site. For binary and discrete categorical traits, this translated to average relative abundances of each trait level, while for continuous traits it was the average value. We then calculated Bray-Curtis distances among sites based on their community-weighted trait means, and visualized sites in trait space using an NMDS ordination.

To examine any geographic signal in the trait composition of these communities, we hierarchically clustered communities in trait space based on average Bray-Curtis distances, separating clusters into discrete groups based on a maximum average distance of 0.1. We then

recalculated group-level community-weighted means for our trait values by considering individuals from all sites within a group to be part of one community.

Data analyses. We first examined how species richness and Shannon-Weiner diversity varied across latitude, both for the entire epifaunal community and separately for gastropods and peracarids. We additionally examined how the relative abundance of each of these two groups varied across latitudes and ocean basins. For both sets of analyses we used generalized linear models, assuming Poisson-distributed species richness and binomially-distributed relative abundance of gastropods and peracarids.

To identify candidate predictors of the relative abundance of peracarids and gastropods across sites, we used the log-transformed ratio of peracarid relative abundance to gastropod relative abundance (hereafter log-ratio) as the response variable in a random forest model that incorporated both abiotic and environmental predictor variables, including the first two principle components of eelgrass morphology (including sheath length, sheath width, longest leaf length, shoot density, and aboveground biomass; Fig. A4.4), and species richness of the entire epifaunal community as well as the gastropod and peracarid components. We transformed predictor variables (Table A4.2) where appropriate to conform to expectations of normality. Variables that showed a pairwise Kendall's τ value of greater than 0.6 were not included in the predictor pool. We tuned each forest model by visually inspecting out-of-bag error rates across all trees in the model, and adjusted the number of trees to the smallest number for which error was consistently low. We identified the top 10 predictors of relative abundance from each forest by the degree to which they increased MSE when removed from the model and the total increase in node impurities when removed from the model.

We then performed a model selection procedure to determine the best predictor of each taxon's relative abundance. First, we created a set of 30 a priori generalized linear models of relative abundance: one set based on the top 10 predictors alone, another set based on the top 10 predictors with an interaction term for ocean basin (Atlantic vs. Pacific; to address differences in historical processes that may affect local species pools), and another set based on the top 10 predictors with an interaction term for continental margin (Eastern vs. Western; to address differences in the slope of abiotic latitudinal gradients that may affect communities). We ranked these initial models using AICc scores (MuMIn package; Bartoń 2020), and then incorporated predictors from the three lowest-scoring models of each set into a set of composite models to

examine the combined effects of multiple predictor types. We then used backwards elimination to select the lowest-scoring model from these composite models. Where two models had a ΔAICc less than 3 units, we selected the model with the fewest parameters for interpretation. To specifically examine the responses of these two taxa to aspects of eelgrass habitat composition and structural complexity, we modelled the richness and total abundance of gastropods and peracarids as a function of eelgrass allelic richness, genotypic richness, and the first two principle components of eelgrass morphology. The significance of model predictors was assessed using the Anova() function in the car package in R.

To test whether gastropods and peracarids contributed distinct, non-overlapping suites of traits to epifaunal communities, we asked whether the log-ratio determined the clustering of sites in trait space. We performed a permutational multivariate ANOVA (PERMANOVA) on the Bray-Curtis distances of community-weighted means between sites, using 9,999 permutations. We also investigated whether the volume of trait space occupied by gastropod-dominated (negative log-ratio) or peracarid-dominated (positive log-ratio) sites differed significantly from each other by measuring the average dissimilarity from individual sites to their group centroid (Anderson et al. 2006). Because this procedure requires discrete categories across which to compare variances, we assigned sites with positive and negative log-ratios to separate groups and compared between them. All statistical analyses were conducted in R v.4.2.2 (R Development Core Team 2022).

RESULTS

As is typical for many marine and terrestrial systems, total epifaunal species richness and Shannon-Weiner diversity declined with increasing latitude, and this was true for both Atlantic and Pacific oceans ($\chi^2_1 = 67.999$, $p < 0.001$; Fig. 3.1A). For peracarids, species richness showed opposite latitudinal clines between ocean basins – in the Pacific, richness tended to increase with increasing latitude, while it declined significantly with increasing latitude in the Atlantic ($\chi^2_1 = 22.331$, $p < 0.001$; Fig. 3.1B). Gastropods showed no significant latitudinal clines in species richness, even after removing Porth Dinllaen, Wales, where the species richness was an anomalously high 17 species (Fig. 3.1C). Shannon-Weiner diversity for peracarids and gastropods did not show any significant latitudinal trends. Species richness increased with total abundance for peracarids, but not for gastropods (Fig. A4.2).

We found striking clines in the relative abundance of both peracarids and gastropods across the 37º of latitude surveyed in our study – at high latitudes, gastropods dominated (up to 99.55% in Seldianaya, Russia; $\chi^2_1 = 58295$, $p < 0.001$), while at lower latitudes, peracarids dominated ($\chi^2_1 = 11284.0$, $p < 0.001$; Fig. 3.2). These patterns also differed by ocean basin – in the Pacific, peracarids dominated (up to 98.54% in Willapa Bay, WA, USA) and declined more slowly with increasing latitude than in the Atlantic ($\chi^2_1 = 3524.8$, $p < 0.001$; Fig. 3.2A), where gastropods dominated and increased more steeply with increasing latitude ($\chi^2_1 = 1722$, $p < 0.001$; Fig. 3.2B). There were few sites dominated by other epifaunal taxa, including anemones, mussels, and polychaete worms, but this dominance of other taxa did not vary significantly by latitude or ocean basin (Fig. 3.2C).

Our random forest model employed to predict the log-ratio of peracarids to gastropods across sites used 4,000 trees with an average of 12.327 nodes per tree and explained 33.83% of the variance in log-ratios. Top predictors in this model included coast, ocean basin, in-situ temperature, eelgrass morphology PC1 (positively correlated with shorter leaf lengths and narrower sheath widths), eelgrass allelic richness, eelgrass leaf carbon content, site peracarid richness, eelgrass genotypic richness, mean water column Chl a, and water column silicate (Table 3.1). The log-ratio of peracarids to gastropods was best explained by an additive model including only 3 variables: peracarid richness, eelgrass allelic richness, and ocean basin ($F_{3,43} = 20.42$, $p < 0.001$). Log-ratios increased (more peracarids than gastropods) with peracarid richness and eelgrass allelic richness (Fig. 3.3A, B), and were greater in the Pacific than in the Atlantic Ocean (Fig. 3.3C). Eelgrass allelic richness declined with increasing latitude in the Atlantic, but not in the Pacific; eelgrass allelic richness and morphological variation were also greater on average in the Pacific than in the Atlantic (Fig A5.4).

Peracarid abundance and richness showed consistently significant responses to eelgrass allelic richness, genotypic richness, and the first two principle components of eelgrass morphology – sites with more genetically diverse eelgrass, eelgrass with wider, longer blades (negative PC1 scores), and more dense shoots and greater aboveground biomass (positive PC2) scores, had more peracarid species and individuals (Table A4.4, Table A4.5). Gastropod species richness showed a significant positive response to PC1 and genotypic richness (Table A4.4), while abundance responded positively only to PC1 (Table A4.5).

Gastropod-dominated epifaunal communities (those with a negative log-ratio) occupied a distinctive area of ordination space from peracarid-dominated communities (positive log-ratio; pseudo $F_{1,45} = 11.918$, $p < 0.001$; Fig. 3.4A). Gastropod and peracarid species also occupied complementary regions of trait space (Fig. A4.3). The proportion of other epifaunal taxa did not significantly affect a community's trait assemblage (pseudo $F_{1,48} = 0.33$, $p = 0.784$). The log-ratio did not significantly affect functional beta diversity among sites with similar proportions of these focal taxa ($F_{1,47} = 0.7606$, $p = 0.3876$). Community-weighted trait means explained 62.48% of the variation in log-ratio, according to a random forest model. Traits that drove the functional distinction between gastropod- and peracarid-dominated communities predictably included those related to parental care and developmental mode – Peracarid-dominance was significantly correlated with more brooding, less egg-case-laying, more direct development, and less broadcast spawning – but communities with more peracarids also had more suspension feeders, carnivores, parasites, and scavengers. Species' average latitudinal ranges and mean latitudes were also smaller in peracarid-dominated communities (Table 3.2).

Our hierarchical clustering scheme produced 5 distinct groups of sites with different mean trait values for both peracarids and gastropods (Fig. 3.4B). The first group ("cold Pacific") consisted of cool-temperate Northeast Pacific sites in British Columbia, the outer coast of Washington State (Willapa Bay), Oregon, and Northern California, as well as sites in Japan (Hokkaido), South Korea, Portugal, and Mediterranean France. The second group consisted only of one site in Croatia, where we only found the snail *Bittium reticulatum*. The third group ("warm sites") consisted of warm-temperate to subtropical sites in Southern California, Mexico (Baja California), Virginia, and North Carolina, as well as one site in the Salish Sea (Dabob Bay). The fourth group ("cold Atlantic") consisted of cold temperate sites on both sides of the Atlantic, including Long Island, Massachusetts, Quebec, Ireland, Wales, Sweden, Finland, Norway, and Russia (White Sea). The fifth group ("Asia") included sites in Japan and South Korea as well as one site in Southern California (San Diego Bay). Groups varied mostly by mean maximum body length (from the literature; group 1: 23.43 mm; group 5: 11.65 mm), latitudinal range (group 2: 68.47º; group 5: 21.79º), and mean latitude (group 4: 52.58º; group 5: 37.78º), while all groups were dominated by microalgal grazers and marine species (Table 3.3).

DISCUSSION

We found a prominent latitudinal gradient in epifaunal species richness, with greater richness at lower latitudes (Fig. 3.1A). At Atlantic sites, peracarids followed this same trend (Fig. 3.1B), but the pattern was not recapitulated by peracarids at Pacific sites or gastropods worldwide (Fig. 3.1C). While the negative correlation between species richness and latitude is typical for many terrestrial systems and some marine systems (Pianka 1966, Gaston 2000), evidence increasingly shows that for most marine taxa, richness peaks at mid-latitudes, with a dip near the equator (Chaudhary et al. 2016, Arfianti and Costello 2020, Thyrring and Peck 2021). Furthermore, previously published analyses place peaks in gastropod species richness between 25-30ºN and peracarid (amphipod) richness between 50-60ºN in the northern hemisphere (Chaudhary et al. 2016, Arfianti and Costello 2020), in direct contrast with our results. However, these analyses pooled species across multiple nearshore habitat types, including seagrasses, coral reefs, rocky shores, and soft sediments, and our observed peaks in richness at lower latitudes for total epifauna and Atlantic peracarids may reflect the responses of these taxa specifically to unique characteristics of eelgrass habitat that obscure broader patterns of species richness.

The composition of epifaunal communities shifts from being peracarid-dominated to gastropod-dominated at high latitudes, especially in the Atlantic (Fig. 3.2A, B). As far as we are aware, this latitudinal gradient in taxonomic turnover has not been documented elsewhere in the literature, although there is some limited evidence that gastropods may be more abundant in high-latitude seagrass beds than in low-latitude beds (Barnes and Ellwood 2011). This gradient in turnover mirrors the pattern we observed for peracarid species richness (Fig. 3.1B), but appears to be independent of any broader patterns in gastropod diversity (Fig. 3.1C). Despite superficially recovering some expected latitudinal patterns, the variation in taxa and relationship with eelgrass genetic diversity suggest these are not likely to be driven directly by the processes that might generate a latitudinal diversity gradient, such as temperature. Instead, the results of our analyses suggest a set of plausible explanations for this pattern that may hinge on the historical legacy created by eelgrass range expansion across the Pacific from Japan to North America and then through the Arctic to the Atlantic (Duffy et al. 2022, Yu et al. in revision).

Despite differences in the relative abundances of peracarids and gastropods between the Pacific and Atlantic (Fig. 3.3C), we still observe significant increases in gastropod dominance and decreases in peracarid dominance with increasing latitude in Pacific sites, suggesting

additional mechanisms acting within ocean basins to drive the latitudinal pattern. Notably, log-ratios increase with eelgrass allelic richness (Fig. 3.3A). Eelgrass genetic diversity and variation in morphology are both greater in the Pacific than the Atlantic, the result of bottlenecks that occurred during its colonization of the Atlantic via the Arctic starting 3.5 million years ago (Olsen et al. 2004, Duffy et al. 2022, Yu et al. in revision; Fig. A4.4A). Within the Atlantic, allelic richness also declines significantly with latitude (Fig. A4.4A). The response of epifaunal communities to structural complexity in eelgrass is well-characterized (Orth 1992, Carr et al. 2011, Lürig et al. 2016), particularly as refuge from predators. Experimental evidence has shown that eelgrass genetic diversity affects the abundance of epifaunal mesograzers, and that genetic diversity is associated with eelgrass trait diversity (Hughes et al. 2009, Abbott et al. 2017, 2018; Fig. A4.4B,C). We found similar associations between genetic diversity and abundance and richness for peracarids (Table A4.4, A5.5). Differences in numbers of leaves, shoot widths, and shoot length as a result of genetic differentiation may potentially create a greater variety of microhabitats that support more peracarid species and individuals – for example, longer leaves create horizontal "canopies" that are distinct from vertical "stem" habitats (Lürig et al. 2016). PC1's place in the top predictors from our random forest model corroborates this result and indicate that aspects of eelgrass morphology, notably leaf length and sheath width, are also important determiners of epifaunal log-ratios (Table 3.2).

Our best model predicting epifaunal log-ratios shows a significant positive relationship with site-level peracarid species richness (Fig. 3.3B), suggesting that greater abundance and richness of peracarids (perhaps facilitated by greater eelgrass structural complexity; Table A4.4) at lower latitudes may occupy more niches and competitively exclude gastropods. Yet our ordinations (Fig. 3.4, Fig. A4.3) point to complementarity in the traits of gastropods and peracarids, rather than overlap or redundancy. However, the limited number of comparable traits we were able to assemble for both gastropods and peracarids may be biased more towards niche differences that promote stabilizing coexistence rather than fitness differences (sensu Mayfield and Levine 2010), obscuring potential interactions between these two taxa that may lead to competitive exclusion. For example, in many cases gastropods and peracarids differ in their feeding rates on microalgae, macroalgae, or detritus (Graça et al. 2000, Aberle et al. 2005, Sampaio et al. 2017), which may lead to competitive exclusion if multiple species are focusing on the same food source. Peracarids tend to be more selective grazers than gastropods, and

greater richnesses of species with complementary diets may contribute to the exclusion of gastropods (Jernakoff and Nielsen 1997, Duffy and Harvilicz 2001). Peracarids may also dislodge or even prey upon small molluscs (Lefcheck et al. 2014). It seems unlikely that these behaviors would have a major effect on global distributions of the two taxa, but this remains to be tested.

Our experimental network is notably biased in its sampling of eelgrass epifauna in the Atlantic and Pacific Oceans. Our 29 Atlantic sites span nearly 33º of latitude – nearly the full latitudinal range of eelgrass in the Atlantic (den Hartog 1970, Green and Short 2003) – and include 14 of our highest-latitude sites (Fig. 3.2C). In the Pacific, the remaining 20 sites span only 18.6º of latitude, excluding both higher-latitude sites in Alaska, British Columbia, and the Sea of Okhotsk as well as lower-latitude sites in Mexico. Our latitudinal pattern thus seems to be in part driven by high-latitude gastropod-dominated Atlantic sites at one extreme, and low-latitude peracarid-dominated Pacific sites at the other (Fig. 3.3C). However, the latitudinal pattern of taxonomic turnover is highly significant across our Atlantic sites, and the trend, while weaker, is still observable in the limited latitudinal range of our Pacific sites (Fig. 3.3A, 3.3B).

Regardless of the proximate mechanisms behind the patterns of taxonomic turnover we observed, they ultimately contribute to significant differences in the functional structure of global eelgrass communities. Gastropod-dominated sites were not only geographically distinct, but also occupied a distinct area of niche space from communities dominated by peracarids (Fig. 3.4A). Functionally similar groups of sites appeared to group according to similar latitudes within ocean basins (Fig. 3.4B), emphasizing the role of distinct ocean basins as well as correlated aspects of eelgrass habitat structure in affecting the structure and functioning of epifaunal communities (Fig. 3.3A, C). Epifaunal mesograzer communities in seagrass beds play a critical role in linking the primary production of algae and seagrass to populations of larger predators, including juveniles of economically important fishery species (Heck et al. 2003, Blandon and zu Ermgassen 2014, McDevitt-Irwin et al. 2016). Because epifauna vary in their ability to consume fouling epiphytes, feed directly on seagrass tissue, and their palatability to predators (Jernakoff and Nielsen 1997, Lewis and Anderson 2012, Reynolds et al. 2018), understanding the functional consequences of variation in taxonomic structure across broad biogeographic regions may help us begin to predict the idiosyncratic and geographically variable dynamics of seagrass ecosystem function (Duffy et al. 2014).

ACKNOWLEDGMENTS

We thank the many lab and field assistants that participated in this research and whose contributions of time and effort were invaluable for making this project happen. The manuscript was improved with comments from SP Lawler, ED Sanford, and SY Strauss. This research was funded by National Science Foundation grants to JED, JJS, and KAH (NSF-OCE 1336206, OCE 1336905, and OCE 1336741). CB was funded by the Åbo Akademi University Foundation.

REFERENCES

Abbott, J. M., K. DuBois, R. K. Grosberg, S. L. Williams, and J. J. Stachowicz. 2018. Genetic distance predicts trait differentiation at the subpopulation but not the individual level in eelgrass, *Zostera marina*. Ecology and Evolution 8:7476–7489.

Abbott, J. M., R. K. Grosberg, S. L. Williams, and J. J. Stachowicz. 2017. Multiple dimensions of intraspecific diversity affect biomass of eelgrass and its associated community. Ecology 98:3152–3164.

Aberle, N., H. Hillebrand, J. Grey, and K. H. Wiltshire. 2005. Selectivity and competitive interactions between two benthic invertebrate grazers (*Asellus aquaticus* and *Potamopyrgus antipodarum*): an experimental study using 13C- and 15N-labelled diatoms. Freshwater Biology 50:369–379.

Anderson, M. J., K. E. Ellingsen, and B. H. McArdle. 2006. Multivariate dispersion as a measure of beta diversity. Ecology Letters 9:683–693.

Arfianti, T., and M. J. Costello. 2020. Global biogeography of marine amphipod crustaceans: latitude, regionalization, and beta diversity. Marine Ecology Progress Series 638:83–94.

Barnes, R. S. K., and M. D. F. Ellwood. 2011. Macrobenthic assemblage structure in a cool-temperate intertidal dwarf eelgrass bed in comparison with those from lower latitudes. Biological Journal of the Linnean Society 104:527–540.

Bartoń, K. 2020, April 14. Multi-Model Inference. R.

Blandon, A., and P. S. E. zu Ermgassen. 2014. Quantitative estimate of commercial fish enhancement by seagrass habitat in southern Australia. Estuarine, Coastal and Shelf Science 141:1–8.

Carr, L. A., K. E. Boyer, and A. J. Brooks. 2011. Spatial patterns of epifaunal communities in San Francisco Bay eelgrass (*Zostera marina*) beds. Marine Ecology 32:88–103.

Chaudhary, C., H. Saeedi, and M. J. Costello. 2016. Bimodality of latitudinal gradients in marine species richness. Trends in Ecology & Evolution 31:670–676.

Duffy, J. E., and A. M. Harvilicz. 2001. Species-specific impacts of grazing amphipods in an eelgrass-bed community. Marine Ecology Progress Series 223:201–211.

Duffy, J. E., A. R. Hughes, and P.-O. Moksnes. 2014. Ecology of seagrass communities. Pages 271–299 *in* M. D. Bertness, J. F. Bruno, and B. R. Silliman, editors. Marine community ecology and conservation. Sinauer Associates, Sunderland, MA, USA.

Duffy, J. E., J. J. Stachowicz, P. L. Reynolds, K. A. Hovel, M. Jahnke, E. E. Sotka, C. Boström, K. E. Boyer, M. Cusson, J. Eklöf, A. H. Engelen, B. K. Eriksson, F. J. Fodrie, J. N. Griffin, C. M. Hereu, M. Hori, A. R. Hughes, M. V. Ivanov, P. Jorgensen, C. Kruschel, K.-S. Lee, J. S. Lefcheck, P.-O. Moksnes, M. Nakaoka, M. I. O'Connor, N. E. O'Connor, R. J. Orth, B. J. Peterson, H. Reiss, K. Reiss, J. P. Richardson, F. Rossi, J. L. Ruesink, S. T. Schultz, J. Thormar, F. Tomas, R. Unsworth, E. Voigt, M. A. Whalen, S. L. Ziegler, and J. L. Olsen. 2022. A Pleistocene legacy structures variation in modern seagrass ecosystems. Proceedings of the National Academy of Sciences 119:e2121425119.

Duffy, J. E., S. L. Ziegler, J. E. Campbell, P. M. Bippus, and J. S. Lefcheck. 2015. Squidpops: a simple tool to crowdsource a global map of marine predation intensity. PLOS ONE 10:e0142994.

Garcia, H. E., R. A. Locarnini, T. P. Boyer, J. I. Antonov, M. M. Zweng, O. K. Baranova, and D. R. Johnson. 2010. World Ocean Atlas 2009, Volume 4: Nutrients (phosphate, nitrate, silicate). Page (S. Levitus, Ed.). U.S. Government Printing Office, Washington, D.C.

Gaston, K. J. 2000. Global patterns in biodiversity. Nature 405:220–227.

GBIF: Global Biogeographic Information Facility. 2023. . https://www.gbif.org/.

Graça, M. A., S. Y. Newell, and R. T. Kneib. 2000. Grazing rates of organic matter and living fungal biomass of decaying *Spartina alterniflora* by three species of salt-marsh invertebrates. Marine Biology 136:281–289.

Green, E. P., and F. T. Short. 2003. World atlas of seagrasses. University of California Press, Berkeley, CA, USA.

Ha, G., and S. L. Williams. 2018. Eelgrass community dominated by native omnivores in Bodega Bay, California, USA. Bulletin of Marine Science 94:1333–1353.

den Hartog, C. 1970. The seagrasses of the world. North Holland Publishing Co., Amsterdam.

Heck, K. L., G. Hays, and R. J. Orth. 2003. Critical evaluation of the nursery role hypothesis for seagrass meadows. Marine Ecology Progress Series 253:123–136.

Hijmans, R. J., and J. van Etten. 2020, November 14. raster: Geographic Data Analysis and Modeling. R.

Hughes, A. R., K. J. Bando, L. F. Rodriguez, and S. L. Williams. 2004. Relative effects of grazers and nutrients on seagrasses: a meta-analysis approach. Marine Ecology Progress Series 282:87–99.

Hughes, A. R., J. J. Stachowicz, and S. L. Williams. 2009. Morphological and physiological variation among seagrass (*Zostera marina*) genotypes. Oecologia 159:725–733.

Hughes, J. E., L. A. Deegan, J. C. Wyda, M. J. Weaver, and A. Wright. 2002. The effects of eelgrass habitat loss on estuarine fish communities of southern New England. Estuaries 25:235–249.

Intergovernmental Oceanographic Commission of UNESCO. 2023. OBIS: Ocean Biodiversity Information System. https://obis.org/.

Jernakoff, P., and J. Nielsen. 1997. The relative importance of amphipod and gastropod grazers in *Posidonia sinuosa* meadows. Aquatic Botany 56:183–202.

Lefcheck, J. S., and J. E. Duffy. 2015. Multitrophic functional diversity predicts ecosystem functioning in experimental assemblages of estuarine consumers. Ecology 96:2973–2983.

Lefcheck, J. S., J. van Montfrans, R. J. Orth, E. L. Schmitt, J. E. Duffy, and M. W. Luckenbach. 2014. Epifaunal invertebrates as predators of juvenile bay scallops (*Argopecten irradians*). Journal of Experimental Marine Biology and Ecology 454:18–25.

Leopardas, V., W. Uy, and M. Nakaoka. 2014. Benthic macrofaunal assemblages in multispecific seagrass meadows of the southern Philippines: Variation among vegetation dominated by different seagrass species. Journal of Experimental Marine Biology and Ecology 457:71–80.

Lewis, L. S., and T. W. Anderson. 2012. Top-down control of epifauna by fishes enhances seagrass production. Ecology 93:2746–2757.

Lindo, Z., and N. Winchester. 2013. Out on a limb: microarthropod and microclimate variation in coastal temperate rainforest canopies. Insect Conservation and Diversity 6:513–521.

Loke, L. H. L., and R. A. Chisholm. 2022. Measuring habitat complexity and spatial heterogeneity in ecology. Ecology Letters 25:2269–2288.

Lürig, M. D., R. J. Best, and J. J. Stachowicz. 2016. Microhabitat partitioning in seagrass mesograzers is driven by consistent species choices across multiple predator and competitor contexts. Oikos 125:1324–1333.

MacArthur, R. H., and J. W. MacArthur. 1961. On bird species diversity. Ecology 42:594–598.

Mayfield, M. M., and J. M. Levine. 2010. Opposing effects of competitive exclusion on the phylogenetic structure of communities. Ecology Letters 13:1085–1093.

McDevitt-Irwin, J. M., J. C. Iacarella, and J. K. Baum. 2016. Reassessing the nursery role of seagrass habitats from temperate to tropical regions: a meta-analysis. Marine Ecology Progress Series 557:133–143.

Montalbetti, E., L. Fallati, M. Casartelli, D. Maggioni, S. Montano, P. Galli, and D. Seveso. 2022. Reef complexity influences distribution and habitat choice of the corallivorous seastar Culcita schmideliana in the Maldives. Coral Reefs 41:253–264.

Olsen, J. L., W. T. Stam, J. A. Coyer, T. B. H. Reusch, M. Billingham, C. Boström, E. Calvert, H. Christie, S. Granger, R. L. Lumière, N. Milchakova, M.-P. Oudot-Le Secq, G. Procaccini, B. Sanjabi, E. Serrão, J. Veldsink, S. Widdicombe, and S. Wyllie-Echeverria. 2004. North Atlantic phylogeography and large-scale population differentiation of the seagrass *Zostera marina* L. Molecular Ecology 13:1923–1941.

Orth, R. J. 1992. A perspective on plant-animal interactions in seagrass: physical and biological determinants influencing plant and animal abundance. Pages 147–164 *in* D. M. John, S. T. Hawkins, and J. H. Price, editors. Plant –animal interactions in the marine benthos. Clarendon Press, Oxford.

Pianka, E. R. 1966. Latitudinal gradients in species diversity: a review of concepts. The American Naturalist 100:33–46.

R Development Core Team. 2022. R: a language and environment for statistical computing.

Reynolds, P. L., J. J. Stachowicz, K. Hovel, C. Boström, K. Boyer, M. Cusson, J. S. Eklöf, F. G. Engel, A. H. Engelen, B. K. Eriksson, F. J. Fodrie, J. N. Griffin, C. M. Hereu, M. Hori, T. C. Hanley, M. Ivanov, P. Jorgensen, C. Kruschel, K.-S. Lee, K. McGlathery, P.-O. Moksnes, M. Nakaoka, M. I. O'Connor, N. E. O'Connor, R. J. Orth, F. Rossi, J. Ruesink, E. E. Sotka, J. Thormar, F. Tomas, R. K. F. Unsworth, M. A. Whalen, and J. E. Duffy. 2018. Latitude, temperature, and habitat complexity predict predation pressure in eelgrass beds across the Northern Hemisphere. Ecology 99:29–35.

Sampaio, E., I. F. Rodil, F. Vaz-Pinto, A. Fernández, and F. Arenas. 2017. Interaction strength between different grazers and macroalgae mediated by ocean acidification over warming gradients. Marine Environmental Research 125:25–33.

Scheltema, A. H. 1997. Aplacophoran molluscs: deep-sea analogs to polychaetes. Bulletin of Marine Science 60:575–583.

Schmitz, O. J., and K. B. Suttle. 2001. Effects of top predator species on direct and indirect interactions in a food web. Ecology 82:2072–2081.

Serra, I. A., A. M. Innocenti, G. Di Maida, S. Calvo, M. Migliaccio, E. Zambianchi, C. Pizzigalli, S. Arnaud-Haond, C. M. Duarte, E. A. Serrao, and G. Procaccini. 2010. Genetic structure in the Mediterranean seagrass *Posidonia oceanica*: disentangling past vicariance events from contemporary patterns of gene flow. Molecular Ecology 19:557–568.

Thyrring, J., and L. S. Peck. 2021. Global gradients in intertidal species richness and functional groups. eLife 10:e64541.

Tyberghein, L., H. Verbruggen, K. Pauly, C. Troupin, F. Mineur, and O. D. Clerck. 2012. Bio-ORACLE: a global environmental dataset for marine species distribution modelling. Global Ecology and Biogeography 21:272–281.

Whalen, M. A., R. D. B. Whippo, J. J. Stachowicz, P. H. York, E. Aiello, T. Alcoverro, A. H. Altieri, L. Benedetti-Cecchi, C. Bertolini, M. Bresch, F. Bulleri, P. E. Carnell, S. Cimon, R. M. Connolly, M. Cusson, M. S. Diskin, E. D'Souza, A. A. V. Flores, F. J. Fodrie, A. W. E. Galloway, L. C. Gaskins, O. J. Graham, T. C. Hanley, C. J. Henderson, C. M. Hereu, M. Hessing-Lewis, K. A. Hovel, B. B. Hughes, A. R. Hughes, K. M. Hultgren, H. Jänes, D. S. Janiak, L. N. Johnston, P. Jorgensen, B. P. Kelaher, C. Kruschel, B. S. Lanham, K.-S. Lee, J. S. Lefcheck, E. Lozano-Álvarez, P. I. Macreadie, Z. L. Monteith, N. E. O'Connor, A. D. Olds, J. K. O'Leary, C. J. Patrick, O. Pino, A. G. B. Poore, M. A. Rasheed, W. W. Raymond, K. Reiss, O. K. Rhoades, M. T. Robinson, P. G. Ross, F. Rossi, T. A. Schlacher, J. Seemann, B. R. Silliman, D. L. Smee, M. Thiel, R. K. F. Unsworth, B. I. van Tussenbroek, A. Vergés, M. E. Yeager, B. K. Yednock, S. L. Ziegler, and J. E. Duffy. 2020. Climate drives the geography of marine consumption by changing predator communities. Proceedings of the National Academy of Sciences 117:28160–28166.

Table 3.1. Top 10 predictors in a random forest model that explained 56.5% of variation in the log-ratio of peracarid relative abundance to gastropod relative abundance across global eelgrass sites. Bolded rows indicate predictors included in the best model of log-ratio.

Predictor	Transformation	% Increase in MSE	% Increase in Node Impurity
Coast	None	23.469200	31.201383
Ocean Basin	**None**	**21.772421**	**29.091206**
In-situ Temperature (ºC)	None	14.963883	11.001778
Eelgrass Morphology PC1 (62.09%)	None	14.214091	30.976627
Eelgrass Allelic Richness (avg. number of alleles per locus, normalized to 7 genets)	**Squared**	**12.844151**	**21.280422**
Mean Eelgrass Leaf % C	None	10.997176	13.525104
Site Peracarid Richness	**log + 1**	**9.401629**	**11.836563**
Genotypic Richness (mean Rozenfeld distance)	None	6.845336	3.603339
Mean Water Column Chl a	log	6.779512	6.117515
Mean Water Column Silicate	log	6.455153	4.595070

Table 3.2. Top 10 candidate traits (continuous) and trait states (categorical) associated with increases in log-ratio peracarid relative abundance to gastropod relative abundance across sites, as output from a random forest model explaining 62.48% of variation in log-ratios. Bolded rows indicate trait states unique to gastropods.

Trait value	% Increase in MSE	Increase in Node Impurity	Spearman ρ	p
Brooder	14.792646	85.317146	0.8086603	6.188e-12
Mean Latitude	14.093822	72.964589	-0.6279949	2.298e-06
Lays Egg Case	**8.811130**	**36.860245**	**-0.7153161**	**1.607e-08**
Direct Developer	6.700999	19.853744	0.56727	3.214e-05
Latitudinal Range	5.559044	21.833437	-0.5122888	0.0002322
Suspension Feeder	5.396012	23.410392	0.5174202	0.0001958
Non-Suspension Feeder	4.523542	13.447565	-0.517311	0.0001965
Non-carnivore/parasite/scavenger	3.554432	10.720121	-0.471435	0.0008231
Broadcast Spawner	**3.516959**	**4.040270**	**-0.1846305**	**0.2141**
Microalgal Grazer	3.066659	5.222737	-0.3014138	0.0395

Table 3.3. Mean trait values of the peracarid and gastropod community in 5 a posteriori groups of eelgrass sites created by hierarchical clustering based on similarities in site-level community-weighted mean trait values. Dominant values for binary and categorical traits are shown, while group-level community-weighted means are supplied for continuous traits. Observed sizes are derived from sieved epifaunal samples. Latitudinal range and mean latitude are derived from observations gathered from GBIF and OBIS.

Group	Diet	Parental Care	Developmental mode	Mode Obs. Size (mm)	Max Obs. Size (mm)
1 - "Cold Pacific"	Microalgal grazer	Brooder	Direct development	2.585	5.556
2 - Croatia	Microalgal grazer, detritivore	Broadcast spawner	Lecithotrophic	2.800	8.000
3 - "Warm Sites"	Microalgal grazer	Brooder	Direct development	1.443	5.042
4 - "Cold Atlantic"	Microalgal grazer, macroalgal grazer	Lays egg case	Direct development	1.440	4.139
5 - "Asia"	Microalgal grazer, detritivore	Brooder	Direct development	1.578	4.959

Table 3.3, continued.

Group	Mean Obs. Size (mm)	Max Lit. Size (mm)	Lat. Range	Lat. Mean	Salinity
1 - "Cold Pacific"	2.473	23.428	32.574º	46.735º	Marine
2 - Croatia	2.364	15.000	68.471º	52.156º	Marine, Brackish, Freshwater
3 - "Warm Sites"	1.669	15.000	38.205º	36.942º	Marine
4 - "Cold Atlantic"	1.474	14.141	45.610º	52.584º	Marine
5 - "Asia"	1.713	11.646	21.788º	37.782º	Marine

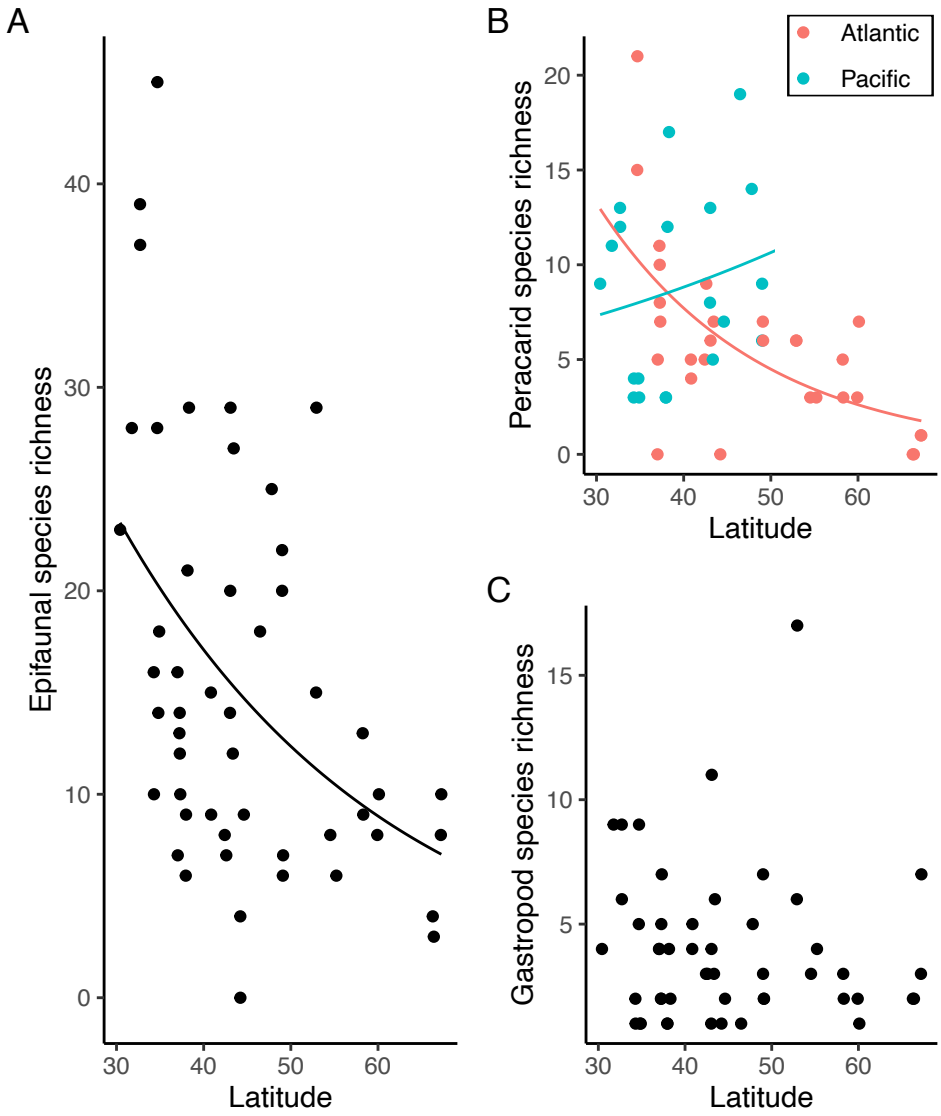

Figure 3.1. Latitudinal clines in species richness for all epifauna (A), peracarids (B), and gastropods (C) across global eelgrass sites. There was a significant relationship between latitude and total epifaunal species richness in both the Atlantic and Pacific oceans ($\chi^2_1 = 67.999$, $p < 0.001$). Peracarids showed opposite patterns of richness with latitude in the Pacific and Atlantic ($\chi^2_1 = 22.331$, $p < 0.001$), while gastropods showed no significant latitudinal richness gradient.

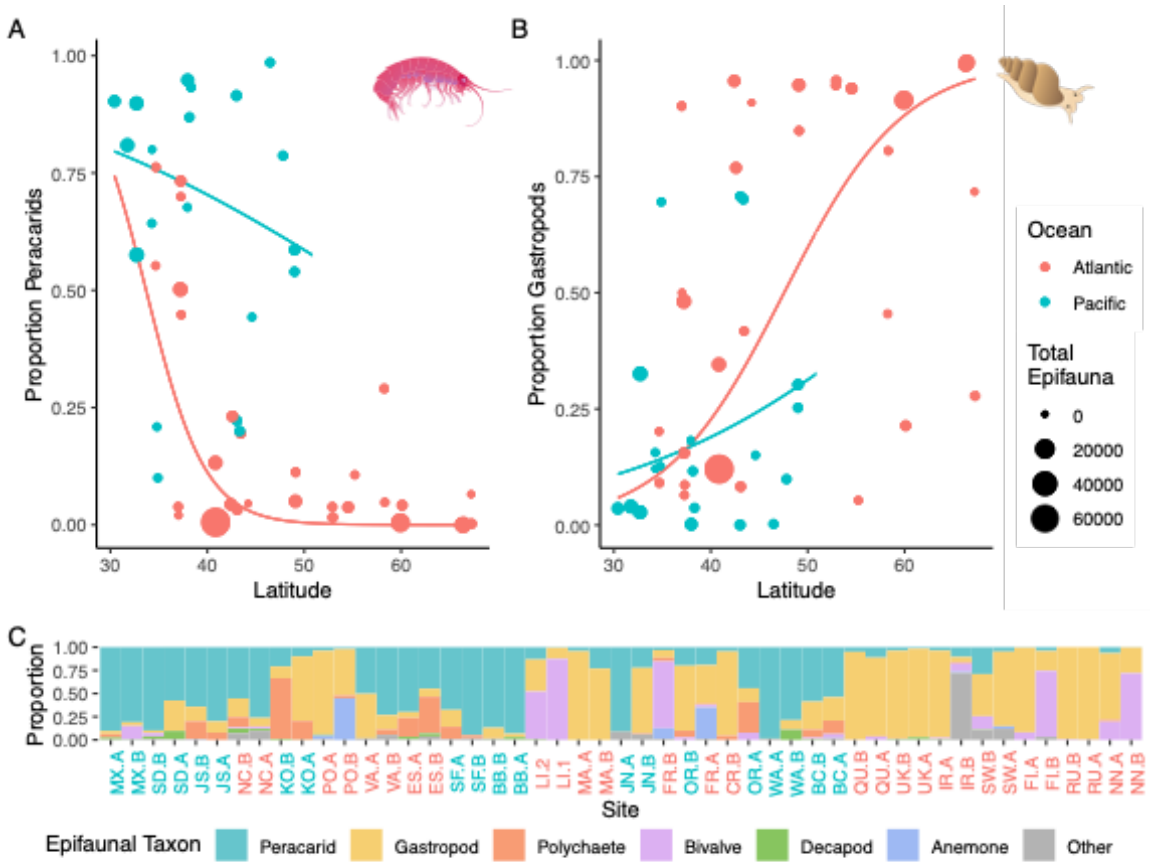

Figure 3.2. Latitudinal clines in the dominance of peracarid crustaceans (A) and gastropods (B) across global epifaunal communities (C). The relative abundance of each taxon changed significantly with latitude (peracarids $\chi^2_1 = 11284.0$, $p < 0.001$; gastropods $\chi^2_1 = 58295$, $p < 0.001$). For both taxa, the latitudinal clines varied significantly between ocean basins (peracarids $\chi^2_1 = 3524.8$, $p < 0.001$; gastropods $\chi^2_1 = 1722$, $p < 0.001$). Site labels in C are colored according to ocean basin as in panels A and B, and arranged from lowest (on the left) to highest latitude (on the right); site locations are shown in Fig. A4.1 and Table A4.1.

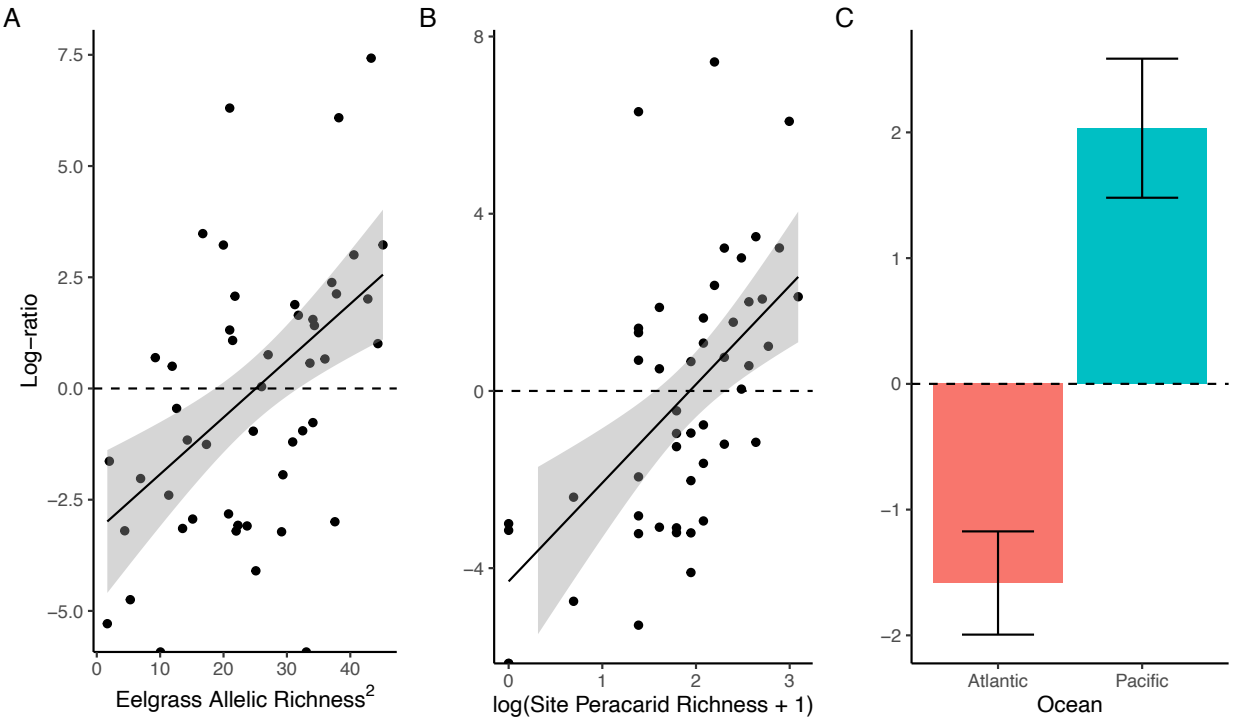

Figure 3.1. The best predictors of the log-transformed ratio of peracarid relative abundance to gastropod relative abundance in epifaunal communities across sites. Log-ratios were best explained by an additive model including eelgrass allelic richness, peracarid species richness, and ocean basin ($F_{3,43} = 20.42$, $p < 0.001$). The horizontal dashed line indicates a 1:1 ratio of gastropods to peracarids.

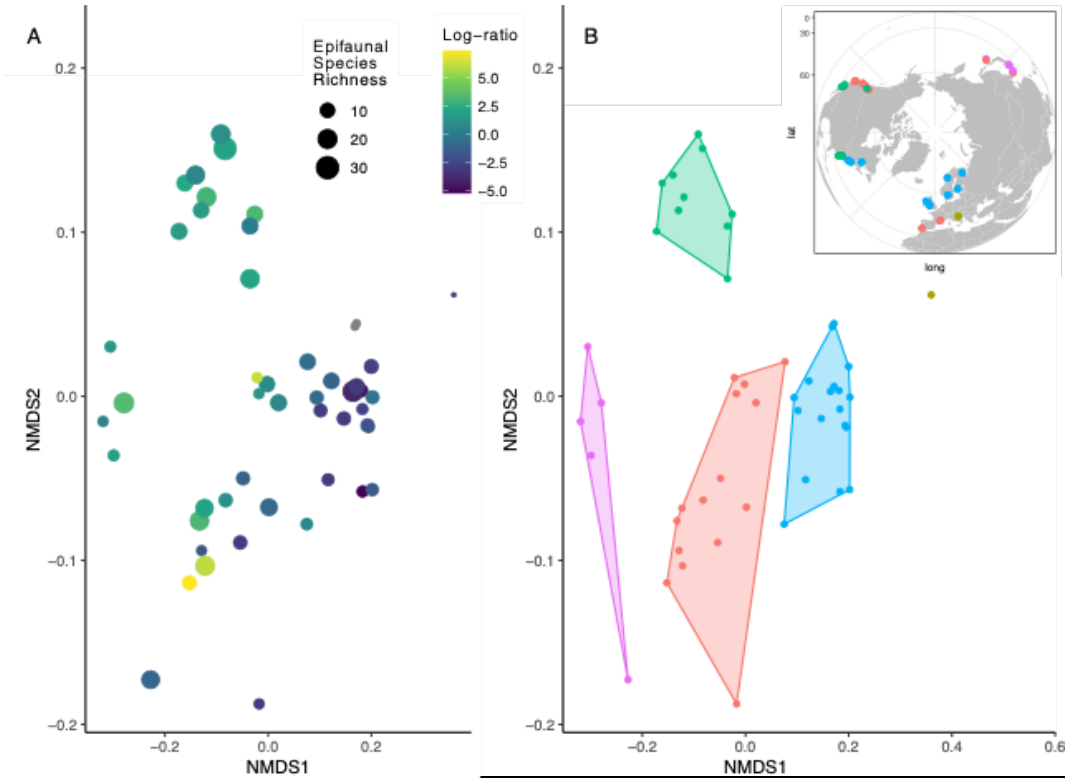

Figure 3.2. NMDS ordinations of eelgrass epifaunal communities in trait space. Points represent individual sites, and points that fall more closely together are more similar in community-weighted mean trait values. In (A), sites are colored by the log-ratio of the relative abundance of peracarids and gastropods; positive log-ratios indicate more peracarids than gastropods, while negative log-ratios indicate more gastropods than peracarids. Log-ratios significantly predicted sites' positions in trait space (pseudo $F_{1,45} = 11.918$, $p < 0.001$). In (B), the same sites are colored according to membership to one of 5 groups created by hierarchical clustering based on similarities in community-weighted mean trait values; inset map shows the geographic location of groups.

APPENDIX 1: Supplementary material for Chapter 1

Table A1.1. Results of t-tests comparing average SES values within ocean basins to zero. SES values are calculated relative to the global species pool; p values in bold represent significance at an a level of 0.05.

Ocean	Metric	Permutation Algorithm	Trait Set	Mean SES	t	df	p
Pacific	MPD	Independent Swap	All	0.393	2.27	19	**0.0352**
			Microhabitat	0.404	2.41	19	**0.0261**
			Diet	0.415	1.66	19	0.114
		Tip Shuffle	All	0.363	2.12	19	**0.0479**
			Microhabitat	0.412	2.86	19	**0.0101**
			Diet	0.381	1.56	19	0.135
	MNTD	Independent Swap	All	0.155	0.589	19	0.563
			Microhabitat	0.686	3.48	19	**0.00254**
			Diet	-0.0449	-0.155	17	0.879
		Tip Shuffle	All	0.221	0.855	19	0.403
			Microhabitat	0.737	3.73	19	**0.00143**
			Diet	0.263	0.684	14	0.505
Atlantic	MPD	Independent Swap	All	-0.156	-1.07	21	0.295
			Microhabitat	-0.0959	-0.518	21	0.61
			Diet	-0.0998	-0.532	20	0.601
		Tip Shuffle	All	-0.699	-4.23	21	**0.000375**
			Microhabitat	-0.505	-2.55	21	**0.0185**
			Diet	-0.382	-2.06	20	0.0531
	MNTD	Independent Swap	All	-0.364	-2.4	21	**0.026**
			Microhabitat	-0.314	-1.74	21	0.0974
			Diet	-0.272	-1.77	19	0.0935
		Tip Shuffle	All	-0.358	-2.35	21	**0.0285**
			Microhabitat	-0.3327	-1.69	21	**0.011**
			Diet	0.00933	0.0394	14	0.9691

Table A1.2. Average predation rate and epiphyte load across ocean basins. Values in the first two rows are mean ± standard deviation. Values in the third row represent the results of two-sample t-tests on untransformed (predation) and log-transformed (epiphytes) data across oceans.

Ocean	Prop. Tethered Prey Removed		g Epiphytes g Eelgrass^{-1}	
Pacific	0.80 ± 0.20		0.30 ± 0.31	
Atlantic	0.64 ± 0.24		0.13 ± 0.12	
Difference	t = 2.18	p = 0.037	t = 1.13	p = 0.27

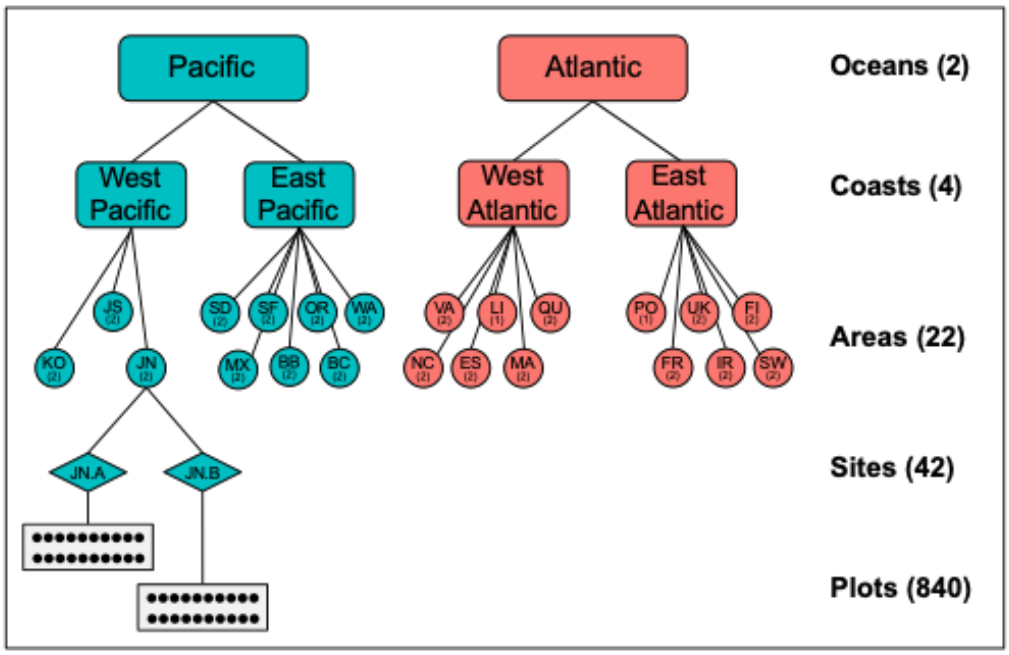

Figure A1.1. Hierarchical design of the ZEN 2014 seagrass ecosystem survey. Sites are nested in one of 22 areas: KO = South Korea; JS = southern Japan (Seto Inland Sea); JN = northern Japan (Hokkaido); SD = San Diego Bay, US; MX = Mexico (Pacific Baja California); SF = San Francisco Bay, US; BB = Bodega and Tomales Bays, US; OR = Oregon, US, BC = British Columbia, Canada; WA = Washington State, US; NC = North Carolina (Back Sound), US; VA = York River, Virginia, US; ES = Virginia Eastern Shore, US; LI = Long Island, US; MA = Massachusetts, US; QU = Quebec (St. Lawrence Estuary), Canada; PO = Algarve, Portugal; FR = Mediterranean France; UK = Wales, UK; IR = Ireland; FI = Archipelago Sea, Finland; SW = Swedish west coast. Numbers in parentheses indicate the number of sites in a given area.

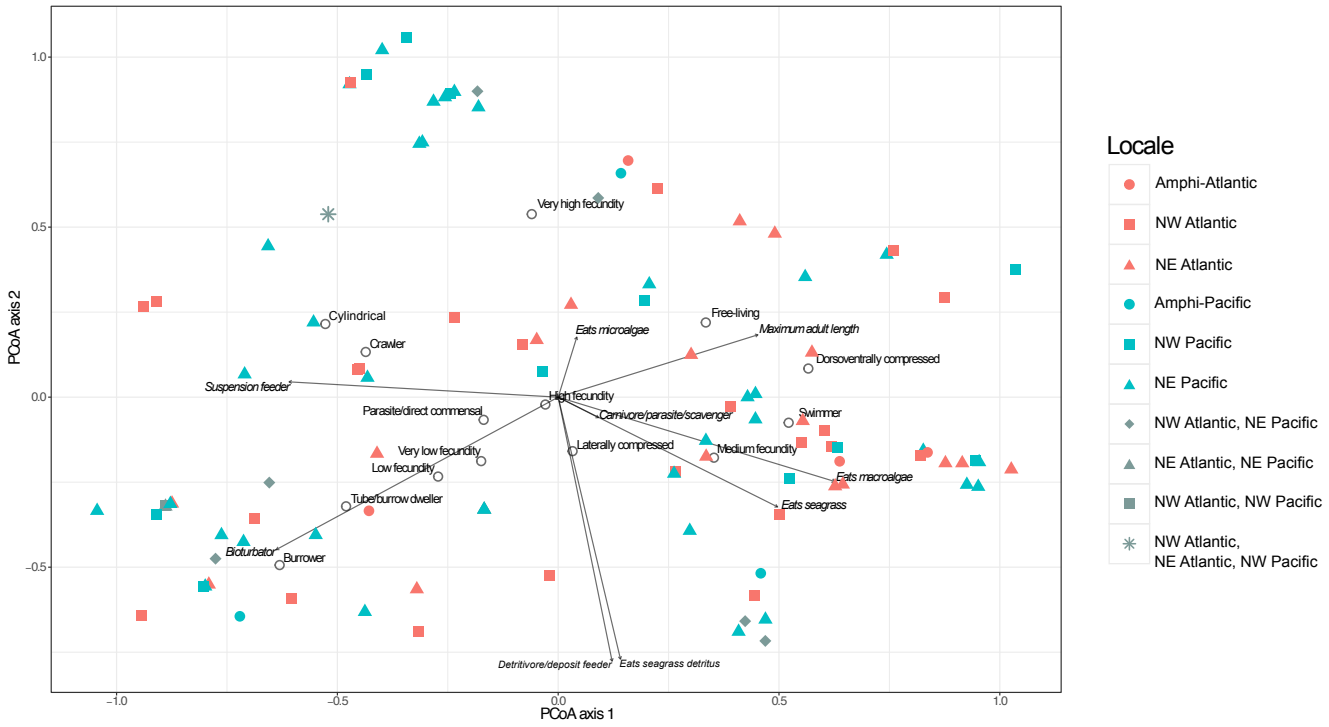

Figure A1.2. Principal coordinates analysis (PCoA) biplot of peracarid species in our global species pool, based on Gower distances. Solid symbols represent species in trait space, with symbol shape and colour corresponding to where they were found in our samples; hollow symbols represent centroids for categorical traits. Traits were fairly independent, and few were strongly correlated. Additionally, locale was not a significant predictor of where a given species fell in trait space (PERMANOVA; pseudo $F_{9,95} = 0.98$, $p = 0.51$). In other words, there were no traits that were particularly distinct to regions. Amphi-Pacific and Amphi-Atlantic distributions refer to species that occur in both the western and eastern margins of the Pacific and Atlantic Oceans, respectively.

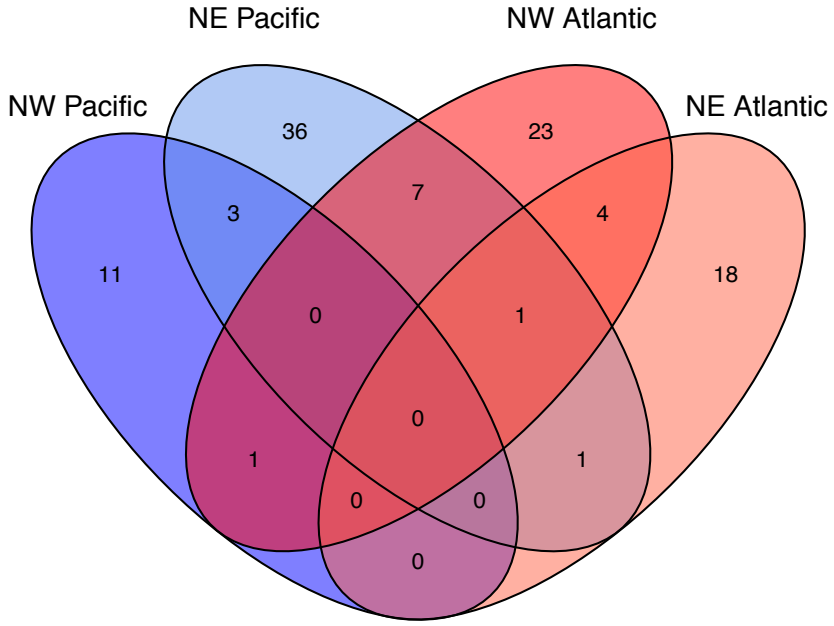

Figure A1.3. Peracarid species richnesses across the four coastlines observed in this study. 55 species were collected from Atlantic sites and 60 species were collected from Pacific sites. Of these, 15 species were collected from the Northwest Pacific, 48 species from the Northeast Pacific, 36 species from the Northwest Atlantic, and 24 species from the Northeast Atlantic. There were 37 genera in 24 families in the Pacific and 40 genera in 22 families in the Atlantic.

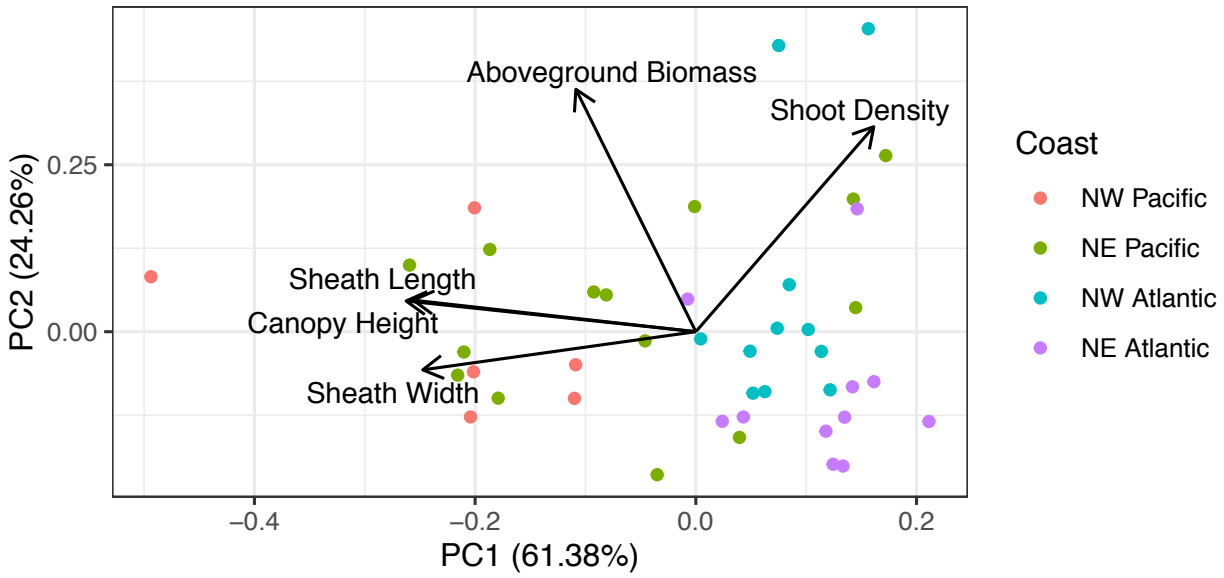

Figure A1.4. Principal component biplot for eelgrass habitat structure across sites. Most of the variation in eelgrass was between short canopies of dense shoots and taller canopies of sparser shoots. The first two principal components accounted for 85.64% of the total variation in habitat structure at the site level. Eelgrass beds in the Atlantic Ocean were mostly characterized by small, densely packed shoots, while those in the Northwest Pacific contained larger, sparser shoots. Northeast Pacific sites contained both of these bed types.

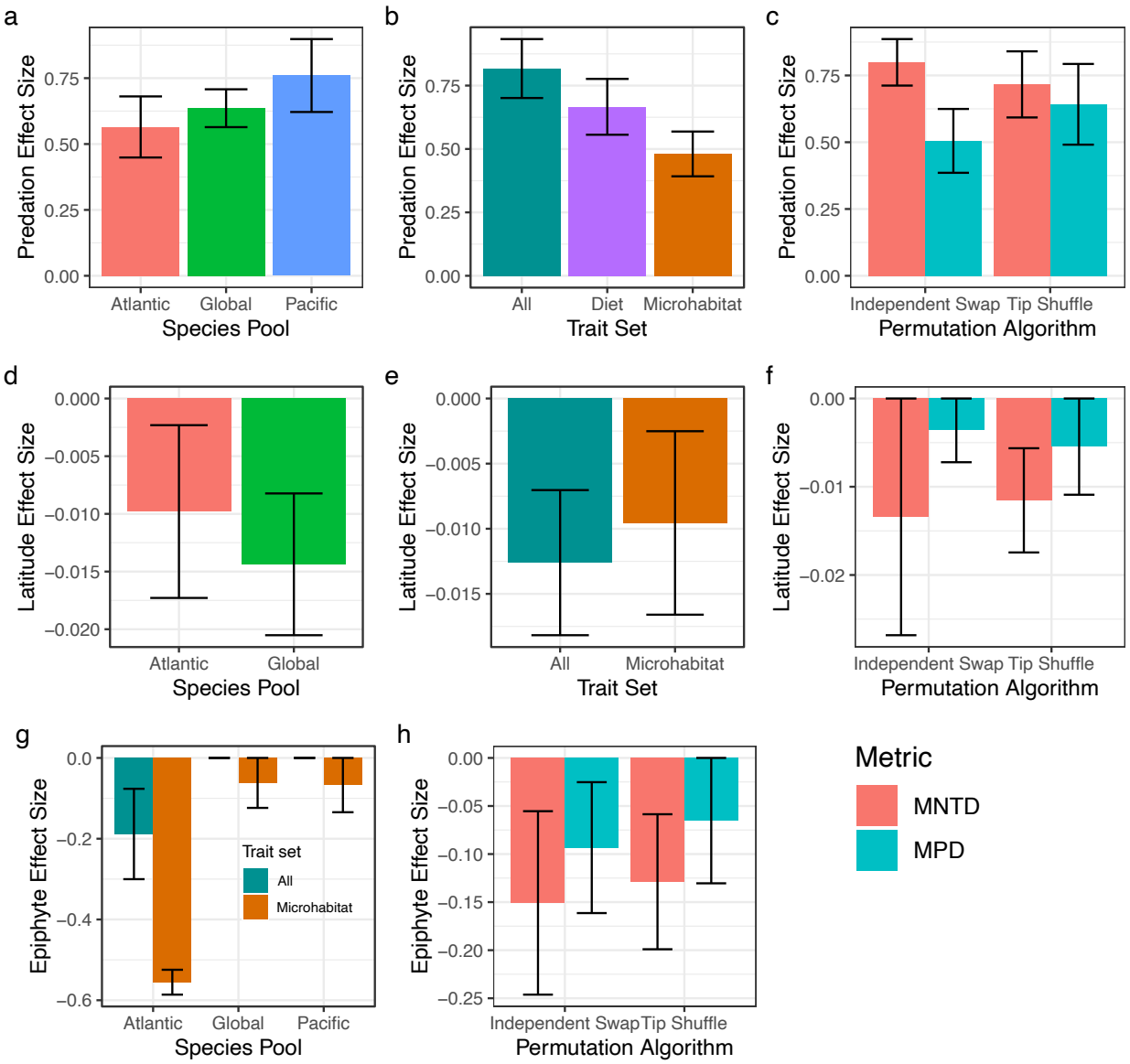

Figure A1.5. Effects of predation (a-c), latitude (d-f), and epiphyte load (g-h) in best models of site-level trait dispersion (SES values) across three species pools (a, d, g), 3 sets of traits (b, e, g), two permutation algorithms, and two dispersion metrics (c, f, h). Columns show mean effect sizes (across best models selected by AICc) averaged across species pools, trait sets, algorithms, and metrics where appropriate; error bars represent standard errors.

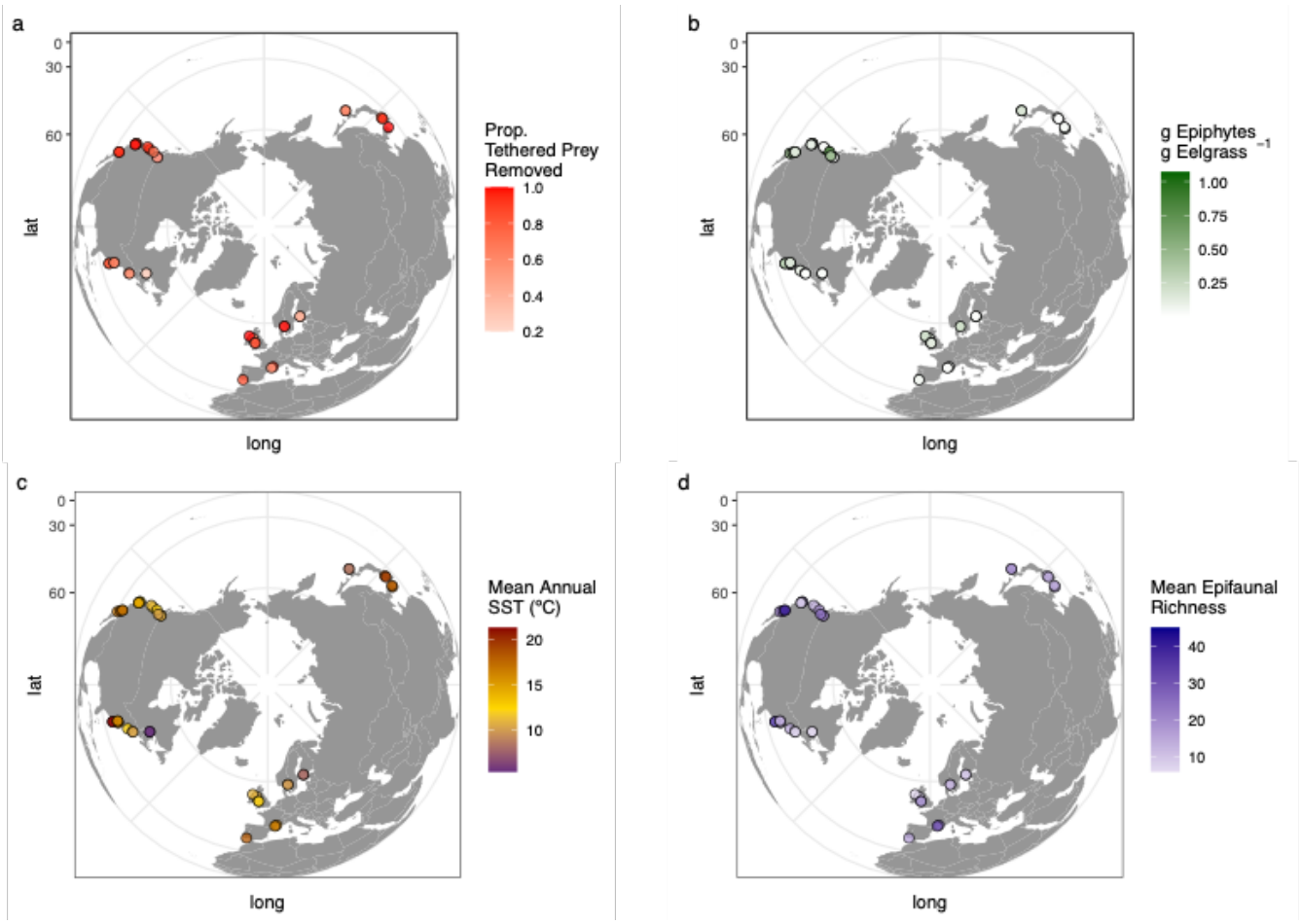

Figure A1.6. Maps of predation intensity (a), epiphyte load (b), mean annual sea surface temperature (c), and epifaunal species richness (d) across sites and ocean basins. None of these predictors varied significantly by ocean basin. See Fig. A1.1 for more detailed information about site locations.

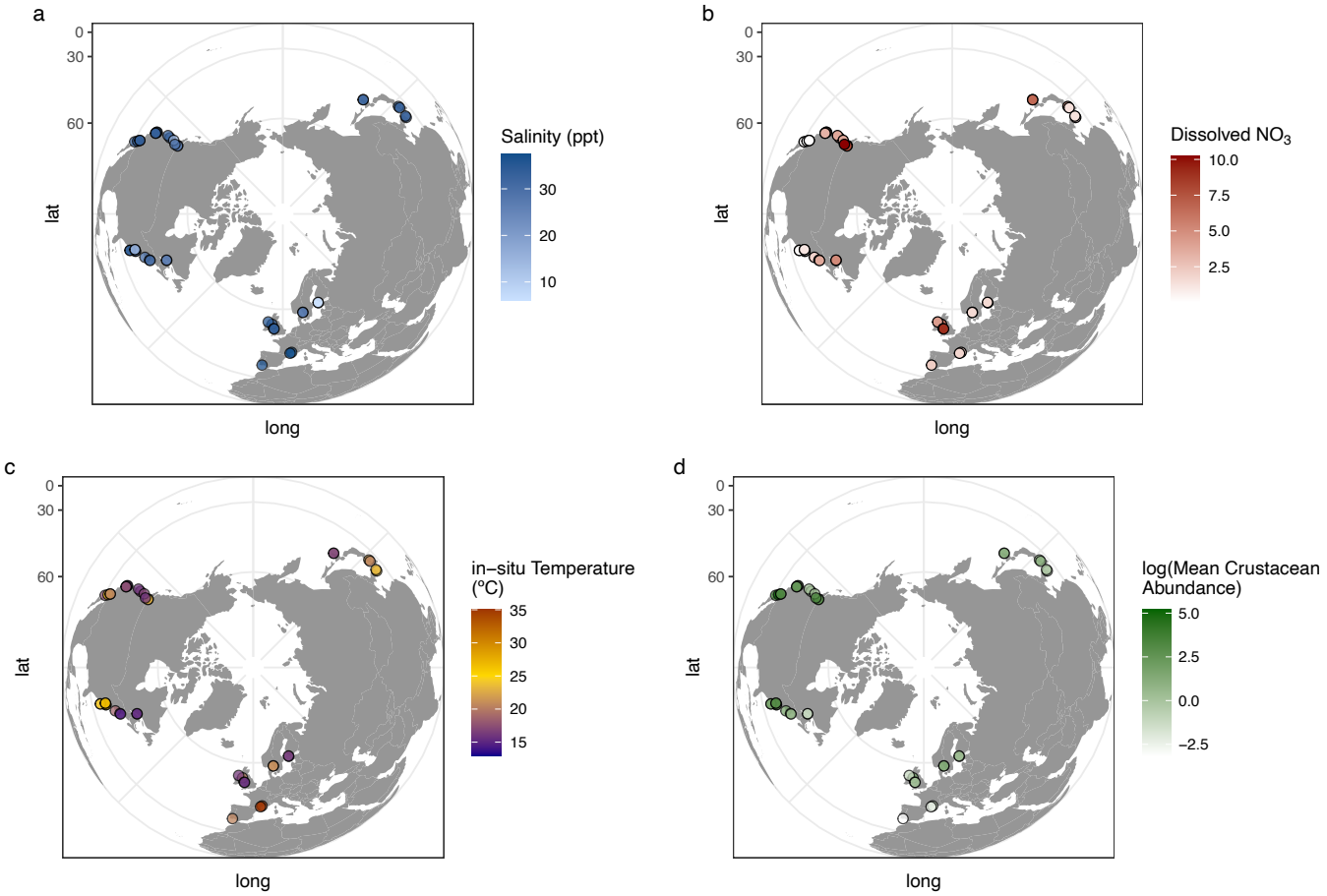

Figure A1.7. Maps of salinity (a), water column nitrate (b), in-situ temperature (c), and crustacean abundance (d) across sites and ocean basins. Of these predictor, only crustacean abundance was significantly greater in the Pacific ($R^2 = 0.076$, $p = 0.043$). See Fig. A1.1 for more detailed information about site locations.

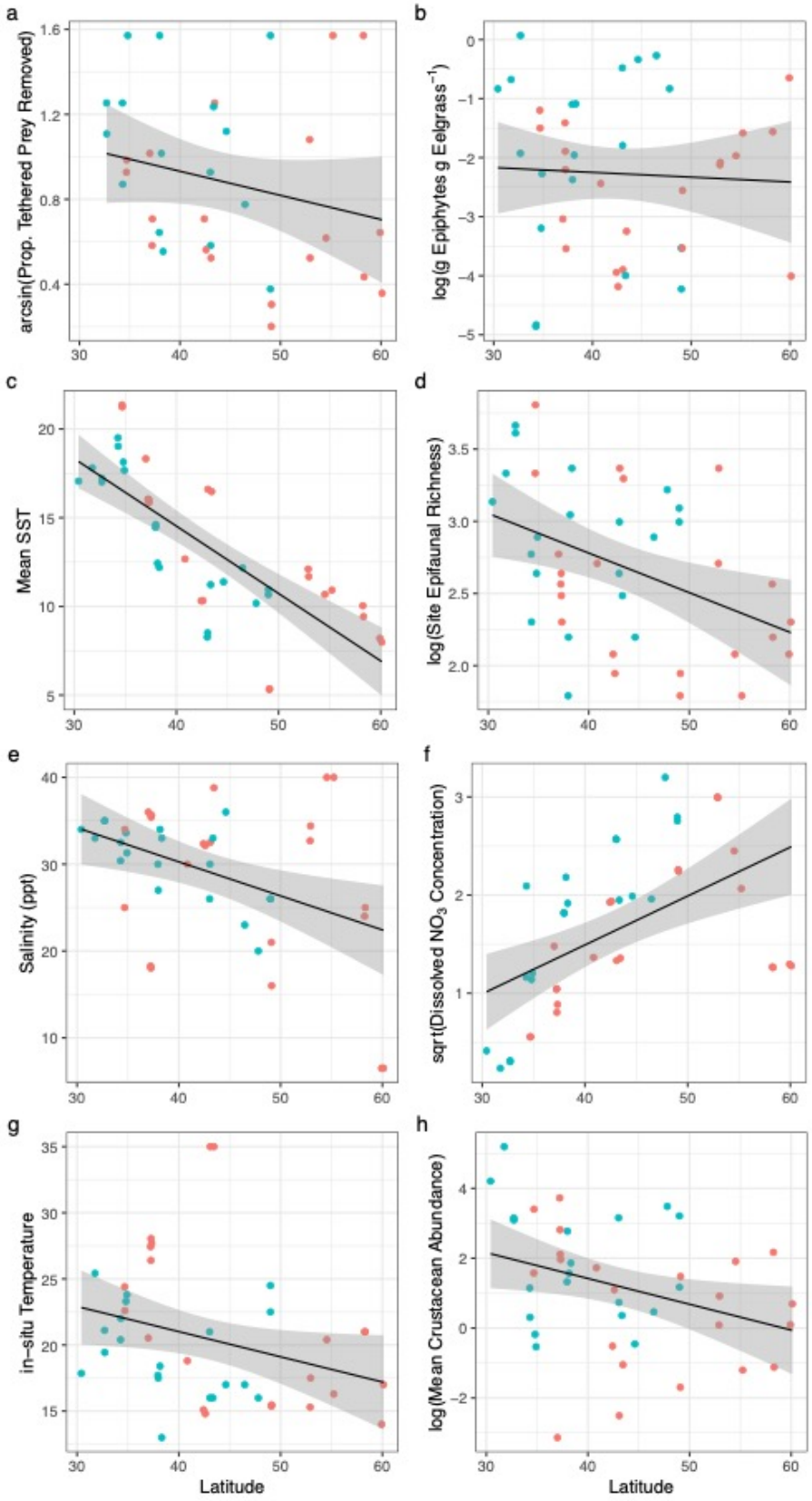
a
arcsin(Prop. Tethered Prey Removed)
b
log (g Epiphytes g Eelgrass^{-1})
c
Mean SST
d
log (Site Epifaunal Richness)
e
Salinity (ppt)
f
sqrt(Dissolved NO_3 Concentration)
g
in−situ Temperature
h
log (Mean Crustacean Abundance)
Latitude
Latitude

Figure S8. Predictors used in models of dispersion, including predation intensity (a), epiphyte load (b), mean sea surface temperature (c), epifaunal richness (d), salinity (e), water column nitrate (f), in-situ temperature (g), and crustacean abundance (h), plotted against latitude. Without accounting for other variables, latitude was a significant predictor of mean sea surface temperature ($R^2 = 0.58$, $p < 0.0001$), site epifaunal richness (log-transformed; $R^2 = 0.15$, $p = 0.0062$), salinity ($R^2 = 0.16$, $p = 0.0056$), nitrate (square root-transformed; $R^2 = 0.26$, $p = 0.00034$), in-situ temperature ($R^2 = 0.074$, $p = 0.046$), and crustacean abundance (log-transformed; $R^2 = 0.092$, $p = 0.029$). Points represent sites, color-coded by ocean; Atlantic sites are in red, Pacific sites are in blue.

APPENDIX 2: References for peracarid trait data used in global analyses of trait dispersion

Arimoto, I. 1976. Taxonomic studies of caprellids (Crustacea, Amphipoda, Caprellidae) found in the Japanese and adjacent waters. Special Publications from the Seto Marine Biological Laboratory 3:234.

Ariyama, H. 2004. Nine Species of the Genus *Aoroides* (Crustacea : Amphipoda : Aoridae) from Osaka Bay, Central Japan. Publications of the Seto Marine Biological Laboratory 40:1–66.

Ashford, O. S., A. J. Kenny, C. R. S. Barrio Froján, M. B. Bonsall, T. Horton, A. Brandt, G. J. Bird, S. Gerken, and A. D. Rogers. 2018. Phylogenetic and functional evidence suggests that deep-ocean ecosystems are highly sensitive to environmental change and direct human disturbance. Proceedings of the Royal Society B: Biological Sciences 285:20180923.

Beermann, J., and H.D. Franke. 2011. A supplement to the amphipod (Crustacea) species inventory of Helgoland (German Bight, North Sea): Indication of rapid recent change. Marine Biodiversity Records 4:1–15.

Best, R. J., and J. J. Stachowicz. 2012. Trophic cascades in seagrass meadows depend on mesograzer variation in feeding rates, predation susceptibility, and abundance. Marine Ecology Progress Series 456:29–42.

Best, R. J., and J. J. Stachowicz. 2013. Phylogeny as a Proxy for Ecology in Seagrass Amphipods: Which Traits Are Most Conserved? PLOS ONE 8:e57550.

Borges, F. O., C. Figueiredo, E. Sampaio, R. Rosa, and T. F. Grilo. 2018. Transgenerational deleterious effects of ocean acidification on the reproductive success of a keystone crustacean (*Gammarus locusta*). Marine Environmental Research 138:55–64.

Borowsky, B. 1996. Laboratory Observations On the Life History of the Isopod *Sphaeroma quadridentatum* Say, 1818. Crustaceana 69:94–100.

Boström, C., and E. Bonsdorff. 1997. Community structure and spatial variation of benthic invertebrates associated with *Zostera marina* (L.) beds in the northern Baltic Sea. Journal of Sea Research 37:153–166.

Brook, H. J., T. A. Rawlings, and R. W. Davies. 1994. Protogynous Sex Change in the Intertidal Isopod *Gnorimosphaeroma oregonense* (Crustacea: Isopoda). The Biological Bulletin 187:99–111.

Cruz-García, R., A. L. Cupul-Magaña, M. E. Hendrickx, and A. P. Rodríguez-Troncoso. 2013. Abundance of three species of Isopoda (Peracarida, Isopoda) associated with a coral reef environment in Pacific Mexico. Crustaceana 86:1664–1674.

Drumm, D. T., and B. Kreiser. 2012. Population genetic structure and phylogeography of *Mesokalliapseudes macsweenyi* (Crustacea: Tanaidacea) in the northwestern Atlantic and Gulf of Mexico. Journal of Experimental Marine Biology and Ecology 412:58–65.

Duffy, J. E., and A. M. Harvilicz. 2001. Species-specific impacts of grazing amphipods in an eelgrass-bed community. Marine Ecology Progress Series 223:201–211.

Duffy, J. E., and M. E. Hay. 1991. Food and shelter as determinants of food choice by an herbivorous marine amphipod. Ecology 72:1286–1298.

Ferreira, A. C., E. S. Ambrosio, and A. R. Capítulo. 2015. Population ecology of *Sinelobus stanfordi* (Crustacea: Tanaidacea) in a temperate southern microtidal estuary. New Zealand Journal of Marine and Freshwater Research 49:462–471.

Fincham, A. A. 1974. Rhythmic swimming of the isopod *Exosphaeroma obtusum* (Dana). New Zealand Journal of Marine and Freshwater Research 8:655–662.

Ford, A. T., T. F. Fernandes, S. A. Rider, P. A. Read, C. D. Robinson, and I. M. Davies. 2003. Reproduction in the amphipod, *Echinogammarus marinus*: a comparison between normal and intersex specimens. Journal of the Marine Biological Association of the United Kingdom 83:937–940.

Gaston, K. J., and J. I. Spicer. 2001. The relationship between range size and niche breadth: a test using five species of *Gammarus* (Amphipoda). Global Ecology and Biogeography 10:179–188.

Gray, A. P., C. A. Richardson, and R. Seed. 1997. Ecological relationships between the valviferan isopod *Edotia doellojuradoi* Giambiagi, 1925, and its host *Mytilus edulis chilensis* in the Falkland Islands. Estuarine, Coastal and Shelf Science 44:231–239.

Greve, L. 1974. *Anatanais normani* (Richardson) found near Bermuda and notes on other *Anatanais* species. Sarsia 55:115–120.

Guerra-García, J. M., and J. M. Tierno de Figueroa. 2009. What do caprellids (Crustacea: Amphipoda) feed on? Marine Biology 156:1881–1890.

Hosono, T. 2014. Temperature explains reproductive dynamics in caprellids at different latitudes. Marine Ecology Progress Series 511:129–141.

Hou, Z., J. Fu, and S. Li. 2007. A molecular phylogeny of the genus *Gammarus* (Crustacea: Amphipoda) based on mitochondrial and nuclear gene sequences. Molecular Phylogenetics and Evolution 45:596–611.

Ingólfsson, A. 2000. Colonization of floating seaweed by pelagic and subtidal benthic animals in southwestern Iceland. Pages 181–189 *in* M. B. Jones, J. M. N. Azevedo, A. I. Neto, A. C. Costa, and A. M. F. Martins, editors. Island, Ocean and Deep-Sea Biology. Springer Netherlands.

Jeong, S. J., O. H. Yu, and H. L. Suh. 2007. Life History and Reproduction of *Jassa slatteryi* (Amphipoda, Ischyroceridae) on a Seagrass Bed (*Zostera marina* L.) in Southern Korea. Journal of Crustacean Biology 27:65–70.

Jung, T. W., S. Jeong, D. Han, M.-S. Kim, and S. Yoon. 2016. The First Record of the Genus *Eogammarus* (Crustacea: Amphipoda: Anisogammridae) from Korea. ASED.

Khalaji-Pirbalouty, V., N. Bruce, and J. W. Wägele. 2013. The genus *Cymodoce* Leach, 1814 (Crustacea: Isopoda: Sphaeromatidae) in the Persian Gulf with description of a new species. Zootaxa 3686.

Kondylatos, G., M. Corsini-Foka, and E. Perakis. 2018. First record of the isopod *Idotea hectica* (Pallas, 1772) (Idoteidae) and of the brachyuran crab *Matuta victor* (Fabricius, 1781) (Matutidae) in the Hellenic waters. Mediterranean Marine Science 19:656–661.

Kunkel, B. Waugh., and B. W. Kunkel. 1918. The Arthrostraca of Connecticut. State Geological and Natural History Survey, Hartford,.

Ledet, J., M. Byrne, and A. G. B. Poore. 2018. Temperature effects on a marine herbivore depend strongly on diet across multiple generations. Oecologia 187:483–494.

Lefcheck, J. S., and J. E. Duffy. 2015. Multitrophic functional diversity predicts ecosystem functioning in experimental assemblages of estuarine consumers. Ecology 96:2973–2983.

Levings, C. D. 1980. The biology and energetics of *Eogammarus confervicolus* (Stimpson) (Amphipoda, Anisogammaridae) at the Squamish River Estuary, B.C. Canadian Journal of Zoology 58:1652–1663.

Lindén, E., M. Lehtiniemi, and M. Viitasalo. 2003. Predator avoidance behaviour of Baltic littoral mysids *Neomysis integer* and *Praunus flexuosus*. Marine Biology 143:845–850.

Lürig, M. D., R. J. Best, and J. J. Stachowicz. 2016. Microhabitat partitioning in seagrass mesograzers is driven by consistent species choices across multiple predator and competitor contexts. Oikos 125:1324–1333.

Mancinelli, G. 2012. To bite, or not to bite? A quantitative comparison of foraging strategies among three brackish crustaceans feeding on leaf litters. Estuarine, Coastal and Shelf Science 110:125–133.

Martínez-Laiz, G., A. Ulman, M. Ros, and A. Marchini. 2019. Is recreational boating a potential vector for non-indigenous peracarid crustaceans in the Mediterranean Sea? A combined biological and social approach. Marine Pollution Bulletin 140:403–415.

Menzies, R. J. 1951. New Marine Isopods, Chiefly from Northern California, with Notes on Related Forms.

Nakamachi, T., H. Ishida, and N. Hirohashi. 2015. Sound Production in the Aquatic Isopod *Cymodoce japonica* (Crustacea: Peracarida). The Biological Bulletin 229:167–172.

Othman, M. S., and D. Pascoe. 2001. Growth, Development and Reproduction of *Hyalella azteca* (Saussure, 1858) in Laboratory Culture. Crustaceana 74:171–181.

Pennafirme, S., and A. Soares-Gomes. 2009. Population biology and reproduction of *Kalliapseudes schubartii* Mañé-Garzón, 1949 (Peracarida, Tanaidacea) in a tropical coastal lagoon, Itaipu, southeastern Brazil. Crustaceana 82:1509–1526.

Pilgrim, E. M., M. J. Blum, D. A. Reusser, H. Lee, and J. A. Darling. 2013. Geographic range and structure of cryptic genetic diversity among Pacific North American populations of the non-native amphipod *Grandidierella japonica*. Biological Invasions 15:2415–2428.

Poore, A. G. B., S. T. Ahyong, J. K. Lowry, and E. E. Sotka. 2017. Plant feeding promotes diversification in the Crustacea. Proceedings of the National Academy of Sciences 114:8829–8834.

Rumbold, C. E., S. M. Obenat, and E. D. Spivak. 2012. Life History of *Tanais dulongii* (Tanaidacea: Tanaidae) in an Intertidal Flat in the Southwestern Atlantic. Journal of Crustacean Biology 32:891–898.

Rumbold, C. E., S. M. Obenat, and E. D. Spivak. 2015. Comparison of life history traits of *Tanais dulongii* (Tanaidacea: Tanaididae) in natural and artificial marine environments of the south-western Atlantic. Helgoland Marine Research 69:231.

Sainte-Marie, B. 1991. A review of the reproductive bionomics of aquatic gammaridean amphipods: variation of life history traits with latitude, depth, salinity and superfamily. Hydrobiologia 223:189–227.

Schückel, U., M. Beck, and I. Kröncke. 2013. Spatial variability in structural and functional aspects of macrofauna communities and their environmental parameters in the Jade Bay (Wadden Sea Lower Saxony, southern North Sea). Helgoland Marine Research 67:121.

Schultz, G. A. 1969. How to know the marine isopod crustaceans. Wm. C. Brown Company Publishers, Dubuque, IA, USA.

Shuster, S. M. 1995. Female reproductive success in artificial sponges in *Paracerceis sculpta* (Holmes) (Crustacea: Isopoda). Journal of Experimental Marine Biology and Ecology 191:19–27.

Skadsheim, A. 1984. Life cycles of *Gammarus oceanicus* and *G. salinus* (Amphipoda) in the Oslofjord, Norway. Ecography 7:262–270.

Smith, G. 1905. The effect of pigment migration on the phototropism of *Gammarus annulatus* S. I. SMITH. American Journal of Physiology-Legacy Content 13:205–216.

Sotka, E. E., T. Bell, L. E. Hughes, J. K. Lowry, and A. G. B. Poore. 2017. A molecular phylogeny of marine amphipods in the herbivorous family Ampithoidae. Zoologica Scripta 46:85–95.

Steele, D. H., and V. J. Steele. 1970. The biology of *Gammarus* (Crustacea, Amphipoda) in the northwestern Atlantic. IV. *Gammarus lawrencianus* Bousfield. Canadian Journal of Zoology 48:1261–1267.

Steele, D. H., and V. J. Steele. 1973. Some aspects of the biology of *Calliopius laeviusculus* (Krøyer) (Crustacea, Amphipoda) in the northwestern Atlantic. Canadian Journal of Zoology 51:723–728.

Steele, D. H., and V. J. Steele. 1974. The blology of *Gammarus* (Crustacea, Amphipoda) ln the northwestern Atlantlc. VIII. Geographlc distribution of the northern specles. Canadian Journal of Zoology 52:1115–1120.

Steele, D. H., and V. J. Steele. 1975. The biology of *Gammarus* (Crustacea, Amphipoda) in the northwestern Atlantic. XI. Comparison and discussion. Canadian Journal of Zoology 53:1116–1126.

Strong, J. A., C. A. Maggs, and M. P. Johnson. 2009. The extent of grazing release from epiphytism for *Sargassum muticum* (Phaeophyceae) within the invaded range. Journal of the Marine Biological Association of the United Kingdom 89:303–314.

Thiel, M. 1997. Reproductive biology of a filter-feeding amphipod, *Leptocheirus pinguis*, with extended parental care. Marine Biology 130:249–258.

Vader, W., and T. Krapp-Schickel. 2012. On some maerid and melitid material (Crustacea: Amphipoda) collected by the Hourglass Cruises (Florida). Part 2: Genera *Dulichiella* and *Elasmopus* , with a key to world *Elasmopus*. Journal of Natural History 46:1179–1218.

Vassallo, L., and D. H. Steele. 1980. Survival and Growth of Young *Gammarus lawrencianus* Bousfield, 1956, on Different Diets. Crustaceana. Supplement:118–125.

Viherluoto, M., H. Kuosa, J. Flinkman, and M. Viitasalo. 2000. Food utilisation of pelagic mysids, *Mysis mixta* and *M. relicta*, during their growing season in the northern Baltic Sea. Marine Biology 136:553–559.

Watling, L. 1981. Amphipoda from the northwestern Atlantic: The genera *Jerbarnia*, *Epimeria*, and *Harpinia*. Sarsia 66:203–211.

APPENDIX 3: Methods and Results – post-hoc modeling of individual peracarid trait dispersion (SES) against environmental predictors in global eelgrass beds

Data analysis. To assess how individual traits responded to ecological filters in our dataset, we built a series of simple post-hoc models with the subset of environmental variables that appeared most often in our best models of broader trait dispersion at the site level: latitude, ocean, epiphyte load, and predation on amphipods. For each of the traits in our dataset, we calculated the standard effect size of MPD and MNTD (SES_{MPD} and SES_{MNTD}) using the independent swap and tip shuffle algorithms across the global pool. We calculated SES_{MPD} for all 13 of our traits (Table 1.1), but because MNTD is sensitive to missing values, we were unable to calculate SES_{MNTD} for fecundity or any of the diet traits in our data.

SES values for each metric and permutation algorithm were used as continuous response variables in each of four models with the univariate predictors of latitude, ocean, epiphyte load, and predation. To account for multiple comparisons, we used a Bonferroni-corrected α-level of 0.0125 when evaluating the significance of the individual predictors. In total, we built 144 models: four predictors, two permutation algorithms, two diversity metrics, two sets of 13 traits, and two sets of five traits.

Results. The majority of trait SES values showed no significant response to any of the four predictors we examined (Table A3.1). However, we found that peracarid communities were more overdispersed in fecundity (SES_{MPD} independent swap and tip shuffle), living habit (SES_{MPD} independent swap and tip shuffle, SES_{MNTD} tip shuffle), motility (SES_{MPD} tip shuffle), and feeding on macroalgae (SES_{MPD} independent swap) at lower latitudes than at higher latitudes (Fig. A3.1). We also found that body size and living habit were significantly more dispersed in the Pacific than the Atlantic Ocean (SES_{MPD} independent swap and tip shuffle; Fig. A3.2), and that communities were increasingly dispersed in feeding on macroalgae as predation increased (SES_{MPD} tip shuffle; Fig. A3.3). These trait dispersion-environment patterns were consistent across other metrics and permutation algorithms for which they were calculated, albeit not significant in every case (Table A3.1).

Table A3.1. Post-hoc models of individual trait dispersion (SES) as a function of latitude, ocean, predation on amphipods, and epiphyte load in eelgrass-associated peracarid crustaceans. Bolded rows indicate models that were significant according to a Bonferroni-corrected α-level of 0.0125.

Permutation Algorithm	Metric	Predictor	Trait	Intercept	Slope	AICc	Adj. R^2
Independent Swap	MPD	Latitude	Maximum adult body length	-0.373	0.012	133.647	-0.017
Independent Swap	**MPD**	**Latitude**	**Maximum fecundity**	**2.565**	**-0.063**	**68.362**	**0.301**
Independent Swap	MPD	Latitude	Body shape	0.954	-0.015	104.648	0.001
Independent Swap	**MPD**	**Latitude**	**Living habit**	**2.734**	**-0.065**	**103.412**	**0.312**
Independent Swap	MPD	Latitude	Motility	1.821	-0.041	122.781	0.088
Independent Swap	MPD	Latitude	Bioturbator	-0.691	0.017	126.783	-0.006
Independent Swap	MPD	Latitude	Eats microalgae	0.271	-0.006	117.443	-0.026
Independent Swap	MPD	Latitude	Eats macroalgae	2.465	**-0.053**	82.125	0.180
Independent Swap	MPD	Latitude	Eats seagrass	1.619	-0.028	76.790	0.026
Independent Swap	MPD	Latitude	Eats seagrass detritus	0.108	0.003	70.142	-0.044
Independent Swap	MPD	Latitude	Suspension feeder	-0.325	0.000	67.632	-0.045
Independent Swap	MPD	Latitude	Detritivore/ deposit feeder	0.719	-0.015	75.792	-0.022
Independent Swap	MPD	Latitude	Carnivore/ parasite/ scavenger	0.800	-0.017	64.469	-0.016
Independent Swap	**MPD**	**Pacific Ocean**	**Maximum adult body length**	**-0.329**	**0.969**	**124.989**	**0.173**
Independent Swap	MPD	Pacific Ocean	Maximum fecundity	-0.625	0.608	75.889	0.085
Independent Swap	MPD	Pacific Ocean	Body shape	0.469	-0.333	103.797	0.021
Independent Swap	**MPD**	**Pacific Ocean**	**Living habit**	**-0.472**	**0.914**	**108.725**	**0.219**
Independent Swap	MPD	Pacific Ocean	Motility	0.040	0.059	127.646	-0.024

Independent Swap	MPD	Pacific Ocean	Bioturbator	-0.048	0.140	127.353	-0.020
Independent Swap	MPD	Pacific Ocean	Eats microalgae	-0.053	0.106	117.439	-0.026
Independent Swap	MPD	Pacific Ocean	Eats macroalgae	-0.021	0.286	88.432	-0.012
Independent Swap	MPD	Pacific Ocean	Eats seagrass	0.444	-0.195	78.270	-0.031
Independent Swap	MPD	Pacific Ocean	Eats seagrass detritus	0.297	-0.085	70.116	-0.043
Independent Swap	MPD	Pacific Ocean	Suspension feeder	-0.485	0.434	66.125	0.018
Independent Swap	MPD	Pacific Ocean	Detritivore/ deposit feeder	-0.079	0.257	75.871	-0.025
Independent Swap	MPD	Pacific Ocean	Carnivore/ parasite/ scavenger	-0.012	0.210	64.982	-0.041
Independent Swap	MPD	arcsin(Mean Amphipod Predation)	Maximum adult body length	0.039	0.287	109.673	-0.018
Independent Swap	MPD	arcsin(Mean Amphipod Predation)	Maximum fecundity	-0.813	0.540	71.273	0.032
Independent Swap	MPD	arcsin(Mean Amphipod Predation)	Body shape	0.150	0.184	88.825	-0.021
Independent Swap	MPD	arcsin(Mean Amphipod Predation)	Living habit	-0.546	0.506	95.522	0.023
Independent Swap	MPD	arcsin(Mean Amphipod Predation)	Motility	-0.140	0.226	105.248	-0.022
Independent Swap	MPD	arcsin(Mean Amphipod Predation)	Bioturbator	0.063	0.099	105.528	-0.029
Independent Swap	MPD	arcsin(Mean Amphipod Predation)	Eats microalgae	-0.462	0.525	101.826	0.004
Independent Swap	MPD	arcsin(Mean Amphipod Predation)	Eats macroalgae	-1.040	1.112	70.734	0.194
Independent Swap	MPD	arcsin(Mean Amphipod Predation)	Eats seagrass	0.143	0.183	64.584	-0.045
Independent Swap	MPD	arcsin(Mean Amphipod Predation)	Eats seagrass detritus	-0.485	0.956	52.352	0.155
Independent Swap	MPD	arcsin(Mean Amphipod Predation)	Suspension feeder	-0.361	0.130	54.402	-0.055

Independent Swap	MPD	arcsin(Mean Amphipod Predation)	Detritivore/ deposit feeder	-0.670	0.890	61.434	0.087
Independent Swap	MPD	arcsin(Mean Amphipod Predation)	Carnivore/ parasite/ scavenger	0.443	-0.700	47.083	0.016
Independent Swap	MPD	log(Mean Epiphyte Load)	Maximum adult body length	-0.189	-0.154	129.301	0.010
Independent Swap	MPD	log(Mean Epiphyte Load)	Maximum fecundity	-0.880	-0.207	74.635	0.065
Independent Swap	MPD	log(Mean Epiphyte Load)	Body shape	-0.172	-0.212	98.913	0.102
Independent Swap	MPD	log(Mean Epiphyte Load)	Living habit	-0.004	-0.001	116.137	-0.026
Independent Swap	MPD	log(Mean Epiphyte Load)	Motility	-0.471	-0.254	118.562	0.090
Independent Swap	MPD	log(Mean Epiphyte Load)	Bioturbator	-0.370	-0.156	121.828	0.018
Independent Swap	MPD	log(Mean Epiphyte Load)	Eats microalgae	-0.268	-0.122	114.464	-0.006
Independent Swap	MPD	log(Mean Epiphyte Load)	Eats macroalgae	-0.291	-0.157	85.502	0.015
Independent Swap	MPD	log(Mean Epiphyte Load)	Eats seagrass	-0.066	-0.191	71.932	0.045
Independent Swap	MPD	log(Mean Epiphyte Load)	Eats seagrass detritus	0.636	0.172	66.344	0.025
Independent Swap	MPD	log(Mean Epiphyte Load)	Suspension feeder	-0.715	-0.149	64.562	0.010
Independent Swap	MPD	log(Mean Epiphyte Load)	Detritivore/ deposit feeder	0.535	0.191	71.167	0.032
Independent Swap	MPD	log(Mean Epiphyte Load)	Carnivore/ parasite/ scavenger	0.620	0.215	59.953	0.050
Independent Swap	MNTD	Latitude	Maximum adult body length	0.078	0.001	125.763	-0.025
Independent Swap	MNTD	Latitude	Body shape	0.175	-0.006	97.761	-0.020

Independent Swap	MNTD	Latitude	Living habit	0.578	-0.021	58.862	0.113
Independent Swap	MNTD	Latitude	Motility	-0.130	-0.003	86.032	-0.023
Independent Swap	MNTD	Latitude	Bioturbator	-0.807	0.017	101.258	0.011
Independent Swap	MNTD	Pacific Ocean	Maximum adult body length	-0.196	0.700	120.284	0.100
Independent Swap	MNTD	Pacific Ocean	Body shape	-0.120	0.083	97.822	-0.022
Independent Swap	MNTD	Pacific Ocean	Living habit	-0.442	0.212	62.895	0.024
Independent Swap	MNTD	Pacific Ocean	Motility	-0.249	-0.034	86.074	-0.024
Independent Swap	MNTD	Pacific Ocean	Bioturbator	-0.011	-0.118	102.525	-0.019
Independent Swap	MNTD	arcsin(Mean Amphipod Predation)	Maximum adult body length	-0.080	0.358	107.974	-0.011
Independent Swap	MNTD	arcsin(Mean Amphipod Predation)	Body shape	-0.225	0.135	83.174	-0.025
Independent Swap	MNTD	arcsin(Mean Amphipod Predation)	Living habit	-0.244	-0.126	56.605	-0.020
Independent Swap	MNTD	arcsin(Mean Amphipod Predation)	Motility	-0.018	-0.271	76.168	-0.003
Independent Swap	MNTD	arcsin(Mean Amphipod Predation)	Bioturbator	0.301	-0.409	86.409	0.015
Independent Swap	MNTD	log(Mean Epiphyte Load)	Maximum adult body length	0.007	-0.071	121.862	-0.016
Independent Swap	MNTD	log(Mean Epiphyte Load)	Body shape	-0.182	-0.048	96.288	-0.018
Independent Swap	MNTD	log(Mean Epiphyte Load)	Living habit	-0.320	0.002	62.545	-0.026
Independent Swap	MNTD	log(Mean Epiphyte Load)	Motility	-0.546	-0.132	80.162	0.057
Independent Swap	MNTD	log(Mean Epiphyte Load)	Bioturbator	-0.308	-0.088	95.046	0.001
Tip Shuffle	MPD	Latitude	Maximum adult body length	-0.059	0.011	148.536	-0.020

Tip Shuffle	**MPD**	**Latitude**	**Maximum fecundity**	**2.783**	**-0.067**	**77.612**	**0.254**
Tip Shuffle	MPD	Latitude	Body shape	1.040	-0.018	94.983	0.022
Tip Shuffle	**MPD**	**Latitude**	**Living habit**	**2.565**	**-0.064**	**103.586**	**0.310**
Tip Shuffle	**MPD**	**Latitude**	**Motility**	**1.958**	**-0.047**	**115.614**	**0.142**
Tip Shuffle	MPD	Latitude	Bioturbator	-1.022	0.017	128.657	-0.007
Tip Shuffle	MPD	Latitude	Eats microalgae	0.219	-0.010	111.643	-0.021
Tip Shuffle	MPD	Latitude	Eats macroalgae	2.262	-0.052	90.555	0.132
Tip Shuffle	MPD	Latitude	Eats seagrass	1.575	-0.021	71.748	0.004
Tip Shuffle	MPD	Latitude	Eats seagrass detritus	-0.040	0.003	73.020	-0.045
Tip Shuffle	MPD	Latitude	Suspension feeder	-0.236	-0.005	68.924	-0.043
Tip Shuffle	MPD	Latitude	Detritivore/ deposit feeder	0.601	-0.016	77.781	-0.020
Tip Shuffle	MPD	Latitude	Carnivore/ parasite/ scavenger	0.728	-0.019	61.796	0.000
Tip Shuffle	**MPD**	**Pacific Ocean**	**Maximum adult body length**	**-0.232**	**1.327**	**136.379**	**0.236**
Tip Shuffle	MPD	Pacific Ocean	Maximum fecundity	-0.697	0.834	81.630	0.139
Tip Shuffle	MPD	Pacific Ocean	Body shape	0.307	-0.108	96.709	-0.019
Tip Shuffle	**MPD**	**Pacific Ocean**	**Living habit**	**-0.695**	**1.038**	**104.831**	**0.290**
Tip Shuffle	MPD	Pacific Ocean	Motility	-0.188	0.272	122.230	-0.005
Tip Shuffle	MPD	Pacific Ocean	Bioturbator	-0.415	0.236	128.873	-0.012
Tip Shuffle	MPD	Pacific Ocean	Eats microalgae	-0.369	0.290	111.125	-0.007
Tip Shuffle	MPD	Pacific Ocean	Eats macroalgae	-0.215	0.323	95.177	-0.012
Tip Shuffle	MPD	Pacific Ocean	Eats seagrass	0.694	-0.120	72.798	-0.037
Tip Shuffle	MPD	Pacific Ocean	Eats seagrass detritus	0.083	-0.004	73.037	-0.045
Tip Shuffle	MPD	Pacific Ocean	Suspension feeder	-0.675	0.589	66.299	0.065
Tip Shuffle	MPD	Pacific Ocean	Detritivore/ deposit feeder	-0.280	0.320	77.711	-0.017
Tip Shuffle	MPD	Pacific Ocean	Carnivore/ parasite/ scavenger	-0.223	0.328	62.245	-0.022

Tip Shuffle	MPD	arcsin(Mean Amphipod Predation)	Maximum adult body length	0.240	0.391	123.622	-0.015
Tip Shuffle	MPD	arcsin(Mean Amphipod Predation)	Maximum fecundity	-0.919	0.701	78.825	0.049
Tip Shuffle	MPD	arcsin(Mean Amphipod Predation)	Body shape	0.031	0.255	83.991	-0.011
Tip Shuffle	MPD	arcsin(Mean Amphipod Predation)	Living habit	-0.805	0.611	96.893	0.043
Tip Shuffle	MPD	arcsin(Mean Amphipod Predation)	Motility	-0.438	0.409	104.419	-0.003
Tip Shuffle	MPD	arcsin(Mean Amphipod Predation)	Bioturbator	-0.317	0.144	108.902	-0.027
Tip Shuffle	MPD	arcsin(Mean Amphipod Predation)	Eats microalgae	-0.645	0.474	96.641	0.003
Tip Shuffle	**MPD**	**arcsin(Mean Amphipod Predation)**	**Eats macroalgae**	**-1.457**	**1.357**	**75.901**	**0.231**
Tip Shuffle	MPD	arcsin(Mean Amphipod Predation)	Eats seagrass	0.454	0.170	62.224	-0.046
Tip Shuffle	MPD	arcsin(Mean Amphipod Predation)	Eats seagrass detritus	-0.750	1.043	53.737	0.172
Tip Shuffle	MPD	arcsin(Mean Amphipod Predation)	Suspension feeder	-0.650	0.279	56.207	-0.042
Tip Shuffle	MPD	arcsin(Mean Amphipod Predation)	Detritivore/ deposit feeder	-0.916	0.960	62.376	0.100
Tip Shuffle	MPD	arcsin(Mean Amphipod Predation)	Carnivore/ parasite/ scavenger	0.139	-0.514	45.163	-0.018
Tip Shuffle	MPD	log(Mean Epiphyte Load)	Maximum adult body length	0.154	-0.124	144.474	-0.009
Tip Shuffle	MPD	log(Mean Epiphyte Load)	Maximum fecundity	-0.668	-0.143	83.871	-0.002
Tip Shuffle	MPD	log(Mean Epiphyte Load)	Body shape	-0.046	-0.133	93.252	0.036

Tip Shuffle	MPD	log(Mean Epiphyte Load)	Living habit	-0.075	0.040	116.091	-0.022
Tip Shuffle	MPD	log(Mean Epiphyte Load)	Motility	-0.474	-0.201	115.002	0.056
Tip Shuffle	MPD	log(Mean Epiphyte Load)	Bioturbator	-0.636	-0.130	123.979	0.003
Tip Shuffle	MPD	log(Mean Epiphyte Load)	Eats microalgae	-0.407	-0.084	109.387	-0.016
Tip Shuffle	MPD	log(Mean Epiphyte Load)	Eats macroalgae	-0.446	-0.147	92.477	-0.001
Tip Shuffle	MPD	log(Mean Epiphyte Load)	Eats seagrass	0.354	-0.138	66.500	0.016
Tip Shuffle	MPD	log(Mean Epiphyte Load)	Eats seagrass detritus	0.585	0.225	68.210	0.063
Tip Shuffle	MPD	log(Mean Epiphyte Load)	Suspension feeder	-0.747	-0.109	66.520	-0.019
Tip Shuffle	MPD	log(Mean Epiphyte Load)	Detritivore/ deposit feeder	0.510	0.254	72.036	0.080
Tip Shuffle	MPD	log(Mean Epiphyte Load)	Carnivore/ parasite/ scavenger	0.453	0.218	57.386	0.066
Tip Shuffle	MNTD	Latitude	Maximum adult body length	0.210	0.005	150.228	-0.024
Tip Shuffle	MNTD	Latitude	Body shape	0.265	-0.008	105.847	-0.017
Tip Shuffle	MNTD	Latitude	Living habit	0.519	**-0.022**	56.049	0.130
Tip Shuffle	MNTD	Latitude	Motility	-0.063	-0.003	107.246	-0.024
Tip Shuffle	MNTD	Latitude	Bioturbator	-0.962	0.021	109.889	0.018
Tip Shuffle	MNTD	Pacific Ocean	Maximum adult body length	-0.033	0.939	144.753	0.101
Tip Shuffle	MNTD	Pacific Ocean	Body shape	-0.133	0.088	106.036	-0.022
Tip Shuffle	MNTD	Pacific Ocean	Living habit	-0.542	0.235	60.250	0.038
Tip Shuffle	MNTD	Pacific Ocean	Motility	-0.163	-0.085	107.177	-0.022
Tip Shuffle	MNTD	Pacific Ocean	Bioturbator	-0.006	-0.124	111.472	-0.019

Tip Shuffle	MNTD	arcsin(Mean Amphipod Predation)	Maximum adult body length	0.090	0.518	128.226	-0.008
Tip Shuffle	MNTD	arcsin(Mean Amphipod Predation)	Body shape	-0.232	0.105	89.054	-0.027
Tip Shuffle	MNTD	arcsin(Mean Amphipod Predation)	Living habit	-0.371	-0.101	52.202	-0.023
Tip Shuffle	MNTD	arcsin(Mean Amphipod Predation)	Motility	0.117	-0.337	94.204	-0.005
Tip Shuffle	MNTD	arcsin(Mean Amphipod Predation)	Bioturbator	0.310	-0.403	93.942	0.006
Tip Shuffle	MNTD	log(Mean Epiphyte Load)	Maximum adult body length	0.193	-0.114	145.966	-0.012
Tip Shuffle	MNTD	log(Mean Epiphyte Load)	Body shape	-0.177	-0.041	104.488	-0.021
Tip Shuffle	MNTD	log(Mean Epiphyte Load)	Living habit	-0.397	0.007	60.495	-0.025
Tip Shuffle	MNTD	log(Mean Epiphyte Load)	Motility	-0.498	-0.140	102.387	0.029
Tip Shuffle	MNTD	log(Mean Epiphyte Load)	Bioturbator	-0.269	-0.071	105.115	-0.012

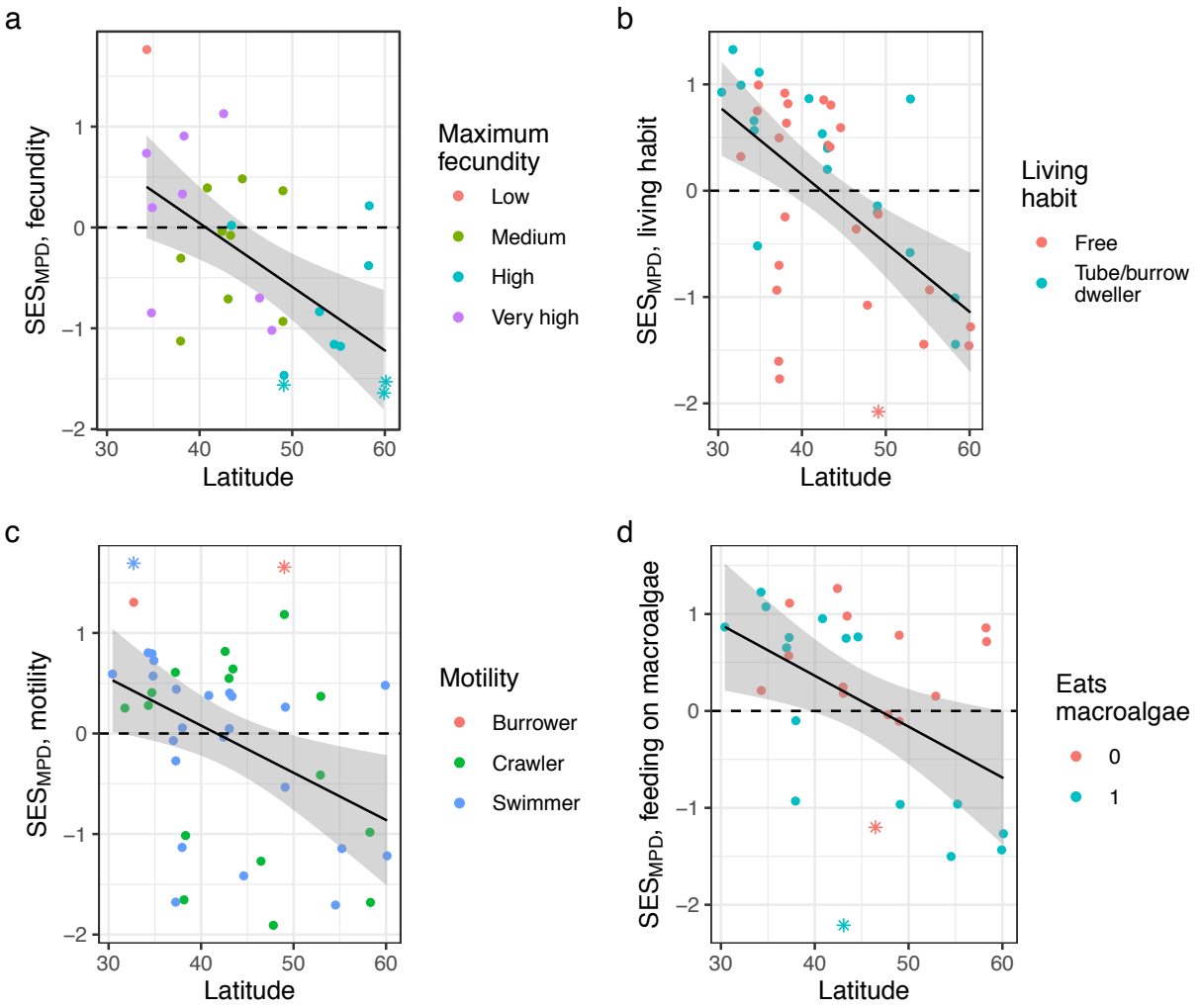

Figure A3.1. Effects of latitude on trait dispersion (measured by SES_{MPD} using the independent swap algorithm in panels A, B, and D and the tip shuffle algorithm in panel C). Permuting across the global species pool, SES_{MPD} declined with latitude for fecundity (A; $R^2 = 0.301$, $p = 0.002$), living habit (B; $R^2 = 0.312$, $p < 0.001$), motility (C; $R^2 = 0.142$, $p = 0.008$), and feeding on macroalgae (D; $R^2 = 0.180$, $p = 0.011$). The dashed horizontal line represents an SES value of 0, indicating an observed value of MPD indistinguishable from random assembly; points displayed as stars represent those for which SES is significantly different from 0 at $\alpha = 0.05$. Colors represent dominant trait values.

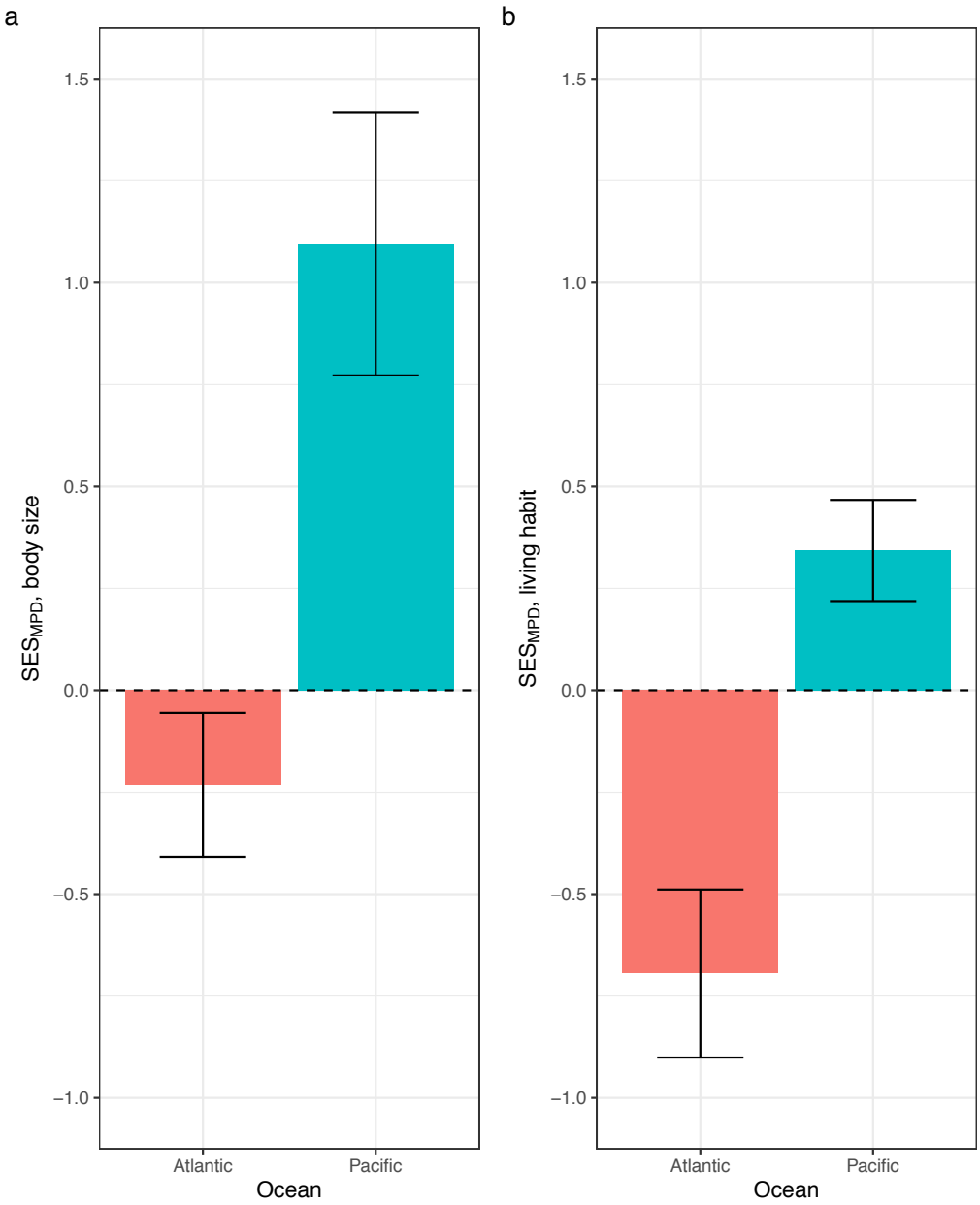

Figure A3.2. Trait dispersion across ocean basins (measured by SES_{MPD} using the tip shuffle algorithm). Permuting across the global species pool, SES_{MPD} was significantly greater in the Pacific than the Atlantic Ocean for maximum adult body length (A; $R^2 = 0.236$, $p < 0.001$) and living habit (B; $R^2 = 0.290$, $p < 0.001$). In the Atlantic, community-weighted mean body size was 14.09 mm; in the Pacific it was 20.79 mm. In both oceans, the majority of species were free-living. The dashed horizontal line represents an SES value of 0, indicating an observed value of MPD indistinguishable from random assembly.

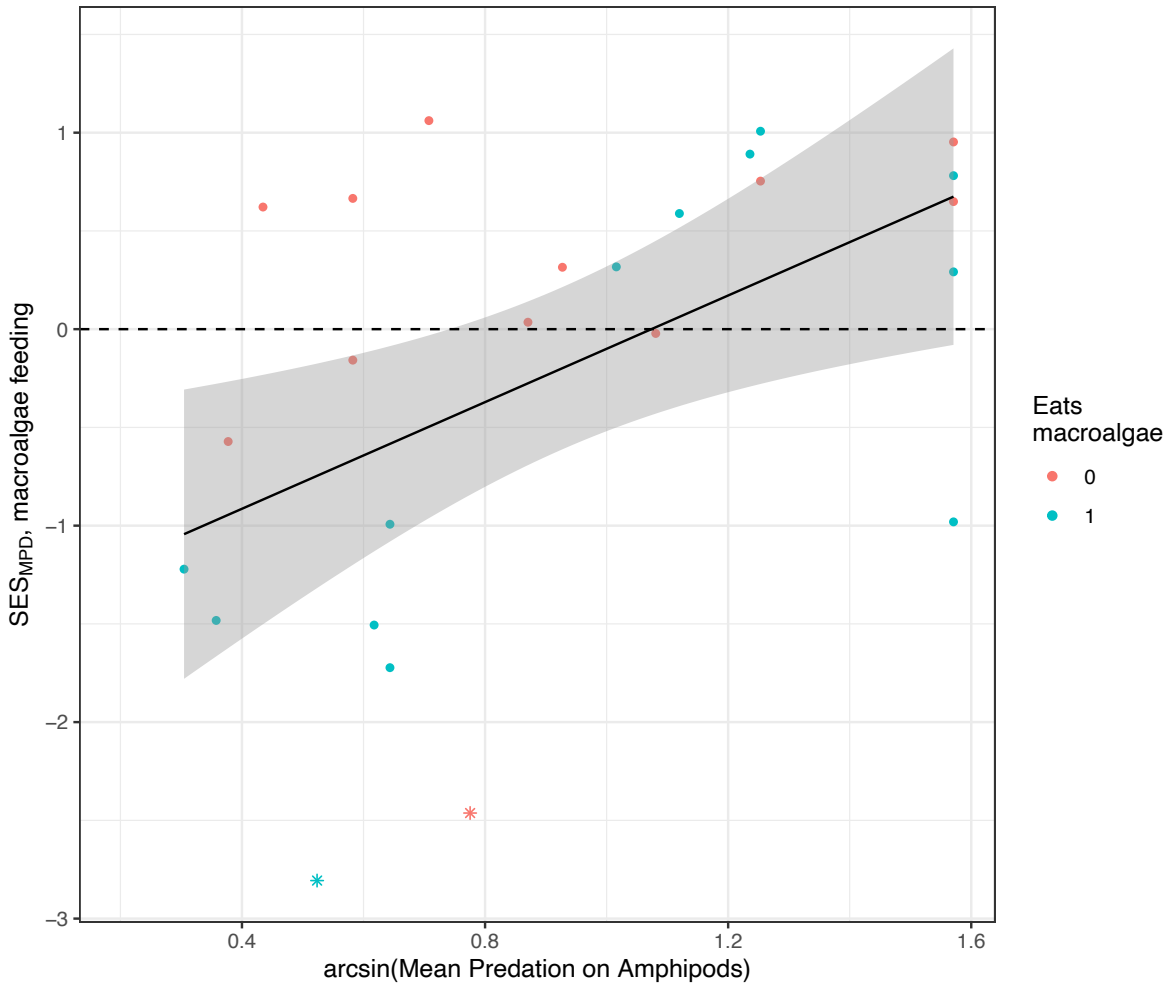

Figure A3.3. Effects of predation intensity on trait dispersion (measured by SES_{MPD} using the tip shuffle algorithm). Permuting across the global species pool, SES_{MPD} increased with increasing predation intensity for macroalgae consumption ($R^2 = 0.231$, $p = 0.009$). The dashed horizontal line represents an SES value of 0, indicating an observed value of MPD indistinguishable from random assembly; points displayed as stars represent those for which SES is significantly different from 0 at $\alpha = 0.05$. Colors represent dominant trait values.

APPENDIX 4: Species and trait data for fish and peracarid communities in Tomales Bay and Bodega Harbor, California

1. FISHES

Across both years and all six sites, we found a total of 35 fish species of which 16 species were retained in our analyses, after removing singletons, species that only occurred in one site-year combination, and species whose abundance totaled fewer than 4 individuals across samples (Table A4.1). The most speciose fish community had 13 species. Four fish species (*Cymatogaster aggregata, Gasterosteus aculeatus, Porichthys notatus,* and *Sebastes carnatus*) were present in discrete size cohorts and counted as separate groups for our analyses (Table A4.2).

We assigned two categorical (vertical position and foraging mode) and one continuous trait (trophic level) to fishes based on Fishbase (Froese & Pauly 2020) and Love (2011; Table A4.3). Vertical position, defined as the orientation of the fish in the water column, had three levels: 1) benthic – resting on the bottom, touching the substrate; 2) benthopelagic – suspended in the water column a short distance from the bottom; and 3) pelagic – suspended in the water column away from benthic structures, not bottom-associated aside from feeding. Foraging mode, defined as the suite of behaviors associated with feeding and foraging, had 5 levels: 1) pursuit predator – actively chases after fast-moving prey; 2) benthic browser – searches for and picks off bottom-associated prey items; 3) epifaunal browser – searches for and picks off prey items associated with eelgrass; 4) planktivore – feeds on suspended prey in the water column; and 5) sit-and-wait – ambush predators that feed on passing prey within reach. We fuzzy-coded vertical position and foraging mode among 5 and 3 levels, respectively, to accommodate species that occupied two or more levels (Ashford et al. 2018).

We collected linear morphometric measurements of fishes from 2-26 specimens of each species and size class collected from seines, and standardized them for ease of comparison across species (Fig. A4.1, Table A4.3). We log-tranformed fish traits where appropriate to conform to a normal distribution. Species-level mean trait values are listed in Table A4.4. We also used principal component analysis (PCA) to condense variation among fish species' linear morphometric traits into 16 axes, the first three of which explained 66% of variation among species (Fig. A4.2).

REFERENCES

Ashford, O. S., A. J. Kenny, C. R. S. Barrio Froján, M. B. Bonsall, T. Horton, A. Brandt, G. J. Bird, S. Gerken, and A. D. Rogers. 2018. Phylogenetic and functional evidence suggests that deep-ocean ecosystems are highly sensitive to environmental change and direct human disturbance. Proceedings of the Royal Society B: Biological Sciences 285:20180923.

Froese, R., and Pauly, D. (eds). 2023. Fishbase. World Wide Web electronic publication, ver. 01/2023

Love, M. 2011. Certainly more than you want to know about the fishes of the Pacific Coast: a postmodern experience. First edition. Really Big Press, Santa Barbara, CA, USA.

Table A4.2. Total counts for all fish species observed across sites and years, including separate size classes for G. aculeatus, C. aggregata, S. carnatus, and P. notatus. Rows in bold indicate species and size classes that were retained for community analyses.

Species	Size class	Total count
Gasterosteus aculeatus	**small**	**2468**
Cymatogaster aggregata	**small**	**729**
Syngnathus leptorhynchus		**563**
Gasterosteus aculeatus	**large**	**146**
Sebastes melanops		**143**
Leptocottus armatus		**51**
Embiotoca lateralis		**50**
Clevelandia ios		**43**
Gibbonsia metzi		**42**
Apodicthhys flavidus		**37**
Brachyistius frenatus		**37**
Sebastes carnatus	**small**	**31**
Atherinops affinus		**19**
Sebastes carnatus	**large**	**18**
Oligocottus snyderi		**17**
Phanerodon vacca		**13**
Cymatogaster aggregata	**large**	**12**
Porichthys notatus	**large**	**10**
Pholis ornata		**9**
Porichthys notatus	**small**	**4**
Aulorhynchus flavidus		5

Acanthogobius flavimanus	4
Citharichthys stigmaeus	4
Scorpaenichthys marmoratus	4
Sebastes caurinus	4
Xiphister mucosus	4
Hexagrammos stelleri	3
Embiotoca jacksoni	2
Oligocottus maculosus	2
Parophrys vetulus	2
Cebidichthys violaceus	1
Clupea pallasii	1
Lepidogobius lepidus	1
Ophiodon elongatus	1
Sebastes paucispinis	1

Table A4.3. Size thresholds for delimiting large vs. small individuals of *G. aculeatus, C. aggregata, S. carnatus,* and *P. notatus*, based on preliminary seine surveys in the same sites as in our study. No individuals were collected of sizes in between the ranges listed.

Species	Size Class	Size threshold (standard length)
Gasterosteus aculeatus	Large	≥ 55 mm
Gasterosteus aculeatus	Small	≤ 45 mm
Cymatogaster aggregata	Large	≥ 60 mm
Cymatogaster aggregata	Small	≤ 56 mm
Sebastes carnatus	Large	≥ 50 mm
Sebastes carnatus	Small	≤ 48 mm
Porichthys notatus	Large	≥ 67 mm
Porichthys notatus	Small	≤ 25 mm

Table A4.4. Traits used to characterize fish communities. Cat = discrete categorical trait, Cont. = continuous trait

Trait	Type	Definition	Standardized	Transformed	Functional Category	Source
Vertical position	Cat.	The orientation of the fish in the water column. Levels: Benthic, Benthopelagic, Pelagic	N/A	N/A	Feeding	Love 2011
Foraging mode	Cat.	Suite of behaviors associated with	N/A	N/A	Feeding	Love 2011

		feeding and foraging. Levels: pursuit predator, benthic browser, epifaunal browser, planktivore, sit-and-wait.				
Trophic level	Cont.	The average trophic level of the species, estimated from food items	N/A	N/A	Feeding	Fishbase
Standard length	Cont.	Body length from snout tip to the end of the caudal peduncle	N/A	N/A	Habitat use, feeding	Measured individuals
Mouth Height	Cont.	Distance from distal tip of the premaxilla to the distal tip of the dentary with the jaws fully extended	Height / Standard Length	N/A	Feeding	Measured individuals
Dorsal Fin Length	Cont.	Straight length from the anterior to posterior end of the dorsal fin; summed where dorsal fins were discontinuous	Length / Standard Length	N/A	Locomotion	Measured individuals
Anal Fin Length	Cont.	Straight length from the anterior to posterior end of the anal fin	Length / Standard Length	N/A	Locomotion	Measured individuals
Caudal Fin Length	Cont.	Straight distance from the end of the caudal peduncle to the distal tip of the longest caudal fin ray	Length / Standard Length	log	Locomotion	Measured individuals
Pectoral Fin Length	Cont.	Length from base to the tip of the longest pectoral ray	Length / Standard Length	N/A	Locomotion, habitat use	Measured individuals
Head Length	Cont.	Distance from posterior margin of the operculum to the distal tip of the premaxilla with the jaws closed	Length / Standard Length	N/A	Feeding	Measured individuals

Body Depth	Cont.	Greatest vertical distance from the top of the fish to the bottom	Depth / Standard Length	N/A	Locomotion, habitat use	Measured individuals
Body Depth Below Midline	Cont.	Greatest vertical distance below a horizontal line drawn from the tip of the snout to the end of the caudal peduncle	Depth / Body Depth	log	Locomotion, habitat use	Measured individuals
Head Depth	Cont.	Vertical distance from the top of the head to the bottom of the head, passing through the eye pupil	Depth / Body Depth	N/A	Feeding	Measured individuals
Eye Position	Cont.	Vertical distance from the pupil to the bottom of the head	Position / Head Depth	N/A	Habitat use	Measured individuals
Eye Diameter	Cont.	Horizontal distance across the eye passing through the pupil	Diameter / Head Length	N/A	Feeding	Measured individuals
Mouth Protrusion	Cont.	Length from distal tip of the premaxilla to the eye pupil with the jaws fully extended	Protrusion / Head Length	log	Feeding	Measured individuals
Snout Length	Cont.	Distance from eye pupil to distal tip of the premaxilla, with the mouth closed	Length / Head Length	N/A	Feeding	Measured individuals
Caudal Peduncle Length	Cont.	Horizontal distance from the end of the caudal peduncle to the end of the anal fin	Length / Standard Length	log	Locomotion	Measured individuals
Caudal Peduncle Depth	Con.	Vertical distance across the narrowest portion of the caudal peduncle	Depth / Body Depth	log	Locomotion	Measured individuals

Table A4.5. Mean trait values for each fish species and size class observed in seines. Continuous morphometric traits are standardized according to Table A4.3; sample size denotes the number of individuals used to collect morphometric measurements.

Species	Vertical position	Foraging mode	Trophic level	Standard length (mm)	Mouth Height	Dorsal Fin Length	Sample size
Apodicththys flavidus	Benthic	Benthic browser, epifaunal browser, sit-and-wait	3.55	94.0000	0.0428	0.8862	10
Atherinops affinus	Pelagic	Benthic browser, planktivore	2.76	42.1667	0.0760	0.1358	9
Brachyistius frenatus	Pelagic	Epifaunal browser, planktivore	3.5	56.0000	0.0860	0.3864	8
Clevelandia ios	Benthic	Benthic browser	3.12	35.4444	0.1299	0.1627	9
Cymatogaster aggregata large	Pelagic, Benthopelagic	Benthic browser, epifaunal browser	2.99	86.0000	0.1137	0.4869	7
Cymatogaster aggregata small	Pelagic	Planktivore	2.99	39.1731	0.1160	0.4282	26
Embiotoca lateralis	Pelagic, Benthopelagic	Benthic browser, epifaunal browser	3.33	64.0000	0.1353	0.4131	7
Gasterosteus aculeatus large	Pelagic, Benthopelagic	Benthic browser, epifaunal browser, planktivore	3.38	65.2500	0.1038	0.2646	12
Gasterosteus aculeatus small	Pelagic, Benthopelagic	Benthic browser, epifaunal browser, planktivore	3.38	25.7727	0.0756	0.2510	11
Gibbonsia metzi	Benthic	Sit-and-wait	3.06	48.5625	0.0911	0.7078	8
Leptocottus armatus	Benthic	Sit-and-wait	3.68	80.7143	0.1727	0.4446	21
Oligocottus snyderi	Benthic	Benthic browser, sit-and-wait	3.16	50.5625	0.1631	0.6191	8

Phanerodon vacca	Pelagic, Benthopelagic	Benthic browser, epifaunal browser	3.38	67.0000	0.0848	0.4216	3
Pholis ornata	Benthic	Benthic browser, epifaunal browser, sit-and-wait	3.55	75.0000	0.0451	0.8854	6
Porichthys notatus large	Benthic, Benthopelagic	Pursuit predator, planktivore	4.04	77.0000	0.1634	0.5039	4
Porichthys notatus small	Benthic, Benthopelagic	Pursuit predator	4.04	24.5000	0.1824	0.5712	2
Sebastes carnatus large	Benthopelagic	Benthic browser, sit-and-wait	3.62	50.0000	0.2195	0.5128	4
Sebastes carnatus small	Benthopelagic	Benthic browser, planktivore	3.62	31.6250	0.2183	0.5078	7
Sebastes melanops	Pelagic, Benthopelagic	Pursuit predator, planktivore	3.9	45.5833	0.2171	0.5574	6
Syngnathus leptorhynchus	Pelagic, Benthopelagic	Epifaunal browser, planktivore	3.24	128.3400	0.0131	0.1129	25

Table A4.4, continued

Species	Anal Fin Length	log(Caudal Fin Length)	Pectoral Fin Length	Head Length	Body Depth	log(Body Depth Below Midline)	Head Depth	Sample size
Apodicthhys flavidus	0.4127	-1.3213	0.0392	0.0956	0.1146	-0.2654	0.4688	10
Atherinops affinus	0.2217	-0.9279	0.1389	0.2090	0.1635	-0.2926	0.6175	9
Brachyistius frenatus	0.3220	-0.8215	0.2123	0.2900	0.3725	-0.3134	0.4749	8
Clevelandia ios	0.2122	-0.7990	0.1120	0.2263	0.1325	-0.2391	0.6821	9
Cymatogaster aggregata large	0.2541	-0.9175	0.2464	0.3073	0.3787	-0.3134	0.5063	7
Cymatogaster aggregata small	0.2477	-0.8154	0.2344	0.3133	0.3623	-0.3214	0.5587	26
Embiotoca lateralis	0.2883	-0.7982	0.2393	0.2989	0.4085	-0.3269	0.5133	7

Gasterosteus aculeatus large	0.1817	-0.9132	0.1327	0.2742	0.1983	-0.1755	0.6826	12
Gasterosteus aculeatus small	0.1639	-0.9809	0.1539	0.2692	0.2364	-0.3194	0.5415	11
Gibbonsia metzi	0.3884	-0.8776	0.1601	0.2141	0.1785	-0.3089	0.5975	8
Leptocottus armatus	0.3112	-0.8138	0.2411	0.3130	0.1889	-0.2324	0.7066	21
Oligocottus snyderi	0.3959	-0.7076	0.2840	0.2572	0.2073	-0.1304	0.7178	8
Phanerodon vacca	0.2739	-0.7846	0.2354	0.3087	0.3868	-0.2999	0.5397	3
Pholis ornata	0.3927	-1.2525	0.0628	0.1150	0.1124	-0.2596	0.4975	6
Porichthys notatus large	0.4883	-0.9009	0.1751	0.2609	0.1774	-0.2417	0.6574	4
Porichthys notatus small	0.4978	-0.7547	0.1492	0.2123	0.1914	-0.2753	0.7659	2
Sebastes carnatus large	0.2023	-0.8042	0.2463	0.3261	0.3055	-0.2512	0.6436	4
Sebastes carnatus small	0.1925	-0.7509	0.2298	0.3681	0.2575	-0.2419	0.8601	7
Sebastes melanops	0.1869	-0.8116	0.2069	0.3322	0.2701	-0.3394	0.6755	6
Syngnathus leptorhynchus	0.0000	-1.5273	0.0203	0.1284	0.0309	-0.2518	0.7862	25

Table A4.4, continued

Species	Eye Position	Eye Diam.	log(Mouth Protrusion)	Snout Length	log(Caudal Peduncle Length + 1)	log(Caudal Peduncle Depth)	Sample size
Apodicththys flavidus	0.6797	0.2387	-0.3886	0.3662	0.0000	-0.4780	10
Atherinops affinus	0.4831	0.2531	-0.3137	0.3552	0.0708	-0.2898	9
Brachyistius frenatus	0.5510	0.2898	-0.2775	0.3960	0.0796	-0.3960	8
Clevelandia ios	0.8090	0.1153	-0.3887	0.3287	0.0675	-0.2702	9
Cymatogaster aggregata large	0.6484	0.2581	-0.2702	0.3950	0.0494	-0.5274	7
Cymatogaster aggregata small	0.5780	0.3552	-0.2315	0.4294	0.0560	1.2031	26
Embiotoca lateralis	0.5784	0.3287	-0.3805	0.3731	0.0630	-0.4818	7

Gasterosteus aculeatus large	0.5319	0.2478	-0.3119	0.4166	0.0507	-0.5158	12
Gasterosteus aculeatus small	0.6582	0.2303	-0.2900	0.4224	0.0540	-0.5753	11
Gibbonsia metzi	0.6632	0.1998	-0.3606	0.3620	0.0313	-0.4292	8
Leptocottus armatus	0.8663	0.1219	-0.3504	0.3282	0.0436	-0.3910	21
Oligocottus snyderi	0.8195	0.2043	-0.3193	0.4333	0.0506	-0.3608	8
Phanerodon vacca	0.5659	0.2846	-0.2959	0.3782	0.0603	-0.4758	3
Pholis ornata	0.7278	0.1710	-0.5043	0.2323	0.0000	-0.4657	6
Porichthys notatus large	1.0048	0.1810	-0.5686	0.2525	0.0000	-0.5855	4
Porichthys notatus small	0.8781	0.1991	0.4096	0.4936	0.0000	-0.5794	2
Sebastes carnatus large	0.7764	0.2604	-0.2458	0.4105	0.0548	-0.4383	4
Sebastes carnatus small	0.6840	0.2753	-0.2326	0.3767	0.0603	-0.3827	7
Sebastes melanops	0.6204	0.2898	-0.2466	0.4023	0.0652	-0.3920	6
Syngnathus leptorhynchus	0.7109	0.0950	-0.2494	0.5647	0.1689	-0.6167	25

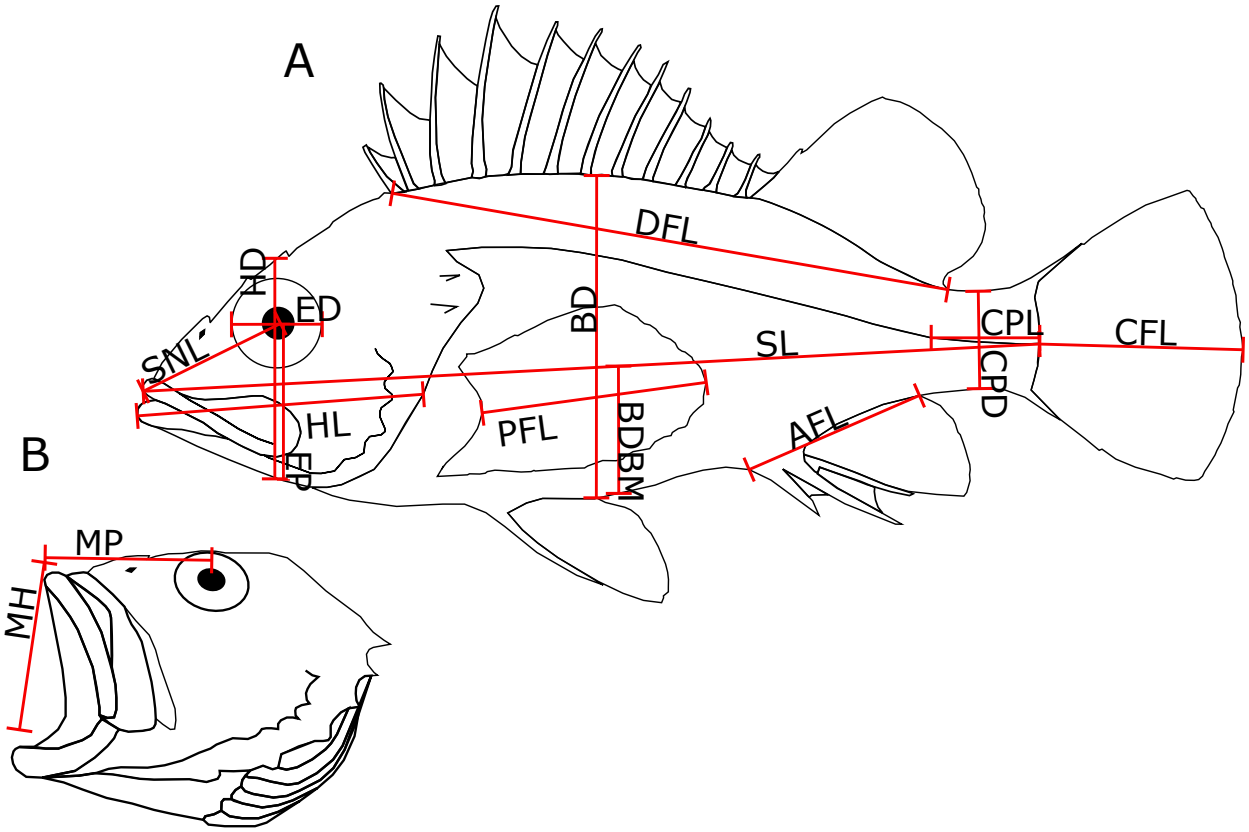

Figure A4.3. Fish morphometric traits used in functional analyses, here measured on a rockfish (*Sebastes* sp.) with its mouth closed (A) and open (B). SNL = snout length; HD = head depth; ED = eye diameter; HL = head length; EP = eye position; PFL = pectoral fin length; BD = body depth; BDBM = body depth below midline; SL = standard length; AFL = anal fin length; CPL = caudal peduncle length; CPD = caudal peduncle depth; CFL = caudal fin length; MP = mouth protrusion; MH = mouth height. Descriptions of individual traits are provided in Table A4.3.

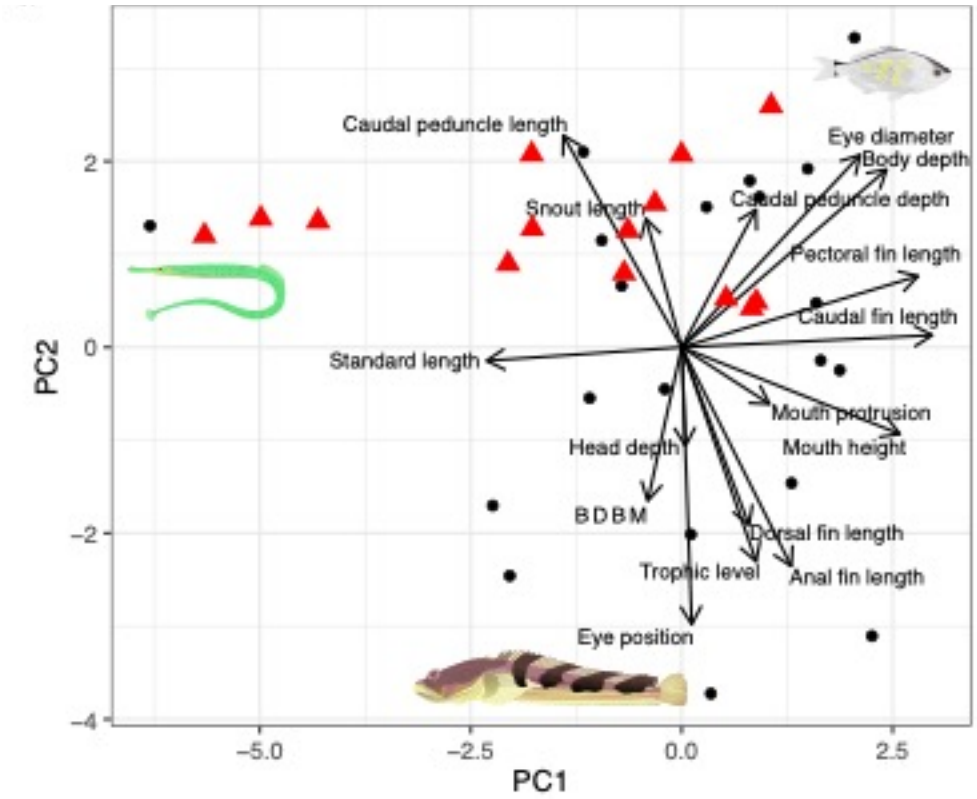

Figure A4.4. Principle coordinates axes of fish morphometric traits. PC1 explained 25.18% of the variation in fish morphology, while PC2 explained 23.10% of the variation. Black circular points represent mean values for species, while red triangles represent community weighted mean values. Species visually represented in morphospace include *Cymatogaster aggregata* (top right), *Syngnathus leptorhynchus* (middle left), and *Porichthys notatus* (bottom middle).

2. PERACARIDS

Across both years and all six sites, we found a total of 28 peracarid species of which 23 species were retained in our analyses, after removing singletons and species that only occurred in one site-year combination (Table A4.5). The most speciose peracarid community in our dataset had 18 species.

We assigned each two categorical traits (body shape and living habit) and one continuous trait (maximum body size) from the literature (Carlton 2007; Table A4.6). We determined tube fidelity for each species according to observations of living and preserved specimens and information in the literature about the presence or absence of silk glands. We ranked tube fidelity along a four-point ordered scale: none = lacks silk glands to build tubes; low = has silk glands but was never observed in tubes when alive or preserved in ethanol; medium = has silk glands

and was observed in tubes when alive but readily flees tube when exposed to ethanol, and high = has silk glands, is tubicolous when alive, and is regularly found inside tubes after preservation in ethanol. Living habit had 3 levels: tubicolous = has silk glands to build tubes, regardless of tube fidelity; clinging = lacks silk glands and typically remains stationary, clinging to eelgrass blades or other structure with well-developed dactyls; and swimming = lacks silk glands, readily swims among vertical structures, and lacks specialized dactyls for clinging. Body shape also had 3 levels: cylindrical = elongated or tube-shaped body, rounded in cross section; dorsoventrally compressed = body wider than it is tall; and laterally compressed = body taller than it is wide.

To measure activity level, we recorded videos of 9-20 individuals of each species, except for *Uromunna ubiquita*. After we started recording, we dropped each individual from a height of 6 centimeters into a cylindrical cup with 150 ml of seawater positioned over a grid on a dark background. We stopped recording 1 minute after the animal was first submerged in the seawater. After recording, we trimmed videos to a length of 1 minute to remove the initial seconds of dropping and splashing, and used FIJI (Schindelin et al. 2012) to record the number of frames during which the animal was not moving, walking, or swimming. We defined a lack of movement as a lack of sustained forward or backward locomotion facilitated by pereopods or pleopods. We defined walking as motion propelled primarily by the pereopod dactyls making contact with the bottom of the cup, while swimming was motion propelled primarily by beating the pleopods and freeing the pereopods from the substrate. We show the pleopods and pereopods of a typical amphipod in Fig. A4.3. We measured continuous morphometric traits from images of 9-22 individuals of each species in FIJI, and standardized and transformed them as described in Table A4.6 and shown in Fig. A4.3. We show species-level mean values for each trait in Table A4.7.

REFERENCES

Ashford, O. S., A. J. Kenny, C. R. S. Barrio Froján, M. B. Bonsall, T. Horton, A. Brandt, G. J. Bird, S. Gerken, and A. D. Rogers. 2018. Phylogenetic and functional evidence suggests that deep-ocean ecosystems are highly sensitive to environmental change and direct human disturbance. Proceedings of the Royal Society B: Biological Sciences 285:20180923.

Carlton, J. T. 2007. The Light and Smith Manual: intertidal invertebrates from Central California to Oregon. Fourth edition. University of California Press.

Schindelin, J., I. Arganda-Carreras, E. Frise, V. Kaynig, M. Longair, T. Pietzsch, S. Preibisch, C. Rueden, S. Saalfeld, B. Schmid, J. Tinevez, D. J. White, V. Hartenstein, K. Eliceiri, P. Tomancak, and A. Cardona. 2012. Fiji: an open-source platform for biological image analysis. Nature Methods 9:676-682.

Table A4.6. Total and standardized counts for all peracarid species observed across sites and years. Standardized abundances are obtained by dividing the number of individuals in a sample by the biomass of macrophytes in the sample Rows in bold indicate species and size classes that were retained for community analyses.

Species	Total count	Standardized total abundance (ind. g^{-1})
Leptochelia sp.	**4468**	**7.92451204**
Photis brevipes	**2757**	**6.94097811**
Caprella californica	**3534**	**6.22669491**
Zeuxo normani	**2159**	**3.98439136**
Monocorophium insidiosum	**2012**	**3.30624947**
Paracorophium sp.	**1524**	**2.71298939**
Ampithoe valida	**1452**	**2.22806836**
Aoroides columbiae	**550**	**1.32119752**
Grandidierella japonica	**567**	**0.83671613**
Ampithoe lacertosa	**390**	**0.7393752**
Pentidotea resecata	**540**	**0.54697383**
Ericthonius brasiliensis	**170**	**0.35707027**
Ischyrocerus anguipes	**204**	**0.35049762**
Paranthura japonica	**96**	**0.17125917**
Uromunna ubiquita	**64**	**0.15066378**
Paracerceis cordata	**62**	**0.11774281**
Melita nitida	**67**	**0.11653687**
Paramicrodeutopus schmitti	**48**	**0.09474279**
Pontogeneia rostrata	**43**	**0.09220466**
Allorchestes angusta	**59**	**0.08527527**
Americorophium spinicorne	**34**	**0.05073408**
Apolochus barnardi	**26**	**0.03992121**
Gnorimosphaeroma sp.	**21**	**0.03192348**
Incisocalliope derzhavini	6	0.00912099
Ampithoe sectimanus	2	0.00617033
Hourstonius vilordes	2	0.00384578
Janiralata occidentalis	1	0.0021857

Megamoera subtener	2	0.00148796

Table A4.7. Traits used to characterize peracarid communities. Traits standardized by body length are standardized by the measured body length of the same individual. Cat = discrete categorical trait, Cont. = continuous trait.

Trait	Type	Definition	Standardized	Transformed	Functional category	Source
Body shape	Cat.	Overall body shape. Levels: Cylindrical, Dorsoventrally compressed, Laterally compressed	N/A	N/A	Microhabitat use	Carlton 2007
Living habit	Cat.	Mode of contact with habitat substrate (eelgrass). Levels: Tubicolous, Clinging, Swimming	N/A	N/A	Microhabitat use	Carlton 2007
Tube fidelity	Ordered Cat.	The degree of association with constructed silk tubes. Levels: None, Low, Medium, High	N/A	N/A	Microhabitat use	Pers. obs.
Maximum body size	Cont.	Body length measured from the tip of the rostrum to the tip of the telson	N/A	log	Microhabitat use, predator susceptibility	Carlton 2007
Mean body size	Cont.	Body length measured from the tip of the rostrum to the tip of the telson	N/A	log	Microhabitat use, predator susceptibility	Measured
% Swimming	Cont.	Percentage of total frames during which pleopod-driven locomotion occurred	N/A	log	Activity level, predator susceptibility	Measured
% Walking	Cont.	Percentage of total frames during which	N/A	N/A	Activity level,	Measured

		pereopod-driven locomotion in contact with the cup surface occurred			predator susceptibility	
% Still	Cont.	Percentage of total frames during which no forward locomotion occurred	N/A	N/A	Activity level, predator susceptibility	Measured
Eye diameter	Cont.	Diameter of a circle with an area equal to that of the eye (eyes are often irregularly-shaped)	Diameter / Body length	N/A	Sensory	Measured
Antenna length 1	Cont.	Distance from the base to the distal tip of antenna 1	Length / Body length	N/A	Sensory	Measured
Antenna length 2	Cont.	Distance from the base to the distal tip of antenna 2	Length / Body length	N/A	Sensory	Measured

Table A4.8. Mean trait values for each peracarid species observed in grab samples. Continuous morphometric traits are standardized according to Table A4.6; sample size denotes the number of individuals used to collect morphometric measurements, followed by the number of individuals used to collect movement data.

Species	Body shape	Living habit	Tube fidelity	log(Max. body size (mm))	log(Mean body size (mm))	Sample size
Allorchestes angusta	Laterally compressed	Swimming	None	1.0000	0.7656	10, 20
Americorophium spinicorne	Cylindrical	Tubicolous	Medium	0.8451	0.5573	20, 9
Ampithoe lacertosa	Laterally compressed	Tubicolous	Medium	1.3802	1.2241	20, 19
Ampithoe valida	Laterally compressed	Tubicolous	Medium	1.0969	0.8336	14, 19
Aoroides columbiae	Laterally compressed	Tubicolous	Low	0.7782	0.7108	22, 14
Apolochus barnardi	Laterally compressed	Clinging	None	0.3979	0.4465	18, 9

Caprella californica	Cylindrical	Clinging	None	1.4771	1.2663	21, 20
Ericthonius brasiliensis	Cylindrical	Tubicolous	High	0.8129	0.7804	20, 15
Gnorimosphaeroma sp.	Dorsoventrally compressed	Clinging	None	1.0000	0.3656	10, 10
Grandidierella japonica	Laterally compressed	Tubicolous	Medium	1.1139	0.6055	12, 11
Ischyrocerus anguipes	Laterally compressed	Tubicolous	Low	1.0792	0.7205	22, 12
Leptochelia sp.	Cylindrical	Tubicolous	Medium	0.4771	0.5380	10, 10
Melita nitida	Laterally compressed	Swimming	None	1.0792	0.6598	14, 10
Monocorophium insidiosum	Cylindrical	Tubicolous	Medium	0.6532	0.4433	18, 15
Paracerceis cordata	Dorsoventrally compressed	Clinging	None	0.8513	0.5545	9, 14
Paracorophium sp.	Laterally compressed	Tubicolous	Low	0.6021	0.3888	16, 17
Paramicrodeutopus schmitti	Laterally compressed	Tubicolous	Low	0.6990	0.7730	10, 10
Paranthura japonica	Cylindrical	Tubicolous	Medium	0.9590	0.9129	10, 11
Pentidotea resecata	Dorsoventrally compressed	Clinging	None	1.6990	1.2320	10, 10
Photis brevipes	Laterally compressed	Tubicolous	High	0.8451	0.6721	21, 13
Pontogeneia rostrata	Laterally compressed	Swimming	None	0.8129	0.7542	22, 14
Uromunna ubiquita	Dorsoventrally compressed	Clinging	None	0.3010	0.0216	13, 0
Zeuxo normani	Cylindrical	Tubicolous	High	0.4771	0.5253	10, 10

Table A4.7, continued. A1 = antenna length 1, A2 = antenna length 2

Species	log(% Swimming)	% Walking	% Still	Eye diam.	A1	A2	Sample size
Allorchestes angusta	-0.2712	0.0560	0.4084	0.0334	0.2656	0.2451	10, 20
Americorophium spinicorne	-0.3674	0.3353	0.2355	0.0230	0.4270	0.5313	20, 9
Ampithoe lacertosa	-0.6914	0.2940	0.5025	0.0151	0.6798	0.4924	20, 19
Ampithoe valida	-0.3708	0.2619	0.3123	0.0200	0.5430	0.4249	14, 19
Aoroides columbiae	-0.9805	0.3705	0.5249	0.0191	0.5919	0.3128	22, 14
Apolochus barnardi	-1.4612	0.0205	0.9449	0.0433	0.2288	0.1896	18, 9
Caprella californica	-1.0288	0.2929	0.6135	0.0077	0.6116	0.2864	21, 20
Ericthonius brasiliensis	-0.9664	0.1314	0.7605	0.0244	0.4831	0.4838	20, 15

Gnorimosphaeroma sp.	-0.8345	0.2346	0.6191	0.0667	0.2593	0.3793	10, 10
Grandidierella japonica	-0.3383	0.1971	0.3441	0.0228	0.5652	0.4371	12, 11
Ischyrocerus anguipes	-1.0569	0.4292	0.4831	0.0177	0.4416	0.4272	22, 12
Leptochelia sp.	-1.1577	0.5021	0.4283	0.0178	0.2144	0.1157	10, 10
Melita nitida	-0.4091	0.0615	0.5487	0.0245	0.5435	0.3654	14, 10
Monocorophium insidiosum	-0.2725	0.1974	0.2687	0.0246	0.3748	0.4900	18, 15
Paracerceis cordata	-1.8909	0.4669	0.5202	0.0739	0.2338	0.3244	9, 14
Paracorophium sp.	-0.6522	0.3501	0.4271	0.0240	0.3082	0.3156	16, 17
Paramicrodeutopus schmitti	-0.6657	0.0013	0.7828	0.0194	0.3932	0.2589	10, 10
Paranthura japonica	-1.1076	0.5976	0.3243	0.0155	0.0831	0.1013	10, 11
Pentidotea resecata	-0.4588	0.5181	0.1341	0.0186	0.0969	0.4472	10, 10
Photis brevipes	-1.6417	0.4967	0.4805	0.0202	0.3877	0.3628	21, 13
Pontogeneia rostrata	-0.2748	0.0401	0.4288	0.0594	0.4266	0.4973	22, 14
Uromunna ubiquita	NA	NA	NA	0.0393	0.2001	0.8503	13, 0
Zeuxo normani	-1.8539	0.8506	0.1354	0.0161	0.1411	0.1284	10, 10

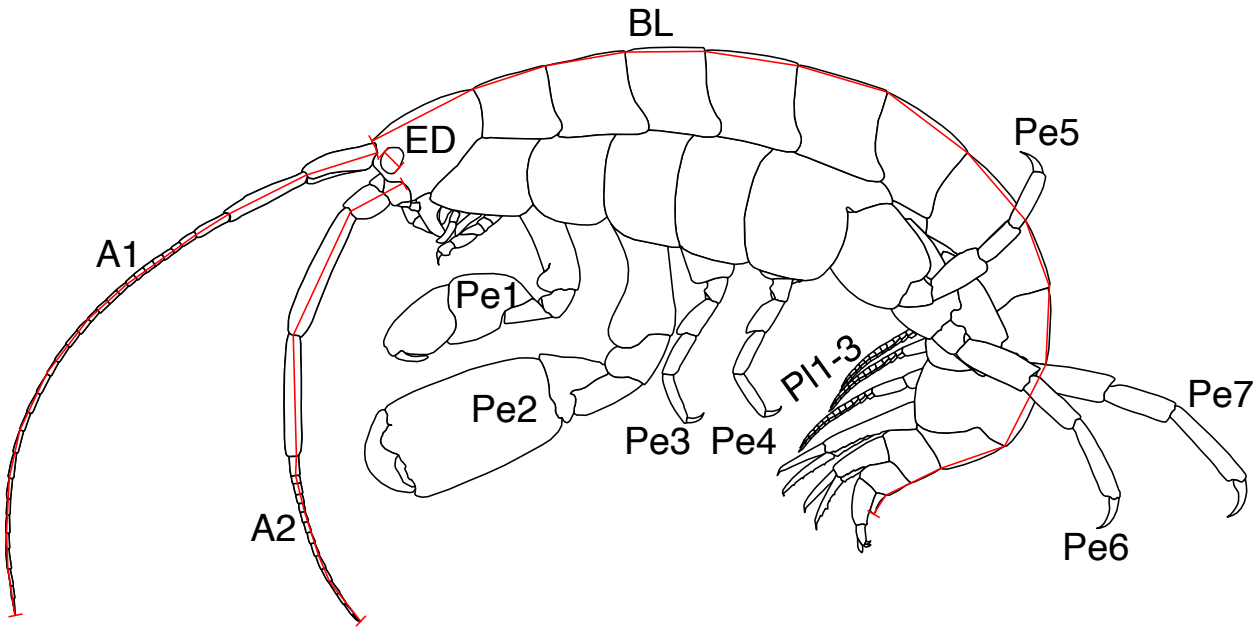

Figure A4.5. Peracarid morphometric traits used in functional analyses, here measured on an amphipod, *Ampithoe valida*. A1 = antenna length 1; A2 = antenna length 2; ED = eye diameter; BL = body length. Pe1-Pe7 denote individual pereopods (walking legs), while Pl1-Pl3 denote individual pleopods (swimming legs). Descriptions of individual traits are provided in Table A4.6.

APPENDIX 5: Supplementary material for Chapter 2.

Table A5.1. Effect sizes of community-weighted mean fish traits on peracarid community trait and phylogenetic dispersion. Bolded cells indicate values significant at the alpha level indicated; the first 103 rows are models for which results are presented in the main text. Italicized rows represent post-hoc tests of individual peracarid community response traits. Rows are colored according to the direction and magnitude of the effect size; red indicates a negative effect while blue indicates a positive effect, and color saturation is proportional to R^2. TS = Tip Shuffle algorithm, IS = Independent Swap algorithm; BDBM = Body Depth Below Midline

Predictor trait	Response trait	Response metric	Response permutation algorithm	Effect size	R^2	alpha level
PC1	all	SES_{MNTD}	TS	0.04471	-0.07225	0.003125
PC2	all	SES_{MNTD}	TS	0.225	-0.01413	0.003125
PC3	all	SES_{MNTD}	TS	0.1713	0.001343	0.003125
PC4	all	SES_{MNTD}	TS	-1.07	0.2779	0.003125
PC5	all	SES_{MNTD}	TS	-0.25312	0.06352	0.003125
PC6	all	SES_{MNTD}	TS	0.2937	0.1789	0.003125
PC7	all	SES_{MNTD}	TS	-0.7743	0.2114	0.003125
PC8	all	SES_{MNTD}	TS	1.249	0.4769	0.003125
PC9	all	SES_{MNTD}	TS	0.9483	0.3428	0.003125
PC10	all	SES_{MNTD}	TS	-1.2957	0.03707	0.003125
PC11	all	SES_{MNTD}	TS	3.65107	0.03478	0.003125
PC12	all	SES_{MNTD}	TS	-3.24415	0.3404	0.003125
PC13	all	SES_{MNTD}	TS	2.48169	0.01732	0.003125
PC14	all	SES_{MNTD}	TS	-5.0352	0.3272	0.003125
PC15	all	SES_{MNTD}	TS	5.4195	0.03951	0.003125
PC16	all	SES_{MNTD}	TS	**14.3565**	**0.6565**	0.003125
Anal fin length	all	SES_{MNTD}	TS	1.4954	-0.06102	0.00263158
BDBM	all	SES_{MNTD}	TS	-13.492	0.5642	0.00263158
Body depth	all	SES_{MNTD}	TS	2.3018	0.004472	0.00263158
Caudal fin length	all	SES_{MNTD}	TS	2.3498	-0.08527	0.00263158
Caudal peduncle depth	all	SES_{MNTD}	TS	0.2568	-0.00711	0.00263158
Caudal peduncle length	all	SES_{MNTD}	TS	0.6436	-0.09203	0.00263158

Dorsal fin length	all	SES_{MNTD}	TS	1.2216	-0.01383	0.00263158
Eye diameter	all	SES_{MNTD}	TS	1.4517	-0.0776	0.00263158
Eye position	all	SES_{MNTD}	TS	7.84	0.2658	0.00263158
Head depth	all	SES_{MNTD}	TS	-3.557	0.05329	0.00263158
Head length	all	SES_{MNTD}	TS	0.8822	-0.09438	0.00263158
Mouth height	all	SES_{MNTD}	TS	3.5411	-0.02024	0.00263158
Mouth protrusion	all	SES_{MNTD}	TS	4.283	0.06329	0.00263158
Pectoral fin length	all	SES_{MNTD}	TS	3.4599	0.007227	0.00263158
Standard length	all	SES_{MNTD}	TS	0.007442	0.005068	0.00263158
Snout length	all	SES_{MNTD}	TS	-0.2739	-0.09941	0.00263158
Trophic level	all	SES_{MNTD}	TS	-0.198	-0.09573	0.00263158
Foraging mode	all	SES_{MNTD}	TS	-0.4545	-0.04048	0.00263158
Vertical position	all	SES_{MNTD}	TS	-0.07623	-0.09513	0.00263158
PC1	phylogeny	SES_{MNTD}	TS	0.04383	-0.08396	0.003125
PC2	phylogeny	SES_{MNTD}	TS	0.3495	0.02462	0.003125
PC3	phylogeny	SES_{MNTD}	TS	0.2277	0.00781	0.003125
PC4	phylogeny	SES_{MNTD}	TS	-1.6731	0.456	0.003125
PC5	phylogeny	SES_{MNTD}	TS	-0.34585	0.08368	0.003125
PC6	phylogeny	SES_{MNTD}	TS	0.4308	0.2609	0.003125
PC7	phylogeny	SES_{MNTD}	TS	-1.0766	0.2622	0.003125
PC8	phylogeny	SES_{MNTD}	TS	**1.7603**	**0.5895**	0.003125
PC9	phylogeny	SES_{MNTD}	TS	1.253	0.3652	0.003125
PC10	phylogeny	SES_{MNTD}	TS	-1.83117	0.06472	0.003125
PC11	phylogeny	SES_{MNTD}	TS	4.9229	0.04743	0.003125
PC12	phylogeny	SES_{MNTD}	TS	-4.41861	0.3911	0.003125
PC13	phylogeny	SES_{MNTD}	TS	2.66958	-0.01832	0.003125
PC14	phylogeny	SES_{MNTD}	TS	-6.7443	0.3611	0.003125
PC15	phylogeny	SES_{MNTD}	TS	6.3838	0.01647	0.003125
PC16	phylogeny	SES_{MNTD}	TS	20.4799	**0.8263**	0.003125
Anal fin length	phylogeny	SES_{MNTD}	TS	1.6601	-0.0711	0.00263158
BDBM	phylogeny	SES_{MNTD}	TS	**-18.736**	**0.6706**	0.00263158
Body depth	phylogeny	SES_{MNTD}	TS	2.7896	-0.007678	0.00263158
Caudal fin length	phylogeny	SES_{MNTD}	TS	1.4752	-0.09651	0.00263158
Caudal peduncle depth	phylogeny	SES_{MNTD}	TS	0.3752	0.0193	0.00263158

Caudal peduncle length	phylogeny	SES_{MNTD}	TS	1.237	-0.08227	0.00263158
Dorsal fin length	phylogeny	SES_{MNTD}	TS	1.476	-0.02431	0.00263158
Eye diameter	phylogeny	SES_{MNTD}	TS	1.5907	-0.08382	0.00263158
Eye position	phylogeny	SES_{MNTD}	TS	10.751	0.314	0.00263158
Head depth	phylogeny	SES_{MNTD}	TS	-4.946	0.07829	0.00263158
Head length	phylogeny	SES_{MNTD}	TS	0.36599	-0.09942	0.00263158
Mouth height	phylogeny	SES_{MNTD}	TS	3.799	-0.04477	0.00263158
Mouth protrusion	phylogeny	SES_{MNTD}	TS	6.184	0.1048	0.00263158
Pectoral fin length	phylogeny	SES_{MNTD}	TS	4.0482	-0.01168	0.00263158
Standard length	phylogeny	SES_{MNTD}	TS	0.01177	0.05813	0.00263158
Snout length	phylogeny	SES_{MNTD}	TS	0.4038	-0.09922	0.00263158
Trophic level	phylogeny	SES_{MNTD}	TS	-0.3671	-0.09117	0.00263158
Foraging mode	phylogeny	SES_{MNTD}	TS	-0.429	-0.0681	0.00263158
Vertical position	phylogeny	SES_{MNTD}	TS	-0.1518	-0.08838	0.00263158
BDBM	*activity level (% still)*	SES_{MNTD}	*TS*	*-6.523*	*0.1309*	*0.0045455*
PC16	*activity level (% still)*	SES_{MNTD}	*TS*	*8.7216*	*0.3152*	*0.0045455*
PC8	*activity level (% still)*	SES_{MNTD}	*TS*	*0.7664*	*0.223*	*0.0045455*
BDBM	*activity level (% swimming)*	SES_{MNTD}	*TS*	*-8.911*	*-0.008397*	*0.0045455*
PC16	*activity level (% swimming)*	SES_{MNTD}	*TS*	*12.7537*	*0.08878*	*0.0045455*
PC8	*activity level (% swimming)*	SES_{MNTD}	*TS*	*1.1776*	*0.06215*	*0.0045455*
BDBM	*activity level (% walking)*	SES_{MNTD}	*TS*	*-10.302*	*-0.000527*	*0.0045455*
PC16	*activity level (% walking)*	SES_{MNTD}	*TS*	*9.3668*	*-0.01727*	*0.0045455*
PC8	*activity level (% walking)*	SES_{MNTD}	*TS*	*0.8837*	*-0.02581*	*0.0045455*
BDBM	*antenna 1 length*	SES_{MNTD}	*TS*	*-9.596*	*0.3811*	*0.0045455*
PC16	*antenna 1 length*	SES_{MNTD}	*TS*	*10.2606*	*0.4533*	*0.0045455*
PC8	*antenna 1 length*	SES_{MNTD}	*TS*	*0.9024*	*0.3311*	*0.0045455*
BDBM	*antenna 2 length*	SES_{MNTD}	*TS*	*1.7397*	*0.329*	*0.0045455*

PC16	*antenna 2 length*	*SES_{MNTD}*	*TS*	*-1.84729*	*0.3866*	*0.0045455*
PC8	*antenna 2 length*	*SES_{MNTD}*	*TS*	*-0.16162*	*0.2753*	*0.0045455*
BDBM	*body shape*	*SES_{MNTD}*	*TS*	*-1.4493*	*0.265*	*0.0045455*
PC16	*body shape*	*SES_{MNTD}*	*TS*	*1.52118*	*0.3045*	*0.0045455*
PC8	*body shape*	*SES_{MNTD}*	*TS*	*0.13093*	*0.2019*	*0.0045455*
BDBM	*eye diameter*	*SES_{MNTD}*	*TS*	*2.5251*	*0.09542*	*0.0045455*
PC16	*eye diameter*	*SES_{MNTD}*	*TS*	*-2.8551*	*0.1513*	*0.0045455*
PC8	*eye diameter*	*SES_{MNTD}*	*TS*	*-0.26376*	*0.1161*	*0.0045455*
BDBM	*living habit*	*SES_{MNTD}*	*TS*	*-1.0751*	*0.1289*	*0.0045455*
PC16	*living habit*	*SES_{MNTD}*	*TS*	*1.05591*	*0.1221*	*0.0045455*
PC8	*living habit*	*SES_{MNTD}*	*TS*	*0.0883*	*0.05653*	*0.0045455*
BDBM	*max body size*	*SES_{MNTD}*	*TS*	*-8.346*	*0.3318*	*0.0045455*
PC16	*max body size*	*SES_{MNTD}*	*TS*	*9.1473*	*0.4218*	*0.0045455*
PC8	*max body size*	*SES_{MNTD}*	*TS*	*0.7703*	*0.2728*	*0.0045455*
BDBM	*mean body size*	*SES_{MNTD}*	*TS*	*0.9199*	*-0.06737*	*0.0045455*
PC16	*mean body size*	*SES_{MNTD}*	*TS*	*-0.587207*	*-0.08662*	*0.0045455*
PC8	*mean body size*	*SES_{MNTD}*	*TS*	*-0.05646*	*-0.08754*	*0.0045455*
BDBM	*tube fidelity*	*SES_{MNTD}*	*TS*	*0.2693*	*-0.09993*	*0.0045455*
PC16	*tube fidelity*	*SES_{MNTD}*	*TS*	*-4.74418*	*-0.07704*	*0.0045455*
PC8	*tube fidelity*	*SES_{MNTD}*	*TS*	*-0.3953*	*-0.08394*	*0.0045455*
PC1	all	SES_{MNTD}	IS	0.06359	-0.0628	0.003125
PC2	all	SES_{MNTD}	IS	0.2856	-0.008355	0.003125
PC3	all	SES_{MNTD}	IS	0.2031	-0.005549	0.003125
PC4	all	SES_{MNTD}	IS	-1.1039	0.1666	0.003125
PC5	all	SES_{MNTD}	IS	-0.25133	0.006855	0.003125
PC6	all	SES_{MNTD}	IS	0.3333	0.138	0.003125
PC7	all	SES_{MNTD}	IS	-0.9344	0.2005	0.003125
PC8	all	SES_{MNTD}	IS	1.3956	0.3774	0.003125
PC9	all	SES_{MNTD}	IS	1.0248	0.2427	0.003125
PC10	all	SES_{MNTD}	IS	-1.28943	-0.01003	0.003125
PC11	all	SES_{MNTD}	IS	3.53332	-0.01634	0.003125
PC12	all	SES_{MNTD}	IS	-3.49097	0.2377	0.003125
PC13	all	SES_{MNTD}	IS	2.98987	0.01287	0.003125
PC14	all	SES_{MNTD}	IS	-5.3802	0.2233	0.003125
PC15	all	SES_{MNTD}	IS	6.4034	0.02909	0.003125
PC16	all	SES_{MNTD}	IS	16.0453	0.5263	0.003125
Anal fin length	all	SES_{MNTD}	IS	1.8311	-0.06126	0.00263158

BDBM	all	SES_{MNTD}	IS	-15.136	0.4541	0.00263158
Body depth	all	SES_{MNTD}	IS	2.9529	0.01395	0.00263158
Caudal fin length	all	SES_{MNTD}	IS	3.7553	-0.07506	0.00263158
Caudal peduncle depth	all	SES_{MNTD}	IS	0.3279	0.0003347	0.00263158
Caudal peduncle length	all	SES_{MNTD}	IS	0.46255	-0.09727	0.00263158
Dorsal fin length	all	SES_{MNTD}	IS	1.367	-0.02848	0.00263158
Eye diameter	all	SES_{MNTD}	IS	2.1562	-0.06725	0.00263158
Eye position	all	SES_{MNTD}	IS	8.291	0.1712	0.00263158
Head depth	all	SES_{MNTD}	IS	-4.147	0.03808	0.00263158
Head length	all	SES_{MNTD}	IS	1.7281	-0.08571	0.00263158
Mouth height	all	SES_{MNTD}	IS	4.3921	-0.01868	0.00263158
Mouth protrusion	all	SES_{MNTD}	IS	4.868	0.03977	0.00263158
Pectoral fin length	all	SES_{MNTD}	IS	4.4111	0.01552	0.00263158
Standard length	all	SES_{MNTD}	IS	0.006985	-0.03865	0.00263158
Snout length	all	SES_{MNTD}	IS	-0.6682	-0.09765	0.00263158
Trophic level	all	SES_{MNTD}	IS	-0.3021	-0.09341	0.00263158
Foraging mode	all	SES_{MNTD}	IS	-0.483	-0.05545	0.00263158
Vertical position	all	SES_MNTD	IS	-0.012752	-0.09991	0.00263158
PC1	phylogeny	SES_MNTD	IS	0.05727	-0.06585	0.003125
PC2	phylogeny	SES_{MNTD}	IS	0.3166	0.0275	0.003125
PC3	phylogeny	SES_{MNTD}	IS	0.2281	0.03479	0.003125
PC4	phylogeny	SES_{MNTD}	IS	-1.3922	0.3798	0.003125
PC5	phylogeny	SES_{MNTD}	IS	-0.28792	0.05869	0.003125
PC6	phylogeny	SES_{MNTD}	IS	0.3784	0.2472	0.003125
PC7	phylogeny	SES_{MNTD}	IS	-0.9775	0.2722	0.003125
PC8	phylogeny	SES_{MNTD}	IS	1.5378	0.5559	0.003125
PC9	phylogeny	SES_{MNTD}	IS	1.1032	0.3495	0.003125
PC10	phylogeny	SES_{MNTD}	IS	-1.54419	0.04602	0.003125
PC11	phylogeny	SES_{MNTD}	IS	4.307	0.04067	0.003125
PC12	phylogeny	SES_{MNTD}	IS	-3.91788	0.3813	0.003125
PC13	phylogeny	SES_{MNTD}	IS	2.56861	-0.005734	0.003125
PC14	phylogeny	SES_{MNTD}	IS	-5.9804	0.352	0.003125
PC15	phylogeny	SES_{MNTD}	IS	5.8831	0.0233	0.003125

PC16	phylogeny	SES_{MNTD}	IS	**17.89997**	**0.7821**	0.003125
Anal fin length	phylogeny	SES_{MNTD}	IS	1.9277	-0.05142	0.00263158
BDBM	phylogeny	SES_{MNTD}	IS	**-16.773**	**0.6699**	0.00263158
Body depth	phylogeny	SES_{MNTD}	IS	2.9711	0.03055	0.00263158
Caudal fin length	phylogeny	SES_{MNTD}	IS	2.7667	-0.08468	0.00263158
Caudal peduncle depth	phylogeny	SES_{MNTD}	IS	0.3562	0.03404	0.00263158
Caudal peduncle length	phylogeny	SES_{MNTD}	IS	0.6981	-0.09296	0.00263158
Dorsal fin length	phylogeny	SES_{MNTD}	IS	1.496	-0.003069	0.00263158
Eye diameter	phylogeny	SES_{MNTD}	IS	2.0708	-0.06581	0.00263158
Eye position	phylogeny	SES_{MNTD}	IS	9.082	0.2682	0.00263158
Head depth	phylogeny	SES_{MNTD}	IS	-4.762	0.106	0.00263158
Head length	phylogeny	SES_{MNTD}	IS	1.153	-0.0928	0.00263158
Mouth height	phylogeny	SES_{MNTD}	IS	4.0495	-0.02177	0.00263158
Mouth protrusion	phylogeny	SES_{MNTD}	IS	5.416	0.09584	0.00263158
Pectoral fin length	phylogeny	SES_{MNTD}	IS	4.3394	0.02651	0.00263158
Standard length	phylogeny	SES_{MNTD}	IS	0.00899	0.01499	0.00263158
Snout length	phylogeny	SES_{MNTD}	IS	-0.2454	-0.09964	0.00263158
Trophic level	phylogeny	SES_{MNTD}	IS	-0.3157	-0.09186	0.00263158
Foraging mode	phylogeny	SES_{MNTD}	IS	-0.4784	-0.05056	0.00263158
Vertical position	phylogeny	SES_{MNTD}	IS	-0.07682	-0.09629	0.00263158
BDBM	*activity level (% still)*	*SES_{MNTD}*	*IS*	*-7.506*	*0.00504*	*0.0045455*
PC16	*activity level (% still)*	*SES_{MNTD}*	*IS*	*11.4922*	*0.1477*	*0.0045455*
PC8	*activity level (% still)*	*SES_{MNTD}*	*IS*	*1.0264*	*0.09906*	*0.0045455*
BDBM	*activity level (% swimming)*	*SES_{MNTD}*	*IS*	*-8.199*	*-0.005406*	*0.0045455*
PC16	*activity level (% swimming)*	*SES_{MNTD}*	*IS*	*11.5614*	*0.08922*	*0.0045455*
PC8	*activity level (% swimming)*	*SES_{MNTD}*	*IS*	*1.0714*	*0.06372*	*0.0045455*
BDBM	*activity level (% walking)*	*SES_{MNTD}*	*IS*	*-7.592*	*0.01645*	*0.0045455*
PC16	*activity level (% walking)*	*SES_{MNTD}*	*IS*	*7.207*	*0.005558*	*0.0045455*

PC8	*activity level (% walking)*	*SES_{MNTD}*	*IS*	*0.6739*	*-0.007018*	*0.0045455*
BDBM	*antenna 1 length*	*SES_{MNTD}*	*IS*	*-10.835*	*0.3396*	*0.0045455*
PC16	*antenna 1 length*	*SES_{MNTD}*	*IS*	*11.5808*	*0.4052*	*0.0045455*
PC8	*antenna 1 length*	*SES_{MNTD}*	*IS*	*1.0178*	*0.2931*	*0.0045455*
BDBM	*antenna 2 length*	*SES_{MNTD}*	*IS*	*3.362*	*0.2894*	*0.0045455*
PC16	*antenna 2 length*	*SES_{MNTD}*	*IS*	*-3.92486*	*0.4338*	*0.0045455*
PC8	*antenna 2 length*	*SES_{MNTD}*	*IS*	*-0.34984*	*0.3273*	*0.0045455*
BDBM	*body shape*	*SES_{MNTD}*	*IS*	*-0.3067*	*-0.02747*	*0.0045455*
PC16	*body shape*	*SES_{MNTD}*	*IS*	*0.233292*	*-0.05778*	*0.0045455*
PC8	*body shape*	*SES_{MNTD}*	*IS*	*0.017372*	*-0.07641*	*0.0045455*
BDBM	*eye diameter*	*SES_{MNTD}*	*IS*	*8.208*	*0.2628*	*0.0045455*
PC16	*eye diameter*	*SES_{MNTD}*	*IS*	*-8.9757*	*0.3365*	*0.0045455*
PC8	*eye diameter*	*SES_{MNTD}*	*IS*	*-0.8018*	*0.251*	*0.0045455*
BDBM	*living habit*	*SES_{MNTD}*	*IS*	*-0.09085*	*-0.09906*	*0.0045455*
PC16	*living habit*	*SES_{MNTD}*	*IS*	*-0.324136*	*-0.08793*	*0.0045455*
PC8	*living habit*	*SES_{MNTD}*	*IS*	*-0.04007*	*-0.08142*	*0.0045455*
BDBM	*max body size*	*SES_{MNTD}*	*IS*	*-10.955*	*0.2785*	*0.0045455*
PC16	*max body size*	*SES_{MNTD}*	*IS*	*11.9026*	*0.3494*	*0.0045455*
PC8	*max body size*	*SES_{MNTD}*	*IS*	*0.9915*	*0.2142*	*0.0045455*
BDBM	*mean body size*	*SES_{MNTD}*	*IS*	*3.816*	*0.02283*	*0.0045455*
PC16	*mean body size*	*SES_{MNTD}*	*IS*	*-3.78075*	*0.0213*	*0.0045455*
PC8	*mean body size*	*SES_{MNTD}*	*IS*	*-0.337*	*-0.002909*	*0.0045455*
BDBM	*tube fidelity*	*SES_{MNTD}*	*IS*	*-0.21395*	*-0.09994*	*0.0045455*
PC16	*tube fidelity*	*SES_{MNTD}*	*IS*	*-2.83726*	*-0.08982*	*0.0045455*
PC8	*tube fidelity*	*SES_{MNTD}*	*IS*	*-0.21927*	*-0.09388*	*0.0045455*
PC1	all	SES_{MPD}	TS	0.02844	-0.08938	0.003125
PC2	all	SES_{MPD}	TS	0.1031	-0.08296	0.003125
PC3	all	SES_{MPD}	TS	0.1541	-0.02243	0.003125
PC4	all	SES_{MPD}	TS	-1.0746	0.2606	0.003125
PC5	all	SES_{MPD}	TS	-0.30594	0.126	0.003125
PC6	all	SES_{MPD}	TS	0.2437	0.08158	0.003125
PC7	all	SES_{MPD}	TS	-0.5432	0.04495	0.003125
PC8	all	SES_{MPD}	TS	1.1196	0.3385	0.003125
PC9	all	SES_{MPD}	TS	0.992	0.3584	0.003125

PC10	all	SES_{MPD}	TS	-1.5469	0.0848	0.003125
PC11	all	SES_{MPD}	TS	4.8927	0.1289	0.003125
PC12	all	SES_{MPD}	TS	-3.40143	0.3575	0.003125
PC13	all	SES_{MPD}	TS	2.21331	-0.01173	0.003125
PC14	all	SES_{MPD}	TS	-5.4347	0.3708	0.003125
PC15	all	SES_{MPD}	TS	4.73924	0.000917	0.003125
PC16	all	SES_{MPD}	TS	12.7554	0.4649	0.003125
Anal fin length	all	SES_{MPD}	TS	1.5383	-0.06098	0.00263158
BDBM	all	SES_{MPD}	TS	-12.423	0.4327	0.00263158
Body depth	all	SES_{MPD}	TS	1.705	-0.04578	0.00263158
Caudal fin length	all	SES_{MPD}	TS	1.1645	-0.09658	0.00263158
Caudal peduncle depth	all	SES_{MPD}	TS	0.1372	-0.07493	0.00263158
Caudal peduncle length	all	SES_{MPD}	TS	0.7863	-0.08874	0.00263158
Dorsal fin length	all	SES_{MPD}	TS	1.3908	0.005655	0.00263158
Eye diameter	all	SES_{MPD}	TS	0.6543	-0.0957	0.00263158
Eye position	all	SES_{MPD}	TS	8.175	0.2763	0.00263158
Head depth	all	SES_{MPD}	TS	-3.15	0.01367	0.00263158
Head length	all	SES_{MPD}	TS	-0.10338	-0.09993	0.00263158
Mouth height	all	SES_{MPD}	TS	3.1774	-0.03926	0.00263158
Mouth protrusion	all	SES_{MPD}	TS	3.561	0.00674	0.00263158
Pectoral fin length	all	SES_{MPD}	TS	2.704	-0.03805	0.00263158
Standard length	all	SES_{MPD}	TS	0.008589	0.03239	0.00263158
Snout length	all	SES_{MPD}	TS	-0.1489	-0.09983	0.00263158
Trophic level	all	SES_{MPD}	TS	0.09102	-0.09915	0.00263158
Foraging mode	all	SES_{MPD}	TS	-0.6671	0.02129	0.00263158
Vertical position	all	SES_{MPD}	TS	-0.1976	-0.06905	0.00263158
PC1	phylogeny	SES_{MPD}	TS	0.05309	-0.07896	0.003125
PC2	phylogeny	SES_{MPD}	TS	0.3247	-0.003811	0.003125
PC3	phylogeny	SES_{MPD}	TS	0.1938	-0.03023	0.003125
PC4	phylogeny	SES_{MPD}	TS	-1.2883	0.1947	0.003125
PC5	phylogeny	SES_{MPD}	TS	-0.2897	0.01521	0.003125
PC6	phylogeny	SES_{MPD}	TS	0.377	0.1471	0.003125
PC7	phylogeny	SES_{MPD}	TS	-1.0497	0.2078	0.003125

PC8	phylogeny	SES_{MPD}	TS	1.5874	0.4013	0.003125
PC9	phylogeny	SES_{MPD}	TS	1.1396	0.244	0.003125
PC10	phylogeny	SES_{MPD}	TS	-1.45346	-0.007229	0.003125
PC11	phylogeny	SES_{MPD}	TS	3.68702	-0.02607	0.003125
PC12	phylogeny	SES_{MPD}	TS	-3.81167	0.2267	0.003125
PC13	phylogeny	SES_{MPD}	TS	3.26063	0.008936	0.003125
PC14	phylogeny	SES_{MPD}	TS	-5.8638	0.2116	0.003125
PC15	phylogeny	SES_{MPD}	TS	7.1662	0.03121	0.003125
PC16	phylogeny	SES_{MPD}	TS	18.21	0.5547	0.003125
Anal fin length	phylogeny	SES_{MPD}	TS	1.4783	-0.07951	0.00263158
BDBM	phylogeny	SES_{MPD}	TS	-16.645	0.4437	0.00263158
Body depth	phylogeny	SES_{MPD}	TS	2.8054	-0.01652	0.00263158
Caudal fin length	phylogeny	SES_{MPD}	TS	2.8572	-0.08828	0.00263158
Caudal peduncle depth	phylogeny	SES_{MPD}	TS	0.3522	-0.006041	0.00263158
Caudal peduncle length	phylogeny	SES_{MPD}	TS	0.9322	-0.091	0.00263158
Dorsal fin length	phylogeny	SES_{MPD}	TS	1.2565	-0.05097	0.00263158
Eye diameter	phylogeny	SES_{MPD}	TS	1.7631	-0.08223	0.00263158
Eye position	phylogeny	SES_{MPD}	TS	9.66	0.1988	0.00263158
Head depth	phylogeny	SES_{MPD}	TS	-4.133	0.01128	0.00263158
Head length	phylogeny	SES_{MPD}	TS	1.2172	-0.09425	0.00263158
Mouth height	phylogeny	SES_{MPD}	TS	4.2515	-0.03816	0.00263158
Mouth protrusion	phylogeny	SES_{MPD}	TS	5.549	0.04739	0.00263158
Pectoral fin length	phylogeny	SES_{MPD}	TS	4.1853	-0.0156	0.00263158
Standard length	phylogeny	SES_{MPD}	TS	0.009002	-0.01731	0.00263158
Snout length	phylogeny	SES_{MPD}	TS	-0.1326	-0.09993	0.00263158
Trophic level	phylogeny	SES_{MPD}	TS	-0.3928	-0.09096	0.00263158
Foraging mode	phylogeny	SES_{MPD}	TS	-0.3937	-0.07598	0.00263158
Vertical position	phylogeny	SES_{MPD}	TS	-0.0519	-0.09879	0.00263158
BDBM	*activity level (% still)*	*SES_{MPD}*	*TS*	*-11.716*	*0.493*	*0.0045455*
PC16	*activity level (% still)*	*SES_{MPD}*	*TS*	***13.51323***	***0.6936***	*0.0045455*
PC8	*activity level (% still)*	*SES_{MPD}*	*TS*	*1.1939*	*0.5241*	*0.0045455*

BDBM	*activity level (% swimming)*	*SES_{MPD}*	*TS*	*-12.082*	*0.05978*	*0.0045455*
PC16	*activity level (% swimming)*	*SES_{MPD}*	*TS*	*12.4202*	*0.06986*	*0.0045455*
PC8	*activity level (% swimming)*	*SES_{MPD}*	*TS*	*1.1517*	*0.04714*	*0.0045455*
BDBM	*activity level (% walking)*	*SES_{MPD}*	*TS*	*-13.287*	*0.116*	*0.0045455*
PC16	*activity level (% walking)*	*SES_{MPD}*	*TS*	*13.3525*	*0.1194*	*0.0045455*
PC8	*activity level (% walking)*	*SES_{MPD}*	*TS*	*1.2181*	*0.08399*	*0.0045455*
BDBM	*antenna 1 length*	*SES_{MPD}*	*TS*	***-15.248***	***0.5752***	*0.0045455*
PC16	*antenna 1 length*	*SES_{MPD}*	*TS*	***17.13355***	***0.7575***	*0.0045455*
PC8	*antenna 1 length*	*SES_{MPD}*	*TS*	***1.5025***	***0.5644***	*0.0045455*
BDBM	*antenna 2 length*	*SES_{MPD}*	*TS*	*0.18411*	*-0.07591*	*0.0045455*
PC16	*antenna 2 length*	*SES_{MPD}*	*TS*	*2.09415*	*-0.06906*	*0.0045455*
PC8	*antenna 2 length*	*SES_{MPD}*	*TS*	*0.18411*	*-0.07591*	*0.0045455*
BDBM	*body shape*	*SES_{MPD}*	*TS*	*6.29*	*0.137*	*0.0045455*
PC16	*body shape*	*SES_{MPD}*	*TS*	*-6.42637*	*0.1488*	*0.0045455*
PC8	*body shape*	*SES_{MPD}*	*TS*	*-0.5253*	*0.06753*	*0.0045455*
BDBM	*eye diameter*	*SES_{MPD}*	*TS*	*-0.4154*	*-0.09141*	*0.0045455*
PC16	*eye diameter*	*SES_{MPD}*	*TS*	*0.75786*	*-0.07125*	*0.0045455*
PC8	*eye diameter*	*SES_{MPD}*	*TS*	*0.05451*	*-0.08501*	*0.0045455*
BDBM	*living habit*	*SES_{MPD}*	*TS*	*-3.714*	*-0.05397*	*0.0045455*
PC16	*living habit*	*SES_{MPD}*	*TS*	*1.93645*	*-0.08741*	*0.0045455*
PC8	*living habit*	*SES_{MPD}*	*TS*	*0.09847*	*-0.09672*	*0.0045455*
BDBM	*max body size*	*SES_{MPD}*	*TS*	*-6.376*	*0.1635*	*0.0045455*
PC16	*max body size*	*SES_{MPD}*	*TS*	*5.10984*	*0.07023*	*0.0045455*
PC8	*max body size*	*SES_{MPD}*	*TS*	*0.4032*	*0.006777*	*0.0045455*
BDBM	*mean body size*	*SES_{MPD}*	*TS*	*-2.766*	*-0.03771*	*0.0045455*
PC16	*mean body size*	*SES_{MPD}*	*TS*	*1.52946*	*-0.08084*	*0.0045455*
PC8	*mean body size*	*SES_{MPD}*	*TS*	*0.09095*	*-0.09317*	*0.0045455*
BDBM	*tube fidelity*	*SES_{MPD}*	*TS*	*-11.093*	*0.1503*	*0.0045455*
PC16	*tube fidelity*	*SES_{MPD}*	*TS*	*9.1219*	*0.07026*	*0.0045455*
PC8	*tube fidelity*	*SES_{MPD}*	*TS*	*0.7595*	*0.01892*	*0.0045455*
PC1	all	SES_{MPD}	IS	0.1312	0.05105	0.003125

PC2	all	SES_{MPD}	IS	0.2099	-0.05275	0.003125
PC3	all	SES_{MPD}	IS	0.34	0.1527	0.003125
PC4	all	SES_{MPD}	IS	-0.7953	0.03207	0.003125
PC5	all	SES_{MPD}	IS	-0.1668	-0.05508	0.003125
PC6	all	SES_{MPD}	IS	0.2603	0.0386	0.003125
PC7	all	SES_{MPD}	IS	-0.6837	0.05357	0.003125
PC8	all	SES_{MPD}	IS	0.9918	0.1301	0.003125
PC9	all	SES_{MPD}	IS	0.8282	0.1136	0.003125
PC10	all	SES_{MPD}	IS	-1.09532	-0.03804	0.003125
PC11	all	SES_{MPD}	IS	4.5731	0.03375	0.003125
PC12	all	SES_{MPD}	IS	-3.34981	0.1967	0.003125
PC13	all	SES_{MPD}	IS	2.08646	-0.04754	0.003125
PC14	all	SES_{MPD}	IS	-5.1499	0.1827	0.003125
PC15	all	SES_{MPD}	IS	3.93297	-0.05352	0.003125
PC16	all	SES_{MPD}	IS	11.8474	0.2259	0.003125
Anal fin length	all	SES_{MPD}	IS	4.3025	0.1041	0.00263158
BDBM	all	SES_{MPD}	IS	-13.779	0.3382	0.00263158
Body depth	all	SES_{MPD}	IS	4.6609	0.171	0.00263158
Caudal fin length	all	SES_{MPD}	IS	8.5411	0.02312	0.00263158
Caudal peduncle depth	all	SES_{MPD}	IS	0.3385	0.002095	0.00263158
Caudal peduncle length	all	SES_{MPD}	IS	-1.5693	-0.07001	0.00263158
Dorsal fin length	all	SES_{MPD}	IS	2.4794	0.1245	0.00263158
Eye diameter	all	SES_{MPD}	IS	4.7839	0.05387	0.00263158
Eye position	all	SES_{MPD}	IS	4.602	-0.02025	0.00263158
Head depth	all	SES_{MPD}	IS	-6.152	0.19	0.00263158
Head length	all	SES_{MPD}	IS	4.327	-0.01447	0.00263158
Mouth height	all	SES_{MPD}	IS	6.1171	0.05055	0.00263158
Mouth protrusion	all	SES_{MPD}	IS	3.466	-0.03238	0.00263158
Pectoral fin length	all	SES_{MPD}	IS	6.8813	0.1683	0.00263158
Standard length	all	SES_{MPD}	IS	0.0007999	-0.09923	0.00263158
Snout length	all	SES_{MPD}	IS	-3.188	-0.04901	0.00263158
Trophic level	all	SES_{MPD}	IS	0.04308	-0.09987	0.00263158
Foraging mode	all	SES_{MPD}	IS	-1.0744	0.1103	0.00263158

Vertical position	all	SES_{MPD}	IS	0.12334	-0.09193	0.00263158
PC1	phylogeny	SES_{MPD}	IS	0.1347	0.1092	0.003125
PC2	phylogeny	SES_{MPD}	IS	0.2708	0.003273	0.003125
PC3	phylogeny	SES_{MPD}	IS	0.3124	0.1801	0.003125
PC4	phylogeny	SES_{MPD}	IS	-0.5609	-0.01375	0.003125
PC5	phylogeny	SES_{MPD}	IS	-0.07359	-0.08852	0.003125
PC6	phylogeny	SES_{MPD}	IS	0.245	0.06123	0.003125
PC7	phylogeny	SES_{MPD}	IS	-0.7439	0.1387	0.003125
PC8	phylogeny	SES_{MPD}	IS	0.8693	0.1321	0.003125
PC9	phylogeny	SES_{MPD}	IS	0.6145	0.05441	0.003125
PC10	phylogeny	SES_{MPD}	IS	-0.61088	-0.0747	0.003125
PC11	phylogeny	SES_{MPD}	IS	2.6675	-0.04025	0.003125
PC12	phylogeny	SES_{MPD}	IS	-2.55808	0.1272	0.003125
PC13	phylogeny	SES_{MPD}	IS	1.98236	-0.03782	0.003125
PC14	phylogeny	SES_{MPD}	IS	-3.8007	0.1022	0.003125
PC15	phylogeny	SES_{MPD}	IS	3.73891	-0.04485	0.003125
PC16	phylogeny	SES_{MPD}	IS	10.4749	0.2345	0.003125
Anal fin length	phylogeny	SES_{MPD}	IS	3.8571	0.1154	0.00263158
BDBM	phylogeny	SES_{MPD}	IS	-12.012	0.3373	0.00263158
Body depth	phylogeny	SES_{MPD}	IS	4.6634	0.2562	0.00263158
Caudal fin length	phylogeny	SES_{MPD}	IS	9.0636	0.08204	0.00263158
Caudal peduncle depth	phylogeny	SES_{MPD}	IS	0.388	0.07606	0.00263158
Caudal peduncle length	phylogeny	SES_{MPD}	IS	-1.7504	-0.05101	0.00263158
Dorsal fin length	phylogeny	SES_{MPD}	IS	2.0368	0.09897	0.00263158
Eye diameter	phylogeny	SES_{MPD}	IS	5.085	0.1283	0.00263158
Eye position	phylogeny	SES_{MPD}	IS	2.932	-0.05749	0.00263158
Head depth	phylogeny	SES_{MPD}	IS	-5.645	0.2206	0.00263158
Head length	phylogeny	SES_{MPD}	IS	4.98	0.04873	0.00263158
Mouth height	phylogeny	SES_{MPD}	IS	5.7597	0.07526	0.00263158
Mouth protrusion	phylogeny	SES_{MPD}	IS	3.272	-0.02085	0.00263158
Pectoral fin length	phylogeny	SES_{MPD}	IS	6.7875	0.2427	0.00263158
Standard length	phylogeny	SES_{MPD}	IS	-0.001581	-0.09606	0.00263158
Snout length	phylogeny	SES_{MPD}	IS	-3.197	-0.03268	0.00263158

Trophic level	phylogeny	SES_{MPD}	IS	-0.1808	-0.09704	0.00263158
Foraging mode	phylogeny	SES_{MPD}	IS	-0.7833	0.0468	0.00263158
Vertical position	phylogeny	SES_{MPD}	IS	0.245	-0.05821	0.00263158
BDBM	*activity level (% still)*	*SES_{MPD}*	*IS*	***-18.077***	***0.5759***	*0.0045455*
PC16	*activity level (% still)*	*SES_{MPD}*	*IS*	***17.8945***	***0.5662***	*0.0045455*
PC8	*activity level (% still)*	*SES_{MPD}*	*IS*	*1.5369*	*0.3951*	*0.0045455*
BDBM	*activity level (% swimming)*	*SES_{MPD}*	*IS*	*-11.559*	*0.1032*	*0.0045455*
PC16	*activity level (% swimming)*	*SES_{MPD}*	*IS*	*10.6291*	*0.07286*	*0.0045455*
PC8	*activity level (% swimming)*	*SES_{MPD}*	*IS*	*0.9597*	*0.04197*	*0.0045455*
BDBM	*activity level (% walking)*	*SES_{MPD}*	*IS*	*-10.427*	*0.1532*	*0.0045455*
PC16	*activity level (% walking)*	*SES_{MPD}*	*IS*	*9.4573*	*0.1095*	*0.0045455*
PC8	*activity level (% walking)*	*SES_MPD*	*IS*	*0.8446*	*0.06836*	*0.0045455*
BDBM	*antenna 1 length*	*SES_{MPD}*	*IS*	*-14.464*	*0.4704*	*0.0045455*
PC16	*antenna 1 length*	*SES_{MPD}*	*IS*	*13.4336*	*0.395*	*0.0045455*
PC8	*antenna 1 length*	*SES_{MPD}*	*IS*	*1.1297*	*0.2527*	*0.0045455*
BDBM	*antenna 2 length*	*SES_{MPD}*	*IS*	*-7.51*	*0.08254*	*0.0045455*
PC16	*antenna 2 length*	*SES_{MPD}*	*IS*	*5.41524*	*-0.004533*	*0.0045455*
PC8	*antenna 2 length*	*SES_{MPD}*	*IS*	*0.4407*	*-0.03628*	*0.0045455*
BDBM	*body shape*	*SES_{MPD}*	*IS*	*2.328*	*-0.08247*	*0.0045455*
PC16	*body shape*	*SES_{MPD}*	*IS*	*-5.1407*	*-0.014*	*0.0045455*
PC8	*body shape*	*SES_{MPD}*	*IS*	*-0.4629*	*-0.02973*	*0.0045455*
BDBM	*eye diameter*	*SES_{MPD}*	*IS*	*-10.391*	*0.1864*	*0.0045455*
PC16	*eye diameter*	*SES_{MPD}*	*IS*	*8.836*	*0.1084*	*0.0045455*
PC8	*eye diameter*	*SES_{MPD}*	*IS*	*0.6975*	*0.03081*	*0.0045455*
BDBM	*living habit*	*SES_{MPD}*	*IS*	*-7.53*	*0.04946*	*0.0045455*
PC16	*living habit*	*SES_{MPD}*	*IS*	*5.137*	*-0.03002*	*0.0045455*
PC8	*living habit*	*SES_{MPD}*	*IS*	*0.3726*	*-0.0629*	*0.0045455*
BDBM	*max body size*	*SES_{MPD}*	*IS*	*-8.346*	*0.112*	*0.0045455*
PC16	*max body size*	*SES_{MPD}*	*IS*	*6.20164*	*0.01777*	*0.0045455*
PC8	*max body size*	*SES_{MPD}*	*IS*	*0.4755*	*-0.03024*	*0.0045455*

BDBM	*mean body size*	*SES_{MPD}*	*IS*	*-5.872*	*0.02926*	*0.0045455*
PC16	*mean body size*	*SES_{MPD}*	*IS*	*4.06398*	*-0.03771*	*0.0045455*
PC8	*mean body size*	*SES_{MPD}*	*IS*	*0.29273*	*-0.06744*	*0.0045455*
BDBM	*tube fidelity*	*SES_{MPD}*	*IS*	*-10.087*	*0.1548*	*0.0045455*
PC16	*tube fidelity*	*SES_{MPD}*	*IS*	*8.1603*	*0.06775*	*0.0045455*
PC8	*tube fidelity*	*SES_{MPD}*	*IS*	*0.6825*	*0.01822*	*0.0045455*

Table A5.2. Effect sizes of fish community trait dispersion on residual peracarid community trait and phylogenetic dispersion, not accounting for the effects of habitat filters on fish dispersion. Bolded cells indicate values significant at alpha = 0.008333; the first 24 rows are effects for which results are presented in the main text. Rows are colored according to the direction and magnitude of the effect size; red indicates a negative effect while blue indicates a positive effect, and color saturation is proportional to R^2. TS = Tip Shuffle algorithm, IS = Independent Swap algorithm; BDBM = Body Depth Below Midline.

Predictor trait	Predictor metric	Predictor algorithm	Response trait	Response metric	Response algorithm	Effect size	R^2
all	SES_{MNTD}	TS	activity level (% still)	SES_{MNTD}	TS	0.1302	-0.01212
BDBM	SES_{MNTD}	TS	activity level (% still)	SES_{MNTD}	TS	-0.2055	0.1616
PC16	SES_{MNTD}	TS	activity level (% still)	SES_{MNTD}	TS	-0.07272	-0.09093
PC8	SES_{MNTD}	TS	activity level (% still)	SES_{MNTD}	TS	-0.13771	0.06993
all	SES_{MNTD}	TS	all	SES_{MNTD}	TS	0.13797	-0.03364
BDBM	SES_{MNTD}	TS	all	SES_{MNTD}	TS	**-0.3945**	**0.5485**
PC16	SES_{MNTD}	TS	all	SES_{MNTD}	TS	0.09154	-0.09034
PC8	SES_{MNTD}	TS	all	SES_{MNTD}	TS	-0.24802	0.2707
all	SES_{MNTD}	TS	antenna 1 length	SES_{MNTD}	TS	0.17849	0.059
BDBM	SES_{MNTD}	TS	antenna 1 length	SES_{MNTD}	TS	-0.30197	0.4439
PC16	SES_{MNTD}	TS	antenna 1 length	SES_{MNTD}	TS	-0.08891	-0.08695
PC8	SES_{MNTD}	TS	antenna 1 length	SES_{MNTD}	TS	-0.16647	0.1391
all	SES_{MNTD}	TS	antenna 2 length	SES_{MNTD}	TS	-0.010598	-0.08479

BDBM	SES_{MNTD}	TS	antenna 2 length	SES_{MNTD}	TS	0.047625	0.2671
PC16	SES_{MNTD}	TS	antenna 2 length	SES_{MNTD}	TS	-0.02119	-0.07988
PC8	SES_{MNTD}	TS	antenna 2 length	SES_{MNTD}	TS	0.029647	0.1058
all	SES_{MNTD}	TS	max. body size	SES_{MNTD}	TS	0.13862	0.0138
BDBM	SES_{MNTD}	TS	max. body size	SES_{MNTD}	TS	-0.28207	0.4631
PC16	SES_{MNTD}	TS	max. body size	SES_{MNTD}	TS	0.03453	-0.09766
PC8	SES_{MNTD}	TS	max. body size	SES_{MNTD}	TS	-0.20856	0.3453
all	SES_{MNTD}	TS	phylogeny	SES_{MNTD}	TS	0.22165	0.003042
BDBM	SES_{MNTD}	TS	phylogeny	SES_{MNTD}	TS	**-0.5742**	**0.7263**
PC16	SES_{MNTD}	TS	phylogeny	SES_{MNTD}	TS	0.1332	-0.08769
PC8	SES_{MNTD}	TS	phylogeny	SES_{MNTD}	TS	-0.39414	0.4632
all	SES_{MNTD}	TS	activity level (% still)	SES_{MNTD}	IS	0.18328	-0.04017
BDBM	SES_{MNTD}	TS	activity level (% still)	SES_{MNTD}	IS	-0.23325	0.01581
PC16	SES_{MNTD}	TS	activity level (% still)	SES_{MNTD}	IS	-0.178	-0.08133
PC8	SES_{MNTD}	TS	activity level (% still)	SES_{MNTD}	IS	-0.15043	-0.03033
all	SES_{MNTD}	TS	all	SES_{MNTD}	IS	0.11902	-0.06727
BDBM	SES_{MNTD}	TS	all	SES_{MNTD}	IS	-0.43018	0.4109
PC16	SES_{MNTD}	TS	all	SES_{MNTD}	IS	0.1613	-0.08012
PC8	SES_{MNTD}	TS	all	SES_{MNTD}	IS	-0.27484	0.2017
all	SES_{MNTD}	TS	antenna 1 length	SES_{MNTD}	IS	0.21427	0.06424
BDBM	SES_{MNTD}	TS	antenna 1 length	SES_{MNTD}	IS	-0.34608	0.412
PC16	SES_{MNTD}	TS	antenna 1 length	SES_{MNTD}	IS	-0.11917	-0.08319
PC8	SES_{MNTD}	TS	antenna 1 length	SES_{MNTD}	IS	-0.19037	0.1241
all	SES_{MNTD}	TS	antenna 2 length	SES_{MNTD}	IS	-0.023894	0.686
BDBM	SES_{MNTD}	TS	antenna 2 length	SES_{MNTD}	IS	0.08781	0.2033
PC16	SES_{MNTD}	TS	antenna 2 length	SES_{MNTD}	IS	-0.01991	-0.09568
PC8	SES_{MNTD}	TS	antenna 2 length	SES_{MNTD}	IS	0.050719	0.04635
all	SES_{MNTD}	TS	max. body size	SES_{MNTD}	IS	0.17243	-0.01043

BDBM	SES_{MNTD}	TS	max. body size	SES_{MNTD}	IS	-0.37488	0.406
PC16	SES_{MNTD}	TS	max. body size	SES_{MNTD}	IS	0.08646	-0.09255
PC8	SES_{MNTD}	TS	max. body size	SES_{MNTD}	IS	-0.29047	0.3394
all	SES_{MNTD}	TS	phylogeny	SES_{MNTD}	IS	0.18771	-0.00787
BDBM	SES_{MNTD}	TS	phylogeny	SES_{MNTD}	IS	**-0.51094**	**0.7157**
PC16	SES_{MNTD}	TS	phylogeny	SES_{MNTD}	IS	0.1362	-0.08396
PC8	SES_{MNTD}	TS	phylogeny	SES_{MNTD}	IS	-0.3461	0.4414
all	SES_{MNTD}	TS	activity level (% still)	SES_{MPD}	TS	0.15091	-0.006004
BDBM	SES_{MNTD}	TS	activity level (% still)	SES_{MPD}	TS	-0.33869	0.4658
PC16	SES_{MNTD}	TS	activity level (% still)	SES_{MPD}	TS	-0.01331	-0.09976
PC8	SES_{MNTD}	TS	activity level (% still)	SES_{MPD}	TS	-0.20024	0.1861
all	SES_{MNTD}	TS	all	SES_{MPD}	TS	0.20343	0.03646
BDBM	SES_{MNTD}	TS	all	SES_{MPD}	TS	**-0.38374**	**0.4803**
PC16	SES_{MNTD}	TS	all	SES_{MPD}	TS	-0.06502	-0.09539
PC8	SES_{MNTD}	TS	all	SES_{MPD}	TS	-0.2103	0.1521
all	SES_{MNTD}	TS	antenna 1 length	SES_{MPD}	TS	0.19853	0.00935
BDBM	SES_{MNTD}	TS	antenna 1 length	SES_{MPD}	TS	**-0.4511**	**0.5746**
PC16	SES_{MNTD}	TS	antenna 1 length	SES_{MPD}	TS	0.007573	-0.09995
PC8	SES_{MNTD}	TS	antenna 1 length	SES_{MPD}	TS	-0.27583	0.2648
all	SES_{MNTD}	TS	antenna 2 length	SES_{MPD}	TS	-0.030261	-0.09386
BDBM	SES_{MNTD}	TS	antenna 2 length	SES_{MPD}	TS	-0.059989	-0.07119
PC16	SES_{MNTD}	TS	antenna 2 length	SES_{MPD}	TS	0.10682	-0.07471
PC8	SES_{MNTD}	TS	antenna 2 length	SES_{MPD}	TS	-0.029769	-0.08974
all	SES_{MNTD}	TS	max. body size	SES_{MPD}	TS	0.11042	-0.02451
BDBM	SES_{MNTD}	TS	max. body size	SES_{MPD}	TS	-0.23592	0.3118
PC16	SES_{MNTD}	TS	max. body size	SES_{MPD}	TS	0.06831	-0.09044
PC8	SES_{MNTD}	TS	max. body size	SES_{MPD}	TS	-0.17195	0.2165
all	SES_{MNTD}	TS	phylogeny	SES_{MPD}	TS	0.1192	-0.07337
BDBM	SES_{MNTD}	TS	phylogeny	SES_{MPD}	TS	-0.46549	0.3855

PC16	SES_{MNTD}	TS	phylogeny	SES_{MPD}	TS	0.189	-0.07784
PC8	SES_{MNTD}	TS	phylogeny	SES_{MPD}	TS	-0.30306	0.1977
all	SES_{MNTD}	TS	activity level (% still)	SES_{MPD}	IS	0.24903	0.02255
BDBM	SES_{MNTD}	TS	activity level (% still)	SES_{MPD}	IS	**-0.56827**	**0.6626**
PC16	SES_{MNTD}	TS	activity level (% still)	SES_{MPD}	IS	0.0647	-0.09726
PC8	SES_{MNTD}	TS	activity level (% still)	SES_{MPD}	IS	-0.35456	0.3294
all	SES_{MNTD}	TS	all	SES_{MPD}	IS	0.22319	0.009846
BDBM	SES_{MNTD}	TS	all	SES_{MPD}	IS	**-0.46525**	**0.4704**
PC16	SES_{MNTD}	TS	all	SES_{MPD}	IS	0.04955	-0.09821
PC8	SES_{MNTD}	TS	all	SES_{MPD}	IS	-0.29018	0.2209
all	SES_{MNTD}	TS	antenna 1 length	SES_{MPD}	IS	0.21298	0.01816
BDBM	SES_{MNTD}	TS	antenna 1 length	SES_{MPD}	IS	**-0.47811**	**0.6116**
PC16	SES_{MNTD}	TS	antenna 1 length	SES_{MPD}	IS	0.08451	-0.09385
PC8	SES_{MNTD}	TS	antenna 1 length	SES_{MPD}	IS	-0.31398	0.3439
all	SES_{MNTD}	TS	antenna 2 length	SES_{MPD}	IS	0.038464	-0.09543
BDBM	SES_{MNTD}	TS	antenna 2 length	SES_{MPD}	IS	-0.23202	0.0989
PC16	SES_{MNTD}	TS	antenna 2 length	SES_{MPD}	IS	0.1815	-0.06629
PC8	SES_{MNTD}	TS	antenna 2 length	SES_{MPD}	IS	-0.15222	0.02383
all	SES_{MNTD}	TS	max. body size	SES_{MPD}	IS	0.13779	-0.04479
BDBM	SES_{MNTD}	TS	max. body size	SES_{MPD}	IS	-0.31445	0.2436
PC16	SES_{MNTD}	TS	max. body size	SES_{MPD}	IS	0.1236	-0.08531
PC8	SES_{MNTD}	TS	max. body size	SES_{MPD}	IS	-0.23535	0.1784
all	SES_{MNTD}	TS	phylogeny	SES_{MPD}	IS	0.12528	-0.05456
BDBM	SES_{MNTD}	TS	phylogeny	SES_{MPD}	IS	-0.38672	0.4175
PC16	SES_{MNTD}	TS	phylogeny	SES_{MPD}	IS	0.1758	-0.0704
PC8	SES_{MNTD}	TS	phylogeny	SES_{MPD}	IS	-0.26378	0.2482
all	SES_{MNTD}	IS	activity level (% still)	SES_{MNTD}	TS	0.12006	0.01551
BDBM	SES_{MNTD}	IS	activity level (% still)	SES_{MNTD}	TS	-0.3024	0.2628
PC16	SES_{MNTD}	IS	activity level (% still)	SES_{MNTD}	TS	-0.013916	-0.09959

PC8	SES_{MNTD}	IS	activity level (% still)	SES_{MNTD}	TS	-0.199	0.09933
all	SES_{MNTD}	IS	all	SES_{MNTD}	TS	0.16135	0.04027
BDBM	SES_{MNTD}	IS	all	SES_{MNTD}	TS	**-0.49631**	**0.5574**
PC16	SES_{MNTD}	IS	all	SES_{MNTD}	TS	0.2819	0.01272
PC8	SES_{MNTD}	IS	all	SES_{MNTD}	TS	-0.29346	0.1915
all	SES_{MNTD}	IS	antenna 1 length	SES_{MNTD}	TS	0.17363	0.1326
BDBM	SES_{MNTD}	IS	antenna 1 length	SES_{MNTD}	TS	-0.38078	0.454
PC16	SES_{MNTD}	IS	antenna 1 length	SES_{MNTD}	TS	0.1119	-0.07458
PC8	SES_{MNTD}	IS	antenna 1 length	SES_{MNTD}	TS	-0.20403	0.1017
all	SES_{MNTD}	IS	antenna 2 length	SES_{MNTD}	TS	-0.015273	-0.05117
BDBM	SES_{MNTD}	IS	antenna 2 length	SES_{MNTD}	TS	0.059638	0.2688
PC16	SES_{MNTD}	IS	antenna 2 length	SES_{MNTD}	TS	-0.04693	0.02137
PC8	SES_{MNTD}	IS	antenna 2 length	SES_{MNTD}	TS	0.032959	0.04284
all	SES_{MNTD}	IS	max. body size	SES_{MNTD}	TS	0.14296	0.08709
BDBM	SES_{MNTD}	IS	max. body size	SES_{MNTD}	TS	**-0.36485**	**0.5036**
PC16	SES_{MNTD}	IS	max. body size	SES_{MNTD}	TS	0.05677	-0.09223
PC8	SES_{MNTD}	IS	max. body size	SES_{MNTD}	TS	-0.2825	0.3589
all	SES_{MNTD}	IS	phylogeny	SES_{MNTD}	TS	0.24844	0.1001
BDBM	SES_{MNTD}	IS	phylogeny	SES_{MNTD}	TS	**-0.7385**	**0.7757**
PC16	SES_{MNTD}	IS	phylogeny	SES_{MNTD}	TS	0.2965	-0.02499
PC8	SES_{MNTD}	IS	phylogeny	SES_{MNTD}	TS	-0.49931	0.4077
all	SES_{MNTD}	IS	activity level (% still)	SES_{MNTD}	IS	0.15697	-0.03216
BDBM	SES_{MNTD}	IS	activity level (% still)	SES_{MNTD}	IS	-0.37822	0.09508
PC16	SES_{MNTD}	IS	activity level (% still)	SES_{MNTD}	IS	-0.09835	-0.09299
PC8	SES_{MNTD}	IS	activity level (% still)	SES_{MNTD}	IS	-0.23597	-0.003703
all	SES_{MNTD}	IS	all	SES_{MNTD}	IS	0.15432	-0.01495
BDBM	SES_{MNTD}	IS	all	SES_{MNTD}	IS	-0.5393	0.4145
PC16	SES_{MNTD}	IS	all	SES_{MNTD}	IS	0.3636	0.02425
PC8	SES_{MNTD}	IS	all	SES_{MNTD}	IS	-0.31799	0.1268
all	SES_{MNTD}	IS	antenna 1 length	SES_{MNTD}	IS	0.20575	0.1341

BDBM	SES_{MNTD}	IS	antenna 1 length	SES_{MNTD}	IS	-0.43648	0.4218
PC16	SES_{MNTD}	IS	antenna 1 length	SES_{MNTD}	IS	0.1094	-0.08258
PC8	SES_{MNTD}	IS	antenna 1 length	SES_{MNTD}	IS	-0.23605	0.09354
all	SES_{MNTD}	IS	antenna 2 length	SES_{MNTD}	IS	-0.030193	-0.05362
BDBM	SES_{MNTD}	IS	antenna 2 length	SES_{MNTD}	IS	0.11801	0.2509
PC16	SES_{MNTD}	IS	antenna 2 length	SES_{MNTD}	IS	-0.08006	-0.01418
PC8	SES_{MNTD}	IS	antenna 2 length	SES_{MNTD}	IS	0.057143	0.004347
all	SES_{MNTD}	IS	max. body size	SES_{MNTD}	IS	0.1823	0.05477
BDBM	SES_{MNTD}	IS	max. body size	SES_{MNTD}	IS	-0.4832	0.4386
PC16	SES_{MNTD}	IS	max. body size	SES_{MNTD}	IS	0.07557	-0.093
PC8	SES_{MNTD}	IS	max. body size	SES_{MNTD}	IS	-0.39588	0.3584
all	SES_{MNTD}	IS	phylogeny	SES_{MNTD}	IS	0.21551	0.0877
BDBM	SES_{MNTD}	IS	phylogeny	SES_{MNTD}	IS	**-0.64641**	**0.7364**
PC16	SES_{MNTD}	IS	phylogeny	SES_{MNTD}	IS	0.2984	-0.005307
PC8	SES_{MNTD}	IS	phylogeny	SES_{MNTD}	IS	-0.4298	0.3689
all	SES_{MNTD}	IS	activity level (% still)	SES_{MPD}	TS	0.15812	0.05951
BDBM	SES_{MNTD}	IS	activity level (% still)	SES_{MPD}	TS	-0.4502	0.5404
PC16	SES_{MNTD}	IS	activity level (% still)	SES_{MPD}	TS	0.1851	-0.0425
PC8	SES_{MNTD}	IS	activity level (% still)	SES_{MPD}	TS	-0.24541	0.1414
all	SES_{MNTD}	IS	all	SES_{MPD}	TS	0.20574	0.1158
BDBM	SES_{MNTD}	IS	all	SES_{MPD}	TS	-0.47088	0.4598
PC16	SES_{MNTD}	IS	all	SES_{MPD}	TS	0.1998	-0.04647
PC8	SES_{MNTD}	IS	all	SES_{MPD}	TS	-0.24609	0.0939
all	SES_{MNTD}	IS	antenna 1 length	SES_{MPD}	TS	0.21032	0.08968
BDBM	SES_{MNTD}	IS	antenna 1 length	SES_{MPD}	TS	-0.58901	0.6369
PC16	SES_{MNTD}	IS	antenna 1 length	SES_{MPD}	TS	0.2411	-0.03438
PC8	SES_{MNTD}	IS	antenna 1 length	SES_{MPD}	TS	-0.33989	0.2112
all	SES_{MNTD}	IS	antenna 2 length	SES_{MPD}	TS	-0.008941	-0.09917

BDBM	SES_{MNTD}	IS	antenna 2 length	SES_{MPD}	TS	-0.053199	-0.08548
PC16	SES_{MNTD}	IS	antenna 2 length	SES_{MPD}	TS	0.1747	-0.01679
PC8	SES_{MNTD}	IS	antenna 2 length	SES_{MPD}	TS	-0.0079275	-0.09959
all	SES_{MNTD}	IS	max. body size	SES_{MPD}	TS	0.12066	0.03933
BDBM	SES_{MNTD}	IS	max. body size	SES_{MPD}	TS	-0.26045	0.2216
PC16	SES_{MNTD}	IS	max. body size	SES_{MPD}	TS	0.09129	-0.07901
PC8	SES_{MNTD}	IS	max. body size	SES_{MPD}	TS	-0.21713	0.1834
all	SES_{MNTD}	IS	phylogeny	SES_{MPD}	TS	0.15893	-0.02679
BDBM	SES_{MNTD}	IS	phylogeny	SES_{MPD}	TS	-0.59703	0.4117
PC16	SES_{MNTD}	IS	phylogeny	SES_{MPD}	TS	0.3938	0.01829
PC8	SES_{MNTD}	IS	phylogeny	SES_{MPD}	TS	-0.3555	0.1301
all	SES_{MNTD}	IS	activity level (% still)	SES_{MPD}	IS	0.27083	0.124
BDBM	SES_{MNTD}	IS	activity level (% still)	SES_{MPD}	IS	**-0.68456**	**0.609**
PC16	SES_{MNTD}	IS	activity level (% still)	SES_{MPD}	IS	0.3288	-0.01309
PC8	SES_{MNTD}	IS	activity level (% still)	SES_{MPD}	IS	-0.42436	0.2455
all	SES_{MNTD}	IS	all	SES_{MPD}	IS	0.23963	0.09572
BDBM	SES_{MNTD}	IS	all	SES_{MPD}	IS	-0.5208	0.3579
PC16	SES_{MNTD}	IS	all	SES_{MPD}	IS	0.2554	-0.04147
PC8	SES_{MNTD}	IS	all	SES_{MPD}	IS	-0.34169	0.15
all	SES_{MNTD}	IS	antenna 1 length	SES_{MPD}	IS	0.2327	0.118
BDBM	SES_{MNTD}	IS	antenna 1 length	SES_{MPD}	IS	**-0.55807**	**0.5211**
PC16	SES_{MNTD}	IS	antenna 1 length	SES_{MPD}	IS	0.2518	-0.03281
PC8	SES_{MNTD}	IS	antenna 1 length	SES_{MPD}	IS	-0.38184	0.2688
all	SES_{MNTD}	IS	antenna 2 length	SES_{MPD}	IS	0.07208	-0.07517
BDBM	SES_{MNTD}	IS	antenna 2 length	SES_{MPD}	IS	-0.23115	0.02647
PC16	SES_{MNTD}	IS	antenna 2 length	SES_{MPD}	IS	0.278	-0.002797
PC8	SES_{MNTD}	IS	antenna 2 length	SES_{MPD}	IS	-0.15378	-0.02901
all	SES_{MNTD}	IS	max. body size	SES_{MPD}	IS	0.15557	0.00879

BDBM	SES_{MNTD}	IS	max. body size	SES_{MPD}	IS	-0.33702	0.1529
PC16	SES_{MNTD}	IS	max. body size	SES_{MPD}	IS	0.1355	-0.07828
PC8	SES_{MNTD}	IS	max. body size	SES_{MPD}	IS	-0.29496	0.1457
all	SES_{MNTD}	IS	phylogeny	SES_{MPD}	IS	0.15761	0.01117
BDBM	SES_{MNTD}	IS	phylogeny	SES_{MPD}	IS	-0.43416	0.3178
PC16	SES_{MNTD}	IS	phylogeny	SES_{MPD}	IS	0.2909	-0.0003524
PC8	SES_{MNTD}	IS	phylogeny	SES_{MPD}	IS	-0.30763	0.166
all	SES_{MPD}	TS	activity level (% still)	SES_{MNTD}	TS	0.033014	-0.0895
BDBM	SES_{MPD}	TS	activity level (% still)	SES_{MNTD}	TS	-0.26964	0.2573
PC16	SES_{MPD}	TS	activity level (% still)	SES_{MNTD}	TS	-0.09467	-0.04211
PC8	SES_{MPD}	TS	activity level (% still)	SES_{MNTD}	TS	-0.2855	0.1996
all	SES_{MPD}	TS	all	SES_{MNTD}	TS	0.013132	-0.09888
BDBM	SES_{MPD}	TS	all	SES_{MNTD}	TS	-0.3601	0.3285
PC16	SES_{MPD}	TS	all	SES_{MNTD}	TS	-0.14598	-0.007435
PC8	SES_{MPD}	TS	all	SES_{MNTD}	TS	-0.3422	0.1895
all	SES_{MPD}	TS	antenna 1 length	SES_{MNTD}	TS	0.029034	-0.09218
BDBM	SES_{MPD}	TS	antenna 1 length	SES_{MNTD}	TS	-0.30374	0.3364
PC16	SES_{MPD}	TS	antenna 1 length	SES_{MNTD}	TS	-0.14081	0.0233
PC8	SES_{MPD}	TS	antenna 1 length	SES_{MNTD}	TS	-0.3108	0.242
all	SES_{MPD}	TS	antenna 2 length	SES_{MNTD}	TS	0.001044	-0.09973
BDBM	SES_{MPD}	TS	antenna 2 length	SES_{MNTD}	TS	0.04179	0.1242
PC16	SES_{MPD}	TS	antenna 2 length	SES_{MNTD}	TS	0.015735	-0.05822
PC8	SES_{MPD}	TS	antenna 2 length	SES_{MNTD}	TS	0.03394	0.01065
all	SES_{MPD}	TS	max. body size	SES_{MNTD}	TS	0.040296	-0.08213
BDBM	SES_{MPD}	TS	max. body size	SES_{MNTD}	TS	-0.26935	0.3072
PC16	SES_{MPD}	TS	max. body size	SES_{MNTD}	TS	-0.1101	-0.01051
PC8	SES_{MPD}	TS	max. body size	SES_{MNTD}	TS	-0.3405	0.3869
all	SES_{MPD}	TS	phylogeny	SES_{MNTD}	TS	0.04277	-0.09287

BDBM	SES_{MPD}	TS	phylogeny	SES_{MNTD}	TS	**-0.5411**	**0.482**
PC16	SES_{MPD}	TS	phylogeny	SES_{MNTD}	TS	-0.21187	0.01731
PC8	SES_{MPD}	TS	phylogeny	SES_{MNTD}	TS	-0.5795	0.3994
all	SES_{MPD}	TS	activity level (% still)	SES_{MNTD}	IS	0.9565	0.029
BDBM	SES_{MPD}	TS	activity level (% still)	SES_{MNTD}	IS	**-0.6395**	**0.8058**
PC16	SES_{MPD}	TS	activity level (% still)	SES_{MNTD}	IS	**-1.083**	**0.6788**
PC8	SES_{MPD}	TS	activity level (% still)	SES_{MNTD}	IS	**-0.6478**	**0.523**
all	SES_{MPD}	TS	all	SES_{MNTD}	IS	0.003516	-0.09995
BDBM	SES_{MPD}	TS	all	SES_{MNTD}	IS	-0.38064	0.2173
PC16	SES_{MPD}	TS	all	SES_{MNTD}	IS	-0.14793	-0.037
PC8	SES_{MPD}	TS	all	SES_{MNTD}	IS	-0.343	0.09281
all	SES_{MPD}	TS	antenna 1 length	SES_{MNTD}	IS	0.037087	-0.09086
BDBM	SES_{MPD}	TS	antenna 1 length	SES_{MNTD}	IS	-0.3506	0.3168
PC16	SES_{MPD}	TS	antenna 1 length	SES_{MNTD}	IS	-0.1646	0.02076
PC8	SES_{MPD}	TS	antenna 1 length	SES_{MNTD}	IS	-0.3666	0.2409
all	SES_{MPD}	TS	antenna 2 length	SES_{MNTD}	IS	0.0023632	-0.09966
BDBM	SES_{MPD}	TS	antenna 2 length	SES_{MNTD}	IS	0.09311	0.1705
PC16	SES_{MPD}	TS	antenna 2 length	SES_{MNTD}	IS	0.03172	-0.05874
PC8	SES_{MPD}	TS	antenna 2 length	SES_{MNTD}	IS	0.06735	0.005886
all	SES_{MPD}	TS	max. body size	SES_{MNTD}	IS	0.05506	-0.08302
BDBM	SES_{MPD}	TS	max. body size	SES_{MNTD}	IS	-0.34674	0.2433
PC16	SES_{MPD}	TS	max. body size	SES_{MNTD}	IS	-0.13929	-0.02717
PC8	SES_{MPD}	TS	max. body size	SES_{MNTD}	IS	-0.457	0.3463
all	SES_{MPD}	TS	phylogeny	SES_{MNTD}	IS	0.032402	-0.0949
BDBM	SES_{MPD}	TS	phylogeny	SES_{MNTD}	IS	-0.4636	0.4326
PC16	SES_{MPD}	TS	phylogeny	SES_{MNTD}	IS	-0.18612	0.01285
PC8	SES_{MPD}	TS	phylogeny	SES_{MNTD}	IS	-0.4911	0.3472
all	SES_{MPD}	TS	activity level (% still)	SES_{MPD}	TS	0.01758	-0.09763
BDBM	SES_{MPD}	TS	activity level (% still)	SES_{MPD}	TS	-0.36203	0.4128

PC16	SES_{MPD}	TS	activity level (% still)	SES_{MPD}	TS	-0.1399	0.0006152
PC8	SES_{MPD}	TS	activity level (% still)	SES_{MPD}	TS	-0.3286	0.216
all	SES_{MPD}	TS	all	SES_{MPD}	TS	0.027224	-0.09546
BDBM	SES_{MPD}	TS	all	SES_{MPD}	TS	-0.3597	0.3045
PC16	SES_{MPD}	TS	all	SES_{MPD}	TS	-0.17114	0.02035
PC8	SES_{MPD}	TS	all	SES_{MPD}	TS	-0.3582	0.2001
all	SES_{MPD}	TS	antenna 1 length	SES_{MPD}	TS	0.027213	-0.09618
BDBM	SES_{MPD}	TS	antenna 1 length	SES_{MPD}	TS	**-0.4601**	**0.4566**
PC16	SES_{MPD}	TS	antenna 1 length	SES_{MPD}	TS	-0.18283	0.01555
PC8	SES_{MPD}	TS	antenna 1 length	SES_{MPD}	TS	-0.4406	0.2819
all	SES_{MPD}	TS	antenna 2 length	SES_{MPD}	TS	-0.021943	-0.094
BDBM	SES_{MPD}	TS	antenna 2 length	SES_{MPD}	TS	-0.009834	-0.09939
PC16	SES_{MPD}	TS	antenna 2 length	SES_{MPD}	TS	-0.006666	-0.09963
PC8	SES_{MPD}	TS	antenna 2 length	SES_{MPD}	TS	0.03169	-0.09523
all	SES_{MPD}	TS	max. body size	SES_{MPD}	TS	0.032259	-0.08803
BDBM	SES_{MPD}	TS	max. body size	SES_{MPD}	TS	-0.15096	0.03375
PC16	SES_{MPD}	TS	max. body size	SES_{MPD}	TS	-0.08894	-0.03897
PC8	SES_{MPD}	TS	max. body size	SES_{MPD}	TS	-0.2445	0.1625
all	SES_{MPD}	TS	phylogeny	SES_{MPD}	TS	0.001917	-0.09999
BDBM	SES_{MPD}	TS	phylogeny	SES_{MPD}	TS	-0.4296	0.228
PC16	SES_{MPD}	TS	phylogeny	SES_{MPD}	TS	-0.1562	-0.04298
PC8	SES_{MPD}	TS	phylogeny	SES_{MPD}	TS	-0.3777	0.08969
all	SES_{MPD}	TS	activity level (% still)	SES_{MPD}	IS	0.039802	-0.09418
BDBM	SES_{MPD}	TS	activity level (% still)	SES_{MPD}	IS	-0.4809	0.3332
PC16	SES_{MPD}	TS	activity level (% still)	SES_{MPD}	IS	-0.22572	0.02544
PC8	SES_{MPD}	TS	activity level (% still)	SES_{MPD}	IS	-0.5246	0.2857
all	SES_{MPD}	TS	all	SES_{MPD}	IS	0.0423	-0.09267
BDBM	SES_{MPD}	TS	all	SES_{MPD}	IS	-0.33234	0.1309
PC16	SES_{MPD}	TS	all	SES_{MPD}	IS	-0.18925	-0.00159
PC8	SES_{MPD}	TS	all	SES_{MPD}	IS	-0.4238	0.1809

all	SES_{MPD}	TS	antenna 1 length	SES_{MPD}	IS	0.04317	-0.09098
BDBM	SES_{MPD}	TS	antenna 1 length	SES_{MPD}	IS	-0.3688	0.2359
PC16	SES_{MPD}	TS	antenna 1 length	SES_{MPD}	IS	-0.18644	0.01282
PC8	SES_{MPD}	TS	antenna 1 length	SES_{MPD}	IS	-0.4552	0.2828
all	SES_{MPD}	TS	antenna 2 length	SES_{MPD}	IS	-0.004148	-0.0999
BDBM	SES_{MPD}	TS	antenna 2 length	SES_{MPD}	IS	-0.09871	-0.07144
PC16	SES_{MPD}	TS	antenna 2 length	SES_{MPD}	IS	-0.06791	-0.08223
PC8	SES_{MPD}	TS	antenna 2 length	SES_{MPD}	IS	-0.12109	-0.06785
all	SES_{MPD}	TS	max. body size	SES_{MPD}	IS	0.0425	-0.09024
BDBM	SES_{MPD}	TS	max. body size	SES_{MPD}	IS	-0.17961	-0.01107
PC16	SES_{MPD}	TS	max. body size	SES_{MPD}	IS	-0.1136	-0.05324
PC8	SES_{MPD}	TS	max. body size	SES_{MPD}	IS	-0.3172	0.1075
all	SES_{MPD}	TS	phylogeny	SES_{MPD}	IS	0.02093	-0.09764
BDBM	SES_{MPD}	TS	phylogeny	SES_{MPD}	IS	-0.25492	0.07834
PC16	SES_{MPD}	TS	phylogeny	SES_{MPD}	IS	-0.13258	-0.03658
PC8	SES_{MPD}	TS	phylogeny	SES_{MPD}	IS	-0.3178	0.1074
all	SES_{MPD}	IS	activity level (% still)	SES_{MNTD}	TS	0.08915	-0.06832
BDBM	SES_{MPD}	IS	activity level (% still)	SES_{MNTD}	TS	-0.15453	0.01039
PC16	SES_{MPD}	IS	activity level (% still)	SES_{MNTD}	TS	0.0127594	-0.09884
PC8	SES_{MPD}	IS	activity level (% still)	SES_{MNTD}	TS	-0.051485	-0.08262
all	SES_{MPD}	IS	all	SES_{MNTD}	TS	0.4155204	0.3628
BDBM	SES_{MPD}	IS	all	SES_{MNTD}	TS	-0.029272	-0.09734
PC16	SES_{MPD}	IS	all	SES_{MNTD}	TS	0.072724	-0.07469
PC8	SES_{MPD}	IS	all	SES_{MNTD}	TS	0.051274	-0.08841
all	SES_{MPD}	IS	antenna 1 length	SES_{MNTD}	TS	0.3505693	0.3717
BDBM	SES_{MPD}	IS	antenna 1 length	SES_{MNTD}	TS	-0.014731	-0.09903
PC16	SES_{MPD}	IS	antenna 1 length	SES_{MNTD}	TS	0.05012	-0.08279
PC8	SES_{MPD}	IS	antenna 1 length	SES_{MNTD}	TS	0.033471	-0.09293

all	SES_{MPD}	IS	antenna 2 length	SES_{MNTD}	TS	-0.06274	0.3099
BDBM	SES_{MPD}	IS	antenna 2 length	SES_{MNTD}	TS	-0.006551	-0.09482
PC16	SES_{MPD}	IS	antenna 2 length	SES_{MNTD}	TS	-0.013763	-0.06478
PC8	SES_{MPD}	IS	antenna 2 length	SES_{MNTD}	TS	-0.01445	-0.0642
all	SES_{MPD}	IS	max. body size	SES_{MNTD}	TS	0.01788	-0.09854
BDBM	SES_{MPD}	IS	max. body size	SES_{MNTD}	TS	-0.23032	0.1802
PC16	SES_{MPD}	IS	max. body size	SES_{MNTD}	TS	-0.03551	-0.08974
PC8	SES_{MPD}	IS	max. body size	SES_{MNTD}	TS	-0.11715	0.002835
all	SES_{MPD}	IS	phylogeny	SES_{MNTD}	TS	0.3510316	0.09874
BDBM	SES_{MPD}	IS	phylogeny	SES_{MNTD}	TS	-0.2364	0.004544
PC16	SES_{MPD}	IS	phylogeny	SES_{MNTD}	TS	0.033958	-0.09668
PC8	SES_{MPD}	IS	phylogeny	SES_{MNTD}	TS	-0.059588	-0.09058
all	SES_{MPD}	IS	activity level (% still)	SES_{MNTD}	IS	0.107	-0.08431
BDBM	SES_{MPD}	IS	activity level (% still)	SES_{MNTD}	IS	-0.21041	-0.02968
PC16	SES_{MPD}	IS	activity level (% still)	SES_{MNTD}	IS	0.029508	-0.09787
PC8	SES_{MPD}	IS	activity level (% still)	SES_{MNTD}	IS	-0.062562	-0.09118
all	SES_{MPD}	IS	all	SES_{MNTD}	IS	0.4769437	0.3041
BDBM	SES_{MPD}	IS	all	SES_{MNTD}	IS	-0.0077435	-0.09988
PC16	SES_{MPD}	IS	all	SES_{MNTD}	IS	0.092329	-0.07296
PC8	SES_{MPD}	IS	all	SES_{MNTD}	IS	0.0776	-0.0824
all	SES_{MPD}	IS	antenna 1 length	SES_{MNTD}	IS	0.3874407	0.3129
BDBM	SES_{MPD}	IS	antenna 1 length	SES_{MNTD}	IS	-0.028704	-0.09737
PC16	SES_{MPD}	IS	antenna 1 length	SES_{MNTD}	IS	0.051007	-0.08722
PC8	SES_{MPD}	IS	antenna 1 length	SES_{MNTD}	IS	0.028051	-0.09644
all	SES_{MPD}	IS	antenna 2 length	SES_{MNTD}	IS	-0.1417	0.4085
BDBM	SES_{MPD}	IS	antenna 2 length	SES_{MNTD}	IS	-0.021817	-0.08603
PC16	SES_{MPD}	IS	antenna 2 length	SES_{MNTD}	IS	-0.037163	-0.03759
PC8	SES_{MPD}	IS	antenna 2 length	SES_{MNTD}	IS	-0.039501	-0.03503

all	SES_{MPD}	IS	max. body size	SES_{MNTD}	IS	-0.04848	-0.09456
BDBM	SES_{MPD}	IS	max. body size	SES_{MNTD}	IS	-0.35215	0.2332
PC16	SES_{MPD}	IS	max. body size	SES_{MNTD}	IS	-0.067544	-0.08113
PC8	SES_{MPD}	IS	max. body size	SES_{MNTD}	IS	-0.18914	0.03635
all	SES_{MPD}	IS	phylogeny	SES_{MNTD}	IS	0.352747	0.1502
BDBM	SES_{MPD}	IS	phylogeny	SES_{MNTD}	IS	-0.17085	-0.03194
PC16	SES_{MPD}	IS	phylogeny	SES_{MNTD}	IS	0.038126	-0.09478
PC8	SES_{MPD}	IS	phylogeny	SES_{MNTD}	IS	-0.030648	-0.09689
all	SES_{MPD}	IS	activity level (% still)	SES_{MPD}	TS	0.4061137	0.4235
BDBM	SES_{MPD}	IS	activity level (% still)	SES_{MPD}	TS	-0.019472	-0.0986
PC16	SES_{MPD}	IS	activity level (% still)	SES_{MPD}	TS	0.084798	-0.05925
PC8	SES_{MPD}	IS	activity level (% still)	SES_{MPD}	TS	0.06188	-0.08
all	SES_{MPD}	IS	all	SES_{MPD}	TS	**0.4852413**	**0.497**
BDBM	SES_{MPD}	IS	all	SES_{MPD}	TS	0.025127	-0.09814
PC16	SES_{MPD}	IS	all	SES_{MPD}	TS	0.073079	-0.07582
PC8	SES_{MPD}	IS	all	SES_{MPD}	TS	0.068623	-0.08035
all	SES_{MPD}	IS	antenna 1 length	SES_{MPD}	TS	0.4735671	0.3784
BDBM	SES_{MPD}	IS	antenna 1 length	SES_{MPD}	TS	-0.062153	-0.09044
PC16	SES_{MPD}	IS	antenna 1 length	SES_{MPD}	TS	0.086683	-0.07138
PC8	SES_{MPD}	IS	antenna 1 length	SES_{MPD}	TS	0.047626	-0.09204
all	SES_{MPD}	IS	antenna 2 length	SES_{MPD}	TS	0.1912914	0.08853
BDBM	SES_{MPD}	IS	antenna 2 length	SES_{MPD}	TS	0.11418	-0.0221
PC16	SES_{MPD}	IS	antenna 2 length	SES_{MPD}	TS	0.047824	-0.07896
PC8	SES_{MPD}	IS	antenna 2 length	SES_{MPD}	TS	0.08659	-0.03644
all	SES_{MPD}	IS	max. body size	SES_{MPD}	TS	0.005722	-0.09984
BDBM	SES_{MPD}	IS	max. body size	SES_{MPD}	TS	-0.15679	0.03574
PC16	SES_{MPD}	IS	max. body size	SES_{MPD}	TS	-0.058124	-0.07128
PC8	SES_{MPD}	IS	max. body size	SES_{MPD}	TS	-0.1059	-0.01215

all	SES_{MPD}	IS	phylogeny	SES_{MPD}	TS	0.5049448	0.2676
BDBM	SES_{MPD}	IS	phylogeny	SES_{MPD}	TS	-0.02663	-0.09881
PC16	SES_{MPD}	IS	phylogeny	SES_{MPD}	TS	0.106704	-0.07069
PC8	SES_{MPD}	IS	phylogeny	SES_{MPD}	TS	0.082716	-0.08377
all	SES_{MPD}	IS	activity level (% still)	SES_{MPD}	IS	0.5028334	0.2842
BDBM	SES_{MPD}	IS	activity level (% still)	SES_{MPD}	IS	-0.08985	-0.08577
PC16	SES_{MPD}	IS	activity level (% still)	SES_{MPD}	IS	0.046504	-0.09413
PC8	SES_{MPD}	IS	activity level (% still)	SES_{MPD}	IS	0.0061558	-0.09991
all	SES_{MPD}	IS	all	SES_{MPD}	IS	0.3459184	0.1029
BDBM	SES_{MPD}	IS	all	SES_{MPD}	IS	-0.0861	-0.08542
PC16	SES_{MPD}	IS	all	SES_{MPD}	IS	-0.0099042	-0.0997
PC8	SES_{MPD}	IS	all	SES_{MPD}	IS	-0.038843	-0.09579
all	SES_{MPD}	IS	antenna 1 length	SES_{MPD}	IS	0.2939826	0.07311
BDBM	SES_{MPD}	IS	antenna 1 length	SES_{MPD}	IS	-0.1488	-0.04857
PC16	SES_{MPD}	IS	antenna 1 length	SES_{MPD}	IS	-0.011551	-0.09952
PC8	SES_{MPD}	IS	antenna 1 length	SES_{MPD}	IS	-0.063766	-0.0866
all	SES_{MPD}	IS	antenna 2 length	SES_{MPD}	IS	0.2270953	0.02261
BDBM	SES_{MPD}	IS	antenna 2 length	SES_{MPD}	IS	0.034939	-0.09663
PC16	SES_{MPD}	IS	antenna 2 length	SES_{MPD}	IS	0.0104468	-0.09954
PC8	SES_{MPD}	IS	antenna 2 length	SES_{MPD}	IS	0.027849	-0.09697
all	SES_{MPD}	IS	max. body size	SES_{MPD}	IS	-0.0264231	-0.09844
BDBM	SES_{MPD}	IS	max. body size	SES_{MPD}	IS	-0.22135	0.02707
PC16	SES_{MPD}	IS	max. body size	SES_{MPD}	IS	-0.09183	-0.06633
PC8	SES_{MPD}	IS	max. body size	SES_{MPD}	IS	-0.15676	-0.009592
all	SES_{MPD}	IS	phylogeny	SES_{MPD}	IS	0.2396337	0.02785
BDBM	SES_{MPD}	IS	phylogeny	SES_{MPD}	IS	-0.09424	-0.07707
PC16	SES_{MPD}	IS	phylogeny	SES_{MPD}	IS	-0.008824	-0.09969
PC8	SES_{MPD}	IS	phylogeny	SES_{MPD}	IS	-0.038022	-0.0947

Table A5.3. Effect sizes of fish community trait dispersion on residual peracarid community trait and phylogenetic dispersion, controlling for the effects of habitat filters on fish dispersion.

Bolded cells indicate values significant at alpha = 0.008333; the first 24 rows are effects for which results are presented in the main text. Rows are colored according to the direction and magnitude of the effect size; red indicates a negative effect while blue indicates a positive effect, and color saturation is proportional to R^2. TS = Tip Shuffle algorithm, IS = Independent Swap algorithm; BDBM = Body Depth Below Midline.

Predictor trait	Predictor metric	Predictor algorithm	Response trait	Response metric	Response algorithm	Effect size	R^2
all	SES_{MNTD}	TS	activity level (% still)	SES_{MNTD}	TS	0.8045	0.443
BDBM	SES_{MNTD}	TS	activity level (% still)	SES_{MNTD}	TS	-0.2636	0.2355
PC16	SES_{MNTD}	TS	activity level (% still)	SES_{MNTD}	TS	-0.7534	-0.006049
PC8	SES_{MNTD}	TS	activity level (% still)	SES_{MNTD}	TS	-0.251	0.2098
all	SES_{MNTD}	TS	all	SES_{MNTD}	TS	0.8525	0.3018
BDBM	SES_{MNTD}	TS	all	SES_{MNTD}	TS	**-0.506**	**0.7316**
PC16	SES_{MNTD}	TS	all	SES_{MNTD}	TS	0.9485	0.0001235
PC8	SES_{MNTD}	TS	all	SES_{MNTD}	TS	**-0.4521**	**0.5757**
all	SES_{MNTD}	TS	antenna 1 length	SES_{MNTD}	TS	**1.103**	**0.8825**
BDBM	SES_{MNTD}	TS	antenna 1 length	SES_{MNTD}	TS	**-0.3873**	**0.5975**
PC16	SES_{MNTD}	TS	antenna 1 length	SES_{MNTD}	TS	-0.9212	0.03522
PC8	SES_{MNTD}	TS	antenna 1 length	SES_{MNTD}	TS	-0.3035	0.3358
all	SES_{MNTD}	TS	antenna 2 length	SES_{MNTD}	TS	-0.06549	-0.006011
BDBM	SES_{MNTD}	TS	antenna 2 length	SES_{MNTD}	TS	0.06108	0.3708
PC16	SES_{MNTD}	TS	antenna 2 length	SES_{MNTD}	TS	-0.2196	0.1085
PC8	SES_{MNTD}	TS	antenna 2 length	SES_{MNTD}	TS	0.05404	0.2751
all	SES_{MNTD}	TS	max. body size	SES_{MNTD}	TS	**0.8565**	**0.6032**
BDBM	SES_{MNTD}	TS	max. body size	SES_{MNTD}	TS	**-0.3617**	**0.6221**
PC16	SES_{MNTD}	TS	max. body size	SES_{MNTD}	TS	0.3578	-0.07579
PC8	SES_{MNTD}	TS	max. body size	SES_{MNTD}	TS	**-0.3802**	**0.7117**
all	SES_{MNTD}	TS	phylogeny	SES_{MNTD}	TS	**1.37**	**0.5367**
BDBM	SES_{MNTD}	TS	phylogeny	SES_{MNTD}	TS	**-0.7364**	**0.9597**
PC16	SES_{MNTD}	TS	phylogeny	SES_{MNTD}	TS	1.38	0.02755

PC8	SES_{MNTD}	TS	phylogeny	SES_{MNTD}	TS	**-0.7185**	**0.9267**
all	SES_{MNTD}	TS	activity level (% still)	SES_{MNTD}	IS	1.133	0.2697
BDBM	SES_{MNTD}	TS	activity level (% still)	SES_{MNTD}	IS	-0.2991	0.04852
PC16	SES_{MNTD}	TS	activity level (% still)	SES_{MNTD}	IS	-1.845	0.09348
PC8	SES_{MNTD}	TS	activity level (% still)	SES_{MNTD}	IS	-0.2742	0.027
all	SES_{MNTD}	TS	all	SES_{MNTD}	IS	0.7354	0.1022
BDBM	SES_{MNTD}	TS	all	SES_{MNTD}	IS	**-0.5517**	**0.5553**
PC16	SES_{MNTD}	TS	all	SES_{MNTD}	IS	1.671	0.106
PC8	SES_{MNTD}	TS	all	SES_{MNTD}	IS	-0.501	0.4499
all	SES_{MNTD}	TS	antenna 1 length	SES_{MNTD}	IS	**1.324**	**0.9149**
BDBM	SES_{MNTD}	TS	antenna 1 length	SES_{MNTD}	IS	**-0.4438**	**0.5567**
PC16	SES_{MNTD}	TS	antenna 1 length	SES_{MNTD}	IS	-1.235	0.07413
PC8	SES_{MNTD}	TS	antenna 1 length	SES_{MNTD}	IS	-0.347	0.3085
all	SES_{MNTD}	TS	antenna 2 length	SES_{MNTD}	IS	-0.1476	0.01612
BDBM	SES_{MNTD}	TS	antenna 2 length	SES_{MNTD}	IS	0.1126	0.289
PC16	SES_{MNTD}	TS	antenna 2 length	SES_{MNTD}	IS	-0.2063	-0.05528
PC8	SES_{MNTD}	TS	antenna 2 length	SES_{MNTD}	IS	0.09246	0.1668
all	SES_{MNTD}	TS	max. body size	SES_{MNTD}	IS	1.065	0.4535
BDBM	SES_{MNTD}	TS	max. body size	SES_{MNTD}	IS	**-0.4808**	**0.5489**
PC16	SES_{MNTD}	TS	max. body size	SES_{MNTD}	IS	0.8959	-0.0228
PC8	SES_{MNTD}	TS	max. body size	SES_{MNTD}	IS	**-0.5295**	**0.701**
all	SES_{MNTD}	TS	phylogeny	SES_{MNTD}	IS	**1.16**	0.4693
BDBM	SES_{MNTD}	TS	phylogeny	SES_{MNTD}	IS	**-0.6553**	**0.9461**
PC16	SES_{MNTD}	TS	phylogeny	SES_{MNTD}	IS	1.411	0.06622
PC8	SES_{MNTD}	TS	phylogeny	SES_{MNTD}	IS	**-0.6309**	**0.8869**
all	SES_{MNTD}	TS	activity level (% still)	SES_{MPD}	TS	**0.9325**	**0.4808**
BDBM	SES_{MNTD}	TS	activity level (% still)	SES_{MPD}	TS	**-0.4344**	**0.6256**
PC16	SES_{MNTD}	TS	activity level (% still)	SES_{MPD}	TS	-0.1379	-0.09749
PC8	SES_{MNTD}	TS	activity level (% still)	SES_{MPD}	TS	-0.365	0.4215
all	SES_{MNTD}	TS	all	SES_{MPD}	TS	**1.257**	**0.7432**
BDBM	SES_{MNTD}	TS	all	SES_{MPD}	TS	**-0.4921**	**0.6442**

PC16	SES_{MNTD}	TS	all	SES_{MPD}	TS	-0.6736	-0.05222
PC8	SES_{MNTD}	TS	all	SES_{MPD}	TS	-0.3834	0.3596
all	SES_{MNTD}	TS	antenna 1 length	SES_{MPD}	TS	**1.227**	**0.5757**
BDBM	SES_{MNTD}	TS	antenna 1 length	SES_{MPD}	TS	**-0.5785**	**0.7652**
PC16	SES_{MNTD}	TS	antenna 1 length	SES_{MPD}	TS	0.07847	-0.09945
PC8	SES_{MNTD}	TS	antenna 1 length	SES_{MPD}	TS	**-0.5028**	**0.5651**
all	SES_{MNTD}	TS	antenna 2 length	SES_{MPD}	TS	-0.187	-0.06209
BDBM	SES_{MNTD}	TS	antenna 2 length	SES_{MPD}	TS	-0.07693	-0.06305
PC16	SES_{MNTD}	TS	antenna 2 length	SES_{MPD}	TS	1.107	0.1621
PC8	SES_{MNTD}	TS	antenna 2 length	SES_{MPD}	TS	-0.05427	-0.08129
all	SES_{MNTD}	TS	max. body size	SES_{MPD}	TS	0.6823	0.3665
BDBM	SES_{MNTD}	TS	max. body size	SES_{MPD}	TS	-0.3026	0.4281
PC16	SES_{MNTD}	TS	max. body size	SES_{MPD}	TS	0.7078	-0.000965
PC8	SES_{MNTD}	TS	max. body size	SES_{MPD}	TS	**-0.3135**	**0.4769**
all	SES_{MNTD}	TS	phylogeny	SES_{MPD}	TS	0.7364	0.06457
BDBM	SES_{MNTD}	TS	phylogeny	SES_{MPD}	TS	**-0.597**	**0.5227**
PC16	SES_{MNTD}	TS	phylogeny	SES_{MPD}	TS	1.958	0.1296
PC8	SES_{MNTD}	TS	phylogeny	SES_{MPD}	TS	-0.5525	0.4427
all	SES_{MNTD}	TS	activity level (% still)	SES_{MPD}	IS	**1.539**	**0.6573**
BDBM	SES_{MNTD}	TS	activity level (% still)	SES_{MPD}	IS	**-0.7288**	**0.878**
PC16	SES_{MNTD}	TS	activity level (% still)	SES_{MPD}	IS	0.6703	-0.07165
PC8	SES_{MNTD}	TS	activity level (% still)	SES_{MPD}	IS	**-0.6463**	**0.6828**
all	SES_{MNTD}	TS	all	SES_{MPD}	IS	**1.379**	**0.5788**
BDBM	SES_{MNTD}	TS	all	SES_{MPD}	IS	**-0.5967**	**0.6315**
PC16	SES_{MNTD}	TS	all	SES_{MPD}	IS	0.5134	-0.08145
PC8	SES_{MNTD}	TS	all	SES_{MPD}	IS	**-0.529**	**0.4851**
all	SES_{MNTD}	TS	antenna 1 length	SES_{MPD}	IS	**1.316**	**0.6302**
BDBM	SES_{MNTD}	TS	antenna 1 length	SES_{MPD}	IS	**-0.6132**	**0.8126**
PC16	SES_{MNTD}	TS	antenna 1 length	SES_{MPD}	IS	0.8756	-0.03623
PC8	SES_{MNTD}	TS	antenna 1 length	SES_{MPD}	IS	**-0.5724**	**0.7092**

all	SES_{MNTD}	TS	antenna 2 length	SES_{MPD}	IS	0.2377	-0.07173
BDBM	SES_{MNTD}	TS	antenna 2 length	SES_{MPD}	IS	-0.2976	0.1551
PC16	SES_{MNTD}	TS	antenna 2 length	SES_{MPD}	IS	1.881	0.2493
PC8	SES_{MNTD}	TS	antenna 2 length	SES_{MPD}	IS	-0.2775	0.1257
all	SES_{MNTD}	TS	max. body size	SES_{MPD}	IS	0.8514	0.2412
BDBM	SES_{MNTD}	TS	max. body size	SES_{MPD}	IS	-0.4033	0.3407
PC16	SES_{MNTD}	TS	max. body size	SES_{MPD}	IS	1.28	0.05219
PC8	SES_{MNTD}	TS	max. body size	SES_{MPD}	IS	-0.429	0.4076
all	SES_{MNTD}	TS	phylogeny	SES_{MPD}	IS	0.7741	0.1808
BDBM	SES_{MNTD}	TS	phylogeny	SES_{MPD}	IS	**-0.496**	**0.5636**
PC16	SES_{MNTD}	TS	phylogeny	SES_{MPD}	IS	1.821	0.2067
PC8	SES_{MNTD}	TS	phylogeny	SES_{MPD}	IS	**-0.4808**	**0.5348**
all	SES_{MNTD}	IS	activity level (% still)	SES_{MNTD}	TS	0.4837	0.3654
BDBM	SES_{MNTD}	IS	activity level (% still)	SES_{MNTD}	TS	-0.3759	0.3511
PC16	SES_{MNTD}	IS	activity level (% still)	SES_{MNTD}	TS	-0.116	-0.09659
PC8	SES_{MNTD}	IS	activity level (% still)	SES_{MNTD}	TS	-0.3868	0.2875
all	SES_{MNTD}	IS	all	SES_{MNTD}	TS	0.65	0.4651
BDBM	SES_{MNTD}	IS	all	SES_{MNTD}	TS	**-0.6171**	**0.7174**
PC16	SES_{MNTD}	IS	all	SES_{MNTD}	TS	**2.351**	**0.8399**
PC8	SES_{MNTD}	IS	all	SES_{MNTD}	TS	-0.5705	0.4666
all	SES_{MNTD}	IS	antenna 1 length	SES_{MNTD}	TS	**0.6995**	**0.8369**
BDBM	SES_{MNTD}	IS	antenna 1 length	SES_{MNTD}	TS	**-0.4734**	**0.5888**
PC16	SES_{MNTD}	IS	antenna 1 length	SES_{MNTD}	TS	0.933	0.112
PC8	SES_{MNTD}	IS	antenna 1 length	SES_{MNTD}	TS	-0.3966	0.2921
all	SES_{MNTD}	IS	antenna 2 length	SES_{MNTD}	TS	-0.06153	0.09672
BDBM	SES_{MNTD}	IS	antenna 2 length	SES_{MNTD}	TS	0.07415	0.3585
PC16	SES_{MNTD}	IS	antenna 2 length	SES_{MNTD}	TS	**-0.3913**	**0.912**
PC8	SES_{MNTD}	IS	antenna 2 length	SES_{MNTD}	TS	0.06407	0.1777
all	SES_{MNTD}	IS	max. body size	SES_{MNTD}	TS	**0.576**	**0.6537**
BDBM	SES_{MNTD}	IS	max. body size	SES_{MNTD}	TS	**-0.4536**	**0.6504**
PC16	SES_{MNTD}	IS	max. body size	SES_{MNTD}	TS	0.4734	-0.03525

PC8	SES_{MNTD}	IS	max. body size	SES_{MNTD}	TS	**-5.492**	**0.792**
all	SES_{MNTD}	IS	phylogeny	SES_{MNTD}	TS	**1.001**	**0.7061**
BDBM	SES_{MNTD}	IS	phylogeny	SES_{MNTD}	TS	**-0.9181**	**0.9888**
PC16	SES_{MNTD}	IS	phylogeny	SES_{MNTD}	TS	**2.472**	**0.5354**
PC8	SES_{MNTD}	IS	phylogeny	SES_{MNTD}	TS	**-0.9706**	**0.8869**
all	SES_{MNTD}	IS	activity level (% still)	SES_{MNTD}	IS	0.6324	0.1733
BDBM	SES_{MNTD}	IS	activity level (% still)	SES_{MNTD}	IS	-0.4703	0.1425
PC16	SES_{MNTD}	IS	activity level (% still)	SES_{MNTD}	IS	-0.82	-0.04156
PC8	SES_{MNTD}	IS	activity level (% still)	SES_{MNTD}	IS	-0.4587	0.08719
all	SES_{MNTD}	IS	all	SES_{MNTD}	IS	0.6217	0.2427
BDBM	SES_{MNTD}	IS	all	SES_{MNTD}	IS	**-0.6705**	**0.5397**
PC16	SES_{MNTD}	IS	all	SES_{MNTD}	IS	**3.031**	**0.936**
PC8	SES_{MNTD}	IS	all	SES_{MNTD}	IS	-0.6182	0.341
all	SES_{MNTD}	IS	antenna 1 length	SES_{MNTD}	IS	**0.8289**	**0.843**
BDBM	SES_{MNTD}	IS	antenna 1 length	SES_{MNTD}	IS	**-0.5427**	**0.5488**
PC16	SES_{MNTD}	IS	antenna 1 length	SES_{MNTD}	IS	0.9123	0.04528
PC8	SES_{MNTD}	IS	antenna 1 length	SES_{MNTD}	IS	-0.4589	0.2762
all	SES_{MNTD}	IS	antenna 2 length	SES_{MNTD}	IS	-0.1216	0.08684
BDBM	SES_{MNTD}	IS	antenna 2 length	SES_{MNTD}	IS	0.1467	0.3363
PC16	SES_{MNTD}	IS	antenna 2 length	SES_{MNTD}	IS	**-0.6675**	**0.6155**
PC8	SES_{MNTD}	IS	antenna 2 length	SES_{MNTD}	IS	0.1111	0.1028
all	SES_{MNTD}	IS	max. body size	SES_{MNTD}	IS	**0.7345**	**0.5235**
BDBM	SES_{MNTD}	IS	max. body size	SES_{MNTD}	IS	**-6.008**	**0.5697**
PC16	SES_{MNTD}	IS	max. body size	SES_{MNTD}	IS	0.6301	-0.04163
PC8	SES_{MNTD}	IS	max. body size	SES_{MNTD}	IS	**-0.7695**	**0.7911**
all	SES_{MNTD}	IS	phylogeny	SES_{MNTD}	IS	0.8682	0.6562
BDBM	SES_{MNTD}	IS	phylogeny	SES_{MNTD}	IS	**-0.8037**	**0.94**
PC16	SES_{MNTD}	IS	phylogeny	SES_{MNTD}	IS	**2.488**	**0.6895**
PC8	SES_{MNTD}	IS	phylogeny	SES_{MNTD}	IS	**-0.8354**	**0.8115**
all	SES_{MNTD}	IS	activity level (% still)	SES_{MPD}	TS	**0.637**	**0.5426**
BDBM	SES_{MNTD}	IS	activity level (% still)	SES_{MPD}	TS	**-0.5597**	**0.6936**

PC16	SES_{MNTD}	IS	activity level (% still)	SES_{MPD}	TS	1.543	0.3795
PC8	SES_{MNTD}	IS	activity level (% still)	SES_{MPD}	TS	-0.4771	0.3692
all	SES_{MNTD}	IS	all	SES_{MPD}	TS	**0.82889**	**0.7692**
BDBM	SES_{MNTD}	IS	all	SES_{MPD}	TS	**-0.5855**	**0.596**
PC16	SES_{MNTD}	IS	all	SES_{MPD}	TS	1.666	0.3463
PC8	SES_{MNTD}	IS	all	SES_{MPD}	TS	-0.4784	0.2769
all	SES_{MNTD}	IS	antenna 1 length	SES_{MPD}	TS	**0.8473**	**0.6642**
BDBM	SES_{MNTD}	IS	antenna 1 length	SES_{MPD}	TS	**-0.7323**	**0.8162**
PC16	SES_{MNTD}	IS	antenna 1 length	SES_{MPD}	TS	2.011	0.4471
PC8	SES_{MNTD}	IS	antenna 1 length	SES_{MPD}	TS	**-0.6607**	**0.5049**
all	SES_{MNTD}	IS	antenna 2 length	SES_{MPD}	TS	-0.03602	-0.09666
BDBM	SES_{MNTD}	IS	antenna 2 length	SES_{MPD}	TS	-0.06614	-0.08195
PC16	SES_{MNTD}	IS	antenna 2 length	SES_{MPD}	TS	**1.457**	**0.5938**
PC8	SES_{MNTD}	IS	antenna 2 length	SES_{MPD}	TS	-0.01541	-0.09921
all	SES_{MNTD}	IS	max. body size	SES_{MPD}	TS	0.4861	0.4613
BDBM	SES_{MNTD}	IS	max. body size	SES_{MPD}	TS	-0.3238	0.2998
PC16	SES_{MNTD}	IS	max. body size	SES_{MPD}	TS	0.7611	0.07502
PC8	SES_{MNTD}	IS	max. body size	SES_{MPD}	TS	-0.4221	0.4509
all	SES_{MNTD}	IS	phylogeny	SES_{MPD}	TS	0.6403	0.1949
BDBM	SES_{MNTD}	IS	phylogeny	SES_{MPD}	TS	**-0.7423**	**0.5362**
PC16	SES_{MNTD}	IS	phylogeny	SES_{MPD}	TS	**3.283**	**0.8863**
PC8	SES_{MNTD}	IS	phylogeny	SES_{MPD}	TS	-0.691	0.3472
all	SES_{MNTD}	IS	activity level (% still)	SES_{MPD}	IS	**1.091**	**0.8025**
BDBM	SES_{MNTD}	IS	activity level (% still)	SES_{MPD}	IS	**-0.8511**	**0.7815**
PC16	SES_{MNTD}	IS	activity level (% still)	SES_{MPD}	IS	**2.742**	**0.6247**
PC8	SES_{MNTD}	IS	activity level (% still)	SES_{MPD}	IS	**-0.8249**	**0.5716**
all	SES_{MNTD}	IS	all	SES_{MPD}	IS	**0.9654**	**0.6885**
BDBM	SES_{MNTD}	IS	all	SES_{MPD}	IS	-0.6475	0.4694
PC16	SES_{MNTD}	IS	all	SES_{MPD}	IS	2.13	0.388
PC8	SES_{MNTD}	IS	all	SES_{MPD}	IS	-0.6642	0.3859
all	SES_{MNTD}	IS	antenna 1 length	SES_{MPD}	IS	**0.9375**	**0.7783**

BDBM	SES_{MNTD}	IS	antenna 1 length	SES_{MPD}	IS	**-0.6939**	**0.6723**
PC16	SES_{MNTD}	IS	antenna 1 length	SES_{MPD}	IS	2.1	0.4602
PC8	SES_{MNTD}	IS	antenna 1 length	SES_{MPD}	IS	**-0.7423**	**0.6168**
all	SES_{MNTD}	IS	antenna 2 length	SES_{MPD}	IS	0.2904	0.00001889
BDBM	SES_{MNTD}	IS	antenna 2 length	SES_{MPD}	IS	-0.2874	0.05725
PC16	SES_{MNTD}	IS	antenna 2 length	SES_{MPD}	IS	**2.318**	**0.7105**
PC8	SES_{MNTD}	IS	antenna 2 length	SES_{MPD}	IS	-0.2989	0.038
all	SES_{MNTD}	IS	max. body size	SES_{MPD}	IS	0.6268	0.3383
BDBM	SES_{MNTD}	IS	max. body size	SES_{MPD}	IS	-0.419	0.2144
PC16	SES_{MNTD}	IS	max. body size	SES_{MPD}	IS	1.13	0.08112
PC8	SES_{MNTD}	IS	max. body size	SES_{MPD}	IS	-0.5734	0.3775
all	SES_{MNTD}	IS	phylogeny	SES_{MPD}	IS	0.635	0.3479
BDBM	SES_{MNTD}	IS	phylogeny	SES_{MPD}	IS	-0.5398	0.4195
PC16	SES_{MNTD}	IS	phylogeny	SES_{MPD}	IS	**2.425**	**0.7309**
PC8	SES_{MNTD}	IS	phylogeny	SES_{MPD}	IS	-0.598	0.4172
all	SES_{MPD}	TS	activity level (% still)	SES_{MNTD}	TS	**1.796**	**0.4713**
BDBM	SES_{MPD}	TS	activity level (% still)	SES_{MNTD}	TS	**-0.4763**	**0.5311**
PC16	SES_{MPD}	TS	activity level (% still)	SES_{MNTD}	TS	-0.7327	0.348
PC8	SES_{MPD}	TS	activity level (% still)	SES_{MNTD}	TS	**-0.5628**	**0.4907**
all	SES_{MPD}	TS	all	SES_{MNTD}	TS	0.7145	-0.03922
BDBM	SES_{MPD}	TS	all	SES_{MNTD}	TS	**-0.6362**	**0.657**
PC16	SES_{MPD}	TS	all	SES_{MNTD}	TS	**-1.13**	**0.6164**
PC8	SES_{MPD}	TS	all	SES_{MNTD}	TS	**-0.6747**	**0.4708**
all	SES_{MPD}	TS	antenna 1 length	SES_{MNTD}	TS	1.58	0.3254
BDBM	SES_{MPD}	TS	antenna 1 length	SES_{MNTD}	TS	**-5.366**	**0.671**
PC16	SES_{MPD}	TS	antenna 1 length	SES_{MNTD}	TS	**-1.09**	**0.8543**
PC8	SES_{MPD}	TS	antenna 1 length	SES_{MNTD}	TS	**-0.6129**	**0.5743**
all	SES_{MPD}	TS	antenna 2 length	SES_{MNTD}	TS	0.0568	-0.08507
BDBM	SES_{MPD}	TS	antenna 2 length	SES_{MNTD}	TS	0.07383	0.2961
PC16	SES_{MPD}	TS	antenna 2 length	SES_{MNTD}	TS	0.1218	0.2234

PC8	SES_{MPD}	TS	antenna 2 length	SES_{MNTD}	TS	0.06692	0.1182
all	SES_{MPD}	TS	max. body size	SES_{MNTD}	TS	**2.192**	**0.8723**
BDBM	SES_{MPD}	TS	max. body size	SES_{MNTD}	TS	**-0.4758**	**0.6194**
PC16	SES_{MPD}	TS	max. body size	SES_{MNTD}	TS	**-0.8523**	**0.5926**
PC8	SES_{MPD}	TS	max. body size	SES_{MNTD}	TS	**-0.6713**	**0.8599**
all	SES_{MPD}	TS	phylogeny	SES_{MNTD}	TS	2.327	0.2879
BDBM	SES_{MPD}	TS	phylogeny	SES_{MNTD}	TS	**-0.9558**	**0.9281**
PC16	SES_{MPD}	TS	phylogeny	SES_{MNTD}	TS	**-1.64**	**0.808**
PC8	SES_{MPD}	TS	phylogeny	SES_{MNTD}	TS	**-1.142**	**0.8847**
all	SES_{MPD}	TS	activity level (% still)	SES_{MNTD}	IS	2.599	0.311
BDBM	SES_{MPD}	TS	activity level (% still)	SES_{MNTD}	IS	-0.662	0.3188
PC16	SES_{MPD}	TS	activity level (% still)	SES_{MNTD}	IS	-0.9429	0.1549
PC8	SES_{MPD}	TS	activity level (% still)	SES_{MNTD}	IS	-0.7479	0.2583
all	SES_{MPD}	TS	all	SES_{MNTD}	IS	0.1913	-0.09711
BDBM	SES_{MPD}	TS	all	SES_{MNTD}	IS	-0.6724	0.4605
PC16	SES_{MPD}	TS	all	SES_{MNTD}	IS	-1.145	0.3876
PC8	SES_{MPD}	TS	all	SES_{MNTD}	IS	-0.6763	0.2801
all	SES_{MPD}	TS	antenna 1 length	SES_{MNTD}	IS	2.018	0.3975
BDBM	SES_{MPD}	TS	antenna 1 length	SES_{MNTD}	IS	**-0.6194**	**0.6363**
PC16	SES_{MPD}	TS	antenna 1 length	SES_{MNTD}	IS	**-1.274**	**0.8347**
PC8	SES_{MPD}	TS	antenna 1 length	SES_{MNTD}	IS	**-0.7228**	**0.5721**
all	SES_{MPD}	TS	antenna 2 length	SES_{MNTD}	IS	0.1286	-0.08141
BDBM	SES_{MPD}	TS	antenna 2 length	SES_{MNTD}	IS	0.1645	0.3778
PC16	SES_{MPD}	TS	antenna 2 length	SES_{MNTD}	IS	0.2455	0.2194
PC8	SES_{MPD}	TS	antenna 2 length	SES_{MNTD}	IS	0.1328	0.1088
all	SES_{MPD}	TS	max. body size	SES_{MNTD}	IS	**2.996**	**0.8236**
BDBM	SES_{MPD}	TS	max. body size	SES_{MNTD}	IS	**-0.6125**	**0.5065**
PC16	SES_{MPD}	TS	max. body size	SES_{MNTD}	IS	-1.078	0.4637
PC8	SES_{MPD}	TS	max. body size	SES_{MNTD}	IS	**-0.9011**	**0.7799**
all	SES_{MPD}	TS	phylogeny	SES_{MNTD}	IS	1.763	0.1775
BDBM	SES_{MPD}	TS	phylogeny	SES_{MNTD}	IS	**-0.8189**	**0.8409**
PC16	SES_{MPD}	TS	phylogeny	SES_{MNTD}	IS	**-1.441**	**0.7735**

PC8	SES_{MPD}	TS	phylogeny	SES_{MNTD}	IS	**-0.9683**	**0.7817**
all	SES_{MPD}	TS	activity level (% still)	SES_{MPD}	TS	0.9565	0.029
BDBM	SES_{MPD}	TS	activity level (% still)	SES_{MPD}	TS	**-0.6395**	**0.8058**
PC16	SES_{MPD}	TS	activity level (% still)	SES_{MPD}	TS	**-1.083**	**0.6788**
PC8	SES_{MPD}	TS	activity level (% still)	SES_{MPD}	TS	**-0.6478**	**0.523**
all	SES_{MPD}	TS	all	SES_{MPD}	TS	1.481	0.1471
BDBM	SES_{MPD}	TS	all	SES_{MPD}	TS	**-0.6355**	**0.6145**
PC16	SES_{MPD}	TS	all	SES_{MPD}	TS	**-1.325**	**0.8315**
PC8	SES_{MPD}	TS	all	SES_{MPD}	TS	**-0.7063**	**0.4917**
all	SES_{MPD}	TS	antenna 1 length	SES_{MPD}	TS	1.481	0.1077
BDBM	SES_{MPD}	TS	antenna 1 length	SES_{MPD}	TS	**-0.8127**	**0.8832**
PC16	SES_{MPD}	TS	antenna 1 length	SES_{MPD}	TS	**-1.415**	**0.7944**
PC8	SES_{MPD}	TS	antenna 1 length	SES_{MPD}	TS	**-0.8687**	**0.653**
all	SES_{MPD}	TS	antenna 2 length	SES_{MPD}	TS	-1.194	0.2262
BDBM	SES_{MPD}	TS	antenna 2 length	SES_{MPD}	TS	-0.01737	-0.09891
PC16	SES_{MPD}	TS	antenna 2 length	SES_{MPD}	TS	-0.05159	-0.09713
PC8	SES_{MPD}	TS	antenna 2 length	SES_{MPD}	TS	0.06248	-0.09059
all	SES_{MPD}	TS	max. body size	SES_{MPD}	TS	**1.755**	**0.5515**
BDBM	SES_{MPD}	TS	max. body size	SES_{MPD}	TS	-0.2667	0.1363
PC16	SES_{MPD}	TS	max. body size	SES_{MPD}	TS	-0.6884	0.3723
PC8	SES_{MPD}	TS	max. body size	SES_{MPD}	TS	-0.4821	0.4176
all	SES_{MPD}	TS	phylogeny	SES_{MPD}	TS	0.1043	-0.0993
BDBM	SES_{MPD}	TS	phylogeny	SES_{MPD}	TS	**-0.7589**	**0.4794**
PC16	SES_{MPD}	TS	phylogeny	SES_{MPD}	TS	-1.209	0.3414
PC8	SES_{MPD}	TS	phylogeny	SES_{MPD}	TS	-0.7447	0.274
all	SES_{MPD}	TS	activity level (% still)	SES_{MPD}	IS	2.166	0.2165
BDBM	SES_{MPD}	TS	activity level (% still)	SES_{MPD}	IS	**-0.8495**	**0.6652**
PC16	SES_{MPD}	TS	activity level (% still)	SES_{MPD}	IS	**-1.747**	**0.8709**
PC8	SES_{MPD}	TS	activity level (% still)	SES_{MPD}	IS	**-1.034**	**0.6604**
all	SES_{MPD}	TS	all	SES_{MPD}	IS	2.302	0.299
BDBM	SES_{MPD}	TS	all	SES_{MPD}	IS	-0.5871	0.3078

PC16	SES_{MPD}	TS	all	SES_{MPD}	IS	**-1.465**	**0.6617**
PC8	SES_{MPD}	TS	all	SES_{MPD}	IS	-0.8356	0.4538
all	SES_{MPD}	TS	antenna 1 length	SES_{MPD}	IS	2.349	0.3908
BDBM	SES_{MPD}	TS	antenna 1 length	SES_{MPD}	IS	**-0.6516**	**0.4934**
PC16	SES_{MPD}	TS	antenna 1 length	SES_{MPD}	IS	**-1.443**	**0.7732**
PC8	SES_{MPD}	TS	antenna 1 length	SES_{MPD}	IS	**-0.8976**	**0.6548**
all	SES_{MPD}	TS	antenna 2 length	SES_{MPD}	IS	-0.2257	-0.09462
BDBM	SES_{MPD}	TS	antenna 2 length	SES_{MPD}	IS	-0.1744	-0.04955
PC16	SES_{MPD}	TS	antenna 2 length	SES_{MPD}	IS	-0.5256	0.03751
PC8	SES_{MPD}	TS	antenna 2 length	SES_{MPD}	IS	-0.2387	-0.03661
all	SES_{MPD}	TS	max. body size	SES_{MPD}	IS	2.312	0.4311
BDBM	SES_{MPD}	TS	max. body size	SES_{MPD}	IS	-0.3173	0.0571
PC16	SES_{MPD}	TS	max. body size	SES_{MPD}	IS	-0.8792	0.2619
PC8	SES_{MPD}	TS	max. body size	SES_{MPD}	IS	-0.6254	0.3092
all	SES_{MPD}	TS	phylogeny	SES_{MPD}	IS	1.139	0.02829
BDBM	SES_{MPD}	TS	phylogeny	SES_{MPD}	IS	-0.4503	0.215
PC16	SES_{MPD}	TS	phylogeny	SES_{MPD}	IS	-1.026	0.3908
PC8	SES_{MPD}	TS	phylogeny	SES_{MPD}	IS	-0.6267	0.309
all	SES_{MPD}	IS	activity level (% still)	SES_{MNTD}	TS	0.1259	-0.05524
BDBM	SES_{MPD}	IS	activity level (% still)	SES_{MNTD}	TS	-0.397	0.1836
PC16	SES_{MPD}	IS	activity level (% still)	SES_{MNTD}	TS	0.1423	-0.08708
PC8	SES_{MPD}	IS	activity level (% still)	SES_{MNTD}	TS	-0.2349	-0.02067
all	SES_{MPD}	IS	all	SES_{MNTD}	TS	**0.587**	**0.5538**
BDBM	SES_{MPD}	IS	all	SES_{MNTD}	TS	-0.0752	-0.09316
PC16	SES_{MPD}	IS	all	SES_{MNTD}	TS	0.8108	0.1822
PC8	SES_{MPD}	IS	all	SES_{MNTD}	TS	0.234	-0.04709
all	SES_{MPD}	IS	antenna 1 length	SES_{MNTD}	TS	**0.4952**	**0.5663**
BDBM	SES_{MPD}	IS	antenna 1 length	SES_{MNTD}	TS	-0.03784	-0.09752
PC16	SES_{MPD}	IS	antenna 1 length	SES_{MNTD}	TS	0.5588	0.0919
PC8	SES_{MPD}	IS	antenna 1 length	SES_{MNTD}	TS	0.1527	-0.06772

all	SES_{MPD}	IS	antenna 2 length	SES_{MNTD}	TS	**-0.08863**	**0.4791**
BDBM	SES_{MPD}	IS	antenna 2 length	SES_{MNTD}	TS	-0.01683	-0.08669
PC16	SES_MPD	IS	antenna 2 length	SES_{MNTD}	TS	-0.1535	0.2927
PC8	SES_MPD	IS	antenna 2 length	SES_{MNTD}	TS	-0.06596	0.06334
all	SES_MPD	IS	max. body size	SES_{MNTD}	TS	0.02527	-0.09794
BDBM	SES_MPD	IS	max. body size	SES_{MNTD}	TS	**-0.5917**	**0.6197**
PC16	SES_MPD	IS	max. body size	SES_{MNTD}	TS	-0.396	0.01435
PC8	SES_{MPD}	IS	max. body size	SES_{MNTD}	TS	-0.5346	0.3692
all	SES_{MPD}	IS	phylogeny	SES_{MNTD}	TS	0.4959	0.1807
BDBM	SES_{MPD}	IS	phylogeny	SES_{MNTD}	TS	-0.6073	0.1686
PC16	SES_{MPD}	IS	phylogeny	SES_{MNTD}	TS	0.3786	-0.06298
PC8	SES_{MPD}	IS	phylogeny	SES_{MNTD}	TS	-0.2719	-0.05701
all	SES_{MPD}	IS	activity level (% still)	SES_{MNTD}	IS	0.1512	-0.07783
BDBM	SES_{MPD}	IS	activity level (% still)	SES_{MNTD}	IS	-0.5405	0.08066
PC16	SES_{MPD}	IS	activity level (% still)	SES_{MNTD}	IS	0.329	-0.07626
PC8	SES_{MPD}	IS	activity level (% still)	SES_{MNTD}	IS	-0.2855	-0.05975
all	SES_{MPD}	IS	all	SES_{MNTD}	IS	**0.6738**	**0.4709**
BDBM	SES_{MPD}	IS	all	SES_{MNTD}	IS	-0.01989	-0.09968
PC16	SES_{MPD}	IS	all	SES_{MNTD}	IS	1.029	0.2015
PC8	SES_{MPD}	IS	all	SES_{MNTD}	IS	0.3541	-0.01968
all	SES_{MPD}	IS	antenna 1 length	SES_{MNTD}	IS	**0.5473**	**0.4833**
BDBM	SES_{MPD}	IS	antenna 1 length	SES_{MNTD}	IS	-0.07374	-0.09325
PC16	SES_{MPD}	IS	antenna 1 length	SES_{MNTD}	IS	0.5687	0.04248
PC8	SES_{MPD}	IS	antenna 1 length	SES_{MNTD}	IS	0.128	-0.08375
all	SES_{MPD}	IS	antenna 2 length	SES_{MNTD}	IS	**-0.2002**	**0.6184**
BDBM	SES_{MPD}	IS	antenna 2 length	SES_{MNTD}	IS	-0.05604	-0.06411
PC16	SES_{MPD}	IS	antenna 2 length	SES_{MNTD}	IS	**-0.4143**	**0.5958**
PC8	SES_{MPD}	IS	antenna 2 length	SES_{MNTD}	IS	-0.1802	0.1965
all	SES_{MPD}	IS	max. body size	SES_{MNTD}	IS	-0.06848	-0.09231

BDBM	SES_{MPD}	IS	max. body size	SES_{MNTD}	IS	**-0.9046**	**0.7559**
PC16	SES_{MPD}	IS	max. body size	SES_{MNTD}	IS	-0.7531	0.1104
PC8	SES_{MPD}	IS	max. body size	SES_{MNTD}	IS	**-0.8631**	**0.5222**
all	SES_{MPD}	IS	phylogeny	SES_{MNTD}	IS	0.4983	0.2534
BDBM	SES_{MPD}	IS	phylogeny	SES_{MNTD}	IS	-0.4389	0.07484
PC16	SES_{MPD}	IS	phylogeny	SES_{MNTD}	IS	0.4251	-0.04182
PC8	SES_{MPD}	IS	phylogeny	SES_{MNTD}	IS	-0.1398	-0.08582
all	SES_{MPD}	IS	activity level (% still)	SES_{MPD}	TS	**0.5737**	**0.6395**
BDBM	SES_{MPD}	IS	activity level (% still)	SES_{MPD}	TS	-0.05002	-0.09641
PC16	SES_{MPD}	IS	activity level (% still)	SES_{MPD}	TS	0.9455	0.3544
PC8	SES_{MPD}	IS	activity level (% still)	SES_{MPD}	TS	0.2824	-0.00876
all	SES_{MPD}	IS	all	SES_{MPD}	TS	**0.6855**	**0.7434**
BDBM	SES_{MPD}	IS	all	SES_{MPD}	TS	0.06455	-0.09523
PC16	SES_{MPD}	IS	all	SES_{MPD}	TS	0.8148	0.1696
PC8	SES_{MPD}	IS	all	SES_{MPD}	TS	0.3131	-0.01036
all	SES_{MPD}	IS	antenna 1 length	SES_{MPD}	TS	**0.669**	**0.5758**
BDBM	SES_{MPD}	IS	antenna 1 length	SES_{MPD}	TS	-0.1597	-0.07545
PC16	SES_{MPD}	IS	antenna 1 length	SES_{MPD}	TS	0.9665	0.2191
PC8	SES_{MPD}	IS	antenna 1 length	SES_{MPD}	TS	0.2173	-0.06367
all	SES_{MPD}	IS	antenna 2 length	SES_{MPD}	TS	0.2702	0.1663
BDBM	SES_{MPD}	IS	antenna 2 length	SES_{MPD}	TS	0.2933	0.1001
PC16	SES_{MPD}	IS	antenna 2 length	SES_{MPD}	TS	0.5332	0.1346
PC8	SES_{MPD}	IS	antenna 2 length	SES_{MPD}	TS	0.3951	0.19
all	SES_{MPD}	IS	max. body size	SES_{MPD}	TS	0.008083	-0.09978
BDBM	SES_{MPD}	IS	max. body size	SES_{MPD}	TS	-0.4028	0.2487
PC16	SES_{MPD}	IS	max. body size	SES_{MPD}	TS	-0.6481	0.2202
PC8	SES_{MPD}	IS	max. body size	SES_{MPD}	TS	-0.4832	0.3009
all	SES_{MPD}	IS	phylogeny	SES_{MPD}	TS	0.7133	0.4193
BDBM	SES_{MPD}	IS	phylogeny	SES_{MPD}	TS	-0.0684	-0.09695
PC16	SES_{MPD}	IS	phylogeny	SES_{MPD}	TS	1.19	0.2268
PC8	SES_{MPD}	IS	phylogeny	SES_{MPD}	TS	0.3774	-0.02594
all	SES_{MPD}	IS	activity level (% still)	SES_{MPD}	IS	0.7103	0.4427

BDBM	SES_{MPD}	IS	activity level (% still)	SES_{MPD}	IS	-0.2308	-0.06346
PC16	SES_{MPD}	IS	activity level (% still)	SES_{MPD}	IS	0.5185	-0.03458
PC8	SES_{MPD}	IS	activity level (% still)	SES_{MPD}	IS	0.02809	-0.09957
all	SES_{MPD}	IS	all	SES_{MPD}	IS	0.4887	0.1866
BDBM	SES_{MPD}	IS	all	SES_{MPD}	IS	-0.2212	-0.06255
PC16	SES_{MPD}	IS	all	SES_{MPD}	IS	-0.1104	-0.09669
PC8	SES_{MPD}	IS	all	SES_{MPD}	IS	-0.1772	-0.08079
all	SES_{MPD}	IS	antenna 1 length	SES_{MPD}	IS	0.4153	0.1446
BDBM	SES_{MPD}	IS	antenna 1 length	SES_{MPD}	IS	-0.3823	0.03213
PC16	SES_{MPD}	IS	antenna 1 length	SES_{MPD}	IS	-0.1288	-0.09468
PC8	SES_{MPD}	IS	antenna 1 length	SES_{MPD}	IS	-0.291	-0.03885
all	SES_{MPD}	IS	antenna 2 length	SES_{MPD}	IS	0.3208	0.07321
BDBM	SES_{MPD}	IS	antenna 2 length	SES_{MPD}	IS	0.08975	-0.09135
PC16	SES_{MPD}	IS	antenna 2 length	SES_{MPD}	IS	0.1165	-0.09483
PC8	SES_{MPD}	IS	antenna 2 length	SES_{MPD}	IS	0.1271	-0.08616
all	SES_{MPD}	IS	max. body size	SES_{MPD}	IS	-0.03733	-0.09779
BDBM	SES_{MPD}	IS	max. body size	SES_{MPD}	IS	-0.5686	0.2264
PC16	SES_{MPD}	IS	max. body size	SES_{MPD}	IS	-1.024	0.2754
PC8	SES_{MPD}	IS	max. body size	SES_{MPD}	IS	-0.7153	0.3125
all	SES_{MPD}	IS	phylogeny	SES_{MPD}	IS	0.3385	0.08061
BDBM	SES_{MPD}	IS	phylogeny	SES_{MPD}	IS	-0.2421	-0.04109
PC16	SES_{MPD}	IS	phylogeny	SES_{MPD}	IS	-0.09838	-0.09655
PC8	SES_{MPD}	IS	phylogeny	SES_{MPD}	IS	-0.1735	-0.07584

APPENDIX 6: Supplementary material for Chapter 3

Table A6.9. ZEN sites. Site names, codes, and geospatial coordinates.

Site	Name	Ocean	Margin	Latitude	Longitude
BB.A	Westside Park, Bodega Bay, CA, USA	Pacific	East	38.319755	-123.05514
BB.B	Sacramento Landing, Tomales Bay, CA, USA	Pacific	East	38.1496437	-122.90638
BC.A	Tsawwassen, BC, Canada	Pacific	East	49	-123.1
BC.B	White Rock, BC, Canada	Pacific	East	49	-122.8
CR	Sveti Duh, Croatia	Atlantic	East	44.2055713	15.4777338
ES.A	South Bay, VA, USA	Atlantic	West	37.265686	-75.812668
ES.B	Cobb Bay, VA, USA	Atlantic	West	37.31855	-75.789076
FI.A	Fårö, Finland	Atlantic	East	59.92025	21.7961833
FI.B	Ängsö, Finland	Atlantic	East	60.10785	21.70995
FR.A	Bouzigues, Etang de Thau, France	Atlantic	East	43.446971	3.661503
FR.B	Peyrac sur mer, Etang de Bages-Sigean, France	Atlantic	East	43.082895	2.973231
IR.A	Greyabbey, Northern Island, UK	Atlantic	East	54.531944	-5.569167
IR.B	Donegal, Ireland	Atlantic	East	55.2225	-7.701944
JN.A	Akkeshi-ko estuary, Hokkaido, Japan	Pacific	West	43.021167	144.903217
JN.B	Akkeshi-bay, Hokkaido, Japan	Pacific	West	43.052222	144.842699
JS.A	Ikunoshima, Hiroshima, Japan	Pacific	West	34.297834	132.91631
JS.B	Onoura, Hiroshima, Japan	Pacific	West	34.274018	132.26617
KO.A	Dongdae Bay, South Korea	Pacific	West	34.8946611	128.020272
KO.B	Koje Bay, South Korea	Pacific	West	34.8009722	128.583694
LI.1	Landscape Lab, Long Island, NY, USA	Atlantic	West	40.85762	-72.45119
LI.2	Tiana Beach, Long Island, NY, USA	Atlantic	West	40.83158	-72.54082
MA.A	Dorothy Cove, MA, USA	Atlantic	West	42.42014	-70.91544
MA.B	Niles Beach, MA, USA	Atlantic	West	42.59697	-70.6556
MX.A	San Quintin Bay, Baja California, Mexico	Pacific	East	30.419675	-115.96419
MX.B	Punta Banda Estuary, Baja California, Mexico	Pacific	East	31.7584722	-116.62278
NC.A	Middle Marsh, NC, USA	Atlantic	West	34.692458	-76.622589
NC.B	Shackleford Island, NC, USA	Atlantic	West	34.670544	-76.574561
NN.A	Misvaerfjorden, Norway	Atlantic	East	67.2147	15.0083
NN.B	Rövika, Norway	Atlantic	East	67.2667233	15.2560633
OR.A	Yaquina Bay, OR, USA	Pacific	East	44.6127333	-124.01413
OR.B	Coos Bay, OR, USA	Pacific	East	43.34625	-124.31828
PO.A	Culatatra, Portugal	Atlantic	East	36.997057	-7.82849
PO.B	Marim, Portugal	Atlantic	East	37.027333	-7.810105

QU.A	Pointe-Lebel, QU, Canada	Atlantic	West	49.11237	-68.17593
QU.B	Baie-St-Ludger, QU, Canada	Atlantic	West	49.08696	-68.32041
RU.A	Seldianaya, Russia	Atlantic	East	66.4061111	33.7230556
RU.B	Nicolskaya, Russia	Atlantic	East	66.2858333	34.0025
SD.A	Shelter Island, San Diego Bay, CA, USA	Pacific	East	32.713756	-117.22547
SD.B	Coronado, San Diego Bay, CA, USA	Pacific	East	32.700762	-117.17289
SF.A	Point Molate, San Francisco Bay, CA, USA	Pacific	East	37.946557	-122.4185
SF.B	Point San Pablo, San Francisco Bay, USA	Pacific	East	37.978118	-122.40594
SW.A	Torseröd, Sweden	Atlantic	East	58.3131	11.5488
SW.B	Bökevik, Sweden	Atlantic	East	58.2488	11.4536
UK.A	Porth Dinllaen, Wales, UK	Atlantic	East	52.942282	-4.565173
UK.B	Penn Y Chain, Wales, UK	Atlantic	East	52.89856	-4.321868
VA.A	Goodwin Islands, Chesapeake Bay, VA, USA	Atlantic	West	37.2204206	-76.401335
VA.B	Allen's Islands, Chesapeake Bay, VA, USA	Atlantic	West	37.2543093	-76.437447
WA.A	Willapa Bay, WA, USA	Pacific	East	46.474	-124.028
WA.B	Dabob Bay, WA, USA	Pacific	East	47.809	-122.815

Table A6.10. Traits used in functional analyses of epifaunal community structure. Traits were selected for their variation both within and among peracarids and gastropods; only parental care and developmental mode are invariant within peracarids (all peracarids are brooding direct developers). Observed sizes were measured by sieving epifauna through a series of 9 sieves with pore sizes of 0.5, 0.71, 1, 1.4, 2, 2.8, 4, 5.6, 8 mm. Latitudinal range was calculated as the range in absolute values of latitude from the combined set of observations from OBIS and GBIF for a given species after using the CoordinateCleaner package to remove inland observations, centroids, and identical latitude-longitude pairs.

Trait	Type	Values	Interpretation	Transformation	Source
Eats Microalgae	Bin.		Dietary niche partitioning		Gross et al. 2022, MRK
Eats Macroalgae	Bin.		Dietary niche partitioning		Gross et al. 2022, MRK
Eats Seagrass	Bin.		Dietary niche partitioning		Gross et al. 2022, MRK
Suspension Feeder	Bin.		Dietary niche partitioning		Gross et al. 2022, MRK
Detritivore	Bin.		Dietary niche partitioning		Gross et al. 2022, MRK

Carnivore, Parasite, Scavenger	Bin.		Dietary niche partitioning		Gross et al. 2022, MRK
Parental Care	Cat.	broadcast spawner, brooder, lays egg case	Dispersal ability		MRK
Developmental Mode	Cat.	lecithotrophic, planktotrophic, direct developer	Dispersal ability		MRK
Mode			Susceptibility to predators, ability to occupy physical space, competitive ability		Empirically measured
Observed Size	Cont.	0.5 - 8 mm		log	
Maximum Observed Size	Cont.	0.5 - 8 mm	Susceptibility to predators, ability to occupy physical space, competitive ability	log	Empirically measured
Mean Observed Size	Cont.	0.5 - 8 mm	Susceptibility to predators, ability to occupy physical space, competitive ability	log	Empirically measured
Maximum Size (Literature)	Cont.	1 - 140 mm	Susceptibility to predators, ability to occupy physical space, competitive ability	log	Light & Smith, Gastropods. com, etc.
Latitudinal Range	Cont.	0 - 72.569º	Thermal niche		OBIS, GBIF
Mean Latitude	Cont.	13.719 - 66.183º	Thermal niche		OBIS, GBIF
Marine	Cont.		Salinity niche		WoRMS
Brackish	Bin.		Salinity niche		WoRMS
Freshwater	Bin.		Salinity niche		WoRMS

Table A6.11. Predictors used in random forest model of the log-transformed ratio of peracarid relative abundance to gastropod relative abundance (log-ratio). Mean in-situ measurements are derived from averaging across measurements from 20 sites; measurements from Bio-ORACLE are yearly averages measured between 2002-2009 within a 10-km radius of each site; measurements from World Ocean Database (WOD) were spatially interpolated based on sea surface measurements in 2009.

Predictor	Values	Transformation	Source
Ocean	Pacific, Atlantic	None	

Coast	West Pacific, East Pacific, West Atlantic, East Atlantic	None	
Margin	West, East	None	
In-Situ Temperature (ºC)	8 - 35	None	In situ
Salinity (ppt)	6.5 - 40	None	In situ
Genotypic Richness (mean Rozenfeld distance)	0.11 - 1.0	None	In situ
Allelic Richness (avg. number of alleles per locus, normalized to 7 genets)	1.29 - 6.72	Squared	In situ
Epiphyte Load (g cm^{-2} eelgrass)	0.00554072 - 1.071013	log	In situ
Macroalgal Abundance (g m^{-2})	0 - 4172.653	log + 1	In situ
Eelgrass morphology PC1 (62.09%)	-6.06524939 - 2.30096651	None	In situ
Eelgrass morphology PC2 (24.34%)	-1.48402338 - 3.59837339	None	In situ
Total Seagrass Biomass (g)	45.74725 - 1364.95000	log	In situ
Mean Leaf % N	1.092617 - 3.049590	None	In situ
Mean Leaf % C	31.59211 - 42.03824	None	In situ
Predation on Amphipods	0.2 - 1	arcsin	In situ
Predation on Gastropods	0 - 0.8	logit	In situ
Predation on Kale	0 - 0.9	None	In situ
Predation on Dried Squid	0 - 1	None	In situ
Mean Total Epifaunal Abundance	0.00 - 795.55	log	In situ
Site Epifaunal Richness	0 - 34	log	In situ
Calcite	0.00031100 - 0.02810775	log	WOD
Mean Chl A	0.613 - 24.016	log	Bio-Oracle
Nitrate	0.05533333 - 10.23499997	square root	WOD
Phosphate	0.034800 - 2.172433	log	WOD
Mean PAR	27.34367 - 42.52075	None	Bio-Oracle
pH	7.705167 - 8.311857	None	Bio-Oracle
Silicate	0.93350 - 39.64817	log	WOD
Maximum SST (ºC)	12.6166 - 29.6965	log	Bio-Oracle
Mean SST (ºC)	4.0669 - 21.3620	None	Bio-Oracle
SST Range (ºC)	3.573667 - 22.870750	None	Bio-Oracle
Peracarid Richness	0 - 21	log + 1	In situ
Gastropod Richness	1 - 17	log	In situ

Table A6.4. Results of generalized linear models examining the effects of eelgrass genetic diversity and morphology on the species richness of peracarids and gastropods across global eelgrass beds. Allelic richness refers to the average number of alleles per locus normalized to 7 genets, while genotypic richness refers to the mean Rozenfeld distance between individuals in a site. PC1 is positively correlated with shorter, thinner shoots, while PC2 is positively correlated with more dense shoots and greater aboveground biomass. Bolded rows indicate significant predictors at $\alpha = 0.05$.

	Predictor	χ^2_1	p	Effect size	pseudo R^2
Peracarid richness	**Allelic Richness**	**37.258**	**1.035e-09**	**0.028996**	**0.2076344**
	Genotypic Richness	**19.88**	**8.247e-06**	**1.125**	**0.1107829**
	PC1	**4.8839**	**0.02711**	**-0.0652**	**0.0271942**
	PC2	**17.978**	**2.235e-05**	**0.1907**	**0.100195**
Gastropod richness	Allelic Richness	2.271	0.1318	0.009235	0.02300632
	Genotypic Richness	**4.8883**	**0.02704**	**0.7009**	**0.04951779**
	PC1	**12.976**	**0.0003154**	**0.16457**	**0.1314531**
	PC2	0.78951	0.3742	0.05649	0.00799295

Table A6.5. Results of linear models examining the effects of eelgrass genetic diversity and morphology on the log-transformed total site-level abundance of peracarids and gastropods across global eelgrass beds. Allelic richness refers to the average number of alleles per locus normalized to 7 genets, while genotypic richness refers to the mean Rozenfeld distance between individuals in a site. PC1 is positively correlated with shorter, thinner shoots, while PC2 is positively correlated with more dense shoots and greater aboveground biomass. Bolded rows indicate significant predictors at $\alpha = 0.05$.

	Predictor	F	p	Effect size	R^2
log(Peracarid abundance + 1)	**Allelic Richness**	**8.968**	**0.00433**	**0.07691**	**0.1399**
	Genotypic Richness	**5.191**	**0.0272**	**2.921**	**0.07879**
	PC1	**4.722**	**0.0347**	**-0.3904**	**0.0706**
	PC2	**9.963**	**0.00276**	**0.8638**	**0.1546**
log(Gastropod abundance + 1)	Allelic Richness	3.171	0.0813	-0.04703	0.04242
	Genotypic Richness	3.162	0.0817	-2.266	0.04226
	PC1	**6.533**	**0.0138**	**0.4402**	**0.1015**
	PC2	0.7402	0.394	0.2503	-0.005331

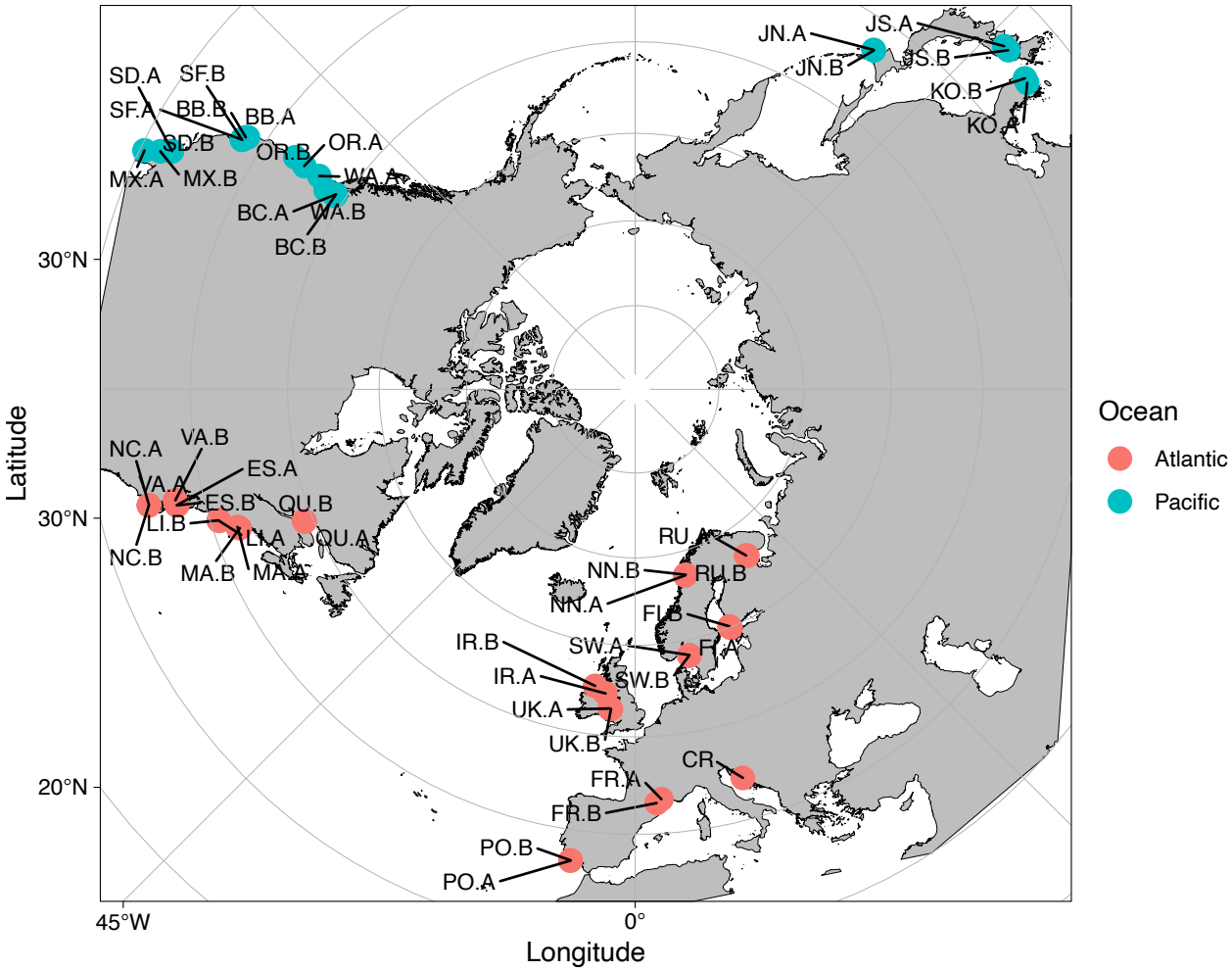

Figure A6.6. ZEN sites in the Atlantic (pink) and Pacific (blue) oceans. See Table A6.1 for site codes.

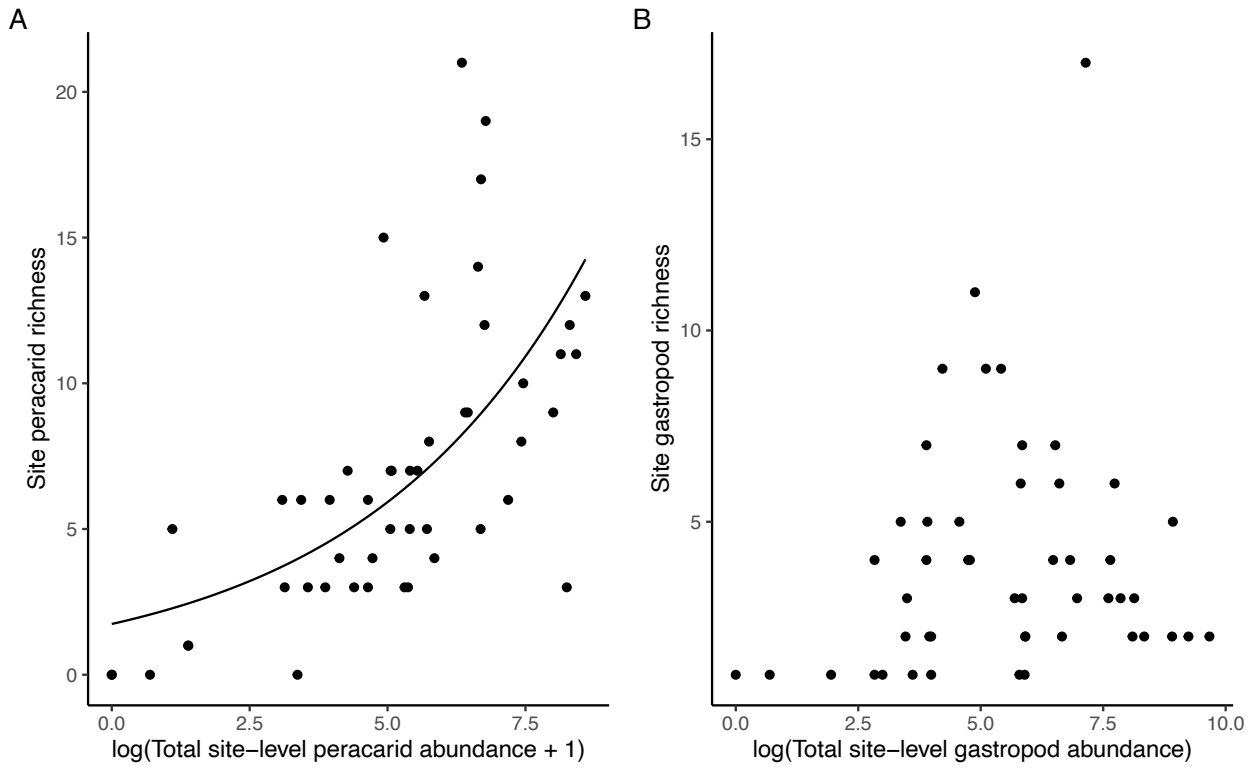

Figure A6.2. Relationships between total site-level abundance (calculated as the sum of plot-level abundances standardized by eelgrass biomass) and species richness for peracarids (A) and gastropods (B) in eelgrass epifaunal communities. Species richness only increased with increasing abundance for peracarids ($\chi^2_1 = 77.038$, $p < 0.001$); gastropods showed no significant trend.

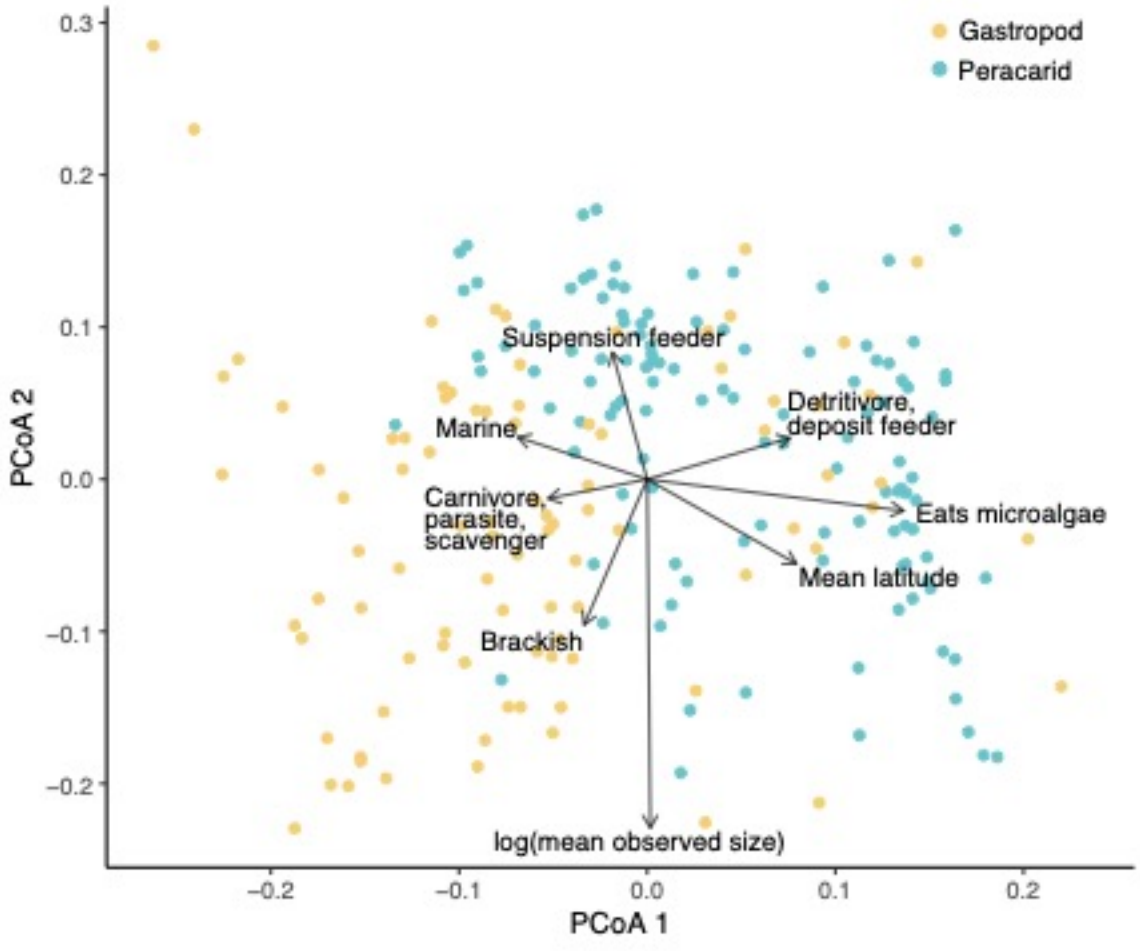

Figure A6.3. Principle components analysis (PCoA) biplot of gastropod and peracarid species in global eelgrass beds. Distances between points (species) are based on weighted Gower distances, which take into account among-species variation in continuous, binary, and categorical traits. For clarity, not all traits are included in this ordination.

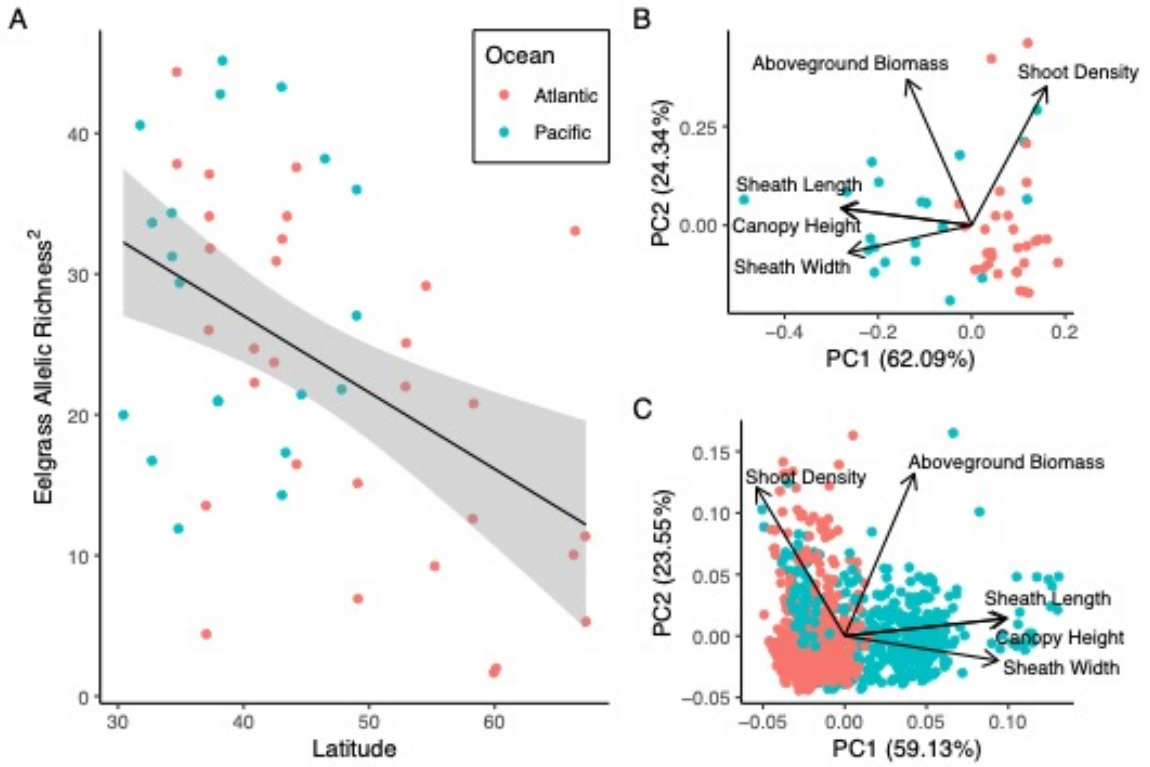

Figure S4. Variation in eelgrass allelic richness and morphology across ocean basins. Allelic richness declined with latitude across sites in both oceans (A; $F_{1,48} = 13.36$, $p = 0.0006375$), and was greater on average in the Pacific, although this was marginally nonsignificant ($F_{1,48} = 3.804$, $p = 0.05699$). Eelgrass morphological variation was greater in the Pacific than in the Atlantic when looking across sites (B) and across plots within sites (C).